D3.1

Modelling, simulation and assessment of vehicle automations and automated vehicles' driver behaviour in mixed traffic

Project Acronym	TransAID
Project Title	Transition Areas for Infrastructure-Assisted Driving
Project Number	Horizon 2020 ART-05-2016 – GA Nr 723390
Work Package	WP3 Modelling and Impact Assessment of Automated Vehicles
Lead Beneficiary	CERTH - HIT (CRT)
Editor / Main Author	Evangelos Mintsis CRT
Reviewer	Sven Maerivoet TML
Dissemination Level	PU
Contractual Delivery Date	30/06/2019 (M22)
Actual Delivery Date	19/09/2019 (M25)
Version	v2.0

This project has received funding from the European Union's Horizon 2020 research and innovation programme under grant agreement No 723390.

Document revision history

Version	Date	Comments
v0.1	2018-05-15	Initial draft version including the structure of Deliverable D3.1.
v0.2	2018-05-31	Chapter 1 “Introduction” and Section 2.1 “Adaptive Cruise Control Model” added.
v0.3	2018-06-14	Sub-section 2.2.1 “Parametrization of SUMO Lane Change Model (LC2013)” added.
v0.4	2018-06-28	Sections 3.1 – 3.4 of Chapter 3 “Simulation Experiments” added.
v0.5	2018-07-19	Chapters 1, 2, and 3 finalized.
v0.6	2018-07-31	Section 4.2 “Scenario 2.1 Prevent ToC/MRM by providing speed, headway and/or lane advice” and Appendix A added.
v0.7	2018-08-08	All chapters finalized apart from conclusions chapter.
v0.8	2018-08-09	Added conclusions chapter, checked all references (literature, figures, and tables).
v0.9	2018-08-10	TML review processed.
v1.0	2018-08-12	Final version.
v0.1	2019-04-08	Updated document structure to reflect work done in the 2nd iteration.
v1.2	2019-04-20	Description of the ToC Model extensions/refinements (Section 2.3.2).
v1.3	2019-05-17	Added description of the Cooperative Cruise Control Algorithm (Section 2.1.2)
v1.4	2019-6-10	New section (2.2.2) on the parametrization of the lane change model for AVs included.
v1.5	2019-06-28	Updated structure of simulation experiments introduced in Section 3.2.
v1.6	2019-07-12	Scenario 4.1 – 5 (Section 4.2.5) finalized.
v1.7	2019-07-19	Scenario 4.2 (Section 4.2.4) finalized.
v1.8	2019-07-29	Scenario 2.1 (Section 4.2.2) finalized.
v1.9	2019-08-30	Scenario 1.3 (Section 4.2.1) finalized.
v1.91	2019-09-02	Scenario 2.3 (Section 4.2.3) finalized.

v1.92	2019-09-03	Added Appendix B, updated conclusions chapter, checked all references (literature, figures, and tables).
v1.93	2019-09-05	TML review processed.
v2.0	2019-09-06	Final version.

Editor / Main author

Evangelos Mintsis (CRT)

List of contributors

Evangelos Mintsis (CRT), Dimitris Koutras (CRT), Kallirroi Porfyri (CRT), Evangelos Mitsakis (CRT), Leonhard Luecken (DLR), Jakob Erdmann (DLR), Yun-Pang Floetteroed (DLR), Robert Alms (DLR), Michele Rondinone (HYU), Sven Maerivoet (TML), Kristof Carlier (TML), Xiaoyun Zhang (DYN), Robbin Blokpoel (DYN), Martijn Harmenzon (MAP), Steven Boerma (MAP)

List of reviewers

Sven Maerivoet (TML)

Dissemination level:

■ PU : Public

□ RE : Restricted to a group specified by the consortium (including the Commission Services)

□ CO : Confidential, only for members of the consortium (including the Commission Services)

Table of contents

Executive Summary

The present document is Deliverable D3.1 entitled "Modelling, simulation and assessment of vehicle automations and automated vehicles' driver behaviour in mixed traffic" which is prepared in the context of the WP3 framework of the TransAID project. In this document, the vehicle/driver models developed to emulate the motion of automated vehicles (AVs) and the driver's behaviour in the event of vehicle disengagements are presented. Namely, an Adaptive Cruise Control (ACC) model and a Cooperative Adaptive Cruise Control (CACC) model that dictate the longitudinal motion of AVs, a parametrized version of the default SUMO lane change model that mimics the lateral motion of AVs, and finally a Transition of Control (ToC) model that determines the actions of the driver/vehicle unit (DVU) during control transitions (transitions between different levels of automation). Details regarding the implementation of these models within SUMO are also provided. Moreover, the setup of the simulation experiments that are conducted for each use case investigated within TransAID is given. To increase the realism of simulation experiments in the 2nd project iteration we also consider Day 1 C-ITS applications. Comprehensive information regarding inputs (vehicle types, traffic demand, vehicle mixes) to the simulation experiments is described separately per project iteration. Additionally, different parametrization schemes of the vehicle/driver models are introduced in each project iteration to facilitate the analysis of the impacts of different DVU behaviour. Simulation results pertaining to traffic safety, traffic efficiency and environmental impacts are provided per examined TransAID scenario. Simulation findings indicate that unmanaged Minimum Risk Manoeuvres (MRMs) can heavily impact traffic operations and induce traffic disruption. On the other hand, successful ToCs can also disturb the traffic flow performance when CV/CAV share is high and ToCs concurrently take place in a confined road section. The latter phenomenon is amplified if CAVs are driving in CACC mode and need to enlarge car-following headways prior to ToC. However, our analysis remains inclusive with respect to the impacts of control transitions on traffic safety and warrant further investigation on the reasons of safety critical events in our baseline simulation experiments.

1. Introduction

1.1 About TransAID

As automated driving (AD) becomes feasible on interrupted and uninterrupted traffic flow facilities, it is important to assess its impacts on traffic safety, traffic efficiency, and the environment. During the early stages of AD market introduction, cooperative and automated vehicles (CAVs), automated vehicles (AVs) of different SAE levels, cooperative vehicles (CVs) able to communicate via vehicle-to-anything (V2X), and legacy vehicles (LVs) will share the same roads with varying penetration rates. In the course of this period, there will be areas and situations on the roads where high automation can be granted, and others where it will not be allowed or feasible due to system failures, highly complex traffic situations, human factors and possibly other reasons. At these areas many AVs will have to change their level of automation. We refer to these areas as "Transition Areas" (TAs).

TransAID develops and demonstrates traffic management procedures and protocols to enable smooth coexistence of (C)AVs, CVs, and LVs in the vicinity of TAs. A hierarchical and centralized approach is adopted, where control actions are implemented at different layers including traffic management centres, roadside infrastructure, and vehicles.

Initially, simulations were run to investigate the efficiency of infrastructure-assisted traffic management solutions in controlling (C)AVs, CVs, and LVs around TAs, taking into account traffic safety, traffic efficiency and environmental metrics. Then, communication protocols for the cooperation between (C)AVs – CVs and the road infrastructure were developed. Traffic measures to detect and inform LVs were addressed. The most promising solutions were implemented as real world prototypes and demonstrated at a test track. Finally, guidelines for advanced infrastructure-assisted driving were formulated. These guidelines include a roadmap that defines necessary activities and upgrades of road infrastructure in the upcoming fifteen years to guarantee a smooth coexistence of (C)AVs, CVs, and LVs.

1.1.1 Iterative project approach

TransAID develops and tests infrastructure-assisted management solutions for mixed traffic at TAs in two project iterations. Each project iteration lasts half of the total project duration.

During the first project iteration, focus is placed on studying Transitions of Control (ToCs) and Minimum Risk Manoeuvres (MRMs) using simplified scenarios. To this end, models for AD and vehicle disengagements are adopted and developed. The simplified scenarios are used for conducting several simulation experiments to analyse the impacts of ToCs at TAs, and the effects of the corresponding mitigating measures.

During the second project iteration, we introduce new vehicle models for CVs/(C)AVs and utilize the experience accumulated during the first project iteration to enhance the existing vehicle/driver models. Moreover, we increase the complexity/realism of our baseline simulation experiments by considering Day 1 C-ITS applications for specific scenarios. New traffic management measures are developed and combined with the existing ones in the proximity of TAs. Finally, we enrich the list of KPIs used for the evaluation of the simulation scenarios.

1.2 Purpose of this document

Deliverable D3.1 encompasses the modelling of vehicle automations and automated vehicles' driver behaviour in SUMO (Simulator of Urban MObility) (Task T3.1), as well as the simulation of baseline scenarios (Task T3.2) previously defined in D2.2.

In the first project iteration, we provide a description of the first stable versions of the vehicle models emulating the longitudinal and lateral motion of (C)AVs and CVs. These vehicle models dictate the motion of (C)AVs and CVs upstream and downstream of TAs where AD is feasible and allowed. Longitudinal motion is determined by an Adaptive Cruise Control (ACC) model, while the lateral motion is determined by the SUMO default lane change model (LC2013). The latter was parametrised to reflect actual (C)AV and CV lane change behaviour. CV's/(C)AVs' driver behaviour is also modelled when a take-over request (ToR) by the vehicle automation is issued. Based on driver's responsiveness, a ToC can either be successful or lead to the execution of an MRM. We also include a detailed description of a combined ToC/MRM model. In the second project iteration, we intorduce a Cooperative Adaptive Cruise Control (CACC) model to replicate the car-following behavior of CVs/CAVs, and conduct enhacments regarding the modelling of AV lane changing and control transitions.

Vehicle demand levels and mixes are defined in the final version of Deliverable D2.2 for the conduct of the baseline simulation experiments in both project iterations. In the first project iteration Delivearble D3.1 further elaborated the discussion on actors by proposing a new vehicle classification that represents actual driving conditions in a more comprehensive manner. The latter vehicle classification scheme is also maintained in the second project iteration.

In the first project iteration we presented a parametrisation scheme of the vehicle/driver models (ACC, LC2013, ToC/MRM) that accounts for simulation experiments exhibiting different effects on traffic safety and efficiency. In the second project iteration we integrate the full spectrum of AV behaviour in a single parametrization scheme of the vehicle/driver models. Baseline simulation results are presented for all the scenarios examined in both project iterations.

Deliverable D3.1 unravels limitations of the simulated driver models, demonstrates the impacts of ToCs and possible MRMs at TAs, and identifys the UCs and scenarios where ToCs/MRMs play a major role in traffic operations. Thus, Deliverable D3.1 provides valuable information for the development of the TransAID measures and the set up of the more detailed simulations (encompassing communication aspects) that will be run on the iTETRIS Platform (WP6).

1.3 Structure of this document

This document is comprised of five chapters and one Appendix. Each chapter is comprised of two major sections reflecting the work conducted in each project iteration separately. Chapter 1 is the introductory chapter where we present a summary of the project, describe the purpose of this document, and provide the structure of Deliverable D3.1 and the Glossary. The driver models developed to emulate the longitudinal and lateral motion of AVs, and the behaviour of automated vehicles' drivers during ToC are outlined in Chapter 2, divided into first and second project iteration work. Chapter 3 includes the description of the simulation experiments (experimental dimensionality, parametrisation of vehicle/driver models, simulation input, simulation runs, and simulation output). We present and analyse the baseline simulation results in Chapter 4, and discuss relevant conclusions in Chapter 5. Finally, in Appendix A we present the information regarding the setup of the baseline simulation experiments.

1.4 Glossary

Abbreviation/Term	Definition
ACC	Adaptive Cruise Control
AD	Automated Driving
ADAS	Advanced Driver Assistance Systems
AV	Automated Vehicle
CACC	Cooperative Adaptive Cruise Control
CAV	Cooperative Automated Vehicle
CV	Cooperative Vehicle
DVU	Driver-vehicle unit
DX.X	Deliverable X.X
HMI	Human Machine Interface
IDM	Intelligent Driver Model
KPI	Key Performance Indicator
LC2013	SUMO Lane Change Model (default)
LOS	Level of Service (from Highway Capacity Manual)
LV	Legacy Vehicle
MRM	Minimum Risk Manoeuvre
RSI	Road-side Infrastructure
SAE	Society of Automotive Engineers
SSM	Surrogate Safety Measure
SUMO	Simulation of Urban MObility
TA	Transition Area
ToC	Transition of Control
ToR	Take-over Request
TransAID	Transition Areas for Infrastructure-Assisted Driving

UC	Use Case
V2X	Vehicle-to-anything
VDIFF	Velocity Difference Model
VMS	Variable Message Signs
WP	Work Package

2 Modelling of vehicle automations

The modelling requirements for the conduct of the baseline simulation analysis (with abstract communications) are specified in D2.2. In line with these specifications, we extended an ACC/CACC model adopted from a previous study in order to replicate the longitudinal motion of (C)AVs/CVs. In addition we parametrised the SUMO LC2013 model to reflect the lateral motion of (C)AVs/CVs, and finally we developed a ToC/MRM model to mimic automated vehicles driver behaviour during ToC (and MRM in case of unsuccessful ToC). A detailed description of the latter vehicle/driver models is presented subsequently.

2.1 (C)AV/CV Car Following Models

2.1.1 First Iteration

2.1.1.1 Adaptive Cruise Control (ACC) Model

2.1.1.1.1 Background

Advanced Driver Assistance Systems (ADAS) have been designed to increase road safety and driving comfort (Blythe & Curtis, 2004). In the past decade, the automobile industry has been deploying ADAS at an increasing rate on new vehicles. ACC is one such a benchmark ADAS, being heavily studied and currently tested in real-world conditions to unravel its impacts on the traffic flow.

ACC systems that are currently available on the market enable automatic following of a preceding vehicle by controlling the throttle and the brake actuators of the ACC vehicle. Specifically, using range sensors, such as radar, lidar and video camera, an ACC system is able to measure the distance and the relative velocity with respect to a preceding vehicle. If the ACC sensors detect a slower preceding vehicle, the ACC equipped vehicle automatically adjusts the speed to maintain a desired space headway (gap-control mode). In the absence of a preceding vehicle, the ACC vehicle operates under the speed-control mode, maintaining the user's chosen desired speed.

Many studies address the impacts of ACC vehicles on traffic flow dynamics with the use of traffic simulation, mainly because large-scale field tests are costly to implement. Some investigations predict a positive effect of ACC (Davis, 2004; Hasebe et al., 2003; Naus et al., 2010; Treiber & Helbing, 2001; van Arem et al., 2006), whereas others are more conservative on the stabilisation results of ACC systems (Marsden, McDonald, & Brackstone, 2001; Milanes et al., 2014).

In (Liang & Peng, 1999) the authors suggested a two-level ACC synthesis method based on optimal control theory. The upper level calculates the desired acceleration rate depending on measurements of the vehicle range (inter-vehicle distance in terms to its predecessor) and range rate (difference in the corresponding speeds), whereas the lower (servo) level deals with the accurate conversion of the higher-level acceleration command into brake or throttle commands. Given that the control signal optimises the range and range errors rate of all vehicles in a platoon, string stability is guaranteed.

In (VanderWerf, Shladover, Kourjanskaia, Miller, & Krishnan, 2001) a mathematical model that incorporates ACC functionality was developed, aiming to predict the effects of the ACC vehicles on overall traffic flow dynamics and safety. A year later this model was used to investigate the effects of different vehicle types (manually driven vehicles and ACC vehicles) on traffic flow capacity, for different market penetration rates (VanderWerf, Shladover, Miller, & Kourjanskaia, 2002). The study showed that conventional ACC systems are unlikely to have significant positive or negative effects on traffic flow.

In (Kesting, Treiber, Schönhof, & Helbing, 2008) the Intelligent Driver Model (IDM) introduced by (Treiber et al., 2000) was used as a reference for incorporating ACC behaviour in traffic flow simulations. According to the simulation results, traffic congestion was eliminated with low ACC market penetration (25%) while significant improvements in travel times were produced for much lower penetration rates (5%).

A car-following control algorithm for ACC equipped vehicles was presented in (S. Shladover, Su, & Lu, 2012). The algorithm was developed based on field data collected through experiments conducted with ACC equipped vehicles proprietary to Nissan. The authors proposed two modes in the developed ACC control algorithm: the speed control and the gap control mode. The former enables vehicles to maintain their desired free-flow speed, while the latter aims to maintain the desired gap between the controlled vehicle and the preceding one. Simulation results demonstrated that increased share of ACC vehicles in the fleet mix is unlikely to increase the capacity significantly.

Within the context of modelling vehicle automations in WP3 (Task T3.1), we integrated a car-following model reflecting ACC behaviour in the microscopic traffic simulator SUMO (Behrisch, Bieker, Erdmann, & Krajzewicz, 2011); it builds upon recent work from (Xiao et al., 2017), where an ACC simulation model originating from a commercial ACC controller (Milanes et al., 2014) was established to guarantee the full-speed range operation of ACC equipped vehicles while considering the collision avoidance constraint.

2.1.1.1.2 ACC Controller

The selected ACC driving model is based on (Liu et al., 2018; Milanés & Shladover, 2014, 2016; Milanes et al., 2014; Xiao et al., 2017), whereby the developed control law in the ACC control algorithm is explicitly divided into three modes based on three different motion purposes: (i) speed (or cruising) control, (ii) gap-closing control, and (iii) gap control. More specifically, the speed control mode is designed to maintain the by the driver chosen desired speed, the gap control mode aims to maintain a constant time gap between the controlled vehicle and its predecessor, while the gap-closing controller enables the smooth transition from speed control mode to gap control mode. In addition, TransAID has introduced a fourth mode (i.e. collision avoidance mode) to the latter controller that prevents rear-end collisions when safety critical conditions prevail. In the following text we present the basic definitions and equations for these four ACC control modes.

2.1.1.1.3 Speed Control Mode

The feedback control law in speed mode is activated when there are no preceding vehicles in the range covered by the sensors, or preceding vehicles exist in a spacing larger of 120 m (Liu et al., 2018; Xiao et al., 2017). This mode aims to eliminate the deviation between the vehicle speed and the desired speed and is given as:

$$a_{i,k+1} = k_1\left(v_d - v_{i,k}\right), k_1 > 0 \quad (1)$$

where $a_{i,k+1}$ represents the acceleration recommended by the speed control mode of the *i*-th consecutive (subject) vehicle for the next time step $k+1$; v_d and $v_{i,k}$ indicate the desired cruising speed and the speed of the *i*-th vehicle at the current time step k, respectively; k_1 is the control gain determining the rate of speed deviation for acceleration. Typical values for this gain range between $0.3 - 0.4\ \mathrm{s}^{-1}$ according to (Xiao et al., 2017); in this study we select $0.4\ \mathrm{s}^{-1}$.

2.1.1.1.4 Gap Control Mode

When the gap control mode is activated, the acceleration in the next time step $k + 1$ is modelled as a second-order transfer function based on the gap and speed deviations with respect to the preceding vehicle; it is defined as:

$$a_{i,k+1} = k_2 e_{i,k} + k_3\left(v_{i-1,k} - v_{i,k}\right), k_2, k_3 > 0 \quad (2)$$

in which $e_{i,k}$ is the gap deviation of the *i*-th consecutive vehicle at the current time step k, and $v_{i-1,k}$ is the current speed of the preceding vehicle (index $i - 1$ refers to the leader of vehicle i); k_2 and k_3 are the control gains on both the positioning and speed deviations, respectively. The proposed optimal values for the gains are $k_2 = 0.23\ \mathrm{s}^{-2}$ and $k_3 = 0.07\ \mathrm{s}^{-1}$ (Xiao et al., 2017). The gap control mode is activated when the gap and speed deviations are concurrently smaller than 0.2 m and 0.1 m/s respectively (Xiao et al., 2017).

Moreover, in this study, and following from (Milanés & Shladover, 2014, 2016; Milanes et al., 2014), the gap deviation of the *i*-th consecutive vehicle ($e_{i,k}$) is defined as:

$$e_{i,k} = x_{i-1,k} - x_{i,k} - t_d v_{i,k} \quad (3)$$

According to Equation (3), the gap deviation is calculated by the current position of the preceding vehicle $x_{i-1,k}$, the current position of the subject vehicle $x_{i,k}$, the current speed of the subject vehicle $v_{i,k}$ and the desired time gap t_d of the ACC controller.

2.1.1.1.5 Gap-closing Control Mode

The initial ACC car-following models by (Milanés & Shladover, 2016) considered the gap-closing controller, but the ACC longitudinal vehicle response under this mode was not modelled in their study. This shortcoming was overcome in (Xiao et al., 2017), where the gap-closing controller was derived by tuning the parameters of the existing gap controller. We also adopted this approach in the current study. In this case, the gap-closing control mode is triggered when the spacing to the preceding vehicle is smaller than 100 m, and the control gains of Equation (2) are set as $k_2 = 0.04\ \mathrm{s}^{-2}$ and $k_3 = 0.8\ \mathrm{s}^{-1}$. If the spacing is between 100 m and 120 m, the controlled vehicle retains the previous control strategy to provide hysteresis in the control loop and perform a smooth transfer between the two strategies (Liu et al., 2018; Xiao et al., 2017).

2.1.1.1.6 Collision Avoidance Mode

We introduced the collision avoidance mode into the ACC car-following model to prevent rear-end collisions occurring during simulations. These may be due to safety critical conditions, i.e. low time-to-collision (TTC) values, or a follower's speed significantly higher than its leader's. We derived the collision avoidance controller by tuning the parameters of the existing gap controller. It is triggered when the spacing to the preceding vehicle is smaller than 100 m, the gap deviation is negative, and the speed deviation is smaller than 0.1 m/s. In this case, the control gains of Equation (2) are set as $k_2 = 0.8\ \mathrm{s}^{-2}$ and $k_3 = 0.23\ \mathrm{s}^{-1}$ to ensure that ACC vehicles can break hard enough to avoid an imminent collision. Similar to the gap-closing control mode, the controlled vehicle retains the previous control strategy to provide hysteresis in the control loop and perform a smooth transfer between the two strategies (Liu et al., 2018; Xiao et al., 2017) if the spacing is between 100 m and 120 m.

2.1.2 Second Iteration

2.1.2.1 Cooperative Adaptive Cruise Control (CACC) Model

2.1.2.1.1 Background

CACC systems, as an extension to ACC functionality, are designed to exploit information provided by vehicle-to-vehicle (V2V) and/or vehicle-to-infrastructure (V2I) communication via wireless technology or ad-hoc networks. Thus, such enhanced systems offer high potential to further improve traffic safety and optimize traffic flow at road networks, since the CACC equipped vehicles can follow their predecessors with higher accuracy, faster response to changes, and shorter time gaps compered to ACC systems (S. Shladover et al., 2012).

Although ACC has been studied by numerous researchers in terms of traffic modelling, capacity and safety improvements, the corresponding literature pertaining to CACC is limited. The California PATH project (S. E. Shladover, 2009) described the development and implementation of CACC systems, focusing on the evaluation of driver's comfort when following a leader using different time gaps. One of the few studies that targeted this paper's area of research was by (VanderWerf, Shladover, & Miller, 2004; VanderWerf et al., 2002), which identified that CACC systems could significantly increase the capacity per lane when using time gaps as short as 0.5 seconds.

Another important study by (van Arem et al., 2006), focused on the impact of CACC equipped vehicles on traffic flow performance. The study showed that CACC vehicles have a positive impact on traffic throughput. Moreover, the highway capacity near a lane drop was increased whereas it was also revealed that the impact of a dedicated CACC lane with a penetration rate less than 40% could lead to a degradation of traffic performance.

A car-following control algorithm for CACC vehicles was also presented in (S. Shladover et al., 2012) which was actually implemented on Nissan test vehicles for field experiments. Simulation results demonstrated that at a high market penetration of CACC equipped vehicles the traffic capacity can potentially double. Based on this approach, in (Milanés & Shladover, 2014) a new control system was introduced and evaluated on four production passenger cars, equipped with CACC and dedicated short-range communication (DSRC) systems to exchange information. Real traffic scenarios, including cut-in and cut-out manoeuvres, were conducted to compare the new CACC controller with respect to the commercially available ACC system. The results revealed that CACC system can improve the response time of the following vehicle, thereby improving the string stability.

Within the context of modelling vehicle automations in WP3 (Task T3.1), we integrated a car-following model reflecting CACC traffic dynamics in the microscopic traffic simulator SUMO (Behrisch et al., 2011); it builds upon the CACC car-following model previously developed by (Milanes et al., 2014; Lin Xiao et al., 2017) where a CACC simulation model was established to guarantee the full-speed range operation of equipped vehicles while considering the collision avoidance constraint.

2.1.2.1.2 CACC Controller

The selected CACC driving model is based on (Liu et al., 2018; Milanés & Shladover, 2014, 2016; Milanes et al., 2014; Xiao et al., 2017), whereby the developed control law in the CACC control algorithm is explicitly divided into three modes based on three different motion purposes: (i) speed (or cruising) control, (ii) gap-closing control, and (iii) gap control. More specifically, the speed control mode is designed to maintain the by the driver chosen desired speed, the gap control mode

aims to maintain a constant time gap between the controlled vehicle and its predecessor, while the gap-closing controller enables the smooth transition from speed control mode to gap control mode. In addition, TransAID has introduced a fourth mode (i.e. collision avoidance mode) to the latter controller that prevents rear-end collisions when safety critical conditions prevail. In the following text we present the basic definitions and equations for these four CACC control modes.

2.1.2.1.3 Speed Control Mode

The speed controller for CACC vehicles is the same with the ACC ones since the additional information exchange between vehicles (V2V) and V2I through wireless communication does not influence the vehicle cruising mode and is triggered when the time-gap is larger than 2 s. Hence, the feedback control law in speed mode is given as:

$$a_{i,k+1} = k_1\left(v_d - v_{i,k}\right), k_4 > 0 \quad (4)$$

where the control gain k_4 is equal to 0.4 s^{-1} (Xiao et al., 2017).

2.1.2.1.4 Gap Control Mode

For the CACC car-following model, the speed of the equipped vehicles in the next time step $k + 1$ is represented by a first-order transfer function, according to:

$$v_{i,k+1} = v_{i,k} + k_5 e_{i,k} + k_6 \dot{e}_{i,k}, \quad k_5, k_6 > 0 \quad (5)$$

where $\dot{e}_{i,k}$ is the derivative of the gap deviation ($e_{i,k}$), and is defined as:

$$\dot{e}_{i,k} = v_{i-1,k} - v_{i,k} - t_d \alpha_{i,k}\,. \quad (6)$$

with t_d being the desired time gap of the CACC controller. The values of the control gains k_5 and k_6 of Equation (5) are set as 0.45 s^{-2} and 0.0125 s^{-1}, respectively (Liu et al., 2018). The gap control mode of the CACC controller is activated when the time-gap is smaller than the minimum threshold (e.g., 1.5 s in this study), and when the gap and speed deviations are concurrently smaller than 0.2 m and 0.1 m/s, respectively.

2.1.2.1.5 Gap-closing Control Mode

As in the case of ACC car-following models, the gap-closing controller was derived by tuning the parameters of the existing gap controller for CACC vehicles. Thus, for CACC car-following models the computed optimal gains of Equation (5) are $k_5 = 0.005\ s^{-2}$ and $k_6 = 0.05\ s^{-1}$ (Liu et al., 2018). This mode is triggered when the time-gap is less than the minimum threshold of 1.5 s. If the time-gap is between the maximum and minimum thresholds, the controlled vehicle retains the control mode implemented during the previous time step (either speed or gap-closing control mode). This introduces hysteresis in the control loop and the CACC controller can perform a smooth transfer between the speed and gap control mode (Liu et al., 2018; Xiao et al., 2017).

2.1.2.1.6 Collision Avoidance Mode

We also introduced the collision avoidance mode into the CACC car-following model to prevent rear-end collisions occurring during simulations. These may be due to safety critical conditions, i.e. low time-to-collision (TTC) values, or a follower's speed significantly higher than its leader's. We derived the collision avoidance controller by tuning the parameters of the existing gap controller. Hence, the collision avoidance mode is activated when the time-gap is less than 1.5 s and the gap

deviation is negative, while the computed optimal control gains of Equation (5) are $k_5 = 0.45\ s^{-2}$ and $k_6 = 0.05\ s^{-1}$.

2.2 (C)AV/CV Lane Change Model

2.2.1 First Iteration

2.2.1.1 Parametrisation of SUMO Lane Change Model (LC2013)

In TransAID we develop driver models for (C)AVs/CVs in SUMO to reflect their car-following and lane-change behaviour. SUMO's inherent default lane change model (i.e. the LC2013 model) was developed to mimic the lane change behaviour of LVs. It is a sophisticated model that accounts for lane changes due to different reasons (i.e. strategic, cooperative, tactical, right-of-way, etc.) and assesses the feasibility of lane changes based on traffic conditions in the surrounding LV road environment. However, (C)AVs/CVs are expected to deviate from human lane change behaviour due to the capabilities of automated driving systems. Currently, the lane change behaviour of CAVs/CVs is OEM-specific.

Parametrisation of the SUMO LC2013 model is an approach that can render the model capable to mimic the lane change behaviour of (C)AVs/CVs in SUMO. Within the context of TransAID the LC2013 lane-change model is parametrized to reflect (C)AVs/CVs lane-change behaviour based on information provided by Hyundai Motor Europe Technical Center (HMETC). The parametrisation process encompasses the adjustment of SUMO's lane change calibration parameters to attain the desired lane change behaviour in terms of SUMO lane change output **(Table 1)**.

Table 1. SUMO lane change output.

Name	Description
id	The id of the vehicle.
type	The type id of the vehicle.
time	The time at which the change took place.
from	The id of the source lane.
to	The id of the destination lane.
pos	The position where the lane-change took place (offset from lane start).
reason	The reason for changing.
dir	The direction of the change (difference in lane indices when staying within one edge).
speed	The current speed of the vehicle.
leaderGap	The longitudinal gap to the nearest leader in the target lane (bumper to bumper) or 'None' if there was no leader.
leaderSecureGap	The required longitudinal gap to the nearest leader to fulfil deceleration constraints or 'None' if there was no leader.
followerGap	The longitudinal gap to the nearest follower in the target lane (bumper to bumper) or 'None' if there was no follower.

followerSecureGap	The required longitudinal gap to the nearest follower to fulfil deceleration constraints or 'None' if there was no follower.
origLeaderGap	The longitudinal gap to the nearest leader on the vehicle's original lane (bumper to bumper) or 'None' if there was no leader.
origLeaderSecureGap	The required longitudinal gap to the nearest leader to fulfil deceleration constraints or 'None' if there was no leader.

The accomplishment of the parametrisation task presumes:

1. Knowledge regarding the logic of the LC2013 model.
2. Information about the lane change behaviour of (C)AVs/CVs in the real world.

The latter information has to be translated into SUMO lane change output for the effective LC2013 model parametrisation. To this end, HMETC provided information with respect to (C)AVs/CVs desired lane change gaps for two specific speed ranges ($0 - 30$ km/h & $30 - 60$ km/h) based on the behaviour of their test vehicles (automation ready).

2.2.1.2 Overview of LC2013 Model

A description of the LC2013 model is provided subsequently, encompassing the model's logic for determining the intention to change lanes (cf. strategic, cooperative, tactical, right-of-way, etc.).

2.2.1.2.1 Lane Change Intention

The LC2013 model considers three main reasons (strategic, cooperative, and tactical) for changing lanes (either right or left) per simulation time step. The ego vehicle initially checks if a right lane change is mandatory[1] or desired based on the logic depicted in **Figure 1**. If a right lane change is not mandatory or desired, a left lane change motivation is determined based on the same rules.

[1] Hence, we assume traffic laws dictating right-hand driving, with overtaking/passing mandatory on the left side.

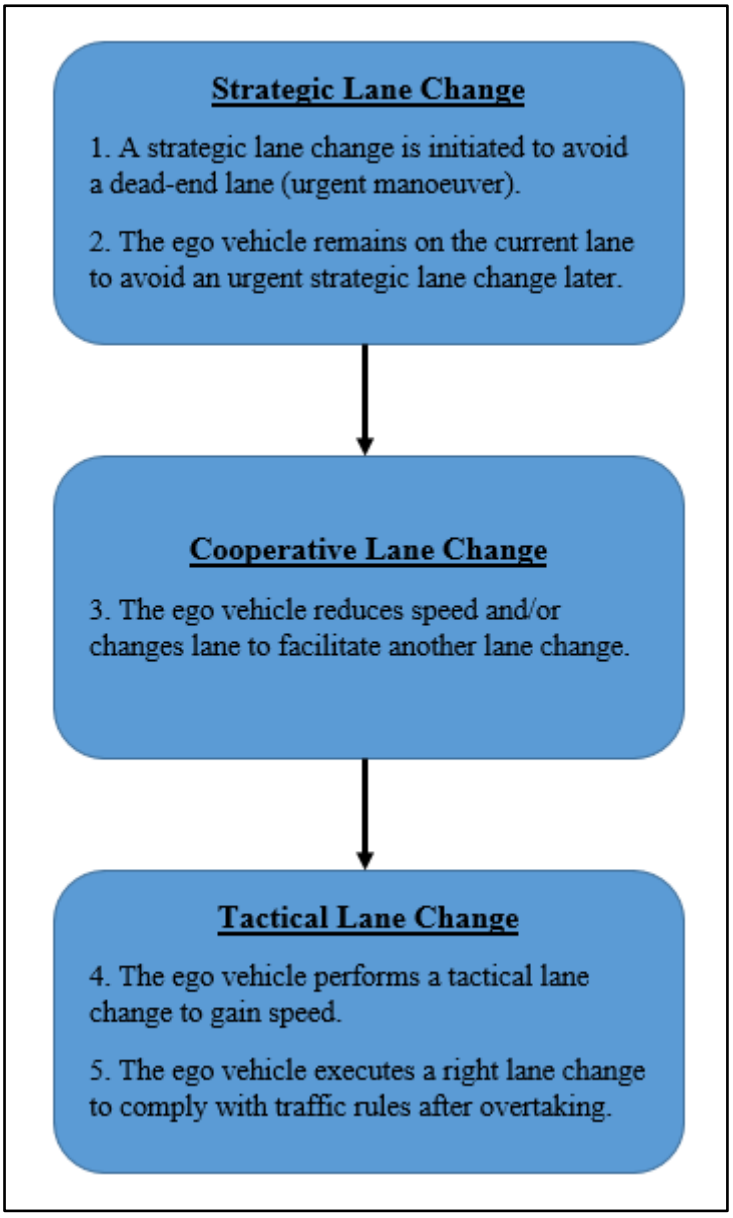

Figure 1. Hierarchy of lane change logic.

Strategic Lane Changes

An ego vehicle approaching a dead-end lane might stay in the strategically advisable lane (if it is already travelling on it), or it might change lanes to the strategically advisable lane (if it is driving in a dead-end lane). The urgency for initiating a strategic lane change manoeuvre is related to the following factors **(Table 2)**:

Table 2. SUMO parameters related to urgency for strategic lane-changing.

Parameter Name	Parameter Description
myLookAheadSpeed (mLAS)	Virtual speed, used to calculate the ideal distance required for the execution of a lane change manoeuvre. It is increasing proportionally to the ego vehicle's current speed. It decays slowly with decreasing vehicle speed, to stimulate an urgent lane change from the ego vehicle.

bestLaneOffset (bLO)	Indicates the number of lane changes required by the ego vehicle to reach an advisable lane. The higher the value the more lanes the ego vehicle should change to continue along its desired path.
miniGap (MG)	Safe bumper-to-bumper vehicle distance at standstill.
laneOccupation (Occ)	The occupied space in a lane by all vehicles (including their miniGap) downstream of the ego vehicle.
freeSpace (FS)	The available free space on a lane downstream of the ego vehicle.
usableDist	The available distance on a dead-end lane where the ego vehicle can drive unimpeded at its desired speed.
laDist	The ideal longitudinal distance for the ego vehicle to execute a lane change manoeuvre.

A physical representation of parameters MG, Occ, FS, and $usableDist$ is depicted in Figure 2.

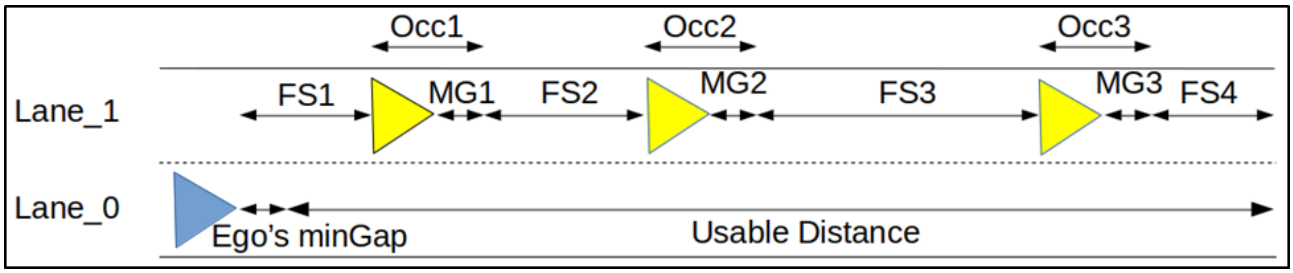

Figure 2. Physical representation of parameters MG, Occ, FS, and $usableDist$.

A strategic lane change manoeuvre is urgent when the available distance is lesser than the ideal:

$$usableDist < laDist \Leftrightarrow RD - Occ < mLAS \times |bLO| \times f \quad (4)$$

where parameters $mLAS$, bLO, and Occ are defined in **Table 2**, RD is the remaining distance between the ego vehicle and the lane end, and f is a factor that encodes the time typically needed to perform a successful change manoeuvre (set to 10 s for right lane changes to right and to 20 s for left lane changes).

The relationship between parameters $usableDist$ and $laDist$ is illustrated for two different cases. One that encompasses an ego vehicle target lane that is free **(Figure 3)**, and one where the ego vehicle target lane is occupied by other vehicles **(Figure 4)**. In **Figure 3a** an ego vehicle travels unimpeded on a dead-end lane. The vehicle approaches the end of the lane (**Figure 3b)** and is not changing lane unless the ideal distance to change lanes is shorter than the available ($usableDist < laDist$) **(Figure 3c)**. If the target lane is occupied by other vehicles, then the free space on the target lane ($usableDist$) is reduced based on the occupation length of each vehicle **(Figure 4)**.

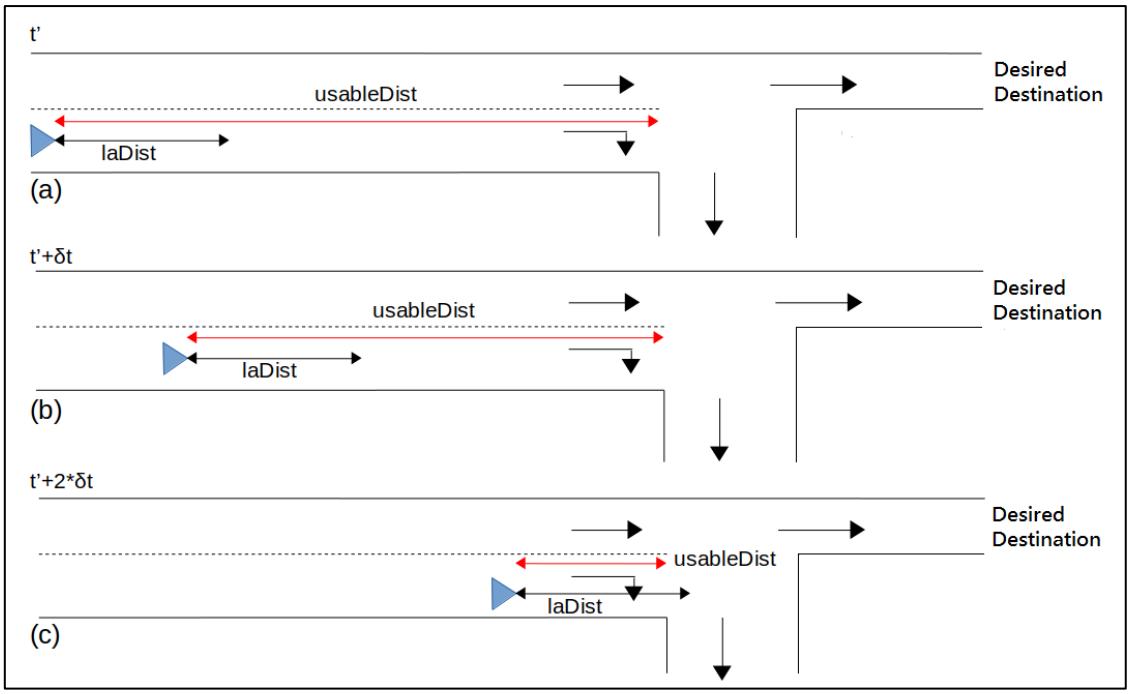

Figure 3. (a) The ego vehicle travels at constant speed on a dead-end lane. **(b)** The available distance on the target lane decreases as the ego vehicle drives towards the dead-end lane. **(c)** The ego vehicle initiates a lane change manoeuvre to the target lane when its ideal distance to perform a lane change ($laDist$) is shorter compared to the available distance on the target lane ($usableDist$).

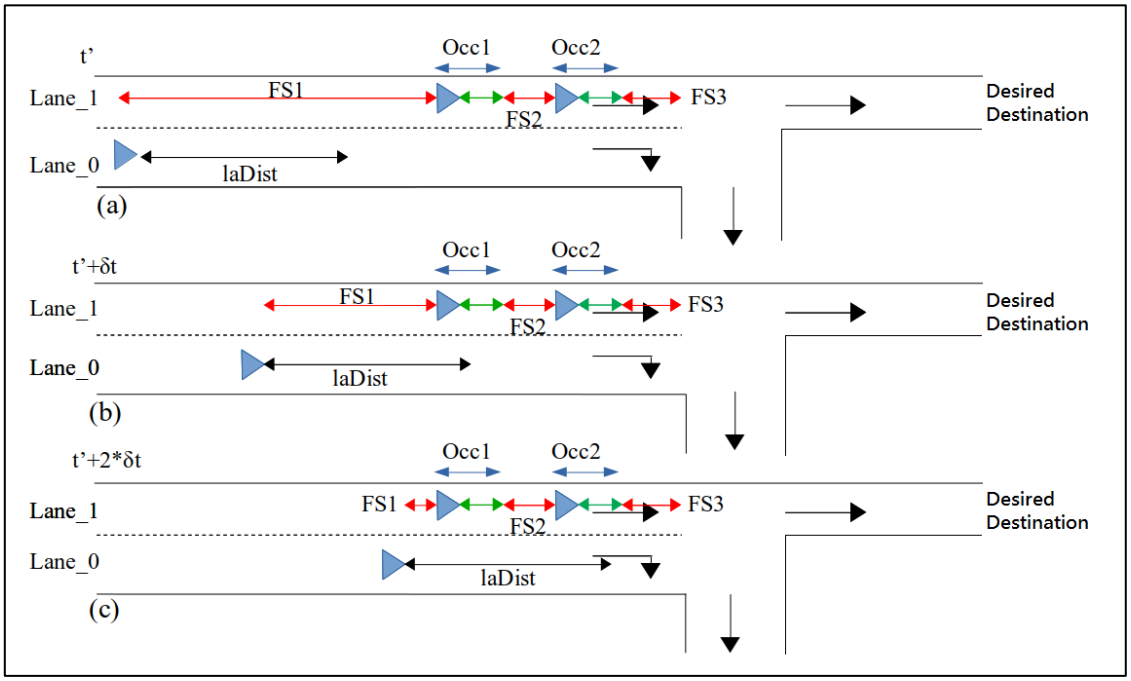

Figure 4. (a) The ego vehicle travels on a dead-end lane and the target lane is partially occupied by other vehicles. **(b)** The available distance for a lane change manoeuvre on the target lane is affected by the presence of other vehicles. **(c)** The ego vehicle performs a lane change when its ideal distance for performing a lane change is lesser than the available free space ($usableDist = FS1 + FS2 + FS3$) on the target lane.

Strategic lane changes might be executed as a consequence of preceding tactical lane changes. Namely, if the ego vehicle performs a lane change for tactical reasons, it might enter into an undesired situation where it will have to execute a strategic lane change manoeuvre soon to avoid a dead-end lane. In this case, the ego vehicle might lose the speed advantage that it gained due to the latter tactical lane change and be finally significantly delayed. Therefore, it would be best in this situation if the ego vehicle stays in the current lane and does not perform a tactical lane change.

Whenever the ego vehicle considers shifting away from the lane with the $bestLaneOffset$, the LC2013 model assesses if the free space on the target lane is sufficient for the imminent strategic lane change. In these cases, the LC2013 model assesses the following inequality to decide upon the feasibility of the tactical lane change:

$$2 \times laDist < neighLeftPlace \quad (5)$$

where $neighLeftPlace$ is the total free space, that the ego vehicle can use on the target dead-end lane to perform a strategic lane change. If the total free space ($neighLeftPlace$) is less than twice the desired distance to change lanes ($laDist$), the ego vehicle will stay in its current lane.

In **Figure 5a** the ego vehicle should stay in Lane_1 in order to reach its desired destination since $2 \times laDist > FS1 + FS2$. However, if the opposite was true and the vehicle could perform a tactical lane change **(Figure 5b),** then it would have to return to Lane_1 based on the aforementioned strategic lane change logic.

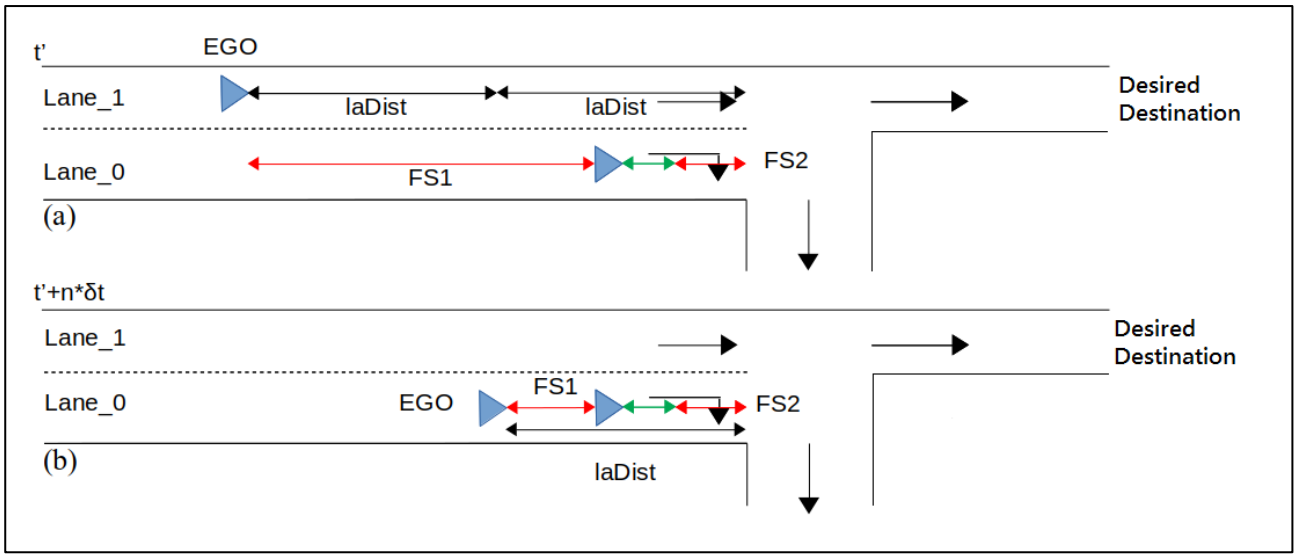

Figure 5. (a) The ego vehicle stays on the current lane since the free space on the neighbouring lane is insufficient to let it move back and forth. **(b)** The ego vehicle has shifted to the dead-end lane and will return based on the strategic lane change logic.

Cooperative Lane Changes

Vehicles also perform cooperative lane changes to facilitate nearby vehicles moving into their desired lanes. When the ego vehicle blocks a nearby vehicle and there are no strategic constraints against lane-changing, the ego vehicle may change lanes to create a gap for the blocked vehicle. Ego vehicles that cannot perform a cooperative lane change manoeuvre may adjust their speed to increase the probability of a successful lane change from a vehicle in a neighbouring lane. However, the ego vehicle shall not adjust speed if leading or following vehicles in the same lane are blocking it.

Tactical Lane Changes

Tactical lane changes take place for speed gains when the ego vehicle is blocked by a slower leader. The decision to execute a tactical lane-change is based on the expected speed gains. Keeping the overtaking lane free (keep right rule) should also be considered apart from the expected speed gains when performing a tactical lane change. Otherwise, slow moving vehicles with minor speed differences might significantly impede traffic flow.

The probability of a tactical lane change (right or left), is reflected by the parameter $speedGainProbability$ for each vehicle. If the magnitude of this parameter exceeds a pre-specified threshold value ($speedGainProbabilityRight$ for right lane changes and $speedGainProbabilityLeft$ for left lane changes), a tactical lane change is desired. The relative gain for moving to the target lane (right or left) is calculated as the relative difference between the expected ego speed for moving to the candidate lane and the expected ego speed for remaining in the current lane:

$$rg = \frac{(neighV - defaultV)}{neighV} \tag{6}$$

where rg is the relative gain from the tactical lane change, $neighV$ is the expected (virtual) ego vehicle speed for moving to the candidate lane, and $defaultV$ is the expected ego speed for remaining in the current lane.

The parameter $speedGainProbability$ is updated per time step based on the estimated relative gain:

$$speedGainProbability = speedGainProbability + rg \times timeStep \tag{7}$$

where $timeStep$ is the time interval between consecutive simulation steps.

If the relative gain is less than a pre-specified threshold value the $speedGainProbability$ value decays. A small relative gain or a negative one indicates that a lane change manoeuvre towards the candidate lane will not only prevent an ego vehicle from increasing speed, but it may finally slow it down. In these cases, $speedGainProbability$ decays according to **Equation 8**:

$$speedGainPobability = speedGainProbability \times SPEEDGAIN\_DECAY\_FACTOR^{timeStep} \tag{8}$$

where $SPEEDGAIN\_DECAY\_FACTOR$ is a factor that indicates the rate of $speedGainProbability$ decay.

In **Figure 2.6**, a heavy vehicle (bus) is preceding a passenger car in Lane_0 and its desired speed is lower than the passenger car's speed. The passenger car is in car-following mode and adjusts its speed based on the actions of the bus. However, since Lane_1 is free, the relative gain for a left lane change is high and $speedGainProbability$ increases until it exceeds $speedGainProbabilityLeft$ and the ego vehicle performs the lane change manoeuvre.

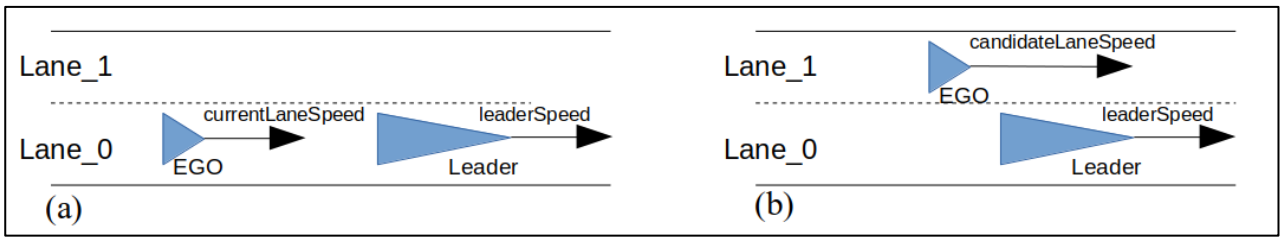

Figure 6. (a) The ego vehicle is in the car-following mode behind a bus. **(b)** The ego vehicle performs a tactical lane-change to gain speed.

However, if a slow-moving leading vehicle exists on Lane_1 as well **(Figure 7)**, then the relative gain for a left lane change will be small and thus the ego vehicle will gain no advantage if it makes a left lane change.

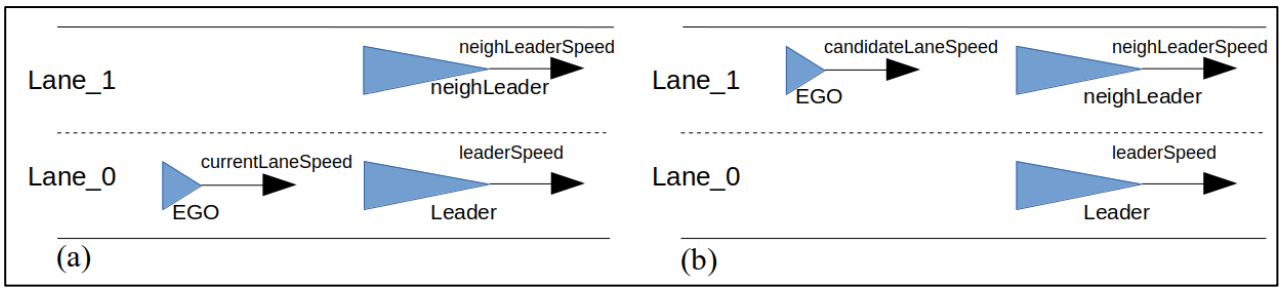

Figure 7. (a) The ego vehicle's speed is impeded by the leader in Lane_0. **(b)** The ego vehicle will be impeded by the leader in the neighbouring lane if it performs a left lane change to Lane_1.

The lane change model initially examines if a right lane change manoeuvre is necessary, after which it investigates whether a left lane change is beneficial. The obligation to clear the overtaking lane is mandatory due to traffic regulations. The probability to make a right lane change after an overtaking manoeuvre is determined by the parameter $keepRightProbability$. When it exceeds a pre-specified threshold value, a right lane change is initiated **(Figure 8)**. The threshold value is the maximum between the value of a constant pre-set parameter $myChangeProbabilityThresholdRight$, and $speedGainProbabilityLeft$. Namely, if the ego vehicle gains speed advantage by traveling on the left lane compared to clearing the overtaking lane by making a right lane change, it will keep on travelling in the left lane.

The ego vehicle determines if an overtaking manoeuvre is advantageous in terms of speed gains based on the gap and speed difference to the leading vehicle on the right. The parameter $keepRightProbability$ is updated accordingly:

$$keepRightProbability = keepRightProbability + \frac{(t \times lV)}{(Vmax \times currentV \times T)} \qquad (9)$$

where, lV is the legal speed limit for the current lane, $Vmax$ is the maximum desired speed of the ego vehicle, $currentV$ is the ego vehicle's current speed, T is a calibration parameter set equal to 7 s, and t is the time interval that the ego vehicle can drive at its maximum desired speed in the right lane prior to an overtaking manoeuvre.

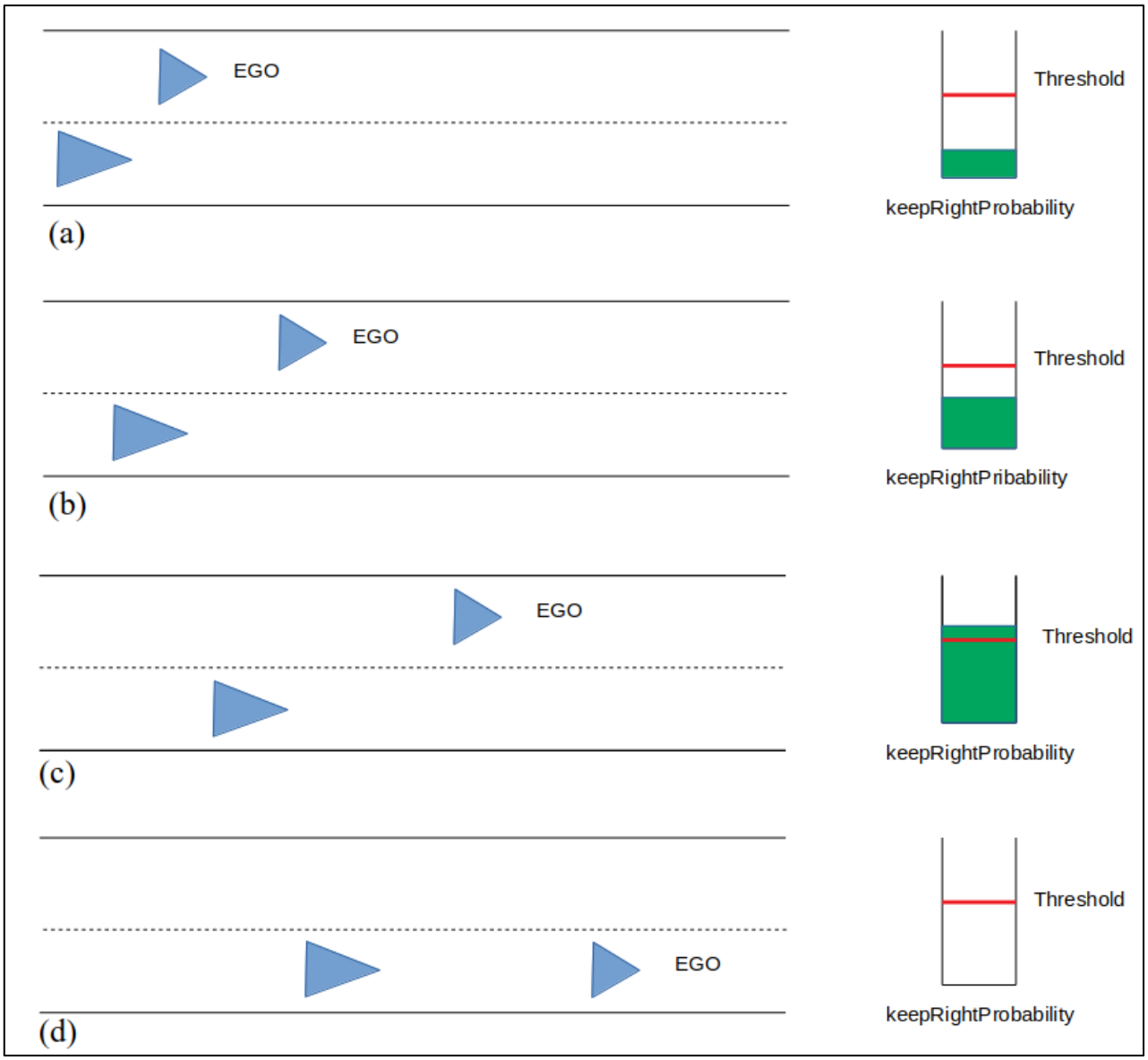

Figure 8. (a) The ego vehicle performed a lane change and is overtaking its previous leader ($keepRightProbability$ is low). **(b)** The ego vehicle has overtaken its previous leader and accelerates to merge safely into the right-most lane ($keepRightProbability$ close to the threshold value). **(c)** The ego vehicle can merge safely into the right-most lane ($keepRightProbability$ exceeded the threshold value). **(d)** The ego vehicle has merged into the right-most lane ($keepRightProbability$ is set equal to zero).

2.2.1.3 Sensitivity Analysis of LC2013 Model

2.2.1.3.1 Introduction

We conducted a sensitivity analysis to facilitate the parametrisation of the LC2013 model for the emulation of (C)AVs/CVs lane change behaviour in SUMO. The sensitivity analysis examines the behaviour of the LC2013 model by identifying the calibration parameters that exhibit the highest impact on its performance. Lane change outputs **(Table 1)** are mapped for predefined calibration parameter spaces and compared to actual (C)AV/CV lane change data to determine the parameters values that demonstrate the desired model behaviour.

A sensitivity analysis investigates the relationships between inputs and outputs of highly complex mathematical models or systems. It studies the uncertainty in the output of the mathematical model or system as a function of the uncertainty in the inputs. There are many available techniques that can be used to examine the sensitivity of a model. Typical techniques are: (i) one-at-a-time (OAT/OFAT), (ii) local methods, (iii) regression analysis, (iv) variance-based methods, (v) Monte Carlo filtering, and (vi) meta-modelling. Comprehensive information about sensitivity analysis can be found in (Saltelli, 2008; Saltelli et al., 2002), which are the main sources used in this study.

In microscopic traffic simulation modelling, sensitivity analysis was mainly used to analyse car-following models. A one-dimensional scan of the Intelligent Driver Model (IDM) and Velocity Difference (VDIFF) car-following model parameters was conducted to assess the models' parameter properties and sensitivity (Kesting & Treiber, 2008). Variance-based sensitivity analysis was applied to the IDM and the Gipps model to identify model parameters that highly contribute to the output uncertainty and thus need to be calibrated (Punzo & Ciuffo, 2011). The Monte Carlo framework was redesigned for variance-based sensitivity analysis of car-following models to estimate the least number of parameters required for credibly replicating actual car-following behaviour (Punzo, Montanino, & Ciuffo, 2015).

This study also applies variance-based sensitivity analysis to analyse the LC2013 model. Variance-based sensitivity analysis is a global sensitivity analysis method (measures sensitivity across the whole input space). It can apportion the variance in the output of a mathematical model or system to inputs or input sets (interaction between inputs is accounted for). For instance, assuming a model with two inputs and one output, the method can determine that x % of the output variance is attributed to the first input, y % to the second, and z % due to the interaction between the two (percentages can be read are measures of sensitivity). Finally, variance-based sensitivity analysis can be applied to nonlinear and non-additive systems.

2.2.1.3.2 Variance-based sensitivity analysis

The sensitivity analysis method used in this study was initially introduced by (Cukier, Fortuin, Shuler, Petschek, & Schaibly, 1973), generalised by (Sobol, 1993; Sobol et al., 2007) with a Monte Carlo-based implementation of the concept, and then improved by (Saltelli et al., 2010) to increase computational efficiency. The existing literature on the topic (Saltelli, 2008; Saltelli et al., 2010, 2002) shows that variance-based methods can overcome the limitations of most commonly used methods, such as OAT/OFAT analysis, local methods, and regression analysis.

This method assumes that variance can credibly represent uncertainty in the outputs and is based on the variance decomposition formula. For a model $Y = f(X_1, X_2, \dots, X_k)$, where $X_i \; \forall i \in [1, k]$ are the input stochastic variables, called $factors$, and Y is the output stochastic variable, the variance of the model can be decomposed as:

$$V(Y) = V_{X_i}\left(E_{\bar{X}_{\sim i}}(Y|X_i)\right) + E_{X_i}\left(V_{\bar{X}_{\sim i}}(Y|X_i)\right) \tag{10}$$

where X_i is the *i*-th factor, and $\bar{X}_{\sim i}$ denotes the vector of all factors but X_i.

The first component $V_{X_i}\left(E_{\bar{X}_{\sim i}}(Y|X_i)\right)$ is called the "main (or first-order) effect" of X_i. The associated sensitivity measure S_i, called the "first-order sensitivity index" is equal to the first-order effect normalised over the total (or unconditional) variance:

$$S_i = \frac{V_{X_i}\left(E_{\bar{X}_{\sim i}}(Y|X_i)\right)}{V(Y)} \tag{11}$$

It can be explained as the portion of the output variance that is only ascribed to the variation of the input factor X_i. Thus, the first order sensitivity index captures only the effect of a single input factor to the model output. However, for non-additive models, the input factor X_i affects the output variance also when interacting with other input factors. Namely, the joint variation of X_i with all (or some of) the input factors may influence the variation of the output. This influence is called the interaction (or higher order) effect related to X_i. The sum of the first-order and higher order effects for all the input factors explains all the output variance. Therefore, when the terms are normalised over the unconditional variance, such summation is equal to 1:

$$\sum_{i=1}^{k} S_i + \sum_{i=1}^{k}\sum_{\substack{j=1 \\ j\neq i}}^{k} S_{i,j} + \sum_{i=1}^{k}\sum_{\substack{j=1 \\ j\neq i}}^{k}\sum_{\substack{l=1 \\ l\neq\{i,j\}}}^{k} S_{i,j,l} + \cdots + \sum_{i=1}^{k}\sum_{\substack{j=1 \\ j\neq i}}^{k} \dots \sum_{\substack{m=1 \\ m\neq\{i,\dots\}}}^{k} S_{i,j,\dots,m} = 1 \qquad (12)$$

where $\sum_{i=1}^{k} S_i$ is the contribution of all the main effects, whereas $1 - \sum_{i=1}^{k} S_i$ is the contribution of all the interaction effects across all the input factors. It is worth noting that in the case of the additive models, there are no interaction effects and $\sum_{i=1}^{k} S_i = 1$, whereas in the case of non-additive models, it results in $\sum_{i=1}^{k} S_i < 1$.

Based on the latter decomposition, the number of higher order effects to calculate would be very high, i.e. $2^k - 1 - k$, with k being the number of factors. Thus, to estimate the total effect of a factor, the "total sensitivity index" is introduced:

$$ST_i = \frac{E_{\bar{X}_{\sim i}}\left(V_{X_i}(Y|\bar{X}_{\sim i})\right)}{V(Y)} = 1 - \frac{V_{\bar{X}_{\sim i}}\left(E_{X_i}(Y|\bar{X}_{\sim i})\right)}{V(Y)} \qquad (13)$$

which is the sum of the first-order effect of X_i and of all the higher order effects that involve X_i. Since higher order effects are computed more times, i.e. in the ST of each factor involved in the interaction (e.g. $S_{i,j} = S_{j,i}$ in both ST_i and ST_j), it results in $\sum_{i=1}^{k} S_i \geq 1$, where the equality holds only for perfectly additive models (for which $S_i = ST_i, \forall\, i = 1, \dots, k$).

According to the aforementioned methodology, it becomes evident that the total sensitivity index is the appropriate measure to identify the factors that significantly influence the output variance. Indeed, $ST_i = 0$ is a necessary and sufficient condition for X_i to be non-influential.

2.2.1.3.3 Application and Results

The LC2013 model encompasses seven calibration parameters that can be modified to alter lane change behaviour in SUMO. Four of these parameters **(Table 2)** were finally analysed within the context of the current sensitivity analysis, per advice of the LC2013 model developers (DLR), based on the parameters' expected influence on the model output. The simulation network of Scenario 2.1 (Prevent ToC/MRM by providing speed, headway, and/or lane advice) was used for the sensitivity analysis, which is a typical motorway merge section where lane changes occur for all the possible reasons considered by the LC2013 model:

- Strategic (on-ramp vehicles to enter the mainline lanes)
- Cooperative (mainline vehicles facilitate on-ramp vehicles' lane changes)
- Tactical (both mainline and on-ramp vehicles to gain speed advantage)
- Right-of-way (both mainline and on-ramp vehicles due to the obligation to keep right)

Thus, the effects of the different calibration parameters on the lane change output can be effectively captured, since a significant number of lane changes will be executed for each reason.

Table 2. LC2013 model calibration parameters encompassed in sensitivity analysis.

Parameter Name	Parameter Definition	Input Range
lcStrategic	The eagerness for performing strategic lane-changing. Higher values result in earlier lane-changing.	[0, inf)
lcKeepRight	The eagerness for following the obligation to keep right. Higher values result in earlier lane-changing.	[0, inf)
lcSpeedGain	The eagerness for performing lane-changing to gain speed. Higher values result in more lane-changing.	[0, inf)
lcAssertive	Willingness to accept lower front and rear gaps on the target lane. The required gap is divided by this value.	Positive reals

The sensitivity analysis was conducted using the SALib library (open source Python library for performing sensitivity analysis). SALib offers a decoupled workflow (it does not directly interface with the mathematical or computational model), where sample functions generate the model inputs, and analyse functions compute the sensitivity indices.

Input samples are generated using a quasi-random sampling technique with low discrepancy sequences (the so-called Sobol's sequences), guaranteeing faster convergence for the indices calculation than other sampling strategies (Saltelli et al., 2010). The generated samples are iteratively input into SUMO and the model is run for the estimation of the lane change output. The first-order and total sensitivity indices are computed for the following lane change output:

- Safe longitudinal gap to leading vehicle in the ego lane ($origLeaderSecureGap$).
- Safe longitudinal gap to leading vehicle in the target lane ($leaderSecureGap$).
- Safe longitudinal gap to following vehicle in the target lane ($followerSecureGap$).

Safe longitudinal gaps to surrounding vehicles for an ego vehicle that is initiating a lane change manoeuvre are depicted in **Figure 11**.

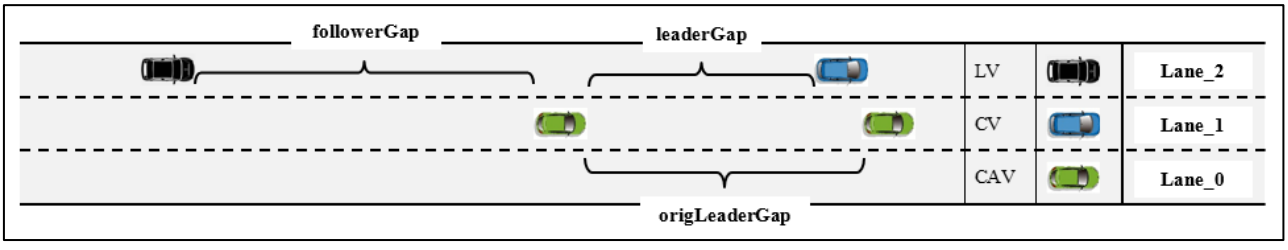

Figure 11. Illustration of SUMO lane change output.

The latter lane change outputs (per input sample) are loaded into SALib, and the corresponding sensitivity indices are estimated per examined model output. The formulas for the estimation of the first-order and total sensitivity indices are obtained by (Saltelli et al., 2010). The values of the first-order (S_i) and total (ST_i) sensitivity indices for the aforementioned lane change output are presented in **Table 3**. Previously it was shown that an appropriate measure for identifying the non-influential parameters is the "total sensitivity index" ST_i, and that $ST_i = 0$ is both necessary and sufficient for the factor X_i to be non-influential. However, in practical applications, a threshold on

ST_i higher than zero is generally set, under which the parameter is considered non-influential (Punzo et al., 2015). In this study, we considered a value of 5% as an acceptable threshold.

Therefore, it becomes clear that the $lcStrategic$ parameter has very limited influence on the output unconditional variance, since ST_i is less than 5 % for all the examined output. The $lcKeepRight$ parameter is only influential for the safe longitudinal gaps between the leading vehicle in the target lane and the ego vehicle. However, since it does not affect the other two types of gaps considered prior to lane-changing, and the ST_i value is close to the specified threshold ($ST_i = 7.57$), this calibration parameter is also fixed in its default value ($lcKeepRight = 1.0$) for the baseline simulations experiments. The $lcSpeedGain$ parameter is found to be influential for two model outputs (the safe gap to leading vehicle in the current lane, and the safe gap to the leading vehicle in the target lane). For the first model output $ST_i = 8.12$, while for the second $ST_i = 22.26$ (i.e. $lcSpeedGain$ is influencing gaps to leading vehicles on the target lane more). Nonetheless, the first-order sensitivity indices are very low for $lcStrategic$, $lcKeepRight$, and $lcSpeedGain$, while being very high for $lcAssertive$. Thus, it is implied that high ST_i values for $lcSpeedGain$ can be ascribed to its interaction with $lcAssertive$. According to the aforementioned considerations, the calibration parameter $lcAssertive$ is explicitly adjusted for the parametrisation of the LC2013 model to reflect (C)AV/CV lane change behaviour.

Table 3. First-order and total sensitivity indexes per calibration parameter and lane change output.

Speed Range [0, 100] (km/h)						
Parameter	**Leader gap (ego lane)**		**Leader gap (target lane)**		**Follower gap (target lane)**	
Sensitivity Index	S_i [%]	ST_i [%]	S_i [%]	ST_i [%]	S_i [%]	ST_i [%]
lcStrategic	0.39	0.62	0.74	2.62	1.14	0.47
lcKeepRight	1.08	0.83	3.32	7.57	1.13	2.26
lcSpeedGain	0.90	8.12	10.92	22.26	0.77	1.37
lcAssertive	59.15	77.03	61.26	80.17	91.40	95.56

The LC2013 model behaviour is mapped (in terms of the aforementioned lane change output) for different values of the $lcAssertive$ parameter. However, information about the actual (C)AV/CV desired gaps (with surrounding vehicles) for lane-changing is necessary, so that it can be compared with the lane change output for different values of $lcAssertive$. Thus, scanning the parameter space of the $lcAssertive$ calibration parameter and comparing against actual lane change data, renders the selection of the $lcAssertive$ values that reproduce the actual (C)AV/CV lane change behaviour feasible. Moreover, we must consider the fact that desired gaps for lane change are a function of the ego vehicle's current speed and its relative speed with its surrounding vehicles that affect the lane change manoeuvre (leader in the current lane, leader in the target lane, and follower in the target lane). Given the latter consideration, actual lane change data for (C)AVs/CVs were provided by HMETC for the parametrisation of the LC2103 model. These data correspond to two different speed ranges ($0 - 30$ km/h, and $30 - 60$ km/h), and represent highly conservative lane change behaviour as stressed by HMETC **(Table 4 – 5)**. This information was used to select appropriate values for the $lcAssertive$ parameter.

Table 4. OEM proposed minimum longitudinal gaps for CAV/CV lane-changing (0 – 30 km/h).

Speed Range (0, 30] (km/h)		
Subject Vehicle	**Relative Speed** $(v_{ego} - v_{obstacle})$	**Desired Gaps [m]**
Leader gap (ego lane)	Positive	22
	Neutral	< 22
	Negative	< 22
Leader gap (target lane)	Positive	17
	Neutral	15
	Negative	< 15
Follower gap (target lane)	Positive	7
	Neutral	20
	Negative	44

Table 5. OEM proposed minimum longitudinal gaps for CAV/CV lane-changing (30 – 60 km/h).

Speed Range (30, 60] (km/h)		
Subject Vehicle	**Relative Speed** $(v_{ego} - v_{obstacle})$	**Desired Gaps [m]**
Leader gap (ego lane)	Positive	50
	Neutral	< 50
	Negative	< 50
Leader gap (target lane)	Positive	35
	Neutral	30
	Negative	< 30
Follower gap (target lane)	Positive	20
	Neutral	44
	Negative	70

Lane change outputs are mapped for $lcAssertive = \{0.5, 0.7, 0.9\}$ and relative speeds of $\pm 5.0\ km/h$. Desired safe gaps for lane-changing increase linearly with vehicle speed, while OEM proposed gaps appear as vertical lines since they are constant within the aforementioned speed ranges **(Figures 10 – 12)**. Desired gaps to the follower in the target lane are shorter compared to the OEM proposed ones for all the tested $lcAssertive$ values and negative relative speed. On the contrary, they are larger for positive relative speeds. Thus, the model behaviour is aggressive compared to the OEM proposed gaps for negative relative speeds, but is conservative for positive relative speeds.

The latter behaviour is not observed though for the other two types of gaps considered in this study (distance to the leader in the current and the target lane). With respect to longitudinal gaps between the ego vehicle and the target leader, $lcAssertive = 0.7$ reproduces actual vehicle behaviour at 30 km/h and 60 km/h respectively (desired gaps coincide at the upper bounds of the speed ranges, and it is reasonable to assume that they would decrease at speeds lower than 30 km/h and 60 km/h). For longitudinal gaps between the ego vehicle and the current leader, $lcAssertive = 0.9$ better emulates LC2013 model behaviour with actual vehicle behaviour.

The LC2013 model does not encompass a calibration parameter that can affect different longitudinal gap types (ego vehicle to target leader, current leader, and target follower) separately. Thus, if a calibration parameter is scaled, then all different gaps considered by the model for the lane change manoeuvre execution are scaled as well. Moreover, no existing calibration parameter can scale desired gaps explicitly for negative or positive relative speeds (even when considering only one type of gap). Therefore, adjusting $lcAssertive$ and/or other calibration parameters to reproduce the given actual (C)AV/CV lane change behaviour in this study is not a possibility according to the current model structure. As a result, the aforementioned $lcAssertive$ values that can replicate OEM proposed behaviour for different types of gaps are used for the baseline simulation experiments.

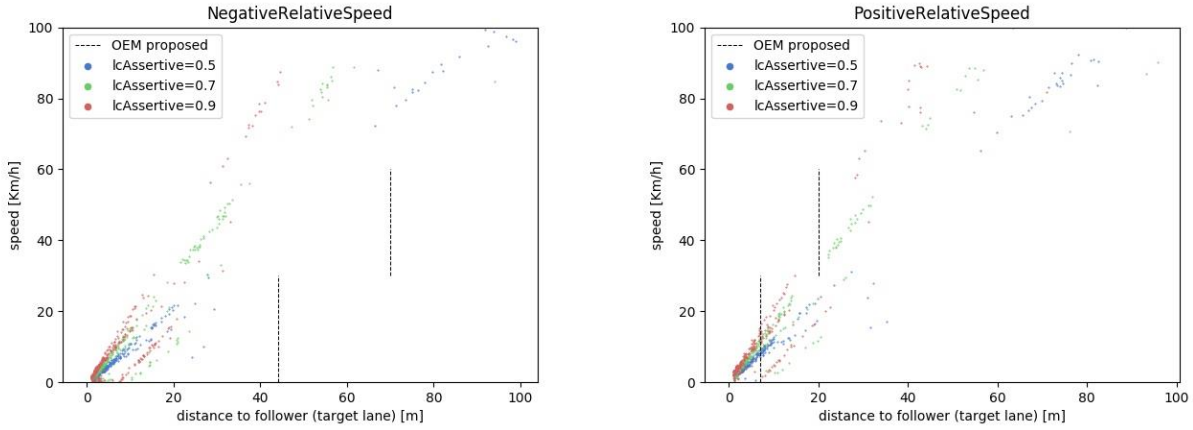

Figure 10. Safe longitudinal gaps to follower (target lane) for different values of $lcAssertive$.

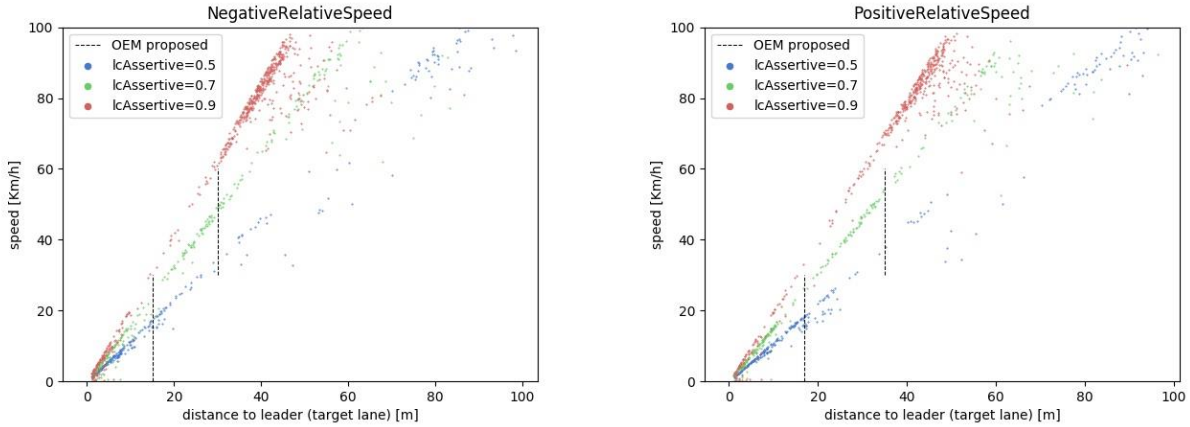

Figure 11. Safe longitudinal gaps to leader (target lane) for different values of $lcAssertive$.

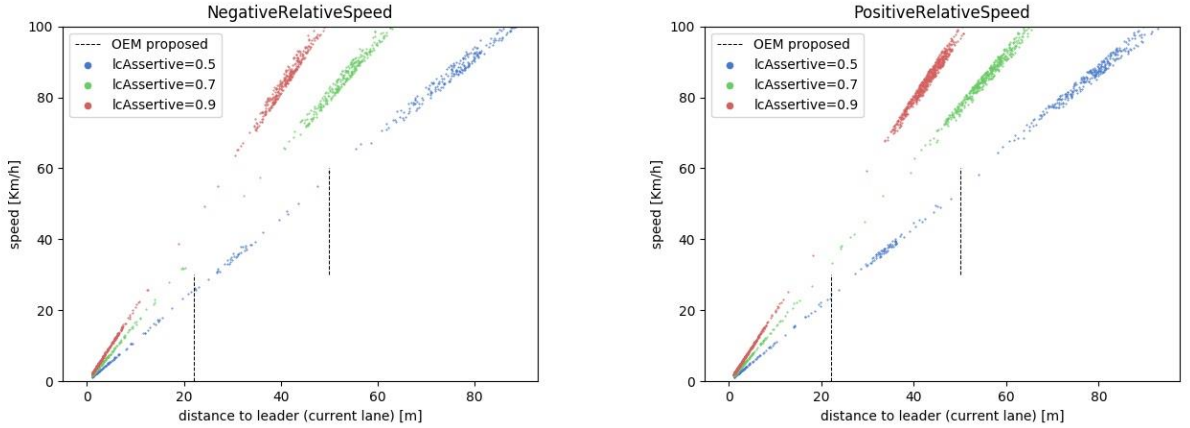

Figure 12. Safe longitudinal gaps to leader (ego lane) for different values of $lcAssertive$.

2.2.2 Second Iteration

2.2.2.1 Revisiting the Parametrisation of the Lane Change Model

According to the simulation findings of the first project iteration, CAVs exhibited rather conservative lane change behaviour in the baseline simulation experiments. The conservativeness of CAV lane changing was especially amplified for low values of $lcAssertive$ (ranging between 0.5 – 0.7) and provoked safety critical events (increased rear-end collision risk) in scenarios encompassing lane drops or lane closures (Scenarios 1.1, 2.1 and 4.2). Moreover, the fact that manual lane changing was selected to be far more aggressive compared to automated ($lcAssertive = 1.3$ for LVs), based on DLR's previous experience with the default SUMO lane change model, intensified the latter issue and additionally caused CAV emergency braking episodes due to cut-in activity by LVs (accepting significantly shorter gaps for lane changing). Hence, we revisit the analysis conducted in the first project iteration with respect to the parametrization of the lane change model to ensure the realism of lane change behaviour (for all simulated vehicle types) in our baseline simulation experiments.

In the second project iteration we enhance **Figures 10 – 12** by making the following adaptations:

- Include simulated lane change output for a wider spectrum of speed difference between ego and foe vehicle (±15 m/s instead of ±5 m/s in the first project iteration)
- Include simulated lane change output for ego vehicle speed ranging between 0 – 130 km/h (in the first project iteration ego vehicle speed ranged between 0 – 100 km/h)
- Include simulated lane change output for $lcAssertive$ values that reflect manual (more aggressive) lane change behaviour (i.e. 1.1 and 1.3)
- Plot the safe gaps (dependent variable) on the vertical y-axis and the ego vehicle speed (independent variable) on the horizontal x-axis

The new **Figures 13 – 15** also depict safe gaps for lane changing estimated by SUMO vs lane change data provided by HMETC (horizontal dashed lines). We note that the HMETC lane change data were collected with the use of a HMETC prototype automated vehicle. The design of the HMETC prototype automated driving logic emphasizes on the aspect of safety, thus rendering the vehicle more conservative on the lateral control task compared to a similar production ready vehicle. Moreover, although the HMETC lane change data appear segmented in the context of this analysis **(Figures 13 – 15)**, the actual prototype's lane change logic can estimate explicit safe gaps per relative speed value.

The *lcAssertive* parameter determines the willingness of a vehicle to accept lower front and rear gaps on the target lane[2]. However, it also indirectly affects the accepted (safe) gaps to the leading vehicle on the current lane. Thus, we examined the variation of the latter type of gaps for varying $lcAssertive$ values in both project iterations as well. Safe gaps are separately shown for negative relative speed between the ego CAV and the foe vehicle (current leader or target leader or target follower) on the left columns, and positive relative speed between the ego CAV and the foe vehicle (current leader or target leader or target follower) on the right columns. Negative relative speed in the following graphs implies that the following vehicle's speed is higher compared to the leader's one, while positive relative speed implies the opposite. **Figure 13** displays safe longitudinal gaps to the target follower, **Figure 14** displays safe longitudinal gaps to the target leader, and finally **Figure 15** displays safe longitudinal gaps to the current leader.

According to **Figure 13**, the model behaviour is significantly more aggressive compared to the HMETC vehicle for values of the *lcAssertive* parameter ranging between 0.7 – 1.3 and negative relative speed between the ego CAV and the follower on the target lane. On the other hand, when the relative speed is positive the behaviour of the HMETC vehicle becomes more aggressive compared to the LC2013 model for *lcAssertive* values ranging between 0.5 – 1.0. Thus, the SUMO vehicle accepts shorter gaps compared to the HMETC for negative relative speed and higher $lcAssertive$ values, while the HMETC vehicle accepts shorter gaps compared to the SUMO vehicle for positive relative speed and lower $lcAssertive$ values.

According to **Figure 14**, the model and the actual vehicle behaviour coincide for *lcAssertive* = 0.9 and negative relative speed between the ego CAV and the leader on the target lane (green dotted line coincides with the right edges of the horizontal dashed lines). When the relative speed between the ego CAV and the leader on the target lane is positive, similar behaviour is attained for *lcAssertive* between 0.7 – 0.9. Thus, when the gap between the ego CAV and the target leader is considered we can approximate the HMETC vehicle lane change behaviour for *lcAssertive* = 0.85.

[2] See https://sumo.dlr.de/wiki/Definition_of_Vehicles,_Vehicle_Types,_and_Routes#Lane-Changing_Models

Finally, **Figure 15** indicates that the SUMO and HMETC vehicle lane change behaviour is identical for *lcAssertive* ranging between 0.55 – 0.6 when the gap between the ego CAV and the leader on the current lane is considered (for both the negative and positive relative speed cases). Examining **Figures 13 – 15** it becomes apparent that the SUMO vehicle exhibits different behaviour compared to the HMETC vehicle for different types of gaps (egoCAV – target leader, egoCAV – current leader, egoCAV – target follower) when the *lcAssertive* parameter is fixed to a specific value. As long as there exists no explicit calibration parameter to adjust separately each type of gap, then it is not feasible to attain the desired lane change behaviour as dictated by the HMETC lane change data.

Moreover, other notable conclusions that can be drawn from the graphs are the following:

1. Safe longitudinal gaps increase linearly with increasing speed for the simulation models
2. Safe longitudinal gaps attain very large values for $egoSpeed > 100\ km/h$ and $lcAssertive < 0.7$

According to the latter analysis and considering that the HMETC prototype AV is more conservative in lane changing in contrast to a similar production ready AV we decide to approximate the AV lane change behaviour by selecting $lcAssertive$ between 0.8 – 0.9 for the baseline simulation experiments of the second project iteration. Moreover, we decided to marginally decrease the aggressiveness in the case of manual lane changing and render CVs more conservative in terms of lane change behaviour compared to LVs taking into account that they are equipped with lane change assistance ADAS. The corresponding $lcAssertive$ values per vehicle type are drawn from normal distributions which are specified in Section 3.2.5.1 for the second project iteration.

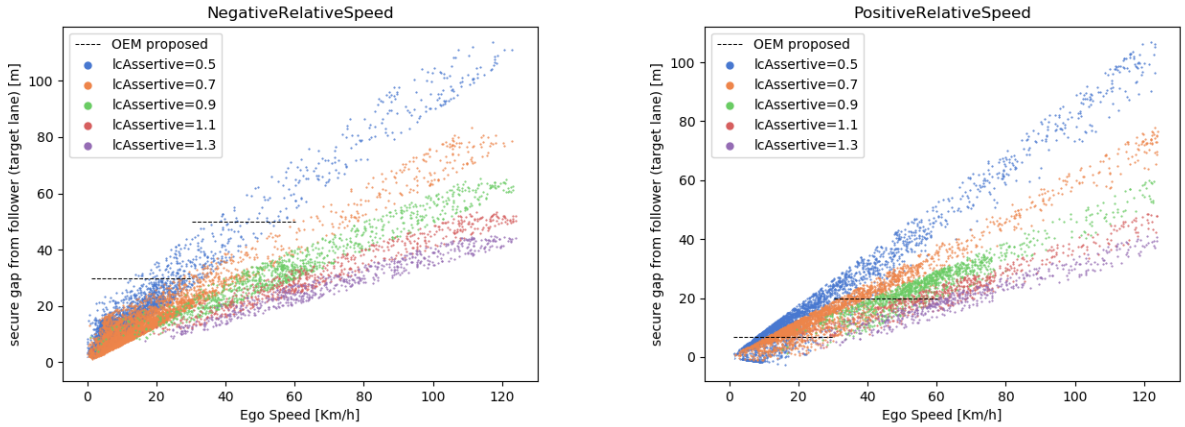

Figure 13. Safe longitudinal gaps to follower on the target lane (relative speed ±15 m/s).

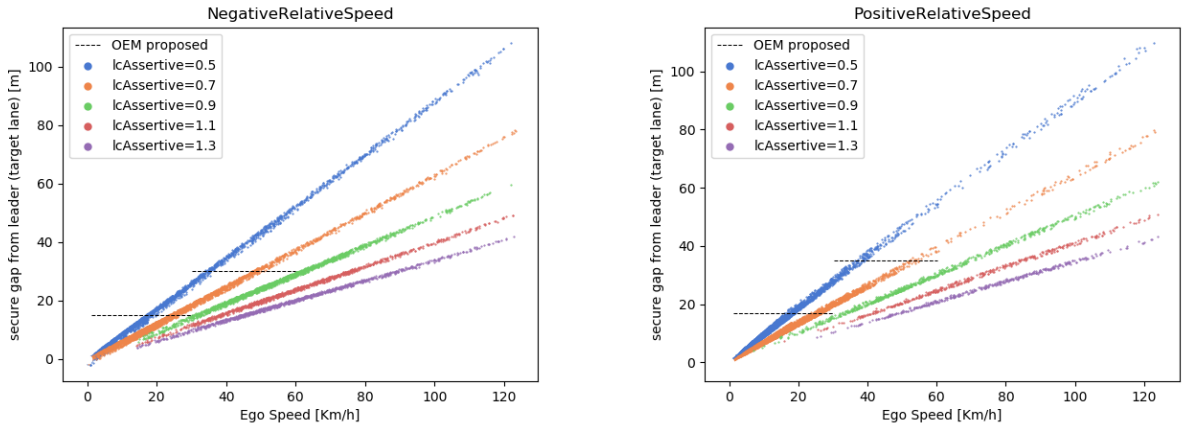

Figure 14. Safe longitudinal gaps to leader on the target lane (relative speed ±15 m/s).

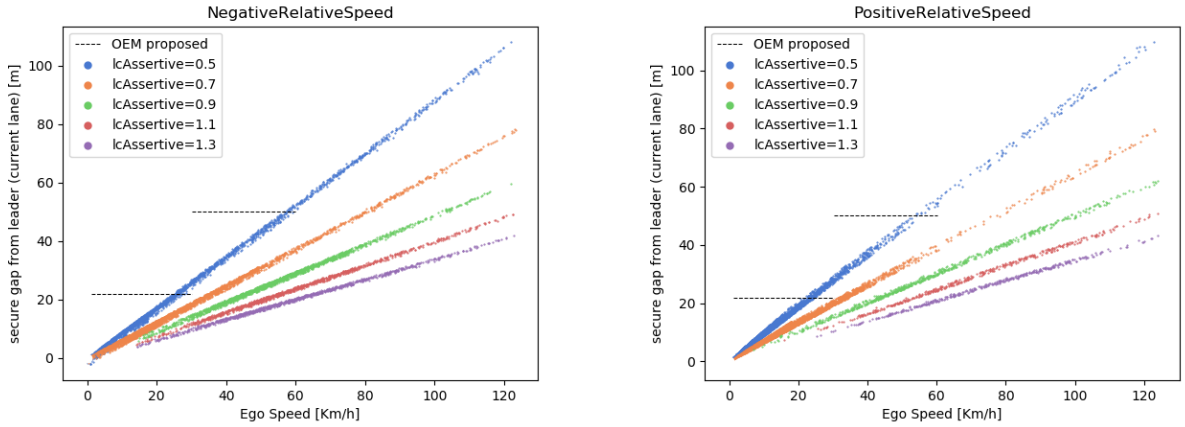

Figure 15. Safe longitudinal gaps to leader on the current lane (relative speed ±15 m/s).

2.3 Simulation of Take-over Process

2.3.1 First Iteration

In this section we give an overview of the important aspects that are considered when modelling ToCs for (C)AVs. We provide details of the implementation in SUMO and propose parameter ranges for parameters to be adopted in baseline simulations of the TransAID project.

2.3.1.1 Structure of Take-over Events

ToCs in (C)AVs can be classified according to several characteristics (Eriksson & Stanton, 2017; Lu et al., 2016). The class of passive, downward transitions is likely to be the most critical as these pose high demands on a potentially distracted human driver in terms of time constraints for the take-over (D2.1).

For simulative studies on the impact of cumulative occurrences of ToCs in TAs, simulation models need to be developed, being capable of reproducing the important processes during such events. **Figure 16** shows a schematic representation of the presumed phases during a downward ToC (Gold et al., 2013).

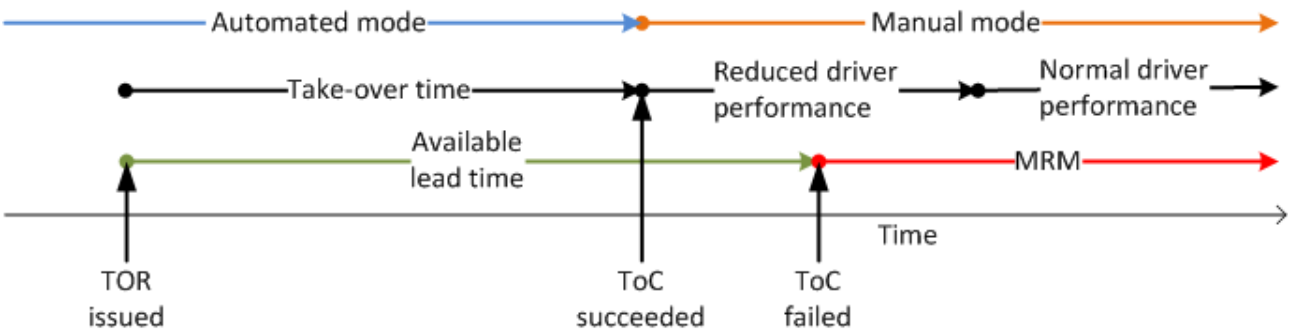

Figure 16. Timeline of a downward transition.

Even though the processes can be described to a higher detail, especially the driver (re)actions prior to the ToC are important (Gold et al., 2013). the level of granularity depicted in **Figure 16** suffices the modelling needs for the purposes in TransAID.

From a modelling perspective it is clear that the time point of switching between automated and manual driving mode requires a careful handling as the model features a discontinuity here. For the implementation, the car-following and lane-change models of the simulated driver-vehicle-unit (DVU) are substituted at this moment and we must ensure that this does not introduce unnaturally high brake rates or similar artefacts.

For the assessment of the impacts of ToCs on traffic safety and efficiency, the choice of parameters of the automated and manual mode is crucial. Especially the phase of reduced driving performance may be conjectured to imply an adverse effect due to irregular or erroneous behaviour, which disturbs a smooth traffic flow. Considerable evidence has been presented to claim that measures of driving performance may drop when a take-over is requested with an insufficient lead time (Blommer et al., 2017; de Winter et al., 2014; Eriksson & Stanton, 2017). Mostly, the available studies are concerned with Level 3 automation and urgency ToCs, and aim at estimating the lead time that permits drivers to operate their vehicle safely after performing the ToC. In general, this lead time was found to be significantly longer if the driver disengages from the driving process, i.e.

more distracted or out of the loop for a longer period of time (de Winter et al., 2014; Louw et al. 2015; Merat et al., 2012). This observation is especially important for the case of highly automated vehicles since the driver is likely to engage in other activities, which distract further from the driving process. Indicators, which were used to quantify the driving performance and are directly related to the driving process, are for instance *speed variation / throttle input* (Blommer et al., 2017; Clark & Feng, 2017), lane keeping (Clark & Feng, 2017; Mok et al., 2017), braking precision / overbraking (Clark & Feng, 2017; Louw et al., 2015; Young & Stanton, 2007), and the type of evasive manoeuvre applied in case of an urgent ToC (Blommer et al., 2017). But also, indirect indicators of attentiveness and situation awareness were studied, e.g. the driver's ability to reconstruct a depicted situation after looking at it for different amounts of time (Lu et al., 2017), and the frequency and type of glances and eye movements (Samuel et al., 2016; Zeeb et al., 2015; Ziegler et al., 2014).

Figure 17 shows a diagram for a model capturing the essential phases and transition during the ToC process. Both driving modes, automated and manual, have a state of normal operation, which corresponds to a normal driver performance for the manual mode and undisrupted functioning for the automated mode. After a take-over request (ToR) has been issued, the model for automated control enters the "Prepare ToC" state, where it resides until the driver responds to the ToR, or until the lead time has elapsed, in case of which it initiates an MRM. The entry point to the manual mode is the "Post-ToC Recovery" period during which a decreased driver performance is assumed. This state is modelled as described in the subsequent Section 2.3.3.

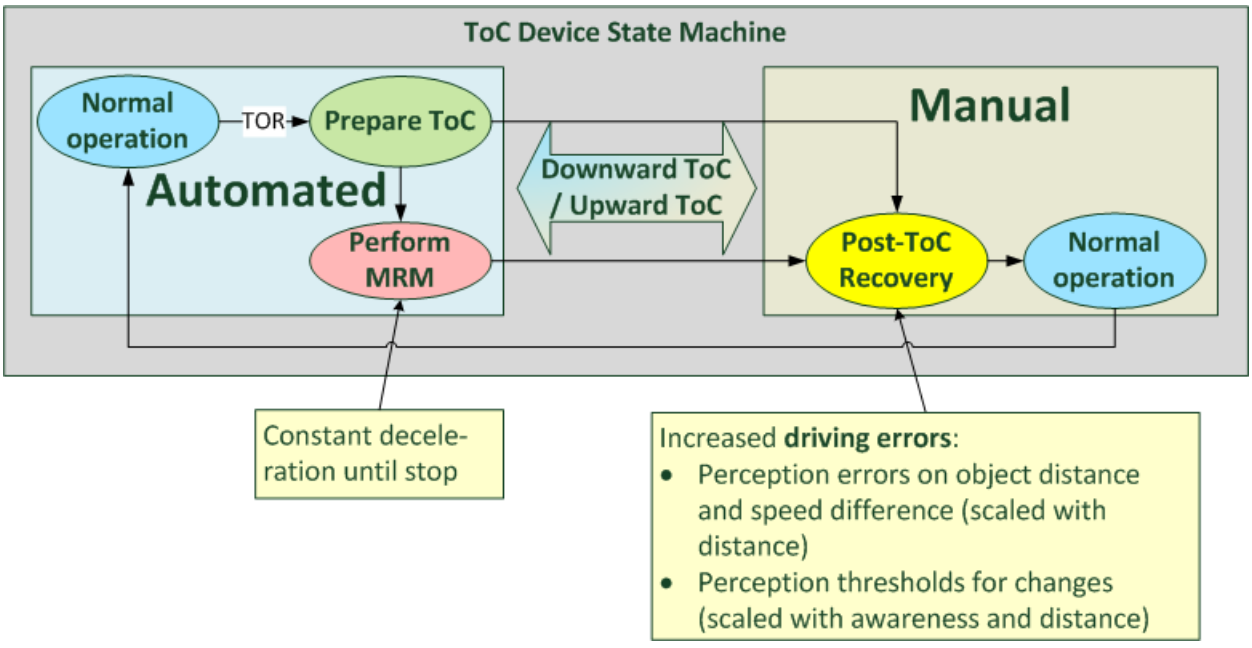

Figure 17. State machine for a ToC process model.

2.3.1.2 Parametrisation of the ToC Model

In TransAID we concentrate the research on situations where the need for a manual overtaking is foreseeable for a certain area. The ToR can be communicated to the driver with a relatively long lead time until the ToC is required to be executed. This means, that the transitions to be modelled are **not urgent but planned**. Unfortunately, the research body on planned ToCs is rather scarce in comparison to urgent ToCs (Eriksson & Stanton, 2017), which received the greatest attention so far because they are likely to lead to the most critical situations.

Due to the hypothetic nature of the parameter assumptions involved in the modelling, we strive to cover a range of possible scenarios by defining a set different parameter schemes (Section 3), corresponding to major, moderate, and minor impacts of the ToC events. For the lead time we fixed a value of 10 seconds for the simulations, which has to be interpreted in conjunction with the distribution of driver response times. This distribution was modified between the different parameter schemes to affect the probability of an MRM being initiated, which presumably represents the largest impact of ToC processes on the traffic flow. **Figure 18** shows the cumulative distribution functions for the different parameter schemes. These are truncated normal distributions with a mean of 7 seconds and variances of 2.1 (minor impact), 2.5 (moderate impact), and 3.0 (major impact). This results in the following probabilities for MRMs:

- Minor impact: P(MRM) = ~7.7%,
- Moderate impact: P(MRM) = ~11.6%
- Major impact: P(MRM) = ~16.2%

Note that a simulated DVU is assumed to switch immediately to the manual mode after the response time has elapsed, even if this requires an abort of an ongoing MRM. Therefore, not only the occurrence of an MRM is an important quantity but also its duration, which is the difference of the response time and the lead time. Thus, the most MRMs occurring in the simulations are of short duration (> 85 % lie within $0 - 3$ s and > 97.5 % within $0 - 5$ s for all parameter schemes) and are interrupted before the vehicle comes to a full stop.

Other important parameters are the initial awareness distribution affecting the driver state at the moment of performing the ToC, and the various coefficients for the driver state model error and perception mechanisms (Section 2.3.3).

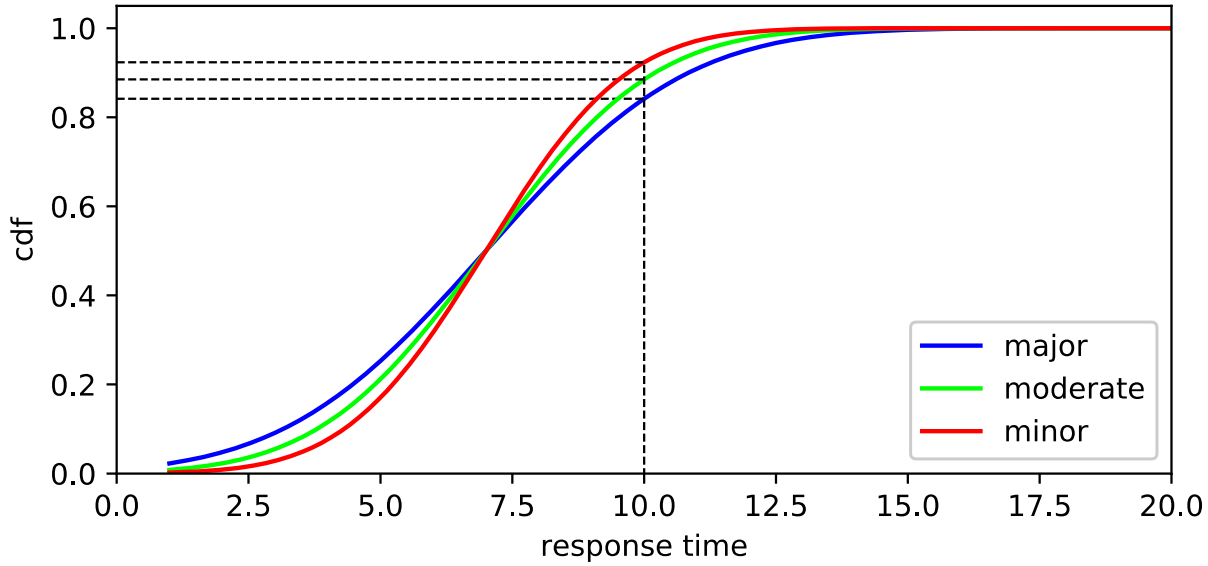

Figure 18. Cumulative distribution functions of the driver response time for the different parameter schemes employed in the baseline simulations. For the different parameter schemes, the intersections of the corresponding dashed lines with the ordinate indicate the probabilities that an AV, which requires a ToC, successfully performs it before initiating an MRM.

2.3.1.3 Modelling of a Decreased Post-ToC Driver Performance

The observations of increasing performance measures with increasing take over time (Section 2.3.1) can be attributed to an underlying recovery process of the driver's awareness and the mental capacity available for the driving process (Fuller, 2005; Lu et al., 2017; Merat et al., 2014; Young & Stanton, 2002).

As this recovery process can be assumed to exhibit a high variability between different drivers and situations, it seems unavoidable that the level of disengagement will be elevated at least for some drivers of automated vehicles after the ToC, even if the granted lead time assures that a good performance can be expected after the ToC for most events.

We capture this assumption by randomly assigning a value for an $initial\ awareness\ A_0$ to the model of each DVU that is performing a ToC in the simulations. The variable A_0 is sampled from a distribution on the interval $[A_{min}, 1]$, see Section 3.5, where a value of $A_0 = 1$ corresponds to full awareness, i.e. normal driving performance, while $A_{min} > 0$ is the minimal level for the initial awareness. Further an $awareness\ recovery\ rate\ r$ is given to the DVU controlling the post-ToC evolution of its awareness $A(t)$ according to $\dot{A}(t) = r$, until the awareness has completely recovered i.e. $A(t) = 1$.

For the period, where the awareness is reduced, i.e., $A(t) < 1$, we assume an increased error rate for the leading DVU. Although errors may enter the driving process at several stages **(Figure 19)**, we restrict the modelling to one source, which is chosen to be the accuracy of the driver's perceptions, i.e. the perception errors. We follow this simplification since it is not obvious how a more detailed error mechanism would to lead to a significant improvement of the model with respect to the modelling purposes within TransAID, because no driver error source specific countermeasures are developed here.

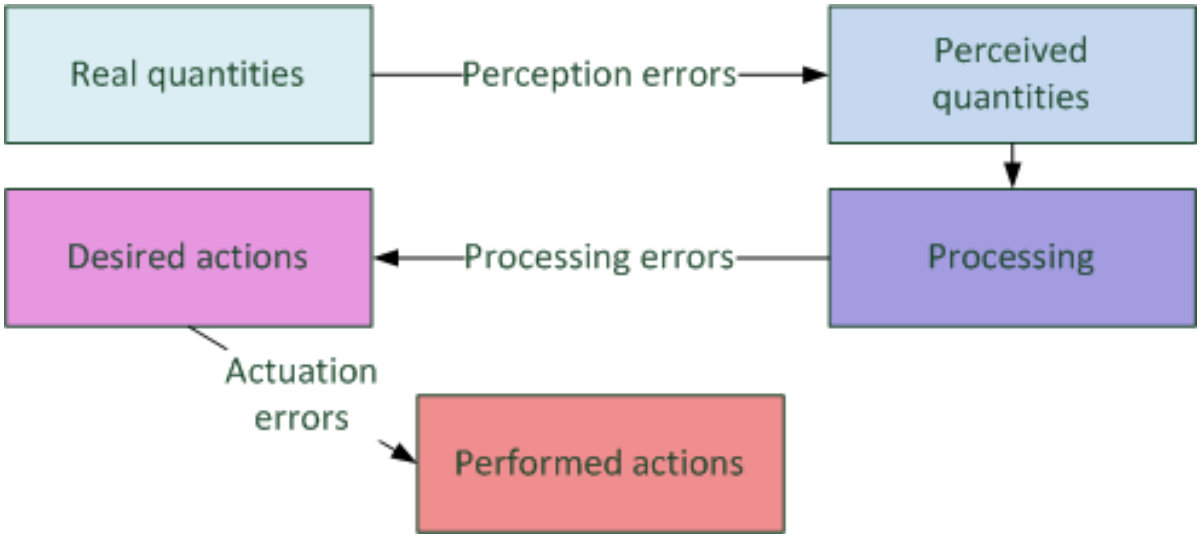

Figure 19. Errors entering the driving process.

Perception errors may be introduced to a car-following model in a generic way. Let us assume that a given model is of the form:

$$\dot{x}(t) = v(t) \tag{14}$$

$$\dot{v}(t) = a(\Delta x(t), \Delta v(t)) \tag{15}$$

where $x(t)$ is the vehicle's position and $v(t)$ its speed at time t. This form assumes that the quantities determining the acceleration $a(t) = a(\Delta x(t), \Delta v(t))$ are the gap $\Delta x(t)$ to the leading vehicle and the corresponding speed difference $\Delta v(t)$. This form is satisfied by a lot of commonly applied car-following models (Treiber & Kesting, 2013), but a generalisation to other forms is not expected to be a difficult task.

Perception errors η_x regarding the gap Δx and η_v regarding the speed difference Δv are used to define the perceived gap $\Delta\tilde{x}$ and the perceived speed difference $\Delta\tilde{v}$ as:

$$\Delta\tilde{x} = \Delta x + \eta_x \tag{16}$$

$$\Delta\tilde{v} = v + \eta_v \tag{17}$$

The erroneous driving behaviour is then described by the equations:

$$\dot{x}(t) = v(t) \tag{18}$$

$$\dot{v}(t) = a(\Delta\tilde{x}(t), \Delta\tilde{v}(t)) \tag{19}$$

Both errors are derived from a scalar Ornstein-Uhlenbeck process H [Gardiner 2009, Kesting 2013] with time-dependent noise intensity σ_t and time scale θ_t. We favoured the implementation of this coloured noise over white noise to capture temporal autocorrelations in driver's deviances from ideal models (Wagner, 2012). The process H evolves according to:

$$d\mathrm{H}_t = -\theta_t \cdot \mathrm{H}_t \cdot dt + \sigma_t \cdot dW_t \tag{20}$$

The effective errors η_x and η_v are assumed to be proportional to the distance to the leading vehicle [Xin et al., 2008] and the main error term H_t, that is:

$$\eta_x(t) = c_x \cdot \Delta x(t) \cdot \mathrm{H}_t \tag{21}$$

$$\eta_v(t) = c_v \cdot \Delta x(t) \cdot \mathrm{H}_t \tag{22}$$

with constant coefficients c_x and c_v. The time scale θ and the noise drive σ of H follow the temporal changes of the awareness $A(t)$ as follows:

$$\theta_t = c_\theta \cdot A(t) \tag{23}$$

$$\sigma_t = c_\sigma \cdot \big(1 - A(t)\big) \tag{24}$$

Roughly speaking, this implies that the higher the awareness, the faster any errors decay and the smaller is their range.

As an additional generic mechanism for imperfect driving, we consider perception specific action points (Todosiev, 1963; Xin et al., 2008). An action point is an instant t where the acceleration $a(t)$ is changing its value according to the dynamical equation of the given car-following model.

Here we assume that a change in a perceived quantity is only recognised if its magnitude surpasses a certain threshold value. Accordingly, a corresponding change in action, here, a change of acceleration, is only taken out when the currently perceived speed difference $\Delta\tilde{v}(t)$ deviates sufficiently from the last recognised value $\Delta\tilde{v}_{\mathrm{rec}}$ or the currently perceived gap $\Delta\tilde{x}(t)$ deviates from the value estimated based on the last recognised quantities. That is, instant t is assumed an action point if either:

$$|\Delta\tilde{x}_{\text{rec}} + (t - t_{\text{rec}}) \cdot \Delta\tilde{v}_{\text{rec}} - \Delta\tilde{x}(t)| > \theta_x, \text{ or } |\Delta\tilde{v}_{\text{rec}} - \Delta\tilde{v}(t)| > \theta_v. \quad (25)$$

Figures 20-22 compare data generated by SUMO's standard model, the proposed model and data from a real car-following episode of an approximate duration of 5.5 min. This episode was extracted from the sim^{TD} database[3].

The experimental setup entailed a simulated car-following situation, where a simulated, model-controlled following vehicle drove behind a simulated vehicle following exactly the recorded speed profile of the real leading vehicle. **Figure 20** shows the trajectory obtained from a Krauss model (the standard SUMO model), and **Figures 20 – 22** show trajectories of the model extended by the perception error mechanism as described above for two different parametrisations.

If not stated otherwise, the following parameter values were used for the driver state model of the following vehicle:

- $c_\theta \equiv 100$, and $c_\sigma = 0.2$
- $c_x = 0.75$, and $c_v = 0.15$
- $\theta_x = \theta_v = 0.1$

The underlying Krauss model had the following configuration parameters:

- $accel = 1.0$,
- $decel = 3.0$,
- $sigma = 0.0$, and
- $tau = 0.72$

The different charts (a)-(d) of Figures 17-19 show different aspects for the trajectory

[3] https://www.sit.fraunhofer.de/de/simtd/

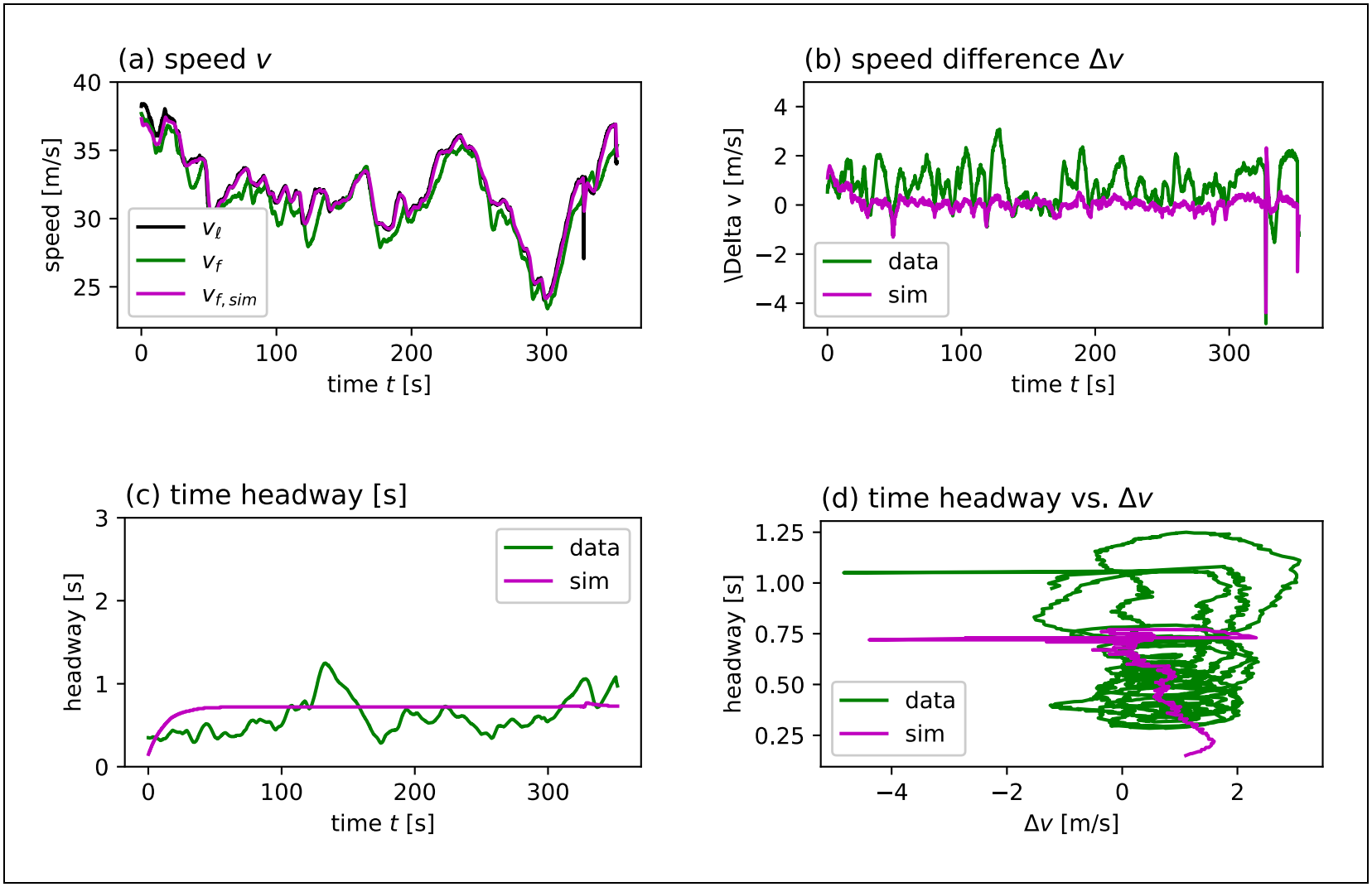

Figure 20. Comparison of SUMO's standard model (Krauss) without driver state extensions and real car-following data.

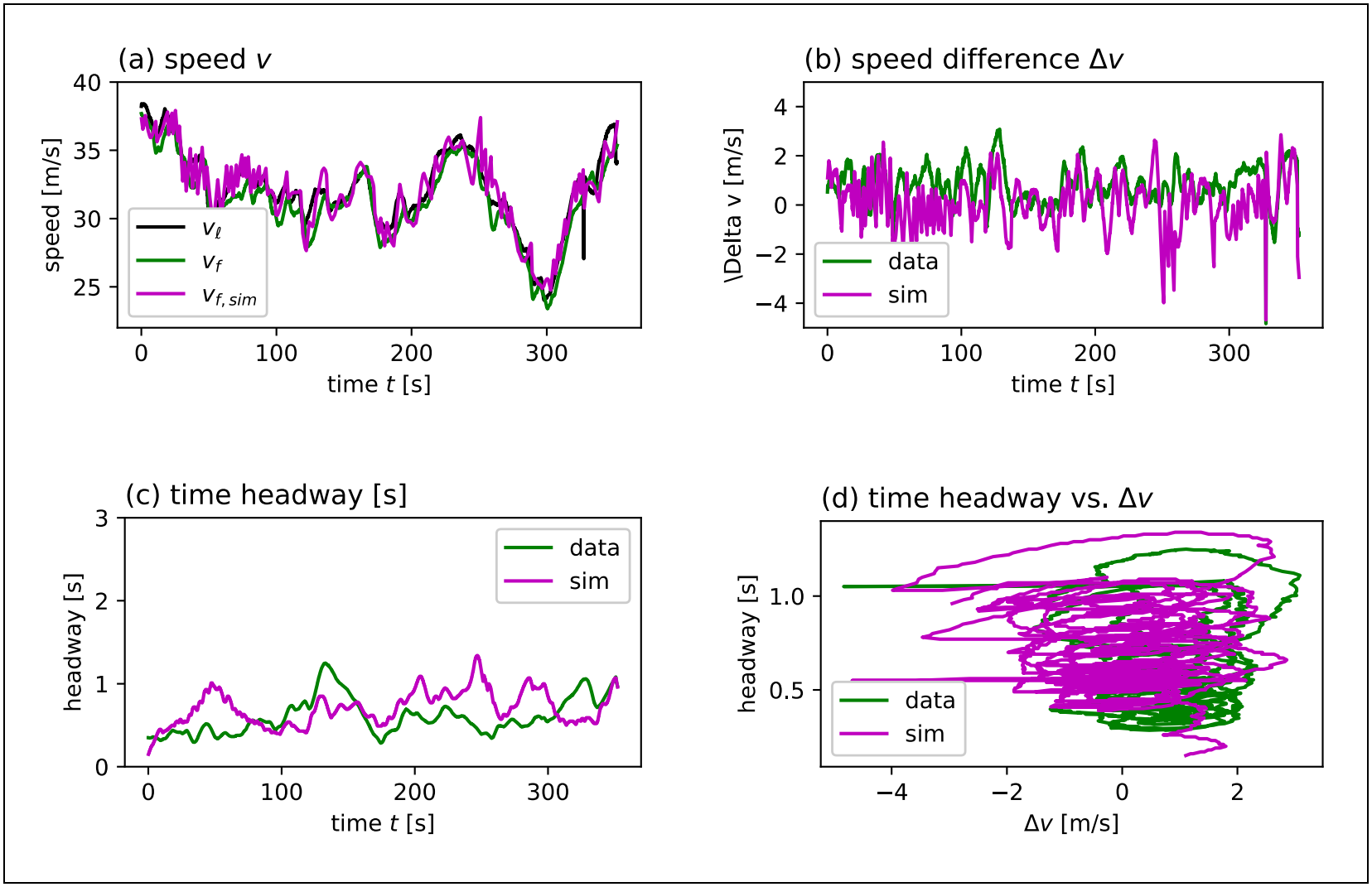
(a) speed v
speed [m/s]
time t [s]
v_ℓ
v_f
$v_{f,sim}$
(b) speed difference Δv
\Delta v [m/s]
time t [s]
data
sim
(c) time headway [s]
headway [s]
time t [s]
data
sim
(d) time headway vs. Δv
headway [s]
Δv [m/s]
data
sim

Figure 21. Comparison of a Krauss model with superposed perception errors and real car-following data. The awareness is held constant with a value of $A(t) \equiv 0.1$.

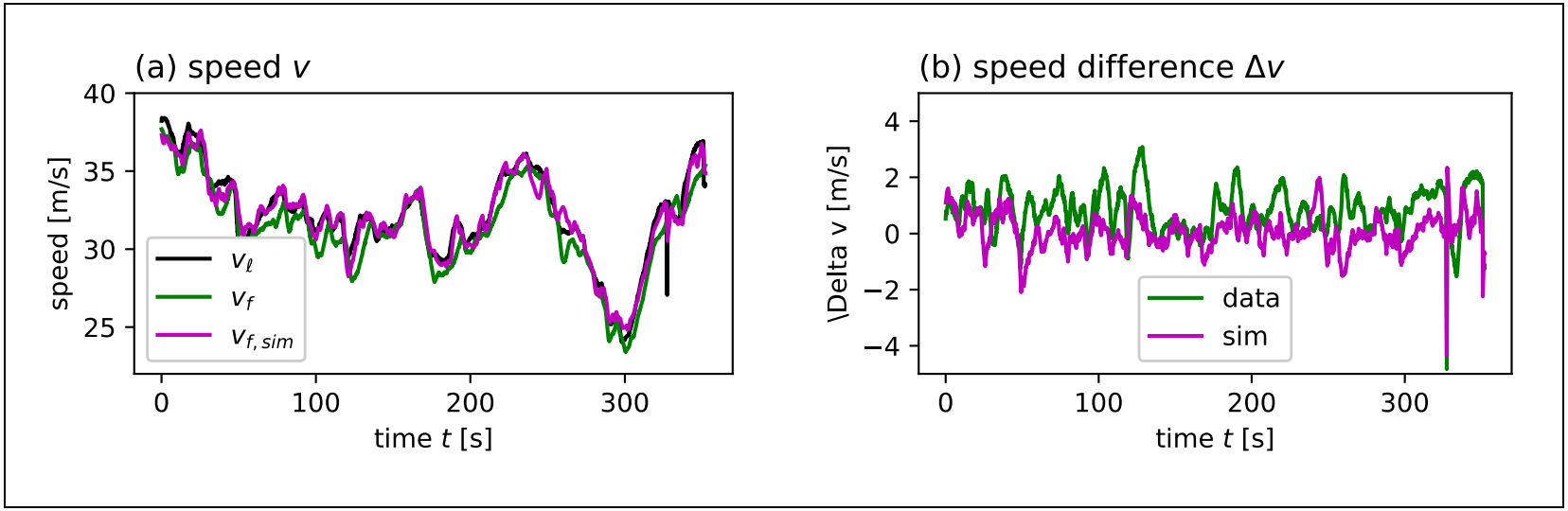

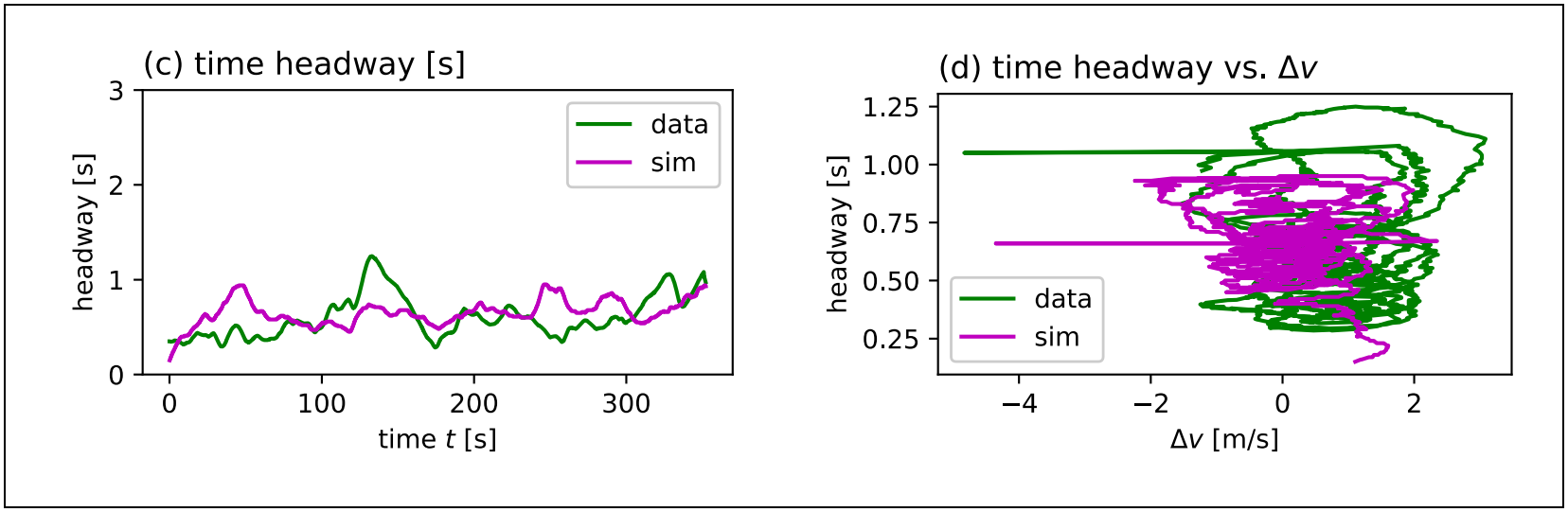

Figure 22. Comparison of a Krauss model with superimposed perception errors and real car-following data. Here, $\theta_x = \theta_v = 0.02$ (other parameters as given above); constant awareness $A(t) \equiv 0.1$.

2.3.1.4 Implementation of the ToC Model in SUMO

To capture the processes during transitions of control in a simulation, a ToC device and a driver state device were implemented in the open source traffic simulation SUMO. The corresponding code is openly available. The relevant source files are MSDevice_ToC.h, MSDevice_ToC.cpp, MSDevice_DriverState.h, and MSDevice_DriverState.cpp in the directory sumo/src/microsim/devices of the SUMO repository at https://github.com/eclipse/sumo.

The parameters for the ToC model are:

- Manual type: SUMO vehicle type (simulation model) for manual driving mode
- Automated type: SUMO vehicle type (simulation model) for automated driving mode
- Response time: The time the driver needs to react to a ToR
- Initial Awareness: Awareness just after a completed ToC
- Recovery rate: Rate by which the awareness recovers to its maximal value after a ToC
- mrmDecel: Value of the constant deceleration rate assumed to be applied during an MRM

To set up a simulated vehicle, which can perform ToCs, the user has to specify at least the two vehicle types, which specify the models for automated and manual driving, as obligatory parameters, see the corresponding Wiki-page[4] for details.

All device parameters are accessible to the user via TraCI (traci.vehicle.setParameter()) and libsumo (libsumo::Vehicle::setParameter()). A special parameter key 'requestToC' combined with the value of the ToC lead time after which an MRM will be initiated, can be used to trigger ToCs for the vehicle during the simulation.

Equipping a SUMO vehicle with a ToC-Device automatically adds a driver state device if none was specified previously. This device provides the error states and parameters for the decreased post-ToC driver performance, see Section 2.3.3. If the driver state is automatically generated, default values are used for its parameters, otherwise the user may specify them as described on the corresponding Wiki-page[5].

2.3.2 Second Iteration

2.3.2.1 ToC Preparation Phase

For the modelling of the preparatory phase between the announcement of a TOR by the vehicle and the actual takeover by the driver in the case of a downward transition we have added a gap control component to SUMO's ToC model. It allows the user to configure a secure headway (parameters $ogNewSpaceHeadway$ and $ogNewTimeHeadway$), which the vehicle automation will try to establish in preparation of the takeover and dynamical aspects of the strategy to achieve this gap (parameters $ogChangeRate$ and $ogMaxDecel$). The process of enlarging the desired headway is as follows: applying change rates dependent on the original and desired new headway the desired headways determining the acceleration choice by the controller are modified. For instance, $ogChangeRate == 0.5$ would imply that the desired headways of the controller change from the old to the new values within two seconds. This modification of the control logic will usually induce

[4] http://sumo.dlr.de/wiki/ToC_Device

[5] http://sumo.dlr.de/wiki/Driver_State

changes in the vehicle's speed. To allow controlling the associated deceleration rate, it is possible to define a maximal value for the associated deceleration via $ogMaxDecel$ (clearly, the headway adaptation process should, for instance, not induce emergency braking).

2.3.2.2 Dynamical Triggering of TORs

In case that an automated vehicle's control wishes to change lanes due to strategic reasons, that is, because this manoeuvre is necessary to continue on the vehicle's designated route, the automation can be expected to request a takeover to let the driver handle the situation. Such a situation may arise if the traffic is too dense or the situation too complex for a necessary lane change to succeed. For instance merging into a crowded highway with dense traffic might pose considerable difficulties for safe automated manoeuvres.

Therefore we have added the option to trigger such situation dependent TORs within SUMO's ToC model. By default the option is deactivated, but it can be set active by handing a parameter $dynamicToCThreshold$ to the configuration of the ToC device. The value of this parameter gives a continuation time (in seconds) without lane changes, which the vehicle automation requires to have granted for its usual operation. As soon as the remaining distance, in which the vehicle may follow its assigned route without performing a lane change, undercuts the value of $dynamicToCThreshold * currentSpeed + MRMDist$, a TOR will be issued to the driver. Here, $currentSpeed$ denotes the current speed the vehicle is traveling at and $MRMDist$ is the distance covered during the braking process associated to an MRM at that speed, i.e. $MRMDist = 0.5 * currentSpeed * currentSpeed/MRMBrakeRate$. The associated lead time is calculated as $leadTime = 0.75 * dynamicToCThreshold$, where the factor 0.75 establishes a safety margin for a timely initiation of the ToC.

The dynamical triggering of a ToC also requires a dynamical sampling of the response time for the driver as we cannot foresee the lead time available to the driver. The distribution underlying the sampling of the response time T_{resp} is assumed to be a truncated Gaussian $N_{\geq 0}(\mu, \sigma)$ as for the static sampling presented in 2.3.1.2 (**Figure 18)**. Given the lead time and a specified probability for an MRM to be triggered, we wish to determine mean μ and variance σ for the Gaussian, which is underdetermined. Therefore, we postulate additionally the relationship:

$$\mu(T_{lead}) = \min\left(2 \cdot \sqrt{T_{lead}}, 0.7 \cdot T_{lead}\right) \quad (26)$$

which is motivated by the ratio ~7:10 of μ and T_{lead} for the assumed static lead time of 10 seconds in the scenarios of the first project iteration, and the fact that we assume the ratio to drop for increasing T_{lead}, see **Figure 23**.

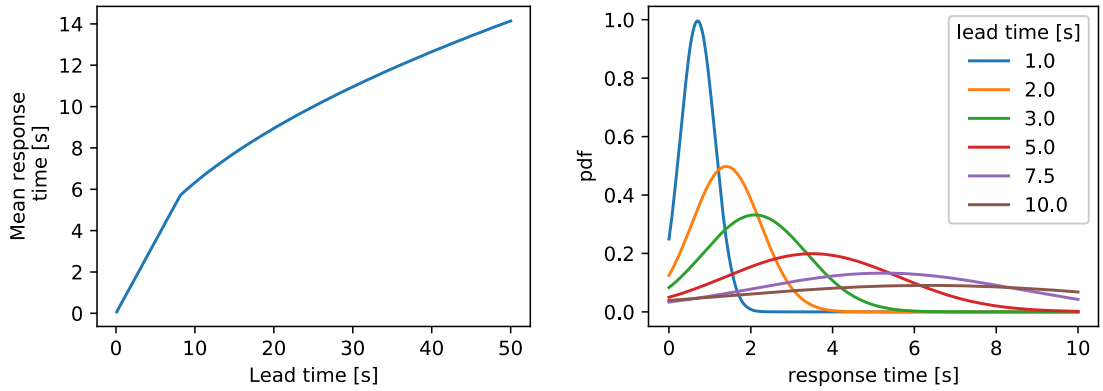

Figure 23. (a) Assumed dependency $\boldsymbol{T_{lead} \mapsto \mu(T_{lead})}$. Resulting probability densities of the response times for some values of $\boldsymbol{T_{lead}}$ (see legend) and $\boldsymbol{p_{MRM} = 0.25}$.

The desired percentage of failing takeovers, i.e., the percentage p_{MRM} of takeover requests leading to an MRM, is then controlled via the variance of the Gaussian. Since we assume moderate lead times and small fractions of failing takeovers, $p_{MRM} \ll 1$, the corresponding equation

$$\mu(T_{lead}) = \min\left(2 \cdot \sqrt{T_{lead}}, 0.7 \cdot T_{lead}\right) \tag{27}$$

is expected to be solvable for σ. We create a corresponding look-up table for a quick calculation of the corresponding mapping $(p_{MRM}, T_{lead}) \mapsto \sigma$. See Appendix B for the script generating the table.

2.3.2.3 Refinement of the ToC Model

Several smaller components of the ToC model (see Section 2.3.1.1) have been refined to enhance the realism of the simulation:

- Lane change abstinence during the recovery phase: there is now a per-vehicle configurable time after the takeover in which the driver will not be able to start lane change manoeuvres.
- Similarly, lane changes are not performed during the ToC preparation phase, since it can be assumed to decrease the safety if drivers overtake control during a lane change.
- The same reasoning applies to acceleration during the ToC preparation, which can now also be confined to a configurable amount below some maximal value.
- "Advanced MRMs" can be simulated by adding the `mrmKeepRight` flag to a vehicles ToC model configuration. This will affect the vehicle to attempt a lane change to the rightmost lane of its current road.

3 Simulation Experiments

3.1 First Iteration

3.1.1 Dimensions of Simulation Experiments

The baseline simulation experiments encompass different traffic demand levels, vehicle mixes, and parameter sets for the (C)AV/CV driver models (ACC, LC2013, ToC/MRM). Whereas Deliverable D2.2 specified traffic demand levels and vehicle mixes for the baseline simulation experiments, we now provide updated vehicle mixes based on a revised definition of actors, considering a more comprehensive set of actual vehicles attributes. Moreover, we here introduce different parametrisation schemes for the (C)AV/CV driver models considering that their behaviour can be aggressive, moderate, or conservative. In addition, the baseline simulation analysis also investigates the effects of a wide range of possible (C)AV/CV behaviours on the Key Performance Indicators (KPIs) defined in D2.1.

3.1.2 Updated Definition of Actors

Deliverable D2.2 categorised actors based on vehicles automation capabilities (longitudinal and/or lateral control), communication capabilities (message types and relevant applications), ToC capabilities (basic or extended), and MRM capabilities (standstill in the ego or the right-most lane).

However, in real life conditions other factors are going to influence the operation of (C)AVs/CVs as well. Early (C)AVs/CVs are expected to be deployed with systems of different automation levels, but system engagement will rely heavily on the driver's discretion. Thus, many (C)AVs/CVs will operate as manual vehicles in several occasions during the first stages of vehicle automation introduction.

Moreover, distracted driving might significantly affect ToCs of Level 1 and 2 AVs. Although drivers of Level 1 and 2 AVs are aware that they should continuously oversee the primary driving tasks when automation is in operation, cases are expected when driver distraction might lead to uncontrolled driving for a short period of time after ToC request (e.g., no acceleration and deceleration until the ego vehicle's distance to leader becomes very short and hard braking must be applied). Finally, there is a possibility that connectivity affects the ToC capabilities of highly automated CAVs (e.g., proactive warning of imminent ToC).

Thus, a revised classification of actors is provided in **Table 6** based on work presented in D2.2 and the newly introduced dimensions with respect to vehicles attributes.

Table 6. Classification of actors (vehicle types).

Class Name	Class Type	Vehicle Capabilities
Class 1	Manual Driving	– Legacy Vehicles – (C)AVs/CVs (any level) with deactivated automation systems
Class 2	Partial Automation	– AVs/CVs capable of Level 1 and 2 automation – Instant TOC (uncontrolled driving in case of distracted driving)

		– No MRM capability
Class 3	Conditional Automation	– (C)AVs capable of Level 3 automation (level 3 systems activated) – Basic ToC (normal duration) – MRM capability (in the ego lane depending on speed and a predetermined desired MRM deceleration level)
Class 4	High Automation	– (C)AVs capable of Level 4 automation (automation activated) – Proactive ToC (prolonged duration) – MRM capability (in the right-most lane depending on speed and a predetermined desired MRM deceleration level)

Uncontrolled driving after ToCs of Level 1 and 2 AVs will not be examined during the 1st project iteration. The ToC/MRM model will be adapted to accommodate the latter mentioned corner case during the 2nd project iteration. Currently, the focus lies on the examination of the aforementioned ToC/MRM model that can replicate regular ToCs of Level 3 and 4 (C)AVs. Within the context of the baseline simulation experiments, we assumed that 75% of (C)AVs/CVs will not be able to autonomously handle traffic situations at the TAs presented in D2.2, and will eventually initiate a ToC manoeuvre. We assume connectivity capabilities for specific portions of the latter defined vehicle classes.

Compliance to TransAID infrastructure-assisted traffic management measures is different per vehicle class based on the corresponding vehicle communication capabilities. Non-cooperative vehicles are expected to follow them manually (i.e. by adapting driving because of shown advices on traffic signs, external human-machine interface (HMI), etc.). Compliance rates for non-cooperative vehicles are expected to be significantly lower compared to cooperative ones. Cooperative vehicles of classes 1 and 2 will follow them manually, and those of classes 3 and 4 automatically.

3.1.3 Traffic Composition

Vehicle mixes for the baseline simulation experiments (1st and 2nd project iteration) are presented in **Tables 7 – 9**, based on the aforementioned vehicle classification. **Table 7** introduces artificial vehicle mixes for the baseline simulation experiments that will be tested during the 1st project iteration. These mixes include explicitly automated vehicles with connectivity capabilities but not non-cooperative vehicles. These latter vehicle classes will be considered during the 2nd project iteration, due to complexities pertaining to conveying TransAID measures to them. Moreover, non-compliant non-cooperative automated vehicles will be disrupting the operations of CAVs when following TransAID measures. Thus, artificial and realistic vehicle mixes encompassing all vehicle classes will be tested during the 2nd project iteration and shown in **Tables 8 – 9**. These mixes will result in more complex but realistic traffic operations. The revised realistic mixes were selected after elaborate discussions within the TransAID consortium considering the work done in D2.2 with respect to projections about future automation and connectivity penetration rates. Please note that TransAID is not linking the penetration rates to specific years, as the key factor is the distribution, not the year.

Table 7. Artificial vehicle mixes for baseline simulations during 1st project iteration.

Vehicle Mix	Class 1	Class 1 (Conn.)	Class 2	Class 2 (Conn.)	Class 3	Class 3 (Conn.)	Class 4	Class 4 (Conn.)
1	60%	10%	-	15%	-	15%	-	-
2	40%	10%	-	25%	-	25%	-	-
3	10%	10%	-	40%	-	40%	-	-

Table 8. Artificial vehicle mixes for baseline simulations during 2nd project iteration.

Vehicle Mix	Class 1	Class 1 (Conn.)	Class 2	Class 2 (Conn.)	Class 3	Class 3 (Conn.)	Class 4	Class 4 (Conn.)
1	60%	10%	5%	5%	5%	5%	5%	5%
2	40%	10%	5%	10%	10%	10%	5%	10%
3	10%	10%	5%	15%	10%	15%	15%	15%

Table 9. Realistic vehicle mixes for baseline simulations during 2nd project iteration.

Vehicle Mix	Class 1	Class 1 (Conn.)	Class 2	Class 2 (Conn.)	Class 3	Class 3 (Conn.)	Class 4	Class 4 (Conn.)
1	60%	3%	5%	4%	9%	8%	6%	5%
2	50%	3%	5%	4%	12%	12%	8%	6%
3	40%	3%	5%	4%	15%	15%	12%	9%

3.1.4 Traffic Demand Levels

The traffic demand dimension of the baseline simulation experiments was addressed in D2.2. Different traffic demand levels (vehicular flows) corresponding to different Levels of Service (LOS) per facility type (urban, rural, motorway) were selected based on information provided in (HCM, 2010). Vehicular flows were converted to passenger car flows based on the fleet composition section described in D2.2. Thus, baseline simulation scenarios encompass only passenger cars. The corresponding flow rates per hour per lane and LOS that will be considered are shown in **Table 10**.

Table 10. Vehicles/hour/lane for LOS A, B and C in urban, rural, and motorway facilities.

Facility Type	Capacity (veh/h/l)	Level of Service (LOS)		
		A	B	C
Urban (50km/h)	1500 veh/h/l	525	825	1155
Rural (80 km/h)	1900 veh/h/l	665	1045	1463
Motorway (120 km/h)	2100 veh/h/l	735	1155	1617
Intensity / Capacity (IC) ratio		0,35	0,55	0,77

Specifically for Scenario 2.1, the capacity of the merge segment is controlled by the capacity of the exiting section as highlighted in (HCM, 2010):

> *"The capacity of a merge area is determined primarily by the capacity of the downstream freeway segment. Thus, the total flow arriving on the upstream freeway and the on-ramp cannot exceed the basic freeway segment."*

Therefore, the two-lane motorway capacity is the basic capacity for the simulation network in Scenario 2.1. The vehicle injection rates on the on-ramp entry link and the upstream freeway entry link together should not exceed downstream two-lane motorway service flow rates, which are $600 \times 2 = 1200$ veh/hr/l, $960 \times 2 = 1920$ veh/hr/l, and $1400 \times 2 = 2800$ veh/hr/l based on (HCM, 2010) and show in **Table 11**. The two entry links – upstream motorway and on-ramp – are then injected with approximately 2/3 and 1/3 of these respective rates.

Table 11. Vehicles/hour/lane for Level of Service A, B and C (Scenario 2.1).

Facility Type	Capacity (veh/h/l)	Level of Service (LOS)		
		A	B	C
On-ramp (80km/h)	1650 veh/h/l	462	726	1056
Intensity (demand volume)/Capacity (IC or VC) ratio		0.28	0.44	0.64
Motorway (100 km/h)	2000 veh/h/l	600	960	1400
Intensity (demand volume)/Capacity (IC or VC) ratio		0.3	0.48	0.7

3.1.5 Parametrisation of Vehicle/Driver Models

The parametrisation of the (C)AV/CV driver models integrates the full spectrum of possible (C)AV/CV behaviours into the baseline simulation experiments, and thus, promotes a holistic understanding of their impacts on traffic safety, efficiency, and the environment. (C)AV/CV driver model parameter values are introduced as normal distributions for aggressive, moderate, and conservative (C)AV/CV. **Table 12** presents the adjusted parameters per driver model to reflect the aforementioned behaviours of (C)AVs/CVs.

Table 12. Adjusted driver model parameters to emulate different (C)AV/CV behaviours.

Driver Model	Parameter Name	SUMO Parameter
ACC (Longitudinal Motion)	Desired time headway	tau
Sub-lane (Lateral Motion)	Desired longitudinal gaps	$lcAssertive$
	Driver response time	$responseTime$
ToC/MRM	Post ToC driver performance	$initialAwareness$
	ToC likelihood (internal and external factors)	$responseTime$
		$timeTillMRM$

The ACC desired time headway (tau) normally spans between 1.2 – 2.2 s (L. Xiao & Gao, 2011). High tau values prompt a conservative ACC behaviour, while low values result in aggressive behaviour. The expected effects of different tau values on traffic safety and efficiency are assessed in qualitative terms in **Table 13**.

Table 13. Expected impacts of ACC desired headway on safety and efficiency.

Driver Model	Parameter Name	Value	Behaviour	Safety	Efficiency
ACC	Desired time headway (tau)	High	Conservative	Positive (+)	Negative (-)
		Moderate	Moderate	Moderate	Moderate
		Low	Aggressive	Negative (-)	Positive (+)

As explained in Section 2.2.1.3, the $lcAssertive$ calibration parameter was identified as the most significant factor in determining desired ego vehicle gaps for lane-changing relative to surrounding traffic (target follower, target leader, and current leader). Higher $lcAssertive$ values dictate a more aggressive vehicle behaviour in accepting shorter gaps, while lower values the opposite. Large desired gaps for lane-changing are expected to have a positive effect on safety and negative on traffic efficiency, and vice versa **(Table14)**.

Table 14. Expected impacts of desired longitudinal gaps for lane-changing on safety and efficiency.

Driver Model	Parameter Name	Value	Behaviour	Safety	Efficiency
Lane Change (LC2013)	Desired longitudinal gaps ($lcAssertive$)	Large	Conservative	Positive (+)	Negative (-)
		Moderate	Moderate	Moderate	Moderate

	Short	Aggressive	Negative (-)	Positive (+)

The ToC/MRM model parameter $responseTime$ determines the driver responsiveness to ToRs by the vehicle automation, while the $initialAwareness$ parameter characterises the driver performance after resuming control from the vehicle. Short $responseTime$ indicates that the driver can efficiently resume vehicle control in a timely manner, thus positively affecting traffic safety and efficiency **(Table 15)**. On the contrary, low $initialAwareness$ values imply that a prolonged time horizon is required for drivers to fully recover their driving capabilities after ToC. In these cases, the effects on safety and efficiency will be negative **(Table 16)**.

The available time for all drivers to take over control during ToC ($timeTillMRM$) is fixed to 10 s for all vehicle classes and scenarios. Note that the exact value of the $timeTillMRM$ has only an effect in relation to the driver's response time and is not as important as in reality, because the models disregard processes preceding the ToC, i.e., in contrast to reality no correlation between the available time and the post-ToC performance of the driver is assumed. The value of $10\ s$ is guided by the time that human drivers usually need to show no significantly reduced performance after a take over in driving simulator experiments, see Section 2.3. When $responseTime$ exceeds $timeTill\ MRM$ the ego vehicle will execute MRM for the time difference of the latter parameters. Thus, it is implied that higher $responseTime$ results in higher MRM frequency and consequently negative impacts on safety and efficiency **(Table 17)**.

Table 15. Expected impacts of driver response time to ToC request on safety and efficiency.

Driver Model	Parameter Name	Value	Behaviour	Safety	Efficiency
TOC/MRM	Driver response time ($responseTime$)	Long	Conservative	Negative (-)	Negative (-)
		Moderate	Moderate	Moderate	Moderate
		Short	Aggressive	Positive (+)	Positive (+)

Table 16. Expected impacts of post ToC driver performance on safety and efficiency.

Driver Model	Parameter Name	Value	Behaviour	Safety	Efficiency
TOC/MRM	Post TOC driver performance ($initialAwareness$)	High	Aggressive	Positive (+)	Positive (+)
		Moderate	Moderate	Moderate	Moderate
		Low	Conservative	Negative (-)	Negative (-)

Table 17. Expected impacts of MRM likelihood on safety and efficiency.

Driver Model	Parameter Name	Value	Safety	Efficiency
MRM	MRM likelihood	High	Negative (-)	Negative (-)
		Moderate	Moderate	Moderate
		Low	Positive (+)	Positive (+)

Driver model parameter attributes implying similar (C)AV/CV driving behaviour (aggressive, moderate, and conservative) might exert conflicting or similar effects on traffic safety and efficiency as shown in **Tables 13 – 17**. Namely, large ACC desired time headways (conservative behaviour) impact safety positively but efficiency negatively **(Table 13)**, while delayed driver response to ToC requests (conservative behaviour) impacts negatively both safety and efficiency. Thus, driver model parameter attributes are grouped into sets (parametrisation schemes) that yield similar effects to traffic safety or efficiency. The adoption of the latter approach generates five parametrisation schemes for the driver models that represent optimistic, moderate, or pessimistic cases with respect to traffic safety and efficiency impacts **(Table 18)**.

Table 18. Driver model parameter attributes per parametrisation scheme.

Parametrization Scheme	ACC	SL2015	ToC/MRM	ToC/MRM	ToC/MRM
	Desired time headway	Desired longitudinal gaps	Driver response time	Post ToC driver performance	MRM likelihood
Pessimistic Safety (PS)	Small	Short	Long	Low	High
Pessimistic Efficiency (PE)	Large	Large	Long	Low	High
Moderate Safety and Efficiency (MSE)	Moderate	Moderate	Moderate	Moderate	Moderate
Optimistic Efficiency (OE)	Small	Short	Short	High	Low
Optimistic Safety (OS)	Large	Large	Short	High	Low

3.1.5.1 Vehicle Properties

Parameter values for the driver models are specified either in the form of constant values or normal distributions. When normal distributions are used, the distribution mean and standard deviation have to be defined, as well as the lowest and highest values that can be possibly selected from the distribution. Parameter values for LV driver models are uniform for all simulation experiments and

were selected based on literature review (Erdmann, 2014; Krauß, 1998) and SUMO developers' knowledge regarding the underlying driver models acquired through previous work **(Table 19)**. Parameter values for (C)AV/CV driver models are provided in **Table 20** considering the aforementioned cases with respect to (C)AV/CV behaviour (aggressive, moderate, and conservative). These values have been selected based on literature review for the ACC and the ToC/MRM model, while parameter values for the lane change model were selected based on the parametrisation analysis of the LC2013 model presented in Chapter 2. CVs have similar parameter values with (C)AVs, except for the $responseTime$ parameter which is set equal to zero for CVs **(Table 21)**, since drivers of these vehicles are expected to instantly resume vehicle control when a take-over request is issued by the vehicle automation.

Table 19. Driver model parameter values for manual driving (LV).

Parameter Name	**Parameter description**	**Parameter values**
$sigma$	The driver's imperfection (between 0 and 1).	normal(0.2, 0.5); [0.0, 1.0]
$tau\ (s)$	The driver's desired (minimum) time headway. For the default Krauss model this is based on the net space between leader back and follower front.	normal(0.6, 0.5); [0.5, 1.6]
$decel\ (m/s^2)$	The deceleration capability of vehicles.	normal(3.5, 1.0); [2.0, 4.5]
$accel\ (m/s^2)$	The acceleration capability of vehicles.	normal(2.0, 1.0); [1.0, 3.5]
$emergencyDecel$ (m/s^2)	The maximum deceleration capability of vehicles.	9.0
$lcAssertive$	Willingness to accept lower front and rear gaps on the target lane.	1.3
$actionStepLength\ (s)$	The interval length for which a vehicle performs its decision logic (acceleration and lane-changing). The given value is processed to the closest (if possible smaller) positive multiple of the simulation step length.	0.1
$speedFactor$	The vehicles expected multiplicator for lane speed limits.	normal(1.1, 0.2); [0.8, 1.2]

Table 20. Driver Model parameter values for (C)AVs.

Parameter Name	Parameter values/(C)AV Behaviour		
	Aggressive	**Moderate**	**Conservative**
$tau\ (s)$	normal(1.2,0.1); [1.1,1.3]	normal(1.6,0.2); [1.3,1.8]	normal(2.0,0.2); [1.8,2.0]
$decel\ (m/s^2)$	normal(3.0,1.0); [2.0,4.0]	normal(3.0,1.0); [2.0,4.0]	normal(3.0,1.0); [2.0,4.0]
$accel\ (m/s^2)$	normal(1.5,1.0); [0.75,2.0]	normal(1.5,1.0); [0.75,2.0]	normal(1.5,1.0); [0.75,2.0]
$emergencyDecel\ (m/s^2)$	9.0	9.0	9.0
$actionStepLength\ (s)$	0.1	0.1	0.1
$lcAssertive$	normal(0.9,0.1); [0.8,1.0]	normal(0.7,0.1); [0.6,0.8]	normal(0.5,0.1); [0.4,0.6]
$responseTime\ (s)$	normal(7,2.1); [2,60]	normal(7,2.5); [2,60]	normal(7,3); [2,60]
$initialAwareness$	normal(0.7,0.3); [0.1,1.0]	normal(0.5,0.3); [0.1,1.0]	normal(0.3,0.3); [0.1,1.0]
$recoveryRate$	normal(0.2,0.1); [0.01,0.5]	normal(0.2,0.1); [0.01,0.5]	normal(0.2,0.1); [0.01,0.5]
$mrmDecel\ (m/s^2)$	3.0	3.0	3.0

Table 21. Driver Model parameter values for CVs.

Parameter Name	Parameter values/CV Behaviour		
	Aggressive	**Moderate**	**Conservative**
$tau\ (s)$	normal(1.2,0.1); [1.1,1.3]	normal(1.6,0.2); [1.3,1.8]	normal(2.0,0.2); [1.8,2.0]
$decel\ (m/s^2)$	normal(3.0,1.0); [2.0,4.0]	normal(3.0,1.0); [2.0,4.0]	normal(3.0,1.0); [2.0,4.0]
$accel\ (m/s^2)$	normal(1.5,1.0); [0.75,2.0]	normal(1.5,1.0); [0.75,2.0]	normal(1.5,1.0); [0.75,2.0]

$emergencyDecel$ (m/s^2)	9.0	9.0	9.0
$actionStepLength\ (s)$	0.1	0.1	0.1
$lcAssertive$	normal(0.9,0.1); [0.8,1.0]	normal(0.7,0.1); [0.6,0.8]	normal(0.5,0.1); [0.4,0.6]
$responseTime\ (s)$	0	0	0
$initialAwareness$	normal(0.7,0.3); [0.1,1.0]	normal(0.5,0.3); [0.1,1.0]	normal(0.3,0.3); [0.1,1.0]
$recoveryRate$	normal(0.2,0.1); [0.01,0.5]	normal(0.2,0.1); [0.01,0.5]	normal(0.2,0.1); [0.01,0.5]
$mrmDecel\ (m/s^2)$	3.0	3.0	3.0

3.1.6 Simulation Runs

Baseline simulation experiments are ran for three different vehicle mixes, three different traffic demand levels, and five different driver model parameter sets per scenario. Thus, 270 simulation runs have to be executed for the six scenarios considered during the 1st project iteration, without accounting for the statistical significance of the simulation output. To ensure that simulation results are statistically significant, we estimated the required number of runs per simulation experiment. Initially, five runs were performed per TransAID scenario and aggregate network-wide performance measurements were collected. Average network speed was selected as the mean statistic to estimate the required number of runs based on the following equation (Ott & Longnecker, 2004):

$$n = \frac{\left(z_{a/2}\right)^2 (s_d)^2}{E} \qquad (\dots)$$

where n is the number of required runs, $z_{a/2}$ is the critical normal distribution value for significance level $(1-a)$, s_d is the standard deviation, and E is the allowable error. The significance level was set at 95%, the tolerable error equal to 0.5 km/h, and the standard deviation was computed based on the simulation output collected during the first five simulation runs executed per scenario. The required number of runs was estimated to be 10 for each simulation scenario. The simulation time-line per simulation run spans to 1 h.

3.1.7 Simulation Output

KPIs were introduced in D2.1 for the assessment of traffic efficiency, safety, environmental impacts, and traffic dynamics at TAs before (baseline scenarios) and after (TransAID measures) the implementation of infrastructure-assisted traffic management schemes at TAs. A set of KPIs for the evaluation of the baseline simulation experiments is chosen from the comprehensive list of KPIs defined in D2.1 **(Table 22)**. These KPIs can be directly estimated and exported by SUMO as simulation output.

Table 22 List of KPIs for the evaluation of baseline simulation experiments.

KPI Name	KPI Description
Average network speed	Average space-mean speed of the vehicular fleet on a specific road network.
Space-mean speed/Edge	Mean speed estimated based on travel time along or road segment.
Total Number of Lane Changes	Number of lane changes performed in the whole network.
Time-to-collision (TTC)	The time required for two vehicles (or a vehicle and an object) to collide if they continue at their present speed and on the same path. Measures a longitudinal margin to lead vehicles or objects.
CO_2 emissions (gr)/km	Total CO_2 emitted per km travelled on the road network during the analysis period.

Traffic efficiency is interpreted through the following aggregated (network-wide) and disaggregated (local) statistics: (i) average network speeds and (ii) space-mean speed per network edge. Traffic dynamics at TAs is investigated in terms of total number of lane changes executed. Total number of lane changes is expected to show the disruption introduced due to lane change manoeuvres per traffic mix and relevant driver behaviour induced by different vehicle types. Since the objective of TransAID is to manage connected and automated vehicles in the presence of mixed traffic along TAs so as to prevent, manage, or distribute ToC/MRM, the estimation of the total number of lane changes will be useful for parallel comparison after TransAID measures encompassing lane change advice are examined.

Traffic safety can be only indirectly assessed in microscopic traffic simulations by means of surrogate safety measures[6] (SSMs). SSMs were selected based on results published in literature and are correlated with crash rates when not enough accident data is available in simulation studies. We chose time-to-collision (TTC) to indicate the probability of safety critical situations for the baseline simulation experiments. There, TTCs are measured under the following conditions: (i) follower has a higher speed than leader, (ii) they travel along the same path, and (iii) the follower's space headway is less than 50 m. We assume that events with TTC lower than three seconds are safety critical conflicts based on SUMO's default threshold for TTC and literature findings (Horst & Hogema, 1993).

Finally, environmental impacts are quantified in terms of CO_2 emissions per km travelled, which are estimated with the use of the PHEMlite model that is incorporated in SUMO. PHEMlite, is a

[6] As traffic safety itself cannot be directly observed, it is relied on other 'proxy' measures such as the space gaps and speed differences between vehicles. These measures are called 'surrogate safety measures' (SSM), and – based on results published in literature – they give an indication of a safe, unsafe, or accident situation. The SSMs can then be analysed to determine the accident risk, and in case of an accident the injury risk. As such, the type of information which should be measured in order to guarantee safety of vehicles in the context of a Transition Areas is known.

simplified version of PHEM, which is an instantaneous vehicle emission model developed by the TU Graz, and is based on an extensive European set of vehicle measurements and covers passenger cars, light duty vehicles and heavy duty vehicles from city buses up to 40 ton semi-trailers (Hausberger et al., 2011).

3.2 Second Iteration

3.2.1 Dimensions of Simulation Experiments

In the second project iteration we also consider three main dimensions (traffic demand, traffic mix, and parametrization scheme of vehicle models) with respect to the baseline simulation experiments. However, the following changes were made in comparison to the first project iteration:

1) Traffic Demand: LOS A is substituted with LOS D
2) Traffic Mix: Heavy Goods Vehicles (HGV) and Light Goods Vehicles (LGV) are introduced into the fleet composition
3) Parametrization Scheme: Aggressive/Moderate/Conservative vehicle/driver behaviour is consolidated into a single parametrization scheme

The rationale regarding the changes to the simulation input in the second project iteration is provided in Deliverable D2.2 (Wijbenga et al., 2019). Comprehensive information regarding each dimension of the baseline simulation experiments is presented in the following sections.

3.2.2 Definition of Actors

In the first version of Deliverable D3.1, vehicles were classified based on their automation, communication and fall-back performance capabilities (cf. Section 3.1.2). The initial vehicle classification is maintained in the baseline simulation experiments of the second iteration as well **(Table 6)**. Moreover, we continue to assume that 25% of CAVs/CVs will be able to handle traffic situations along TAs in automated mode, while 75% of them will be not. However, this assumption now holds only for Scenarios 1.3 and 4.1 – 5.1. In order to increase the realism of the baseline simulation experiments in the 2nd project iteration we introduce Day 1 C-ITS applications in Scenarios 2.1, 2.3 and 4.2. Thus, drivers of CVs are manually taking over vehicle control upon message reception upstream of the TA, while CAVs are grouped in two distinct categories (CAV_G1 and CAV_G2) that exhibit different behaviour. The first group of CAVs (CAV_G1) will be issuing TORs upon message reception, while the second group of CAVs (CAV_G2) will be able to cope with incidents and work zones in automated mode unless lane changing becomes challenging due to dense surrounding traffic. In the latter case, TORs will be triggered dynamically with situation specific available lead times (cf. Section 2.3.2.2). Additionally, we note that drivers of CAVs_G2 will be able to take-over vehicle control more easily compared to drivers of CAVs_G1 due to increased situational awareness and recovery rate resulting from the C-ITS message reception. Thus, we consider the case that connectivity influences the fall-back performance of the DVU.

In the first project iteration we suggested that driver's distraction during ToC might lead to uncontrolled driving for CVs. However, production ready CVs equipped with automation systems of Level 1 and 2 apply emergency braking in case of unsuccessful system-initiated control transitions. In our baseline simulation experiments for the second project iteration we finally decided not to examine the latter emergency braking events so as to explicitly capture the traffic disruption occurring from control transitions of Level 3 and 4 automated vehicles (which is the

scope of TransAID). However, and to this end, we enhanced the capabilities of the ToC/MRM model so that control transitions can be dynamically triggered by the automation according to the complexity of traffic conditions as aforementioned. Hence, the realism of vehicle disengagements for Level 3 and 4 CAVs in our baseline simulation experiments is significantly increased.

3.2.3 Traffic Composition

In the first project iteration we indicated that we are going to consider non-cooperative/connected AVs in the second project iteration. However, as explained in the second version of Deliverable D2.2 vehicle interactions are already complex in the presence of the vehicle classes examined in the baseline simulation experiments of the first iteration. Thus, non-cooperative/connected AVs will be only implicitly considered in the traffic management simulation experiments by assuming a compliance rate for CVs/CAVs (non-compliance resulting from not understanding or receiving messages). Therefore, we use the same artificial mixes for CAVs/CVs/ as in the first project iteration **(Table 7)**. However, we introduce HGVs and LGVs in our simulation experiments. Distribution for passenger cars, LGVs, and HGVs for both urban road and motorways are determined by studying reports from the Belgian road authorities and the TREMOVE project and are depicted in **Table 23**.

Table 23. Distribution of passenger vehicles, LGVs and HGVs on urban roads and motorways.

Vehicle type	Share on urban roads	Share on motorways
Passenger vehicle	87%	77%
LGV	10%	10%
HGV	3%	13%

3.2.4 Traffic Demand Levels

During the first project iteration three different traffic demand levels were considered corresponding to Levels of Service (LOS) A, B, and C. Consideration was also given to road type (urban, rural, and motorway) for the selection of the corresponding hourly volume per LOS. Higher demand levels were not considered initially due to the following reasons:

- insufficient capacity remains to efficiently manage traffic,
- marginal impact of ToC/MRM is expected on the traffic flow, and
- high variability of results (difficult to map KPIs to a specific cause).

However, simulation results presented in Deliverables D3.1 and D4.2 during the first iteration showed that further examination of LOS A is of limited interest. For all the examined scenarios (i.e. 1.1, 2.1, 3.1, 4.2, and 5.1) free-flow traffic conditions prevailed irrespective of the traffic mix and the parametrization of the vehicle/driver models. Thus, the benefits generated by the implementation of the TransAID measures were of minor significance. On the contrary, it was observed that for some scenarios (1.1, 4.2 – Urban), the examination of LOS D would be meaningful, since traffic conditions did not substantially deteriorate for LOS C. Hence, if demand is increased and traffic flow performance is reduced in the baseline simulations, it can be expected that the implementation of the TransAID measures will yield benefits that are more substantial. Therefore, we exclude LOS A and include LOS D with respect to the baseline simulations of the scenarios selected for the second project iteration. The hourly volumes per lane corresponding to the proposed LOS and the respective intensity/capacity ratios are depicted in **Table 24**.

Table 24. Vehicles/hour/lane for LOS B, C and D in urban, rural, and motorway facilities.

Facility Type	Capacity (veh/h/l)	Level of Service (LOS)		
		B	C	D
Urban (50km/h)	1500 veh/h/l	825	1155	1386
Rural (80 km/h)	1900 veh/h/l	1045	1463	1756
Motorway (120 km/h)	2100 veh/h/l	1155	1617	1940
Intensity / Capacity (IC) ratio		0,55	0,77	0.92

Since the capacity of the merge segment is controlled by the capacity of the exiting section (as highlighted in (HCM, 2010)), LOS B, C, and D in scenario 2.1 should be calibrated to determine the traffic demand levels on the on-ramp and on the mainline respectively, shown in **Table 25**. Henceforward, the vehicle inputs on the on-ramp and on the mainline can be derived from **Table 25**.

The two entry links – the upstream motorway entry link and the on-ramp – are then injected with approximately 3/4 and 1/4 of the respective rates.

Table 25. Vehicles/hour/lane for Level of Service A, B and C (Scenario 2.1).

Facility Type	Capacity (veh/h/l)	Level of Service (LOS)		
		B	C	D
On-ramp (100km/h)	2000 veh/h/l	880	1280	1460
Intensity (demand volume)/Capacity (IC or VC) ratio		0.44	0.64	0.73
Motorway (100 km/h)	2000 veh/h/l	960	1400	1600
Intensity (demand volume)/Capacity (IC or VC) ratio		0.48	0.7	0.80

3.2.5 Parametrisation of Vehicle/Driver Models

In the first project iteration we developed a scheme to investigate the effects that different parametrizations of the vehicle automations would inflict on safety and traffic efficiency. Namely, we adjusted specific parameters of the vehicle/driver models **(Table 12)**, we developed to emulate automated driving, so that we can analyse the impacts of different AV behaviours (aggressive, moderate, and conservative) on safety and traffic flow performance. The outcomes of the proposed parametrization scheme that was adopted for the baseline simulation experiments of the first project iteration were summarized in the first version of this Deliverable D3.1 (cf. Section 5.1). In the second project iteration we unify the full spectrum of AV behaviour into a single parametrization scheme to accurately reflect actual traffic conditions in our baseline simulation experiments.

Corresponding parameter values for the vehicle/driver models are provided in the following section per simulated vehicle class.

3.2.5.1 Vehicle Properties

As in the first project iteration parameter values for the vehicle/driver models are specified either in the form of constant values or normal distributions. When normal distributions are used, the distribution mean and standard deviation have to be defined, as well as the lowest and highest values that can be possibly selected from the distribution. Since we use one distribution per model parameter to encapsulate varying vehicle/driver behaviour in the new parametrization scheme, the mean, standard deviation and bounds of these distributions are adjusted accordingly.

Parameter values for LVs are shown in **Table 26**. They are similar to the first project iteration with the exception of the $lcAssertive$ calibration parameter. Based on the simulation findings of the first project iteration with respect to the parametrization of the lane change model it was identified that $lcAssertive = 1.3$ represents rather aggressive lane change behaviour for LVs. Thus, we introduce a distribution for the selection of $lcAssertive$ values for LVs that corresponds to a wider range of safe gaps for lane changing which are though more conservative compared to the ones accepted in the first project iteration.

Table 26. Driver model parameter values for manual driving (LV).

Parameter Name	Parameter description	Parameter values
$sigma$	The driver's imperfection (between 0 and 1).	normal(0.2, 0.5); [0.0, 1.0]
$tau\ (s)$	The driver's desired (minimum) time headway. For the default Krauss model this is based on the net space between leader back and follower front.	normal(0.6, 0.5); [0.5, 1.6]
$decel\ (m/s^2)$	The deceleration capability of vehicles.	normal(3.5, 1.0); [2.0, 4.5]
$accel\ (m/s^2)$	The acceleration capability of vehicles.	normal(2.0, 1.0); [1.0, 3.5]
$emergencyDecel\ (m/s^2)$	The maximum deceleration capability of vehicles.	9.0
$lcAssertive$	Willingness to accept lower front and rear gaps on the target lane.	normal(1.2, 0.05); [1.1, 1.3]
$actionStepLength\ (s)$	The interval length for which a vehicle performs its decision logic (acceleration and lane-changing). The given value is processed to the closest (if possible smaller) positive multiple of the simulation step length.	0.1
$speedFactor$	The vehicles expected multiplicator for lane speed limits.	normal(1.1, 0.2); [0.8, 1.2]

Parameter values for CVs are shown in **Table 27**. In contrast to the first project iteration we increase the $responseTime$ to TORs to 1.5 secs (previously selected to be 0 secs which is not practically feasible). Moreover, we also increase the $initialAwareness$ and $recoveryRate$ as we assume that drivers of CVs are continuously monitoring the primary driving task and can instantly take-over vehicle control if required.

Table 27. Driver Model parameter values for CVs.

Parameter Name	Parameter description	Parameter values
$tau\ (s)$	The driver's desired (minimum) time headway.	0.6
$tauCACCToACC\ (s)$	The driver's desired (minimum) time headway when switching from CACC to ACC model.	normal(1.5,0.2); [1.1,2.0]
$decel\ (m/s^2)$	The deceleration capability of vehicles.	normal(3.0,1.0); [2.0,4.0]
$accel\ (m/s^2)$	The acceleration capability of vehicles.	normal(1.5,1.0); [0.75,2.0]
$emergencyDecel\ (m/s^2)$	The maximum deceleration capability of vehicles.	9.0
$lcAssertive$	Willingness to accept lower front and rear gaps on the target lane.	normal(1.15, 0.05); [1.1, 1.25]
$actionStepLength\ (s)$	The interval length for which a vehicle performs its decision logic (acceleration and lane-changing). The given value is processed to the closest (if possible smaller) positive multiple of the simulation step length.	0.1
$responseTime\ (s)$	The time it takes the driver after the TOR to take back the control over the vehicle.	1.5
$initialAwareness$	The awareness assigned to the driver after a ToC. The value must lie within [0.0, 1.0], where 1.0 corresponds to normal driving performance and lower values lead to increased perception errors.	normal(0.7,0.2); [0.6,1.0]
$recoveryRate$	The rate (in [1/s]) at which the driver's performance recovers after the ToC.	normal(0.2,0.1); [0.1,0.5]
$mrmDecel\ (m/s^2)$	The braking rate at which the vehicle brakes if the driver does not take back control within a specified time.	3.0

Due to the deployment of Day 1 C-ITS applications in Scenarios 2.3 and 4.2 of the second project iteration we divided CAVs into two groups according to their capabilities to deal with TAs (cf.

Section 3.2.2). The first group of CAVs (CAV_G1) cannot deal with TAs and thus triggers TOR at fixed locations upon message reception, while CAVs belonging to the second group (CAV_G2) only trigger TOR dynamically if strategic lane changing is blocked by surrounding traffic (message reception does not trigger ToC). Thus, we assume that CAVs_G2 have shorter $responseTime$ and increased $initialAwareness$ and $recoveryRate$ compared to CAVs_G1. Moreover, we assume that CAVs considered in Scenarios 1.3 and 4.1 – 5.1 belong to the first group (CAVs_G1) in the baseline simulation experiments. Parameter values for CAVs_G1 are presented in **Table 28**, and for CAVs_G2 are depicted in **Table 29**.

Table 28. Driver Model parameter values for CAVs_G1.

Parameter Name	Parameter description	Parameter values
$tau\ (s)$	The driver's desired (minimum) time headway.	0.6
$tauCACCToACC\ (s)$	The driver's desired (minimum) time headway when switching from CACC to ACC model.	normal(1.5,0.2); [1.1,2.0]
$decel\ (m/s^2)$	The deceleration capability of vehicles.	normal(3.0,1.0); [2.0,4.0]
$accel\ (m/s^2)$	The acceleration capability of vehicles.	normal(1.5,1.0); [0.75,2.0]
$emergencyDecel\ (m/s^2)$	The maximum deceleration capability of vehicles.	9.0
$lcAssertive$	Willingness to accept lower front and rear gaps on the target lane.	normal(0.85, 0.02); [0.8, 0.9]
$actionStepLength\ (s)$	The interval length for which a vehicle performs its decision logic (acceleration and lane-changing). The given value is processed to the closest (if possible smaller) positive multiple of the simulation step length.	0.1
$responseTime\ (s)$	The time it takes the driver after the TOR to take back the control over the vehicle.	normal(7,2.1); [2,60]
$initialAwareness$	The awareness assigned to the driver after a ToC. The value must lie within [0.0, 1.0], where 1.0 corresponds to normal driving performance and lower values lead to increased perception errors.	normal(0.3,0.3); [0.1,1.0]
$recoveryRate$	The rate (in [1/s]) at which the driver's performance recovers after the ToC.	normal(0.2,0.1); [0.01,0.5]
$ogNewTimeHeadway$	The target time headway during the preparatory phase before a ToC.	1.6

$ogChangeRate$	The change rate of headway adaption during the preparatory phase before a ToC.	0.8
$mrmDecel\ (m/s^2)$	The braking rate at which the vehicle brakes if the driver does not take back control within a specified time.	3.0

Table 29. Driver Model parameter values for CAVs_G2.

Parameter Name	Parameter description	Parameter values
$tau\ (s)$	The driver's desired (minimum) time headway.	0.6
$tauCACCToACC\ (s)$	The driver's desired (minimum) time headway when switching from CACC to ACC model.	normal(1.5,0.2); [1.1,2.0]
$decel\ (m/s^2)$	The deceleration capability of vehicles.	normal(3.0,1.0); [2.0,4.0]
$accel\ (m/s^2)$	The acceleration capability of vehicles.	normal(1.5,1.0); [0.75,2.0]
$emergencyDecel\ (m/s^2)$	The maximum deceleration capability of vehicles.	9.0
$lcAssertive$	Willingness to accept lower front and rear gaps on the target lane.	normal(0.85, 0.02); [0.8, 0.9]
$actionStepLength\ (s)$	The interval length for which a vehicle performs its decision logic (acceleration and lane-changing). The given value is processed to the closest (if possible smaller) positive multiple of the simulation step length.	0.1
$responseTime\ (s)$	The time it takes the driver after the TOR to take back the control over the vehicle.	normal(4,2); [2,15]
$initialAwareness$	The awareness assigned to the driver after a ToC. The value must lie within [0.0, 1.0], where 1.0 corresponds to normal driving performance and lower values lead to increased perception errors.	normal(0.6,0.2); [0.3,1.0]
$recoveryRate$	The rate (in [1/s]) at which the driver's performance recovers after the ToC.	normal(0.3,0.1); [0.1,0.5]
$ogNewTimeHeadway$	The target time headway during the preparatory phase before a ToC.	1.6
$ogChangeRate$	The change rate of headway adaption during the preparatory phase before a ToC.	0.8

$mrmDecel\ (m/s^2)$	The braking rate at which the vehicle brakes if the driver does not take back control within a specified time.	3.0

Finally, parameter values are provided for HGVs and LGVs in **Tables 30 – 31**.

Table 30. Driver Model parameter values for HGVs.

Parameter Name	Parameter description	Parameter values
$sigma$	The driver's imperfection (between 0 and 1).	normal(0.1, 0.2); [0.0, 1.0]
$tau\ (s)$	The driver's desired (minimum) time headway. For the default Krauss model this is based on the net space between leader back and follower front.	normal(1.2, 0.5); [1.0, 1.6]
$decel\ (m/s^2)$	The deceleration capability of vehicles.	normal(4.0, 1.0); [2.0, 5.0]
$accel\ (m/s^2)$	The acceleration capability of vehicles.	normal(2.0, 1.0); [1.0, 3.0]
$maxSpeed\ (m/s)$	The vehicle's maximum velocity.	25
$vClass$	An abstract vehicle class.	truck
$length\ (m)$	The vehicle's netto-length.	15
$width\ (m)$	The vehicle's width.	2.4
$emergencyDecel\ (m/s^2)$	The maximum deceleration capability of vehicles.	9.0
$lcAssertive$	Willingness to accept lower front and rear gaps on the target lane.	normal(1.0, 0.05); [0.9, 1.1]
$actionStepLength\ (s)$	The interval length for which a vehicle performs its decision logic (acceleration and lane-changing). The given value is processed to the closest (if possible smaller) positive multiple of the simulation step length.	0.1
$speedFactor$	The vehicles expected multiplicator for lane speed limits.	normal(1.0, 0.1); [0.9, 1.1]
$emissionClass$	The emission class of the vehicle type.	HBEFA3/HDV_D_EU4

Table 31. Driver Model parameter values for LGVs.

Parameter Name	Parameter description	Parameter values
$sigma$	The driver's imperfection (between 0 and 1).	normal(0.1, 0.2); [0.0, 1.0]
$tau\ (s)$	The driver's desired (minimum) time headway. For the default Krauss model this is based on the net space between leader back and follower front.	normal(1.0, 0.3); [0.7, 1.6]
$decel\ (m/s^2)$	The deceleration capability of vehicles.	normal(4.5, 1.0); [2.0, 5.0]
$accel\ (m/s^2)$	The acceleration capability of vehicles.	normal(2.5, 1.0); [1.0, 3.5]
$vClass$	An abstract vehicle class.	delivery
$length\ (m)$	The vehicle's netto-length.	8
$width\ (m)$	The vehicle's width.	2.0
$emergencyDecel\ (m/s^2)$	The maximum deceleration capability of vehicles.	9.0
$lcAssertive$	Willingness to accept lower front and rear gaps on the target lane.	normal(1.1, 0.05); [1.0, 1.1]
$actionStepLength\ (s)$	The interval length for which a vehicle performs its decision logic (acceleration and lane-changing). The given value is processed to the closest (if possible smaller) positive multiple of the simulation step length.	0.1
$speedFactor$	The vehicles expected multiplicator for lane speed limits.	normal(1.0, 0.1); [0.9, 1.1]
$emissionClass$	The emission class of the vehicle type.	HBEFA3/LDV_D_EU4

3.2.6 Simulation Runs

Baseline simulation experiments are run for three traffic demand levels, three vehicle mixes, and one driver model parameter set per scenario in the second project iteration. Thus, 54 simulation runs have to be executed for the six scenarios considered during the 1st project iteration, without accounting for the statistical significance of the simulation output. To ensure that simulation results are statistically significant, we estimated the required number of runs per simulation experiment following the same approach as in the first project iteration (cf. Section 3.1.6). The required number of runs was estimated to be 10 for each simulation scenario.

3.2.7 Simulation Output

A list of KPIs proposed in **Table 22** was used for the evaluation of the baseline simulation experiments in the first project iteration. The latter list was comprised of KPIs for the evaluation of safety, traffic efficiency and environmental impacts of control transitions. The safety and environmental KPIs used in the first project iteration (i.e. number of critical events and CO_2 emissions per km travelled) are maintained in the second project iteration as well. On the contrary, we use new KPIs for the assessment of traffic efficiency in the baseline simulation experiments. Moreover, we introduce explicit KPIs for the quantitative analysis of control transitions.

Instead of estimating average network speed (averaging edge speeds weighted by the respective edge flows) to assess network-wide traffic efficiency, we now calculate mean travel time per km travelled for the entire network and fleet. The latter KPI represents more accurately prevailing traffic conditions in our simulation analysis. Additionally, we create tempo-spatial contour plots of speed and flow based on output from simulation detectors, and vehicle trajectory plots (vehicle location over time) on a lane basis. The contour and trajectory plots facilitate the visualization of traffic disruption stemming from control transitions and differences in car-following behaviour between ACC, CACC and manual driving modes. Finally, we also estimate KPIs to explicitly examine ToC/MRM events (i.e. duration of ToCs/MRMs and proportion of MRMs). The complete list of KPIs and the respective SUMO data sources used for their estimation in the baseline simulation experiments of the second project iteration are presented in **Table 32**.

Table 32. List of KPIs for the evaluation of baseline simulation experiments.

KPI	Units	Description	Data source
Travel time	sec/km	The trip duration of vehicles per distance travelled.	SUMO: trip information output
Mean speed for selected cross sections	km/h	Time average of the observed speed at given locations in the road network.	SUMO: virtual induction loop
Mean flow for selected cross sections	#Vehicles/h	Time average of the observed flow at given locations in the road network.	SUMO: virtual induction loop
Vehicle trajectory	-	Vehicle location over time.	SUMO: vehicle probe data
Number of lane changes	#LCs/km	Number of lane changes per kilometre travelled	SUMO: lane change output
Number of critical events	#Events/km	Number of observed episodes with a time-to-collision value below a given threshold θ divided by the total kilometres travelled.	SUMO: trip information output and SSM device output
CO_2 emissions	g/km	Carbon dioxide emissions per kilometre	SUMO: trip information output

		travelled	and emissions output (PHEMlight model)
Duration of ToCs	s	Average duration of control transitions.	SUMO: ToC device output
Proportion of MRMs	-	Number of initiated minimum risk manoeuvres divided by the number of AVs.	SUMO: ToC device output
Duration of MRMs	s	Average duration of initiated minimum risk manoeuvres.	SUMO: ToC device output

4 Baseline Simulation Scenarios

4.1 First Iteration

4.1.1 Scenario 1.1 Provide path around road works via bus lane

4.1.1.1 Scenario Description

In the case of road works, the existence of a bus lane serves as an alternative route to circumvent lane closures. However, (C)AVs/CVs might not be able to understand that driving on the bus lane is permitted in the given situation (unable to detect correct road lane markings), and therefore ToCs become mandatory. Especially in urban situations, such lane markings may not always be available (in every country). If the road side infrastructure (RSI) provides an explicit path around the road works, (C)AVs/CVs can drive without disrupting their AD mode (preventing ToCs). Thus, it is clear where the (C)AV/CV can break the traffic rules and drive across the bus lane.

In this scenario, road works are carried out on a two-lane urban road adjacent to a bus lane **(Figure 20)**. The RSI has planned a path and distributes it; thus, when (C)AVs/CVs approach the road works, they receive the path information from the RSI which allows them to drive around the road works.

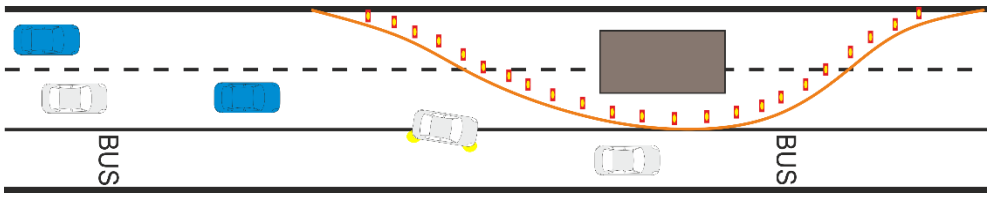

Figure 20. Schematic overview of Scenario 1.1.

More details about the simulation network of Scenario 1.1 can be found in **Table 33.**

Table 33. Network configuration details for Scenario 1.1.

Scenario 1.1	Settings	Notes
Road section length	1.85 km	
Road priority	3	
Allowed road speed	13.89 m/s	• 50 km/h
Number of nodes	11	• n0 – n10
Number of edges	10	
Number of O-D relations	1	• from n0 to n8
Number of lanes	3	• 2 normal lanes; 1 bus lane (the rightmost lane)
Work zone location	from n5 to n6	• 250 m
Closed edges[1, 2] (defined in the file closeLanes.add.xml)	workzone	• 2 normal lanes
	safetyzone1_1	• the leftmost lane
	safetyzone1_2	• 2 normal lanes
	safetyzone2_1	• 2 normal lanes
	safetyzone2_2	• the leftmost lane

Disallowed vehicle classes	• normal lanes: pedestrians, tram, rail_urban, rail, rail_electric, ship	• from n0 to n10
	• bus lane: all expect buses, coaches and emergency vehicles	• from n0 to n2 • from n9 to n10
	• bus lane: same as the normal lanes with custom_1	• from n2 to n9 • custom_1: AVs without providing information
Filenames	• network: UC1_1.net.xml • lane closure: closeLanes.add.xml • traffic signs: shapes.add.xml	
Intended control of lane usage Around the construction site, the bus lane's *vClass* permissions are altered to allow all classes but the class 'custom1' which is assigned to automated vehicles, which were not informed about the possible circumvention along the bus lane. As soon as they are informed, their *vClass* should be switched to the default class ("passenger"), which in turn allows them to use the bus lane in the specified region.		
Network layout 		
Road segments n0→n1: Insertion and backlog area (300 m) n0→n2: Bus only on bus lane (650 m) n2→n9: all *vClasses* but uninformed automated allowed (class "custom1") on bus lane (800 m) n3→n4: the leftmost lane closed (safety zone 1_1) (25 m) n4→n5: the second leftmost lane closed as well (safety zone 1_2 (25 m)) n5→n6: the second leftmost lane closed as well (work site (250 m)) n6→n7: the second leftmost lane closed as well (safety zone 2_1 (25 m)) n7→n8: the leftmost lane closed (safety zone 2_2 (25 m)) n9→n10: Bus only on bus lane (400 m)		

[1] Required minimum safety distance according to the German Technical Rules for Workplaces ASR A5.2: 10 m with allowed maximum speed 30 km/h; 50 m with allowed maximum speed 50 km/h; 100 m with allowed maximum speed 100 km/h. Each safety area is divided into two parts: one is with one-lane closure and the other one is with two-lane closure for smoother transition; [2] The placement of the traffic signs is based on the German Guidelines for road job security (RSA).

4.1.1.2 Results

4.1.1.2.1 Impacts on Traffic Efficiency

Network-wide Impacts

Figure 21 shows the average network speed in the different scenarios. The two columns of the figure show the same data in a distinct grouping to allow an easier visual assessment with respect to the different traffic mixes (left column) and the different levels of service (right column).

For the first column we observe that regardless of the level of service and the parameter scheme, the average speed is decreasing with an increased share of automated vehicles. This capacity loss by the introduction of automated vehicles in the absence of special measures is caused by different factors, which affect the dynamics of automated vehicle models: (i) the required headway is estimated larger for automated vehicles, (ii) their acceleration rate is lower (the downstream end of jams dissolves slower), (iii) driver performance decreases after ToC, and (iv) MRMs may occur.

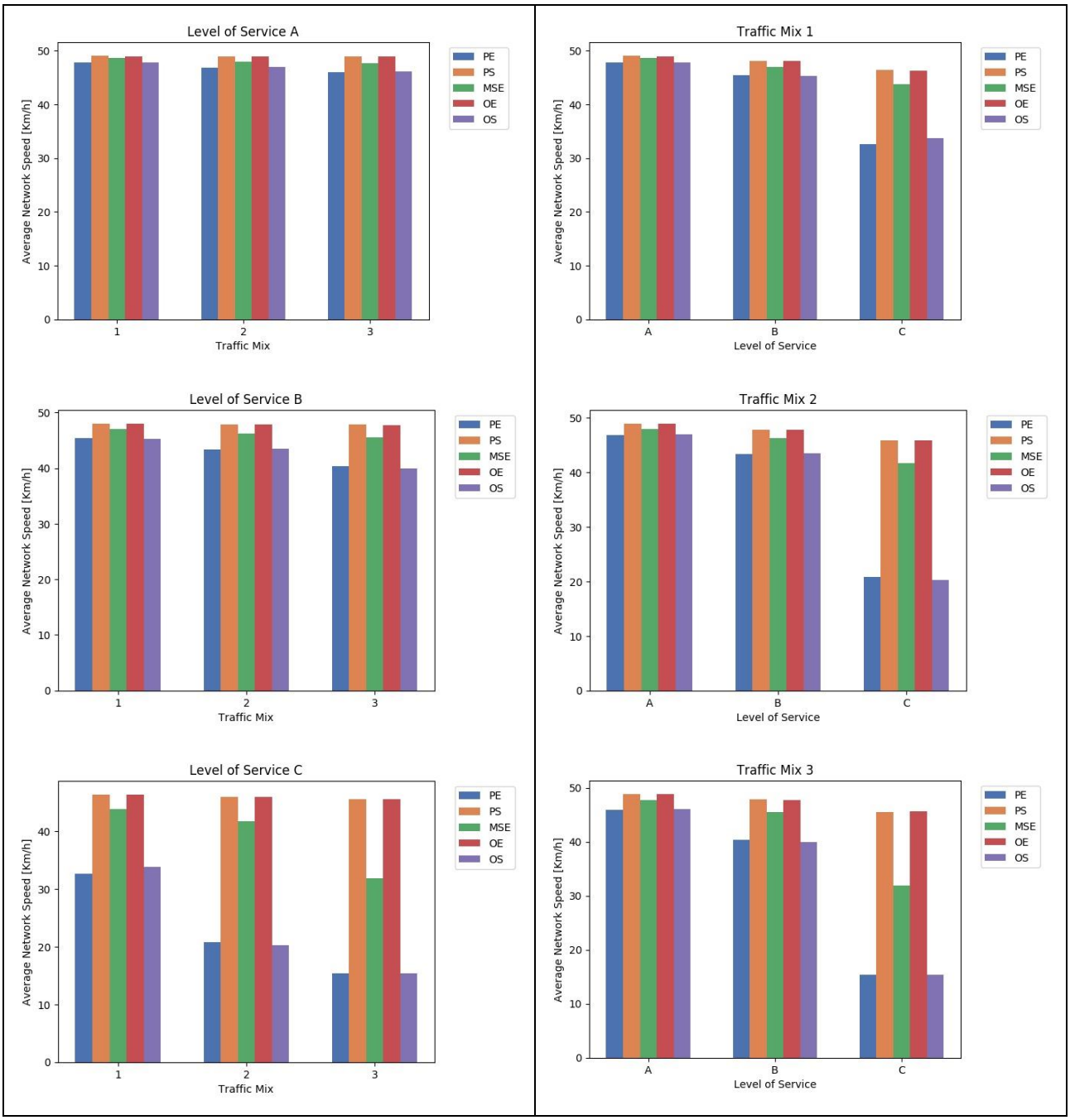

Figure 21. Average network speed for Scenario 1.1 baseline simulation experiments (varying parameter scheme, LOS, and traffic mix). Different bar colours correspond to different parameter schemes. The left column groups results by LOS, the right column by traffic mix.

The right column shows, that accordingly the average speed decrease from LOS A to LOS B is more dramatic in the presence of a larger number of CAVs/CVs, as these decrease the capacity and consequently the region of free flow.

Local Impacts

Figure 22 shows the average speed (taken over 5 minutes) on the edge 'approach_2', which is located just before the bottleneck induced by the subsequent lane drops at the beginning of the

construction site, see **Figure 23**. The left column shows the results for different shares of AVs for LOS C and the right column for different LOS levels for traffic mix 3. The average speed drops for the parameter schemes OS and PE already at LOS B to some intermediate state, and completely deteriorates at LOS C indicating heavy merging problems at the beginning of the construction side. Level MSE also show a tendency for passing the point to the congestion-induced capacity drop as can be suspected from the long term transient for the combination LOS C / Mix 3.

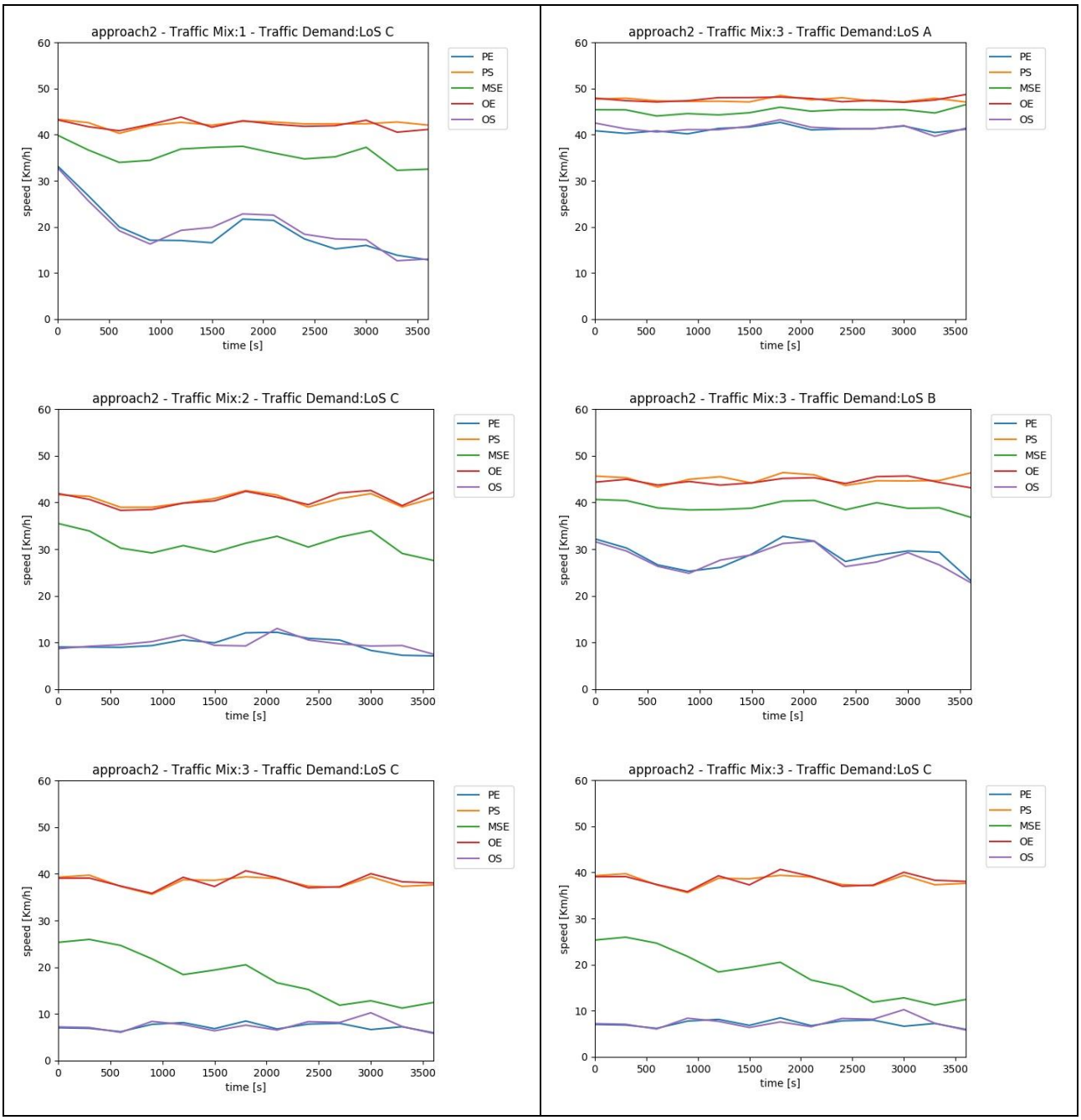

Figure 22. Average speed at the edge ‘approach_2’ for the different parameter sets. Left column: varying traffic mix at LOS C; right column: varying demand level at traffic mix 3.

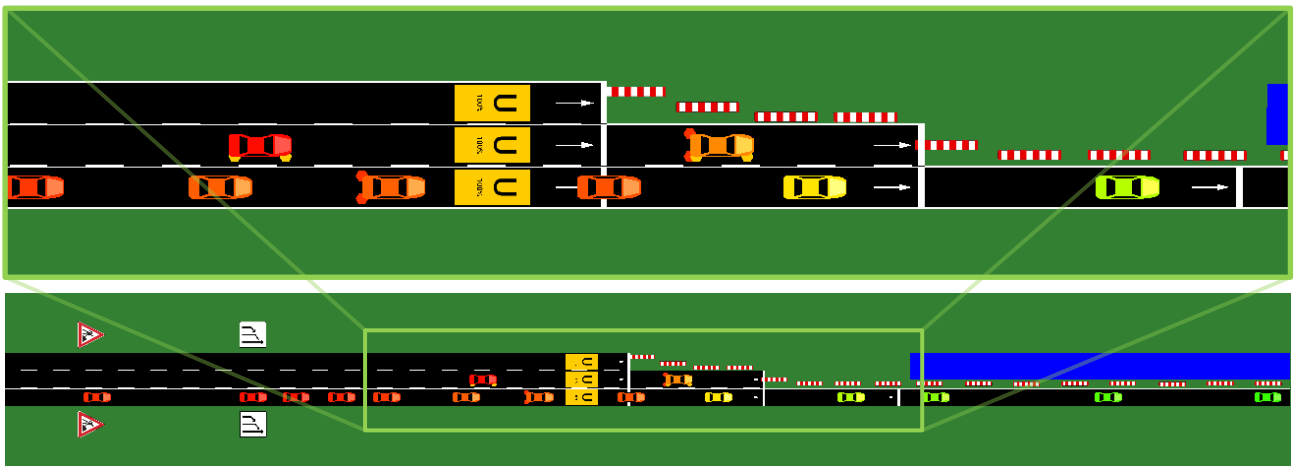

Figure 23. Queueing situation at the merge point, where two lanes are closed. Vehicles are coloured according to their current speed, with red corresponding to speeds close to 0 km/h and green to 50 km/h.

In **Figure 24** we show the average lengths of the queues (during the last 150 seconds) building up on the edge 'approach_2' during the simulation. The queue length is defined as the back position of the last vehicle on the edge, which is slower than 5 km/h.

For congested scenarios a constant queue of length ~250 m builds up on the edge 'approach_2' (the edge's length is 350 m), while in other scenarios (Mix 1/LOS C and Mix 3/LOS B) the queue length strongly fluctuates during alternating episodes of relatively smooth flow and disruptions arising from merging problems. Note the inhomogeneous length-scale on the ordinate.

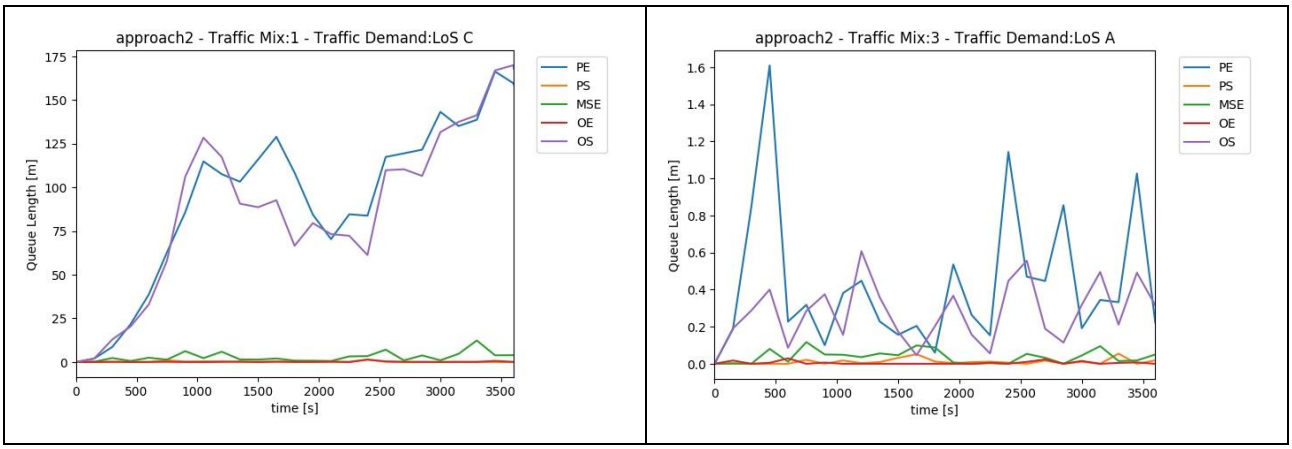

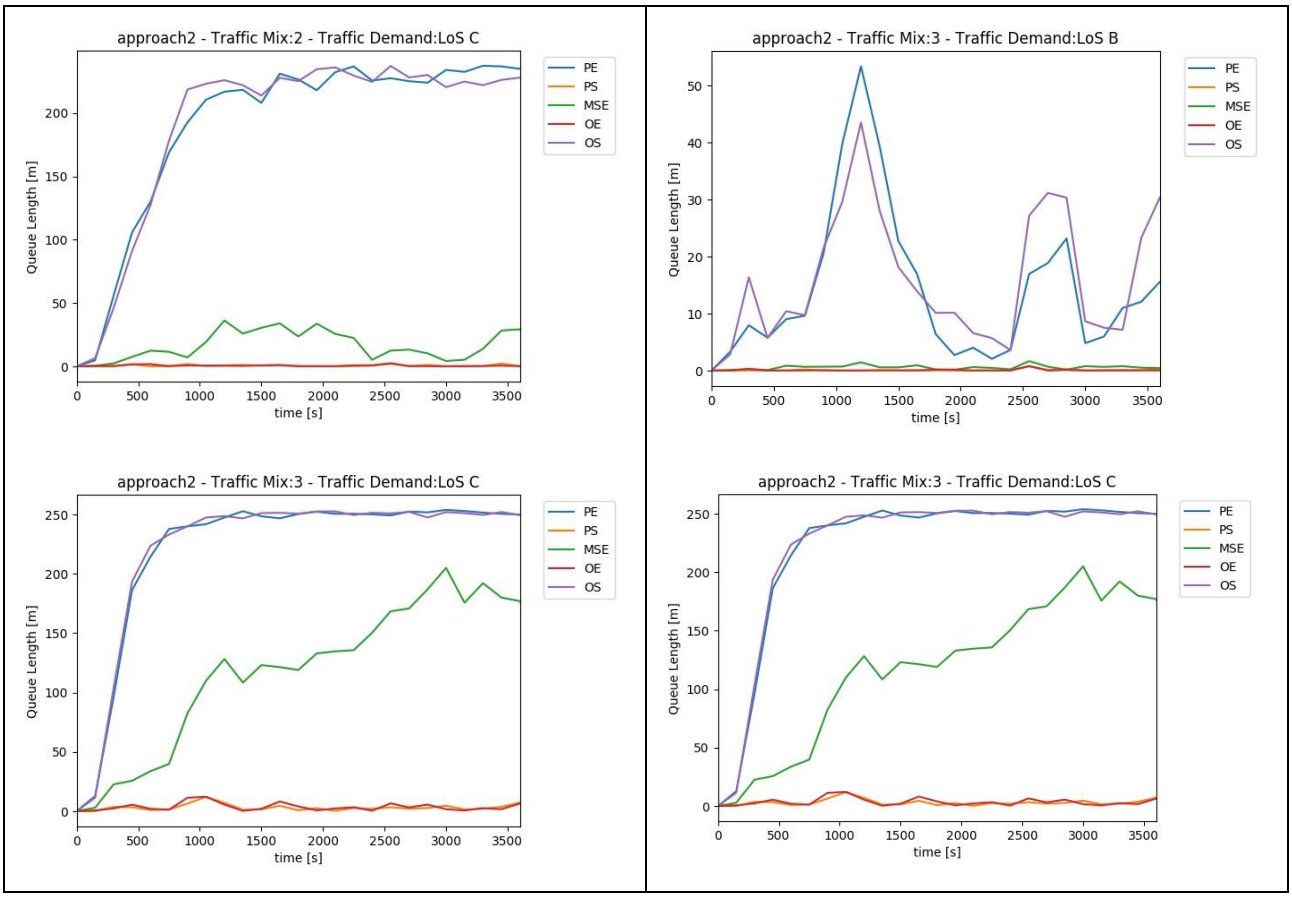

Figure 24. Average queue length at the edge 'approach_2' for the different parameter sets. Left column: varying traffic mix at LOS C; right column: varying demand level at traffic mix 3.

4.1.1.2.2 Impacts on Traffic Dynamics

Figure 25 shows the total number of lane changes for each simulated scenario (accumulated over the ten executed runs). For mainly uncongested scenarios (LOS A and B, and LOS C for parameter schemes OE/PS) the number varies only slightly and is roughly proportional to the number of vehicles with a constant factor of approximately three lane changes per vehicle, indicating homogeneous flow conditions.

For congested conditions, the number of lane changes per vehicle increases, cf. LOS C simulations for parameter schemes PE/OS, and to some also scheme MSE for traffic mix 3. Interestingly, the number does not seem to be a monotonic function of the share of CAVs/CVs, respectively the congestion level, as one can observe a decrease from mix 2 to mix 3 for LOS C.

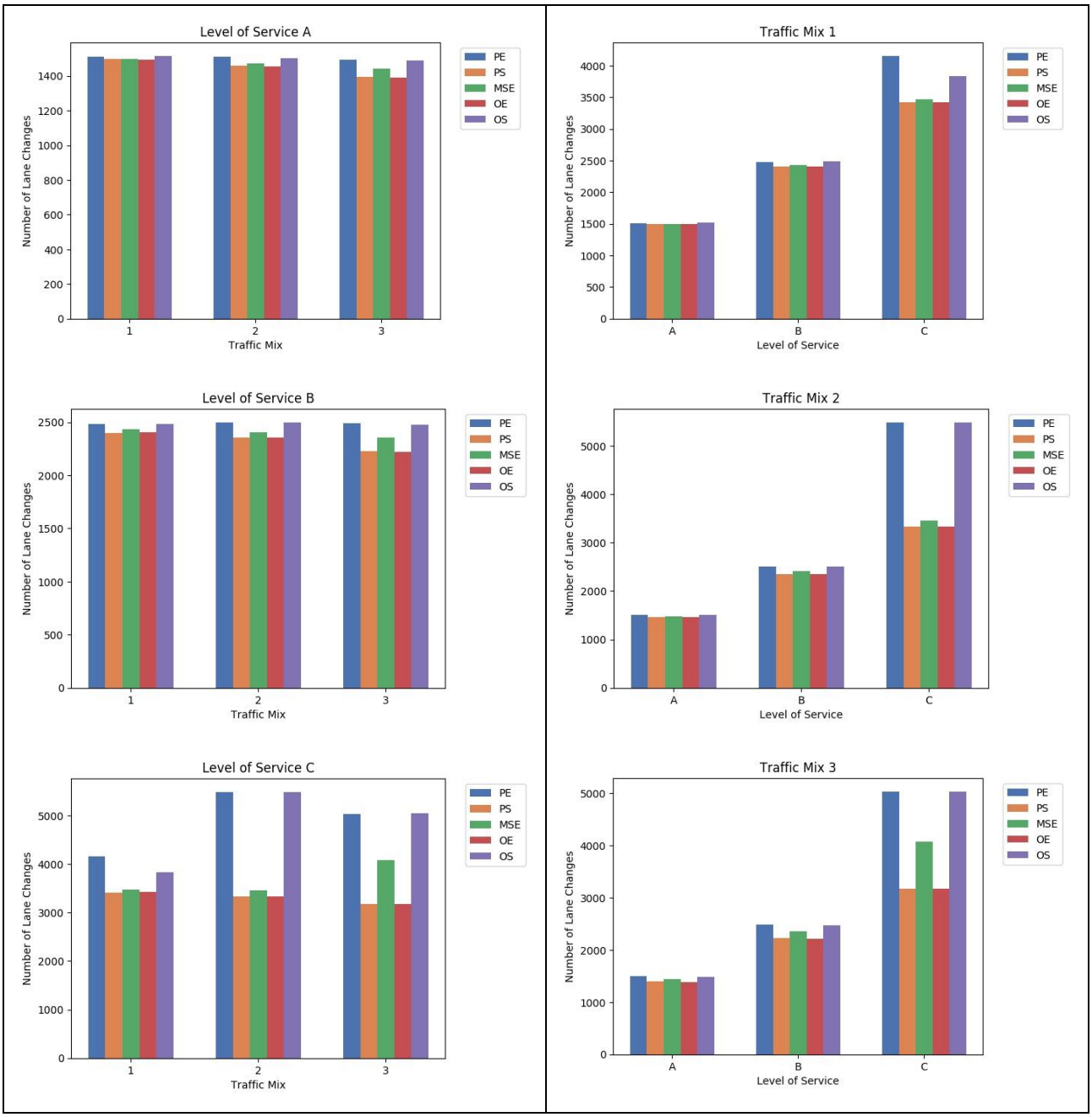

Figure 25. Number of lane changes for Scenario 1.1 baseline simulation experiments (varying parameter scheme, LOS, and traffic mix). Different bar colours correspond to different parameter schemes. The left column groups results by LOS, the right column by traffic mix.

4.1.1.2.3 Impacts on Traffic Safety

Figure 26 shows the average number of events with TTC below three seconds (termed 'critical' below). The dependence on the LOS is monotonic by and large, giving an increasing number of critical events for increasing demand. In dependence of the traffic mix the number of TTCs seems to have a more complex form for several parameter schemes and LOSs.

Most notable there seems to be a positive influence of efficiency on safety in the scenario (in terms of TTC frequency) as higher values for the efficiency indicators (See Section 4.1.2.1) correlate with

a lower number of TTCs below three seconds. This effect even overrules the direct injection of parameter values, which seem favourable for the traffic safety (e.g., larger desired gaps and decreased perception errors), but may have an adverse effect on the efficiency.

The main reason for critical situations observed in the simulations is the reduction of the number of lanes. Indeed, the situations, where the increased TTCs are recorded almost always correspond to rear end conflicts involving vehicles, which have to reduce their speed significantly because they could not find a merging gap on their right before the end of a lane in time, see Sections 4.4.2.1.3 and 4.4.2.2.3 for similar phenomena.

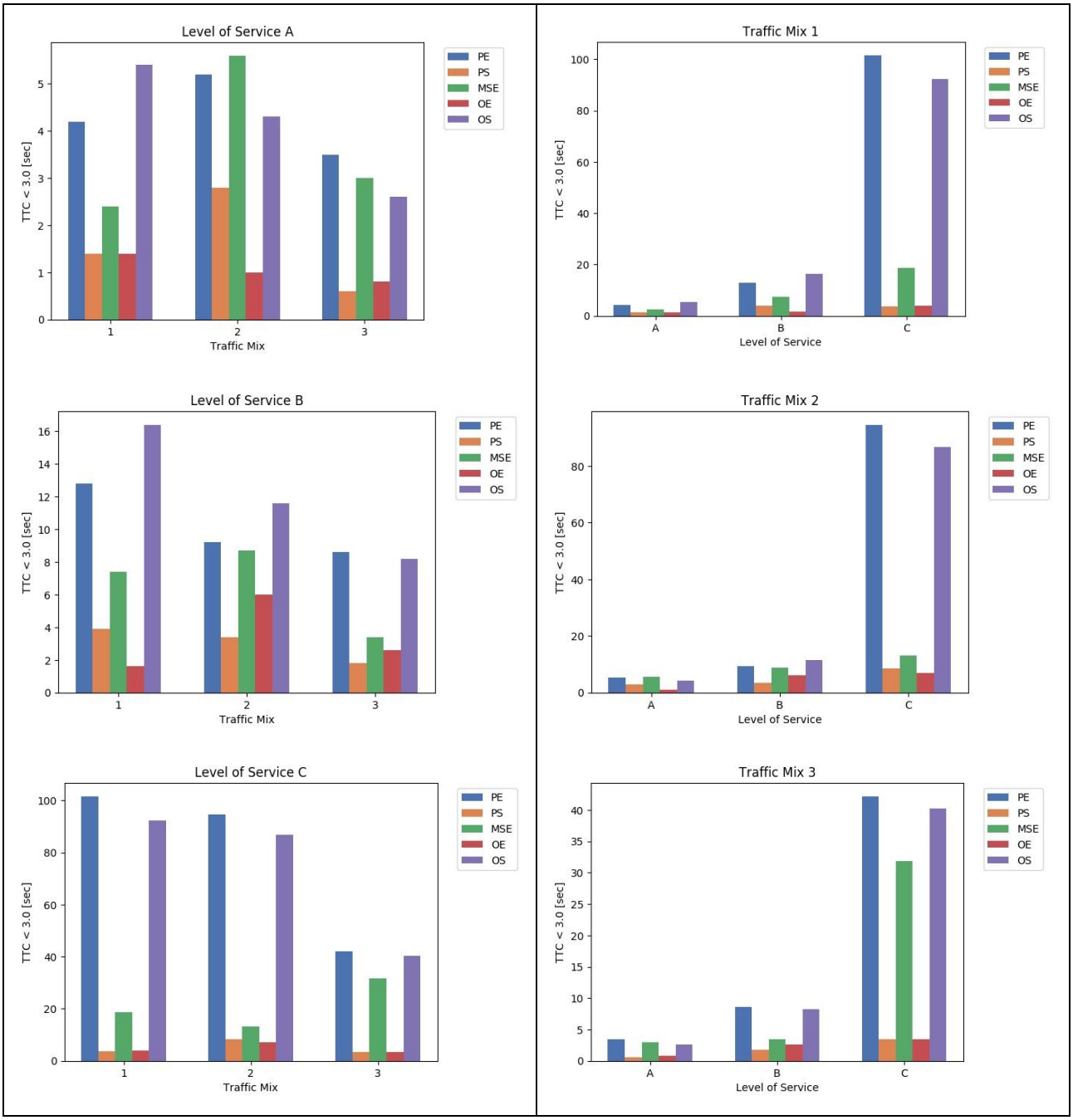

Figure 26 Average number of events with TTCs below 3.0 seconds for Scenario 1.1 baseline simulation experiments (varying parameter scheme, LOS, and traffic mix). Different bar colours

correspond to different parameter schemes. The left column groups results by LOS, the right column by traffic mix.

4.1.1.2.4 Environmental Impacts

Figure 27 shows the average CO_2 emissions per travelled kilometre. We observe that increased emission levels are directly related to increased congestion, see **Figure 21**. The highest values (> 200 g CO_2/km) are observed for LOS C, where also the average speed is below 35 km/h. Again, indirect benefits following from efficiency benefits override assumingly favourable microscopic parameters which seem to promote a more homogeneous driving style, e.g., moderate desired acceleration and deceleration rates and larger desired headways.

Another interesting implication of the results is that more CO_2 emissions are observed in the presence of a larger number of CAVs/CVs. This can be seen by comparing the essentially constant emission levels of uncongested scenarios (parameter schemes PS and OE in the right column of **Figure 27**) when the traffic mix is fixed with the increasing emission levels for uncongested scenarios when the share of CAVs/CVs is increased. This may be due to the disturbances caused by ToCs and MRMs, which would also explain the distribution between the different parameter schemes.

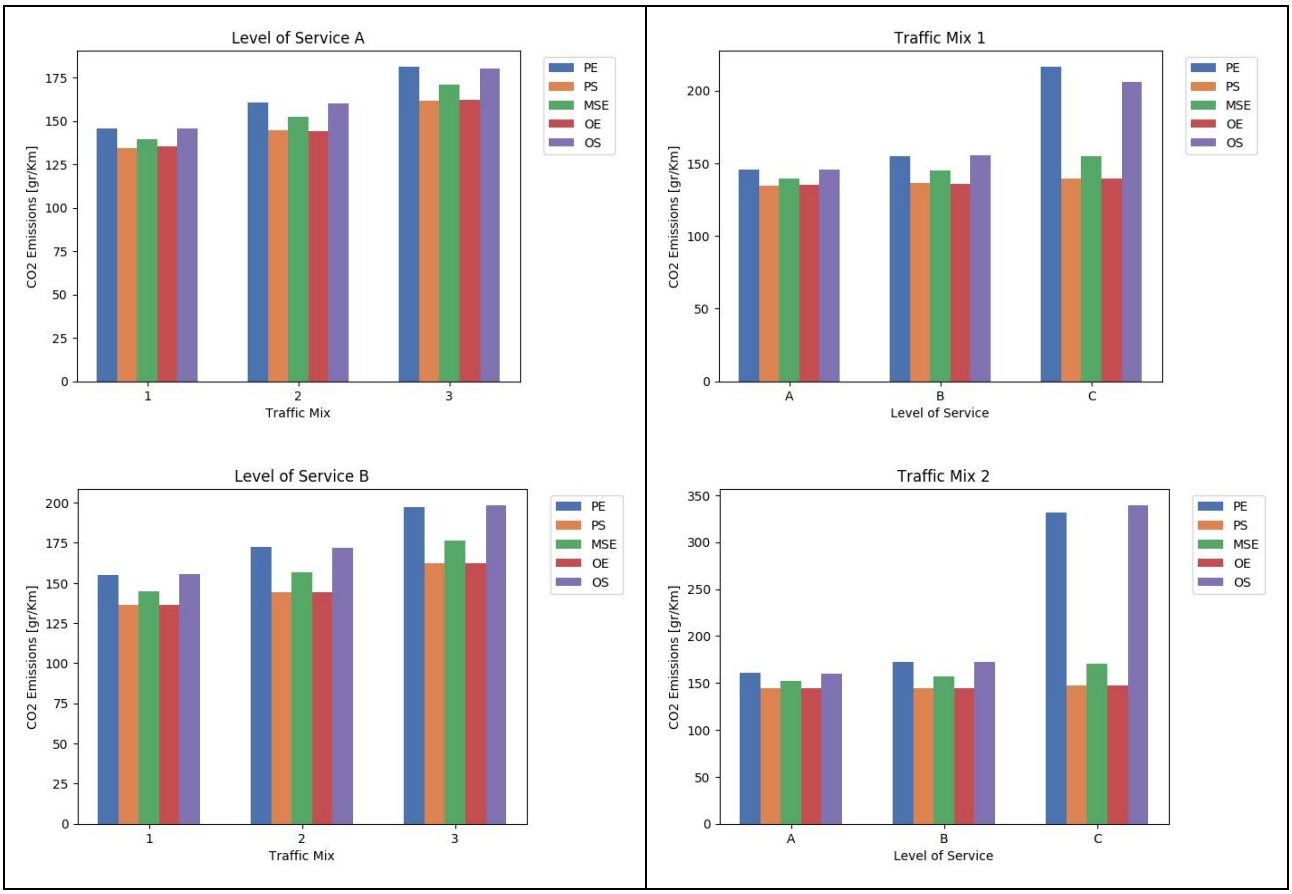

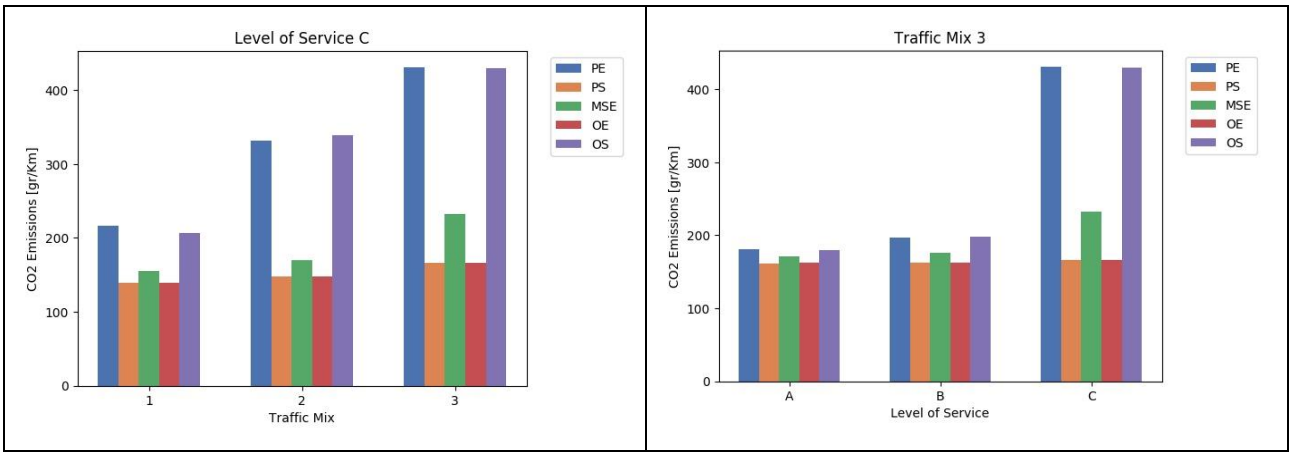

Figure 27. Average CO_2 emissions per km travelled for Scenario 1.1 baseline simulation experiments (varying parameter scheme, LOS, and traffic mix). Different bar colours correspond to different parameter schemes. The left column groups results by LOS, the right column by traffic mix.

4.1.2 Scenario 2.1 Prevent ToC/MRM by providing speed, headway and/or lane advice

4.1.2.1 Scenario Description

The simulation network of Scenario 2.1 is a typical one-lane on-ramp joining a one-direction two-lane motorway segment **(Figure 28)**. Scenario 2.1 (baseline experiments) encompasses CAVs, CVs, and LVs traveling along a motorway merge segment or entering the mainline motorway lanes through an on-ramp. While LVs on the mainline can speed up, slow down, or perform cooperative lane changes to the left, in order to create bigger gaps for the merging vehicles, CAVs on the mainline may not break up platoons or create bigger gaps with temporary acceleration/deceleration for merging vehicles encountering limited space to merge. Due to the complexity of driver behaviour, which is induced by the multiple vehicle types and mixes, it is essential for the RSI to oversee and monitor traffic operations along the motorway, especially at TAs.

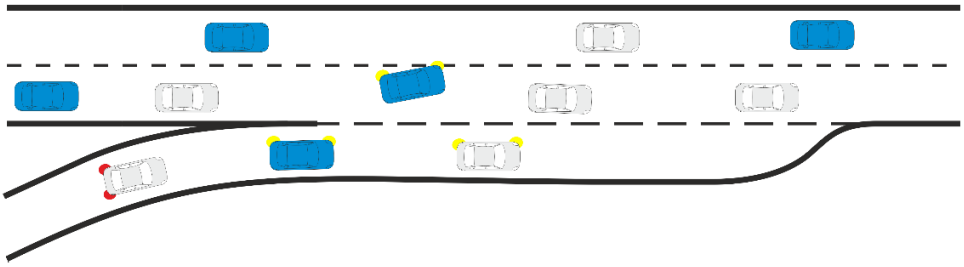

Figure 28. Schematic overview of Scenario 2.1.

The infrastructure detects the available gaps on the right-most mainline lane to estimate speed and lane advice for CAVs/CVs entering the mainline motorway from the on-ramp. We also assume that CAVs/CVs constantly update (near real-time) their speed and lane information to the RSI. The RSI integrates this information with measurements collected by the available road-side sensors. The speeds and locations of LVs can be estimated based on the information gathered via the road-side sensors and on the location (and available sensing information) of CAVs/CVs. With this information, the infrastructure has the option to advise vehicles on the network, for example, lane advice including position and time of the lane change, speed advice, headway advice, or lane change advice on the mainline motorway.

Without the aforementioned infrastructure-assisted measures, vehicles might be impeded or involved in certain safety critical situations under specific traffic conditions (e.g., incidents) or automated driving operations (e.g., platooning at motorway merge/diverge segments). Under these circumstances, CAVs/CVs might request ToCs or execute consequently MRMs at TAs for safety reasons.

The network configuration details are described in **Table 34**. To have a clear view of the merging area (beginning from the on-ramp and ending at the mainline motorway), which is part of the transition area, a more detailed network schematic is added under the SUMO network layout.

The general scenario description in this section showed that a typical on-ramp to motorway merging scenario can be complex due to various driver behaviours generated by different vehicle types and their interactions. The actions and interactions of vehicles (actors) on the network will take place mainly at TAs, and so will the ToCs or MRMs.

Table 34. Network configuration details for Scenario 2.1.

UC2_1	Settings	Notes
Road section length	• Highway: 1.5 km • On-ramp: 0.5 km	
Road priority	3	
Allowed road speed	• Highway: 27.78 m/s • On-ramp: 22.22 m/s	• Highway: 100 km/h • On-ramp: 80 km/h
Number of nodes	7	• jun1 - jun7 priority nodes
Number of edges	6	
Number of O-D relations (routes)	2	• from jun1 to jun7 • from jun3 to jun7
Number of lanes	1-2-3-2	• 1 lane on-ramp • 2 normal lanes on highway • 3 lanes at merging zone (from jun4 to jun5, including acceleration lane) • 2 lanes downstream of the merging zone. Thus, a lane drop from 3 to 2 lanes at the end of merging zone.
Filenames	• network: UC2_1.net.xml	
Network layout 		
Network Schematic 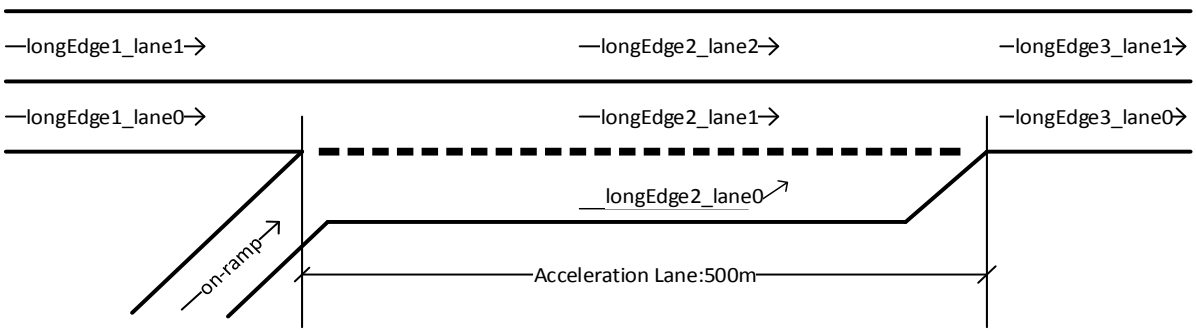		

Road segments

jun1→ jun2: Insertion and backlog area (100 m, 2 lanes)

jun2→ jun4: mainline motorway (500 m, 2 lanes)

jun3→ jun4: on-ramp (500 m, 1 lane)

jun4→ jun5: mainline motorway with acceleration lane (500 m, 3 lanes)

jun5→ jun6: mainline motorway (300 m, 2 lanes)

jun6→ jun7: exit (100 m, 2 lanes)

In Section 3.1.2 we introduced an updated actors' definition, in which three classes of actors (vehicle types) are proposed: manual driving, partial automation, and conditional automation. In the baseline simulation, actors are interpreted into three types of artificial vehicles: LVs, CVs, and CAVs. LVs are modelled to perform motorway merging as human driven vehicles in the real world. On the contrary, CAVs and CVs might request ToCs or consequently execute MRMs at TAs.

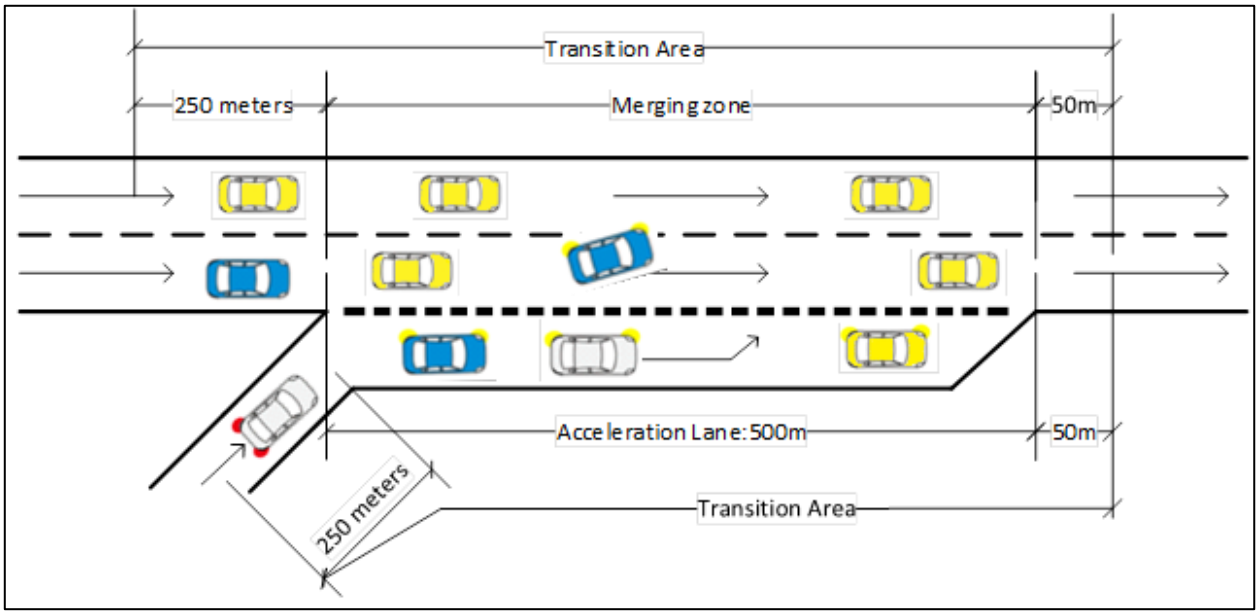

Figure 29. Merging zone schematic of UC2_1 network.

The merging zone is 500 m in length and is composed of one acceleration lane (right-most lane) and two mainline motorway lanes **(Figure 29)**. At the end of the merging zone, a merging bottleneck is formed due to the lane drop. In the merging zone, mandatory lane changes (from the acceleration lane to main motorway lanes) frequently take place, which lead to downwards ToCs of CAVs and CVs upstream of the merging zone. In the baseline simulation experiments, a take-over request is issued 250 m (both in main motorway and on-ramp lanes) upstream of the merging zone.

As introduced in the timeline of a downward transition in **Figure 13**, if the driver response time exceeds the available lead time ($timeTillMRM$ in the simulation), the requested ToC fails and the execution of MRM begins, which is performed as a constant deceleration of 3 m/s^2 on the ego-lane for CAVs and CVs in baseline simulation. The duration of MRMs is explained in Section 2.3.1.2.

4.1.2.2 Results

4.1.2.2.1 Impacts on Traffic Efficiency

Network-wide Impacts

The average network speed is presented in the form of bar charts for three LOSs and three traffic mixes (six plots in **Figure 30**). The left three plots depict average network speed for traffic mix 1, 2 and 3, under LOS A, B and C; the right plots depict average network speed for LOS A, B and C, under traffic mix 1, 2 and 3. For each plot, average network speed is shown for each of the five parametrisation schemes: PE, PS, MSE, OE, and OS.

Starting from the upper left plot, we observe that parametrisation schemes PS and OE exhibit the highest average network speed, followed by the MSE scheme, and finally by the PE and OS schemes. As traffic intensity increases (from LOS A to C in the left plots), the average network speed decreases for all five schemes. For higher traffic intensity, the differences between five schemes are more significant. The highest decrease in average network speed (approximately 47%) occurs for schemes PE and OS for traffic mix 3, from LOS B to LOS C.

The above trend is normal and can be explained by the fundamental diagram of traffic flow theory. Increasing traffic flow prior to the point of critical density (capacity drop point) causes speeds to drop slightly, which is the case for the transition from LOS A to LOS B; when the critical density of the network is reached, increasing traffic flow incurs significant speed drop. This is the case for schemes PE and OS for the transition from LOS B to LOS C under mix 3 that encompasses the highest CAVs/CVs penetration rate, where high ToC and MRM occurrences are causing more variation in speed and flow perturbation.

Schemes PS and OE exhibit the best performance in terms of average network speed and this can be explained given the driver model parameter attributes per parametrisation scheme in **Tables 19, 20,** and **21**. For scheme PS, the desired time headways for car-following and desired longitudinal gaps for lane-changing are short, which results in increased traffic efficiency. Additionally, the driver response time to ToC is also short for scheme OE, which further contributes to increased traffic efficiency.

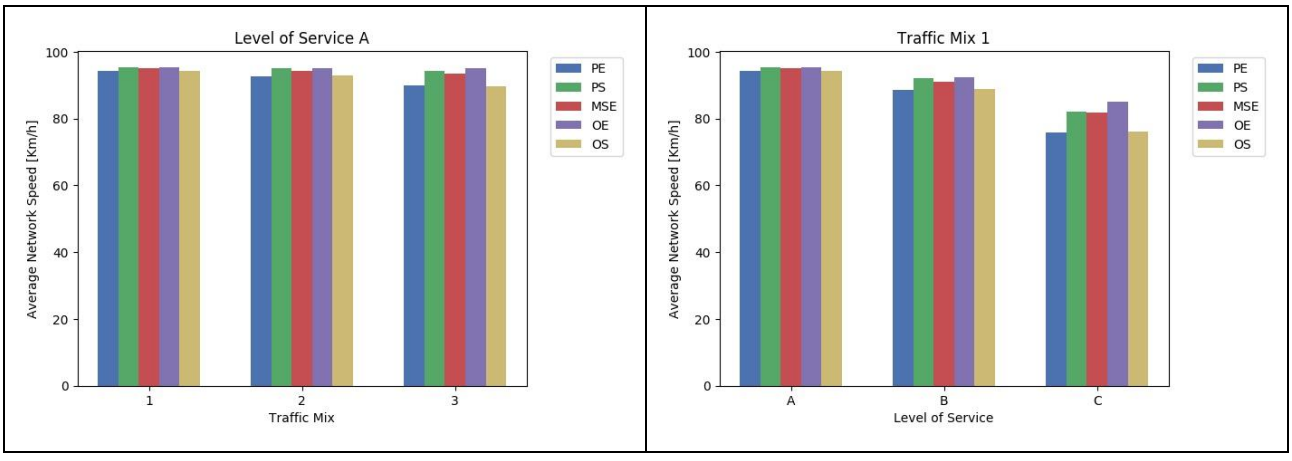

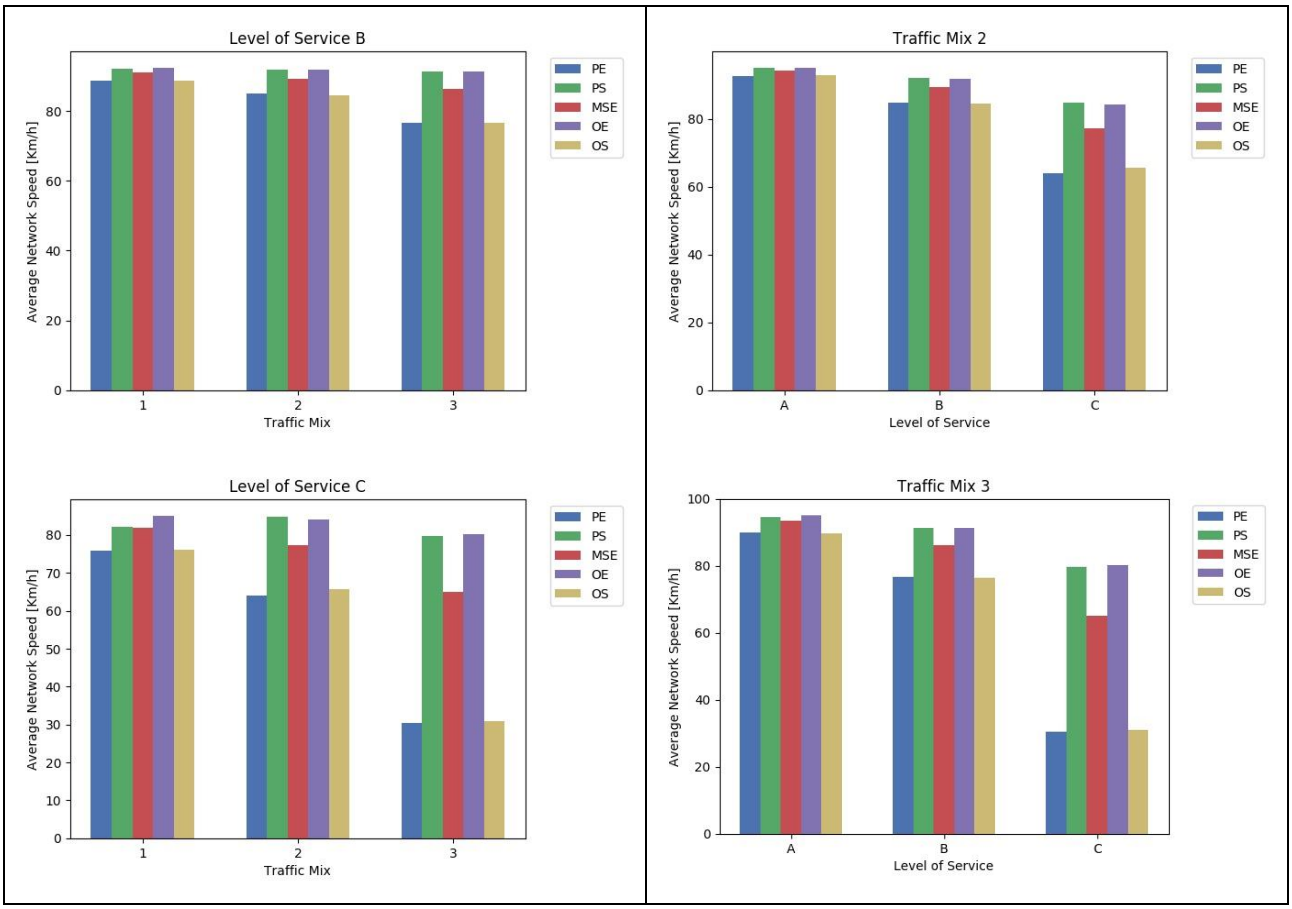

Figure 30. Average network speed for Scenario 2.1 baseline simulation experiments (varying parameter scheme, LOS, and traffic mix). Different bar colours correspond to different parameter schemes. The left column groups results by LOS, the right column by traffic mix.

The right three plots show that the average network speed decreases generally for schemes PE and OS when the CAVs/CVs penetration in traffic mix increases, but not in the cases for schemes PS and OE. For scheme PE, it is self-explanatory because all five attributes in this set are not optimal. It is interesting to point out that scheme OS is equally underperforming as PE. They shared the same attributes regarding desired time headway and desired longitudinal gaps are. It can also be observed **(Figure 33)** that the total number of lane changes does not increase with higher CAVs/CVs penetration rates. Therefore, a preliminary conclusion is that large desired time headway and longitudinal gaps of CAVs/CVs affect average network speed adversely.

Local impacts

To investigate the local impacts on traffic efficiency, the queue length of the merging zone edge and the on-ramp edge, as well as the space-mean speed of the merging zone edge, are presented in **Figure 31** and **Figure 32**.

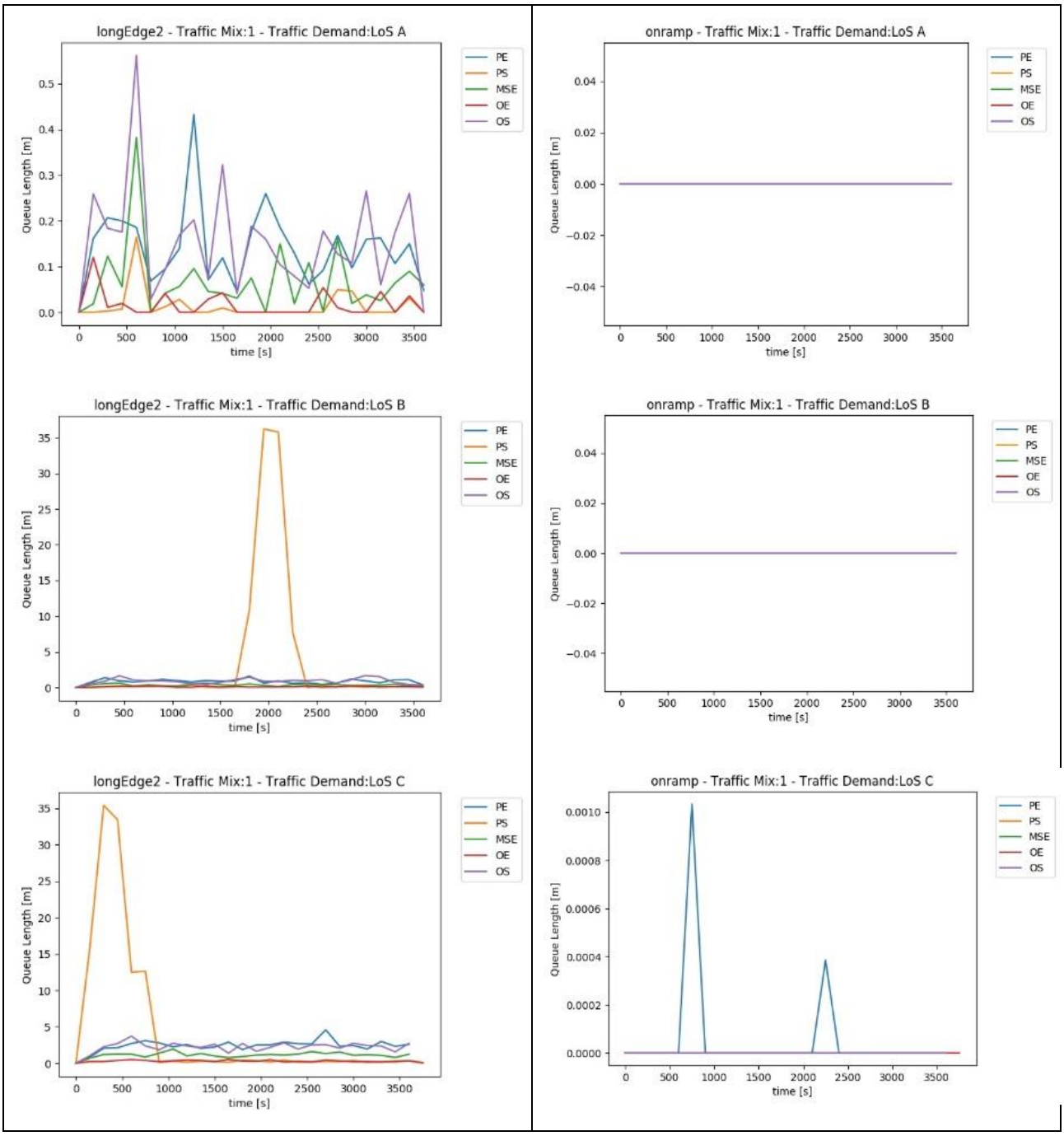
longEdge2 - Traffic Mix:1 - Traffic Demand:LoS A
onramp - Traffic Mix:1 - Traffic Demand:LoS A
longEdge2 - Traffic Mix:1 - Traffic Demand:LoS B
onramp - Traffic Mix:1 - Traffic Demand:LoS B
longEdge2 - Traffic Mix:1 - Traffic Demand:LoS C
onramp - Traffic Mix:1 - Traffic Demand:LoS C
PE
PS
MSE
OE
OS
Queue Length [m]
time [s]

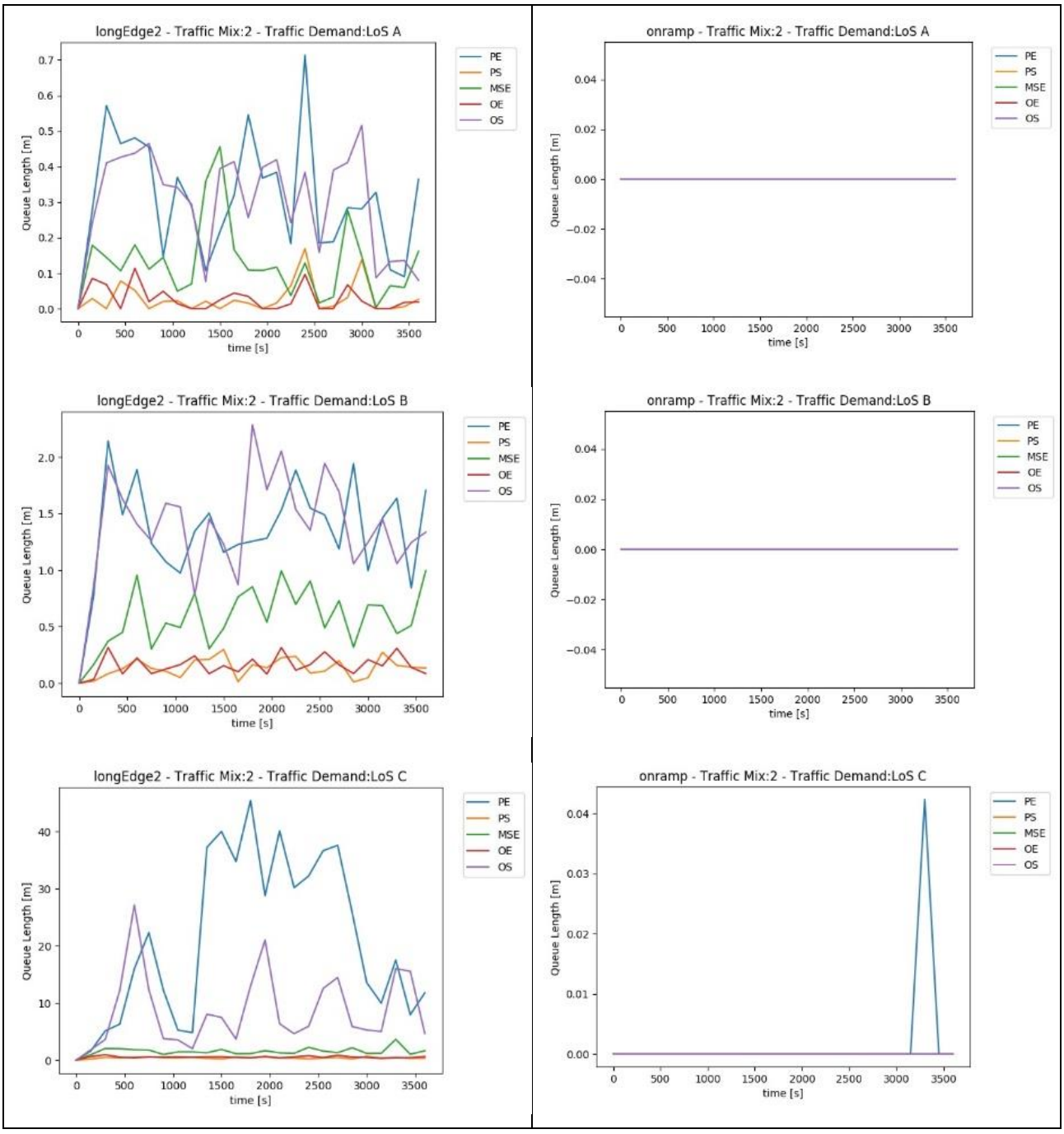
longEdge2 - Traffic Mix:2 - Traffic Demand:LoS A
onramp - Traffic Mix:2 - Traffic Demand:LoS A
longEdge2 - Traffic Mix:2 - Traffic Demand:LoS B
onramp - Traffic Mix:2 - Traffic Demand:LoS B
longEdge2 - Traffic Mix:2 - Traffic Demand:LoS C
onramp - Traffic Mix:2 - Traffic Demand:LoS C
PE
PS
MSE
OE
OS
Queue Length [m]
time [s]

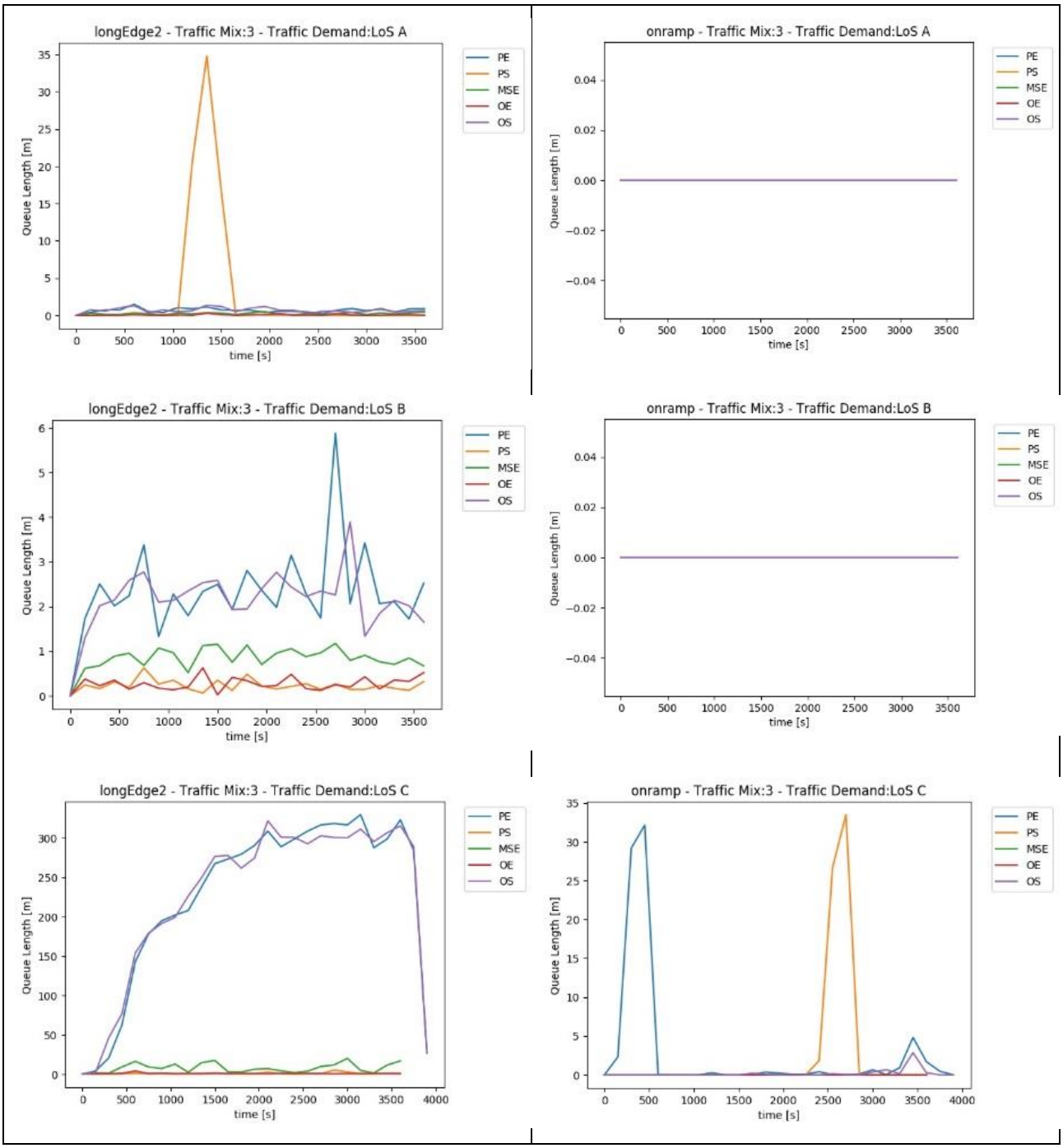

Figure 31. Queue lengths on longEdge2 and on-ramp for Scenario 2.1 baseline simulation experiments.

The left nine plots **(Figure 31)** show the queue length on longEdge2 (see the network schematic of **Table 34** for position reference), under three LOSs and then over three traffic mixes. For each traffic mix, the queue length increases with increasing traffic demand as expected. A few spikes of approximate 35 m queue can be spotted on all LOSs, which could be caused by the following reasons:

1. Several continuous unsuccessful merging cases that lead to vehicles stuck at the end of acceleration lane. This will result in high-risk merging situation that induces a spillback queue upstream to the beginning of the edge in general.
2. Some vehicles are still in the process of MRM (ToC begins on halfway on-ramp) in the beginning of acceleration lane; or some vehicles are in recovery after MRM. Both situations have negative effect (slow speed, large speed deviation) on traffic efficiency regarding queue length.

We also observe that, for schemes PE and OS, noticeable long queues were formed gradually on the merging zone under traffic mix 3 and LOS C, which is again due to the "non-optimal" driver model attributes of large desired time headways for car-following and large desired longitudinal gaps for lane-changing. Meanwhile, the queue length on the on-ramp is mostly stable with a few small spikes (under traffic mix 3 and traffic demand LOS C) that could be caused by vehicles that performed ToCs and consequently longer than normal MRMs, which in turn could result in queue to the beginning of the on-ramp.

The average space-mean speed of longEdge2 is shown in **Figure 32,** under three traffic mixes and three LOSs. As the LOS increases, the average speed decreases, especially for schemes PE and OS which show a higher decrease in average speed. This result corresponds to the inefficiency of these two schemes regarding their driver model attributes.

Looking at the nine plots horizontally and vertically, on the one hand, the five schemes are more "spread-out" in speed range when LOS or CAVs/CVs penetration rate increases. On the other hand, the negative effect of "non-optimal" schemes PE and OS are showing the same patterns and they are more pronounced under worsened traffic conditions, such as higher traffic intensity or higher ToCs and MRM events, which is generated by higher CAVs/CVs penetration rate. The phenomenon agree with the preliminary conclusions on traffic efficiency, traffic dynamic, and environmental impacts.

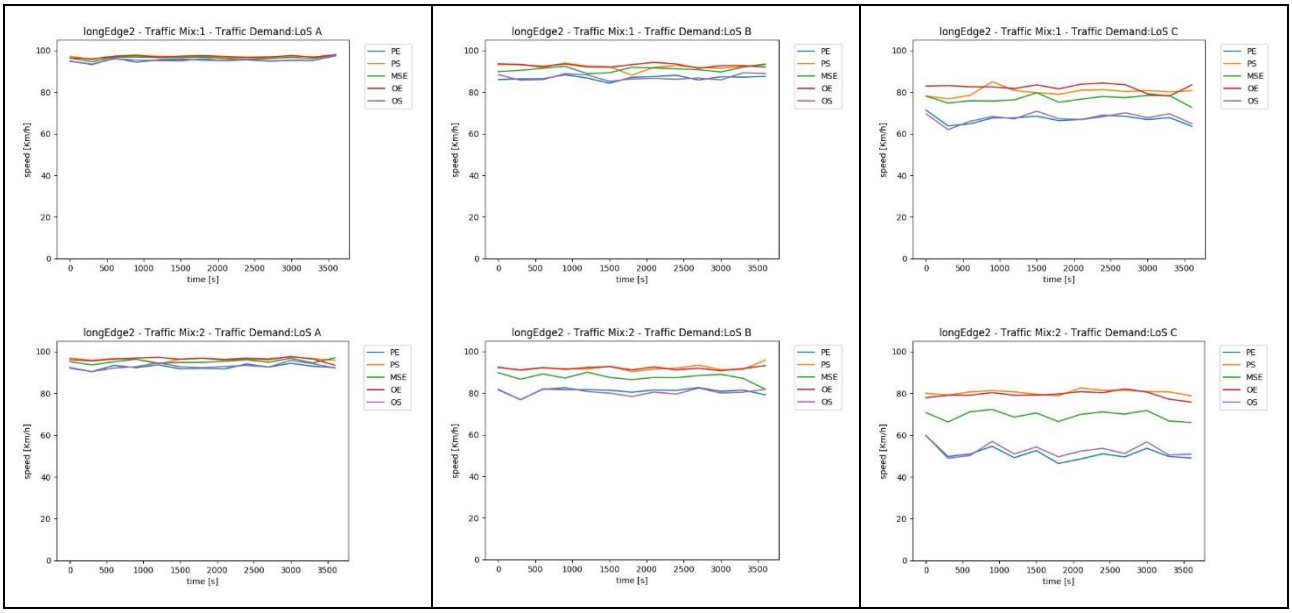

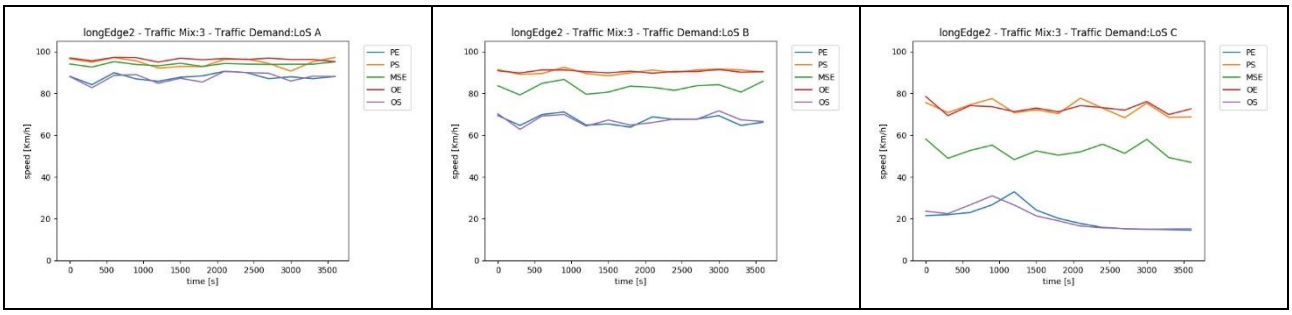

Figure 32. Average speed on longEdge2 for Scenario 2.1 baseline simulation experiments.

4.1.2.2.2 Impacts on Traffic Dynamics

The total number of lane changes is reported to show the disruption caused in the traffic flow by lane change manoeuvres per traffic composition, in which different vehicle types embody different driver behaviours. Results are depicted in **Figure 33** below.

The left three plots indicate that the total number of lane changes for all five schemes generally increase at the same rate as traffic intensity. Thus, the increased rates of traffic intensity did not affect lane changes of mixed traffic significantly under baseline scenario. The right plots show that the total number of lane changes decrease for all five schemes when the penetration rate of CAVs/CVs increases due to relatively higher accepted lane change gaps for CAVs/CVs.

The seemingly more "optimal" scheme OE in terms of traffic efficiency exhibits the lowest total number of lane changes, while less "optimal" schemes PE, OS show a higher total number of lane changes.

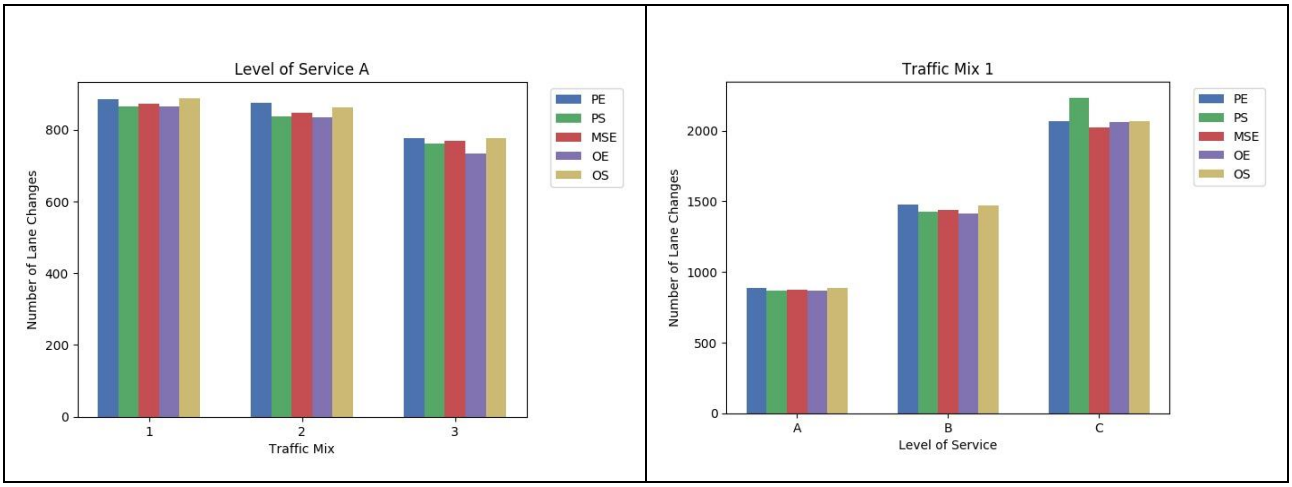

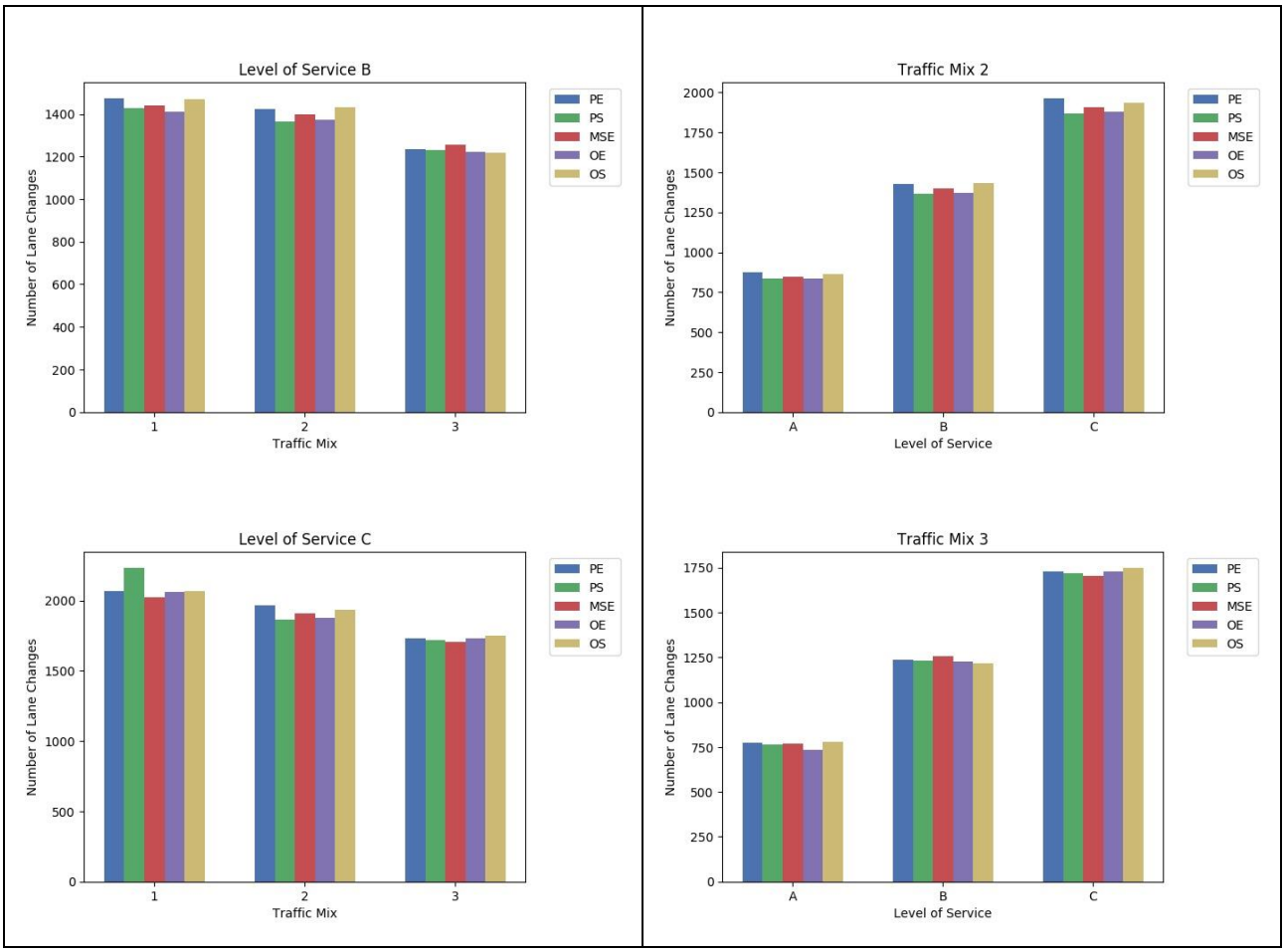

Figure 33. Number of lane changes for Scenario 2.1 baseline simulation experiments (varying parameter scheme, LOS, and traffic mix). Different bar colours correspond to different parameter schemes. The left column groups results by LOS, the right column by traffic mix.

4.1.2.2.3 Impacts on Traffic Safety

As explained in Section 3.1.7, time-to-collision (TTC) measures a longitudinal margin to lead vehicles or objects, and is a proxy for traffic safety. **Figure 34** includes six plots that depict the number of conflicts corresponding to $TTC < 3.0\,\mathrm{s}$ (threshold value indicating safety critical events) for the different LOSs, traffic mixes, and parametrisation schemes.

The left three plots show number of conflicts per scheme as LOS increases. Schemes PE and OS yield most of the safety critical events. Looking at the driver model parameter attributes of these two schemes in **Table 18**, it appears that both of them correspond to large desired time headways for car-following and large desired longitudinal gaps for lane-changing, thus inducing more conflicts at the lane drop location.

The right three plots also show a mixed behaviour among different traffic mixes. It seems that conflicts for all five schemes increase from traffic mix 1 to 3, where CAVs/CVs penetration increases from 30% to 50%, and finally to 80% . We also observe that conflicts for all five schemes (with a few exceptions) increase when traffic intensity increases, under the same traffic mix.

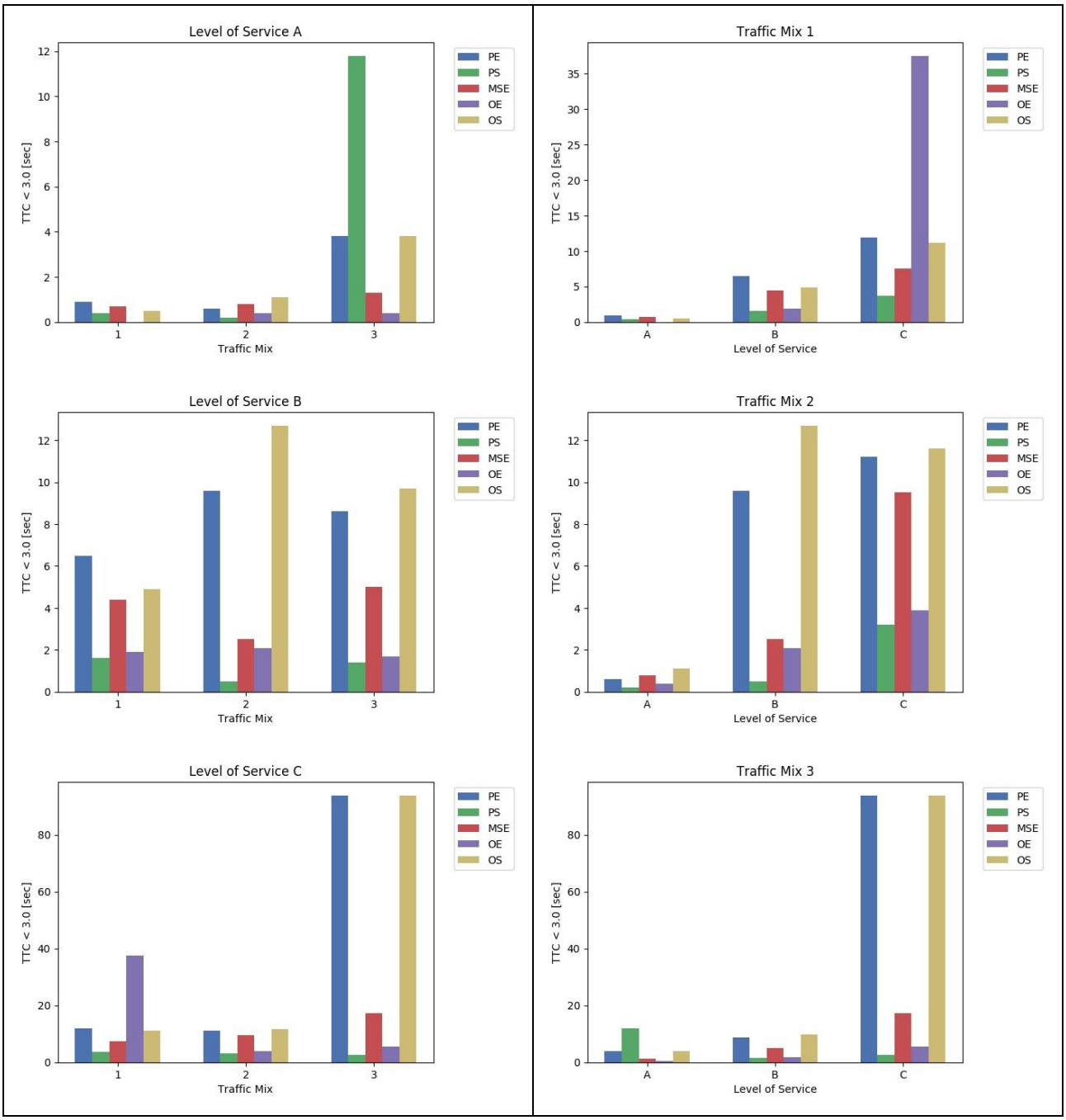

Figure 34. Number of conflicts ($TTC < 3$ s) for Scenario 2.1 baseline simulation experiments (varying parameter scheme, LOS, and traffic mix). Different bar colours correspond to different parameter schemes. The left column groups results by LOS, the right column by traffic mix.

4.1.2.2.4 Environmental Impacts

The total CO_2 emissions for all vehicle types are shown in the six plots of **Figure 35**. The left three plots indicate that the total CO_2 emissions for all five schemes increase when the LOS increases. The increase rate for all schemes is comparable to the increase rate of traffic demand, except for schemes PE and OS under traffic mix 3 and LOS C. For these two schemes, the total CO_2 emissions values are almost one and a half times the values under LOS B. This result complies with average network speed for the same schemes, traffic mix, and LOS. These two schemes are less optimal in

terms of traffic efficiency, thus causing stop and go traffic, where the CO_2 emissions increase significantly.

The right three plots show that under the same traffic intensity, the CO_2 emissions of all five schemes slightly increase when the traffic mix changes from 1 to 3. This is rather emphasised for schemes PE and OS under higher traffic intensity (LOS C). It can be explained by the higher number of ToC and MRM occurring in the merging area, which generate more changes in speed, and in return, increased CO_2 emissions.

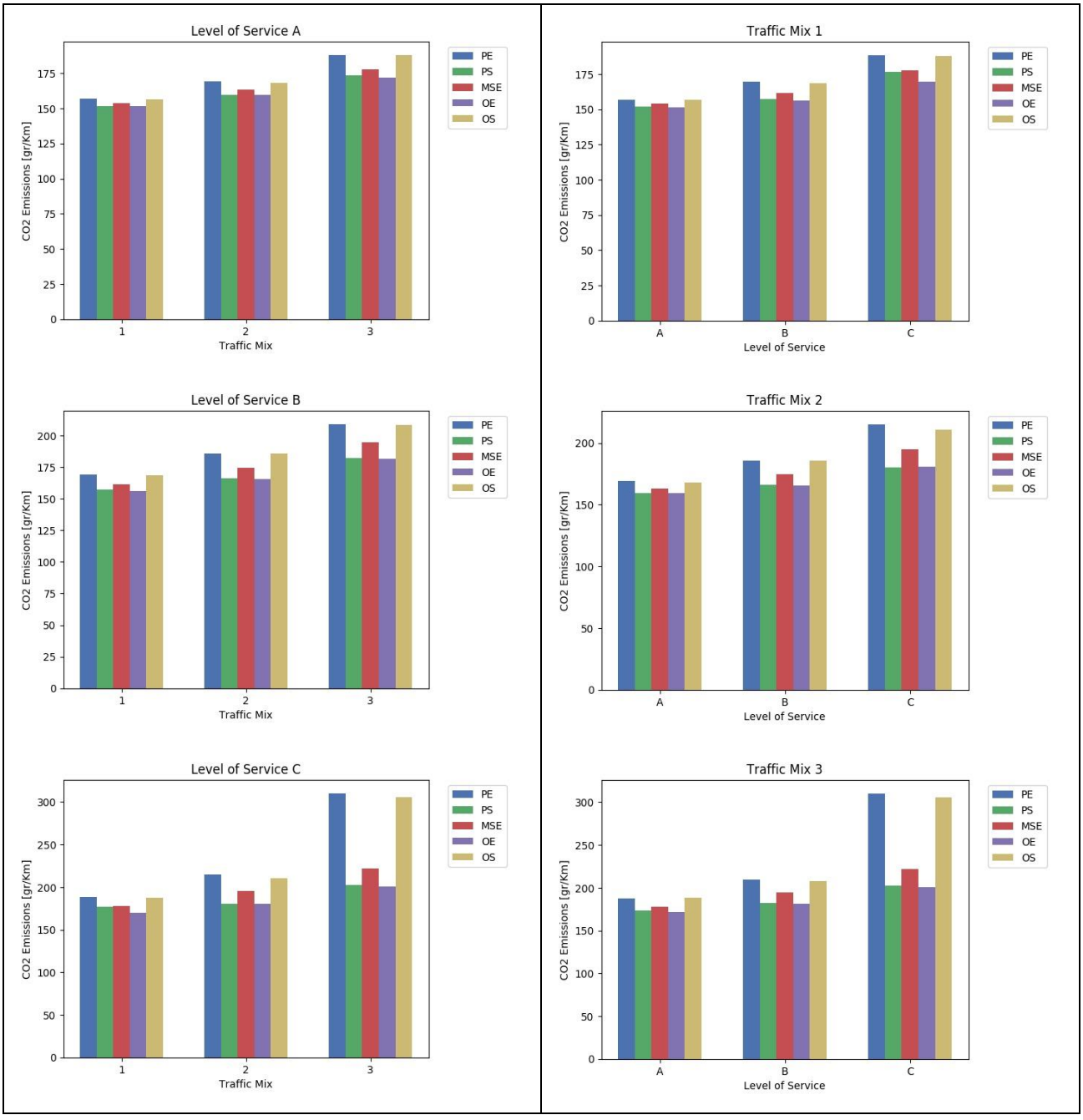

Figure 35. Total CO_2 emissions for Scenario 2.1 baseline simulation experiments (varying parameter scheme, LOS, and traffic mix). Different bar colours correspond to different parameter schemes. The left column groups results by LOS, the right column by traffic mix.

4.1.3 Scenario 3.1 Apply traffic separation before motorway merging/diverging

4.1.3.1 Scenario Description

In Scenario 3.1 (C)AVs, CVs and LVs drive along two two-lane motorways merging into a four-lane motorway **(Figure 36)**. RSI monitors traffic composition upstream of the merge area through collective perception but also via Cooperative Awareness Message (CAM) receptions, and infrared sensors.

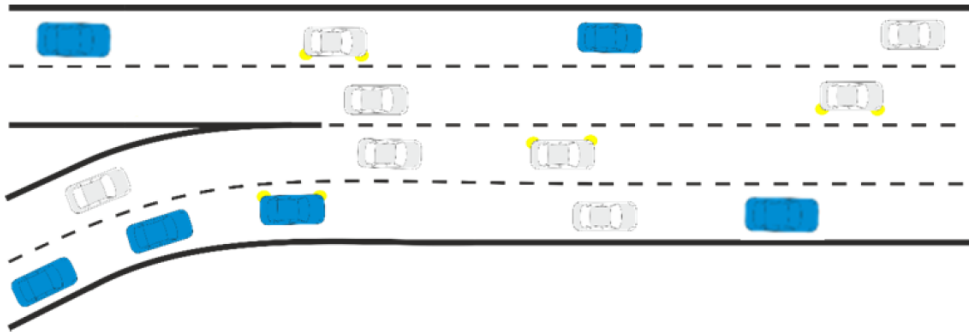

Figure 36. Schematic overview of Scenario 3.1.

(C)AVs/CVs move to the left lane on the left two-lane motorway and to the right on the right two-lane motorway at some point upstream of the merging area according to the selected traffic separation policy. LVs move to the other lanes not allocated to (C)AVs/CVs. Thus, (C)AVs/CVs enter the four-lane section on the outer lanes, giving space to manually driven vehicles (LVs) to occupy the central lanes (in many of these situations human driving still may generate risky and dangerous traffic conditions).

The proposed traffic separation policy is expected to significantly mitigate the total number of risky situations occurring in the merge area, thus resulting in lesser ToCs issued in this area. At some point downstream of the merging area, traffic separation is disabled, and all vehicles can gradually start changing lanes to reach their target destination.

More details about the simulation network of Scenario 3.1 can be found in **Table 35**.

Table 35. Network configuration details for Scenario 3.1.

Scenario 3.1	Settings	Notes
Road section length	2.3 km	• for each motorway
Road priority	9	
Allowed road speed	36.11 m/s	130 km/h
Number of nodes	5	• n0 – n5
Number of edges	4	
Number of start nodes	2	• n0, n4
Number of end nodes	1	• n3
Number of O-D relations	2	• From n0 to n3 • From n4 to n3
Number of lanes upstream	2	

of the merging area		
Number of lanes upstream of the merging area	4	• from n1 to n2
Merging area length	1.3 km	
Filename	• network: UC3_1.net.xml	
Intended control of lane usage There is no control on lane usage. In the sub-scenario 1, Based on the RSI provided traffic separation policy, CAVs and CAV Platoons move to the left lane of the left 2-lane motorway and to the right on the right 2-lane motorway some point upstream of the merging point. CVs move to other lanes than the CAVs and CAV Platoons. CAVs and CAV Platoons thus enter the 4-lane section on the outer lanes, giving space to other vehicle types to merge.		
Network layout 		
Road segments n0→n1: Insertion and backlog area (500 m) n4→n1: Insertion and backlog area (500 m) n1→n2: Merging area (1300 m) n2→n3: Leaving area (500 m)		

4.1.3.2 Results

4.1.3.2.1 Impacts on Traffic Efficiency

Network-wide Impacts

Figure 37 depicts the average network speed for all baseline simulation experiments of Scenario 4.2 (urban network) encompassing the different demand levels, traffic mixes, and parametrisation schemes. The two columns present the same data in a different format to facilitate the visual assessment with respect to the different traffic mixes (left column), and the different traffic demand levels (right column).

All plots indicate that traffic conditions are uncongested irrespective of the demand level, traffic mix, and parametrisation scheme. This implies that no major breakdown occurs at the merge area of the two motorways. Increasing penetration rate of CAVs/CVs does not affect traffic efficiency for LOS A. On the contrary, average network speed is slightly reduced when CAVs/CVs increase for LOS B due to the higher number of vehicles executing ToCs (and possibly MRM) upstream and along the merge area. An interesting finding is that the latter trend is reversed for LOS C. In this case, it seems that denser traffic urges LVs to make more tactical lane changes for speed gain reasons thus inducing turbulence to the traffic flow. Results suggest that the effect of lane-changing on average network speed is more significant compared to that of ToC/MRM.

Plots in the right column show that average network speed decreases with increasing demand. We observe that the latter speed reduction is more significant for parametrisation schemes PE and OS, where driving behaviour was assumed to be more conservative.

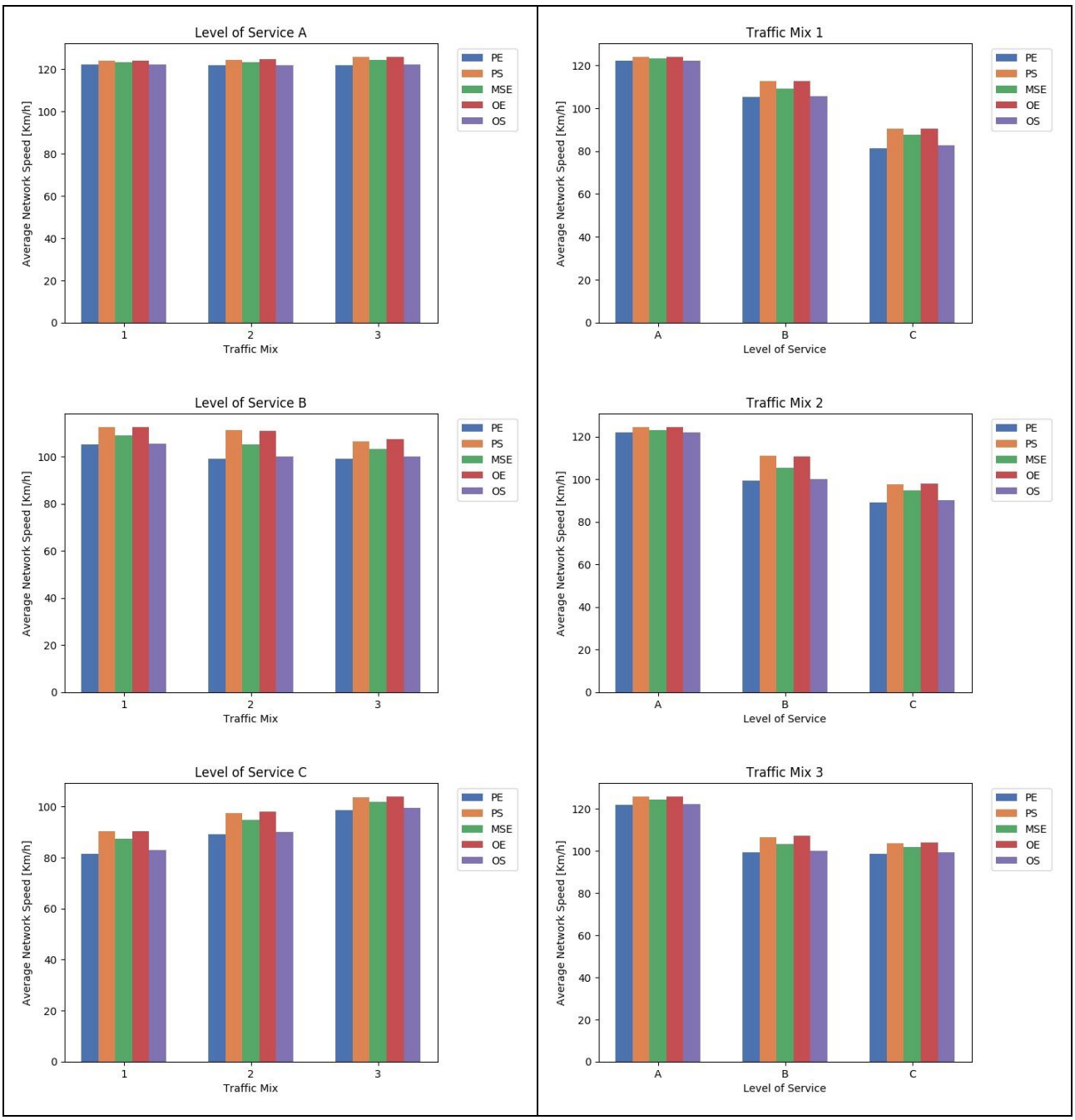

Figure 37. Average network speed for Scenario 3.1 baseline simulation experiments (varying parameter scheme, LOS, and traffic mix). Different bar colours correspond to different parameter schemes.

Local Impacts

Figure 38 shows the average speed (taken over five minutes) on the edge 'start_north', which is located just upstream of the merging area (see network schematic in **Table 35**). The left-most column indicates that free flow traffic operations prevail on the edge for any traffic mix and LOS A.

Space-mean speed is reduced for parametrisation schemes PE and OS for higher share of CAVs/CVs (traffic mix 3) due to their conservative behaviour in terms of car-following and lane-changing. When demand increases (LOS B in middle column), the distinct effects of parametrisation schemes become clear in the presence of more dense traffic. Finally, as traffic density further increases these distinct effects fade out for LOS C, and average edge speed slightly fluctuates around 65 km/h.

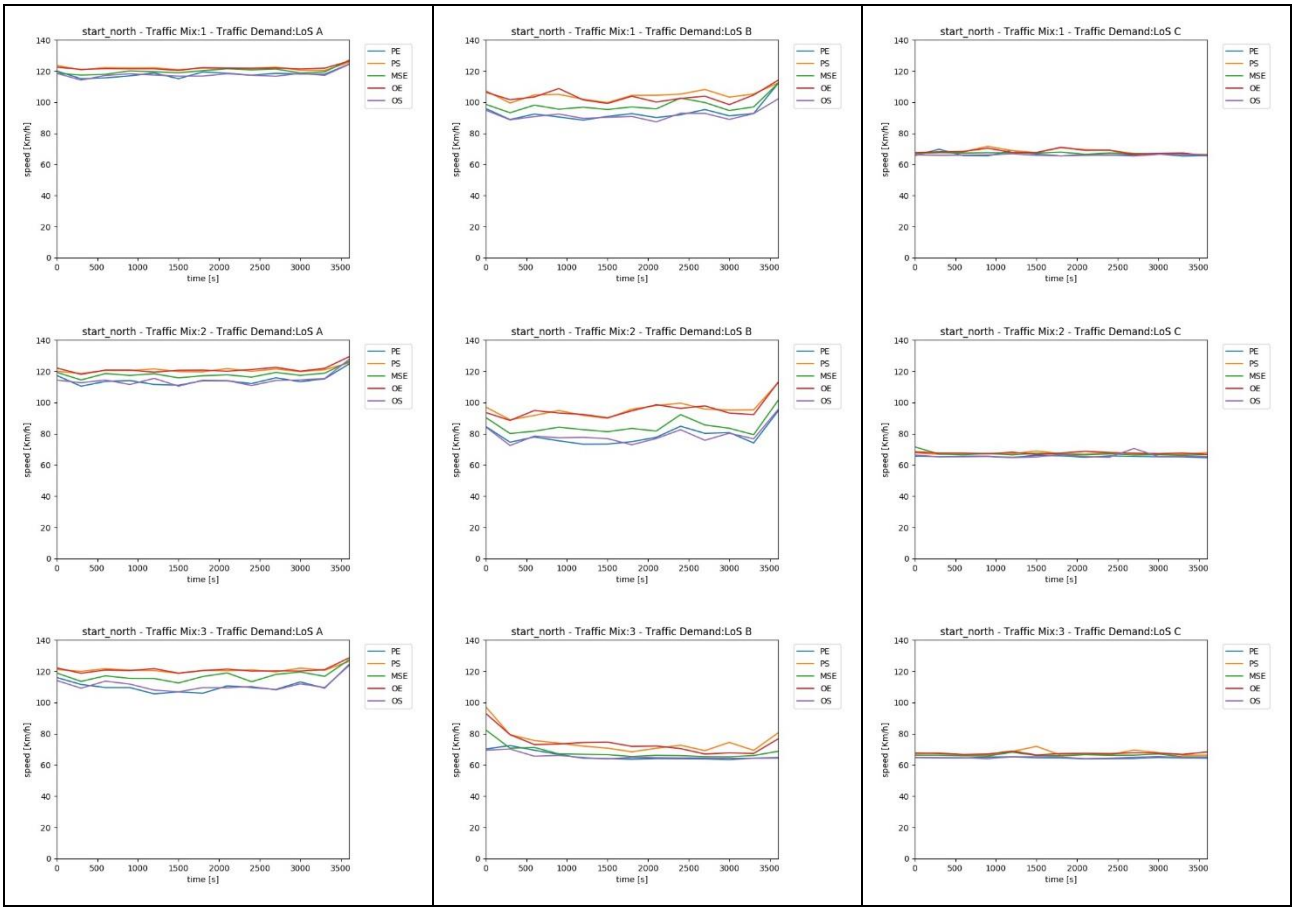

Figure 38. Average speed at the edge 'start_north' for the different parameter sets. First row: varying LOS at traffic mix 1; second row: varying LOS at traffic mix 2; third row: varying LOS at traffic mix 3.

Figure 39 shows the average queue lengths (during the last 150 seconds) building up on the edge 'start_north' during the simulation. The queue length is defined as the back position of the last vehicle on the edge, which is slower than 5 km/h.

It can be observed that traffic operations remain uncongested along the edge irrespective of the traffic mix, demand level, and parametrisations scheme, since no queue spillback is formed on the edge.

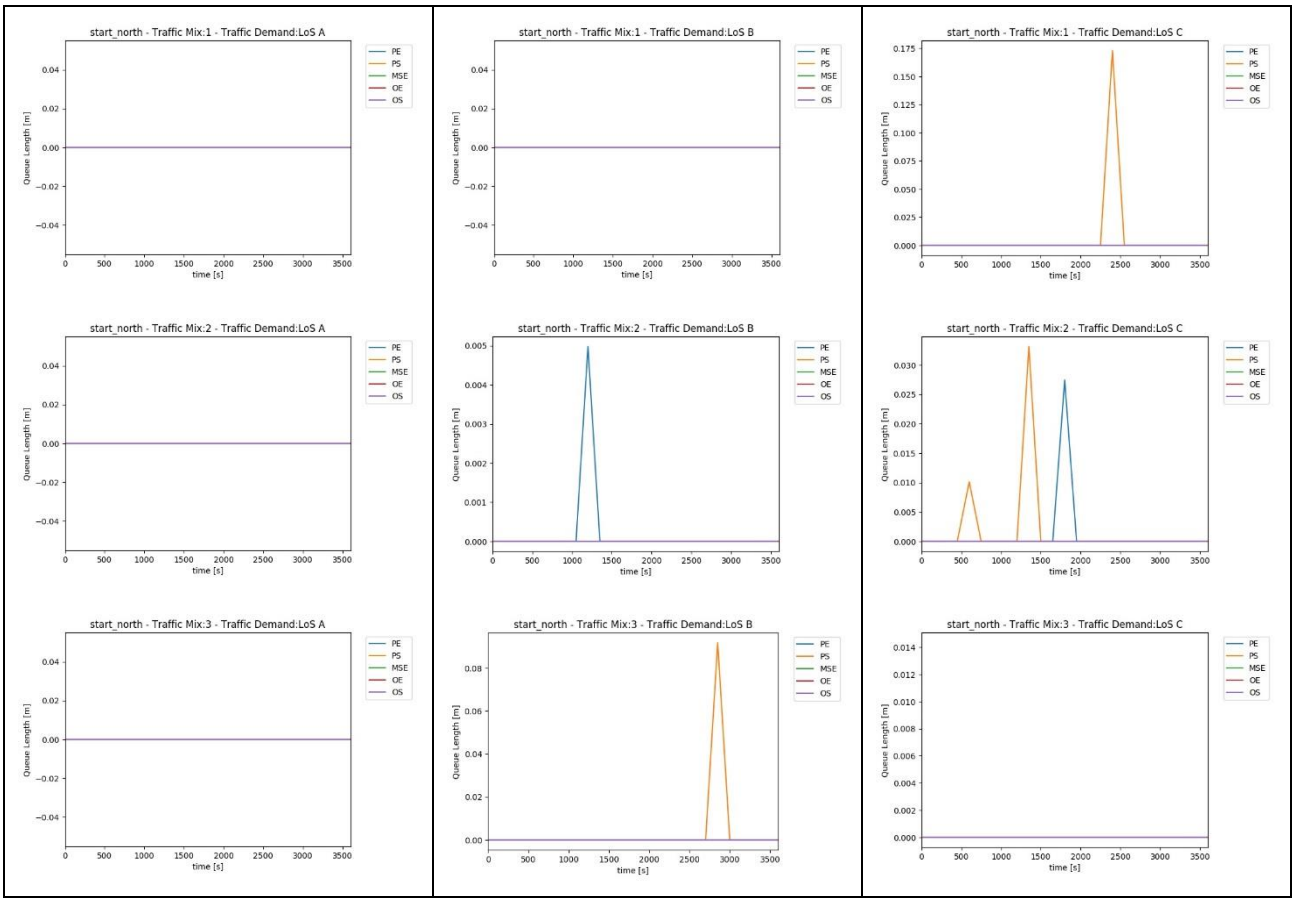

Figure 39. Average queue length at the edge 'approach_2' for the different parameter sets. First row: varying LOS at traffic mix 1; second row: varying LOS at traffic mix 2; third row: varying LOS at traffic mix 3.

4.1.3.2.2 Impacts on Traffic Dynamics

Figure 40 shows the total number of lane changes per simulated scenario. Lane change intensity decreases for higher shares of CAVs/CVs. This is expected since the *lcAssertive* parameter (i.e. the willingness to accept lower front and rear gaps on the target lane) is in general higher for LVs compared to CAVs/CVs. The latter effect is more pronounced for parametrisation schemes PE and OS, where CAVs/CVs exhibit the most conservative behaviour in terms of lane-changing. Additionally, it is shown that the total number of lane changes increases with increasing demand. However, it noteworthy that for Scenario 3.1, less than 1 lane change per vehicle correspond to each simulated scenario. Thus limited turbulence is induced to the traffic due to lane changing, since several vehicles can follow their desired routes without changing lanes.

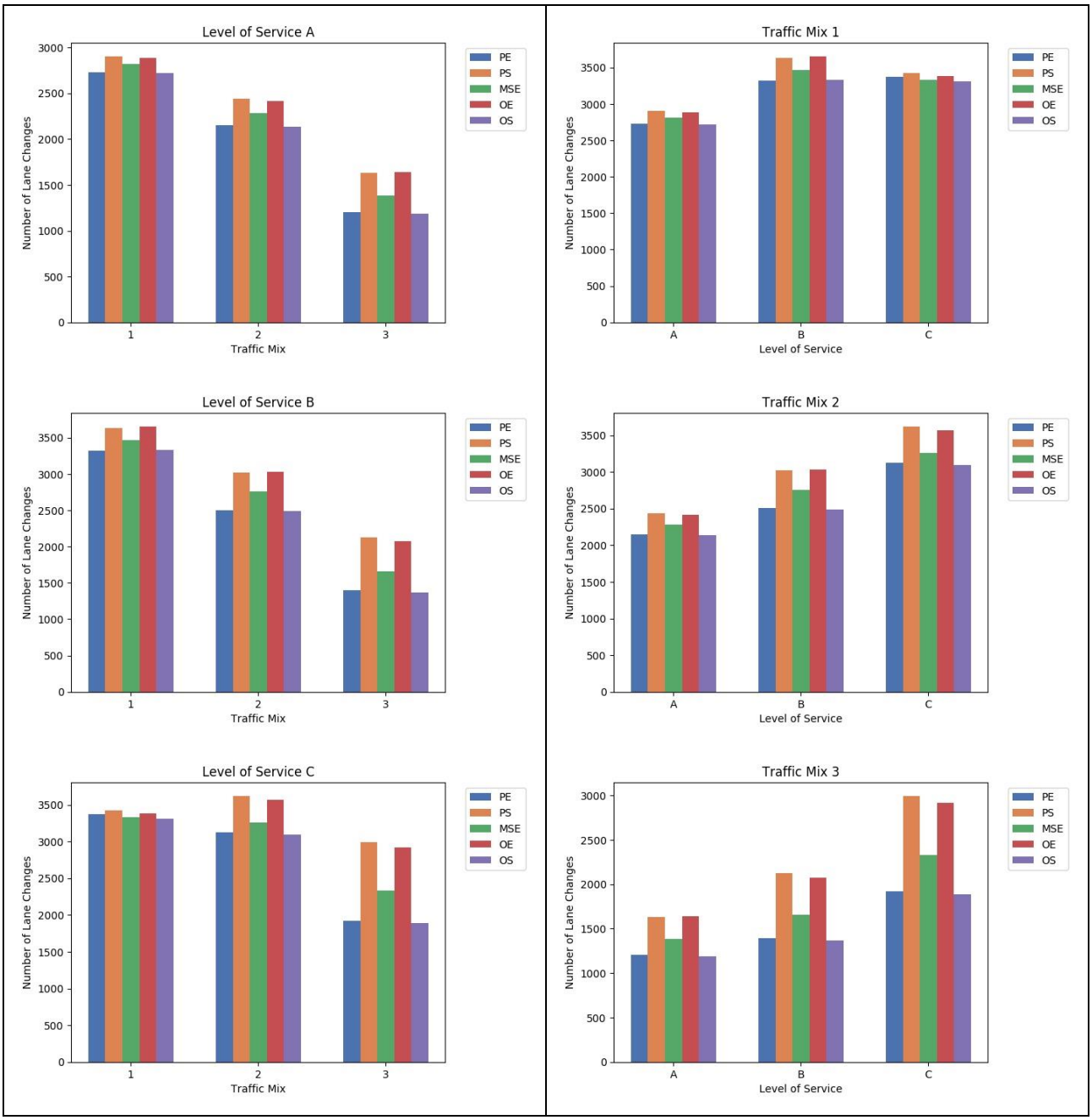

Figure 40. Number of lane changes for Scenario 3.1 baseline simulation experiments (varying parameter scheme, LOS, and traffic mix). Different bar colours correspond to different parameter schemes. The left column groups results by LOS, the right column by traffic mix.

4.1.3.2.3 Impacts on Traffic Safety

Figure 41 presents the average number of events with $TTC < 3.0$ s (termed 'critical' below). It is evident that almost no conflicts take place per simulated scenario. Simulation scenarios corresponding to LOS A exhibit no safety critical events (plots not included for this reason). Similar conditions can be observed for other cases (traffic mix 2 and 3 for LOS B, traffic mix 3 for LOS C). The very few existing events with $TTC < 3.0$ s correspond to parametrisation scheme PE, where reduced driver performance during ToC generates rear-end conflicts with following vehicles.

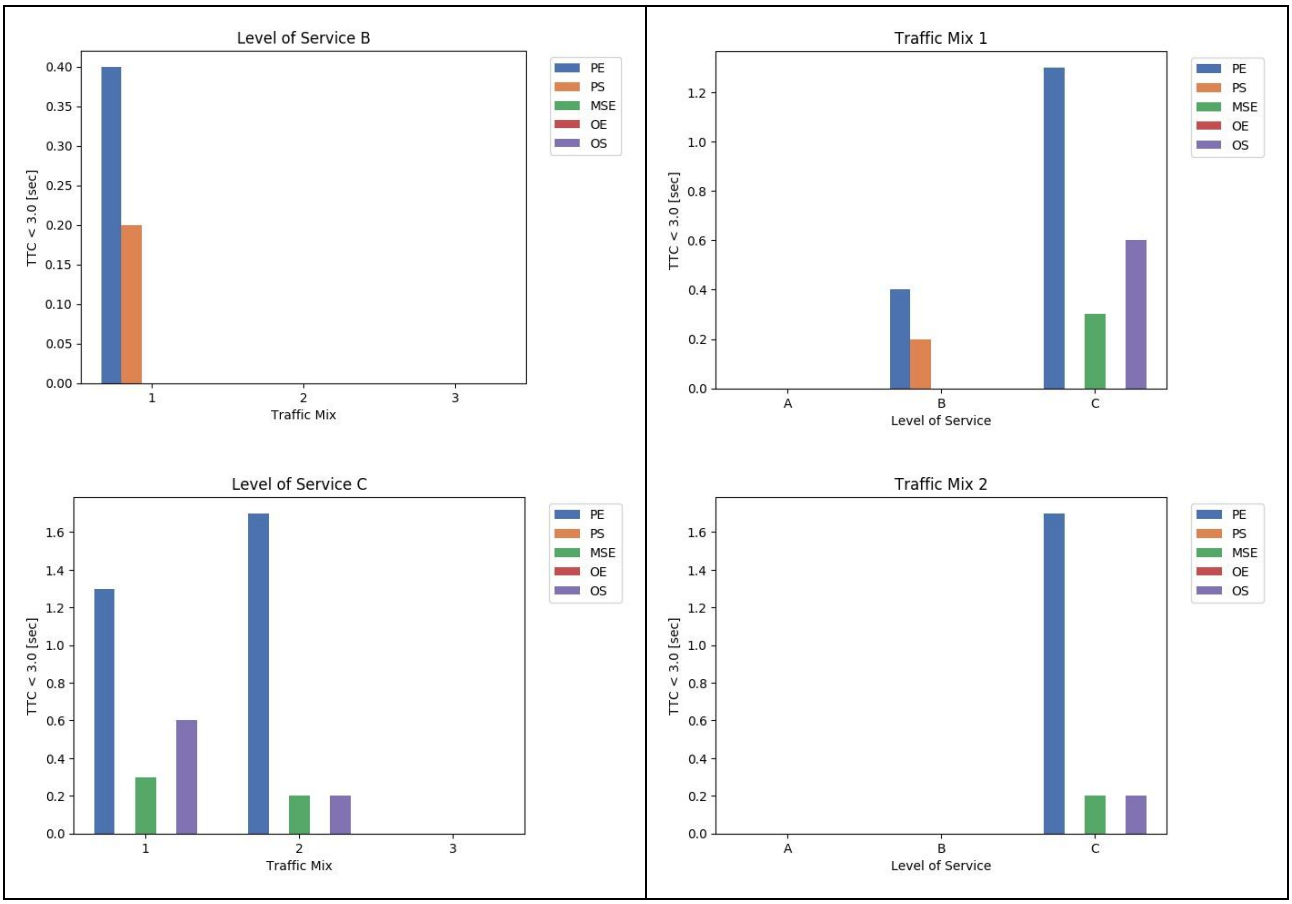

Figure 41. Average number of events with TTCs below 3.0 seconds for Scenario 3.1 baseline simulation experiments (varying parameter scheme, LOS, and traffic mix). Different bar colours correspond to different parameter schemes. The left column groups results by LOS, the right column by traffic mix.

4.1.3.2.4 Environmental Impacts

Figure 42 depicts average CO_2 emissions per kilometre travelled. It can be seen that CO_2/km increases with increasing demand (plots in the right column). However, it was shown in Section 4.3.2.1 that as demand increases average network speed decreases from 120 km/h (LOS A) to approximately 85 km/h (LOS C). For steady-state traffic flow (in the uncongested traffic flow regime) it would be expected that CO_2 emissions per kilometre travelled would decrease for the aforementioned speed drop. Thus, the observed increase of the emissions levels can be only explained by the disturbance introduced in the traffic stream by MRMs. This disturbance is increasing with increasing penetration rate of CAVs/CVs, thus yielding higher emissions levels.

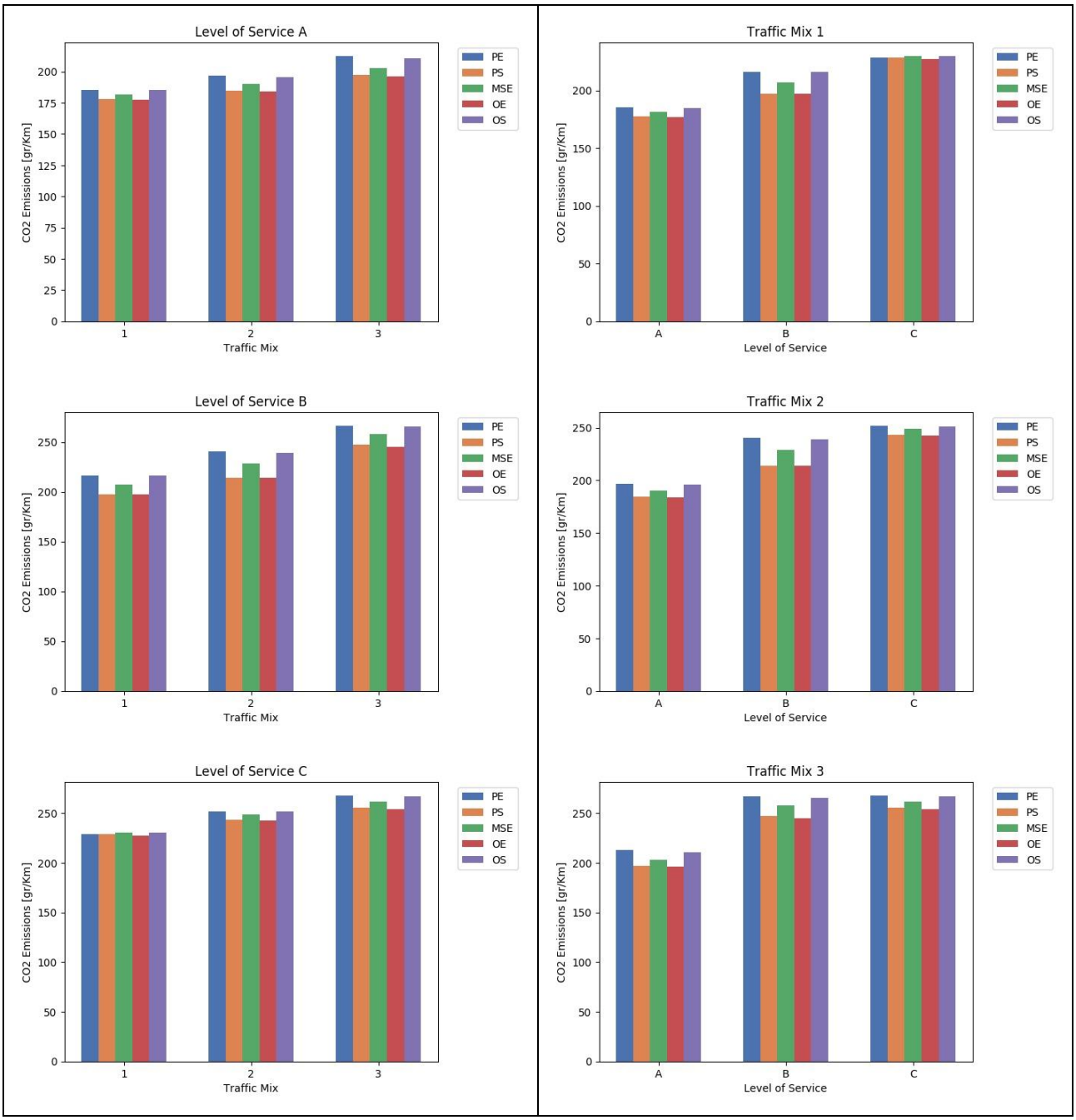

Figure 42. Average CO_2 emissions per km travelled for Scenario 3.1 baseline simulation experiments (varying parameter scheme, LOS, and traffic mix). Different bar colours correspond to different parameter schemes. The left column groups results by LOS, the right column by traffic mix.

4.1.4 Scenario 4.2: Safe spot in lane of blockage

4.1.4.1 Scenario Description

A construction site occupies the left lane of a two-lane road in Scenario 4.2 (urban and motorway cases considered) **(Figure 42)**. The RSI is informed about the construction site and the surrounding environment, and shares the relevant information with the approaching CAVs/CVs.

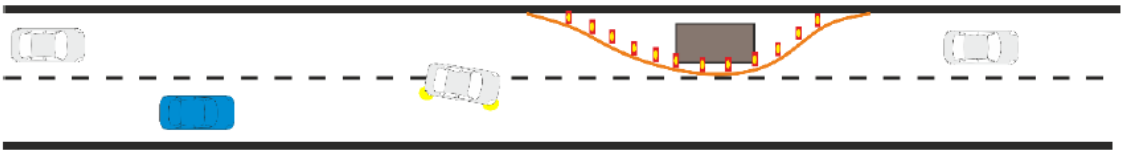

Figure 42. Schematic overview of Scenario 4.2.

However, there are CAVs that cannot drive along the construction site without additional guidance. Therefore, they need to perform a ToC; in case that a ToC is unsuccessful, the corresponding CAV must perform an MRM. Without additional measures the CAV would brake and come to a full stop in the ego lane, thus disrupting the traffic flow when that happens in the right lane. To prevent the latter case, the RSI also monitors the area just in front of the construction site and provides this place as a safe stop to the vehicle, if it is not occupied. The CAV uses the safe spot information to come to a smooth and safe stop in case of an MRM.

More details about the simulation networks (urban and motorway cases) of Scenario 4.2 can be found in **Table 36** & **37.**

Table 36. Network configuration details for Scenario 4.2 (urban).

Scenario 4.2_urban	**Settings**	**Notes**
Road section length	1.85 km	
Road priority	3	
Allowed road speed	13.89 m/s	• 50 km/h
Number of nodes	9	• n0 – n8
Number of edges	8	
Number of O-D relations	1	• from n0 to n8
Number of lanes	2	
Work zone location	from n4 to n5	• 250 m
Closed edge[1,2] (defined in the file: closeLanes.add.xml)	workzone	• the leftmost lane (250 m)
	safetyzone1	• the leftmost lane (50 m)
	Safetyzone2	• the leftmost lane (50 m)
Filenames	• network: UC4_2_urban.net.xml • lane closure: closeLanes.add.xml • traffic signs: shapes.add.xml	
Intended control of lane usage There is no control on lane usage. The RSI knows about it and provides this information to the approaching CAVs. Some CAVs are not able to pass the construction site and perform a ToC. Some of the ToCs are unsuccessful, so the respective CAV must perform a MRM. It uses the safe spot information just in front of the construction site to come to a safe stop.		

Network layout

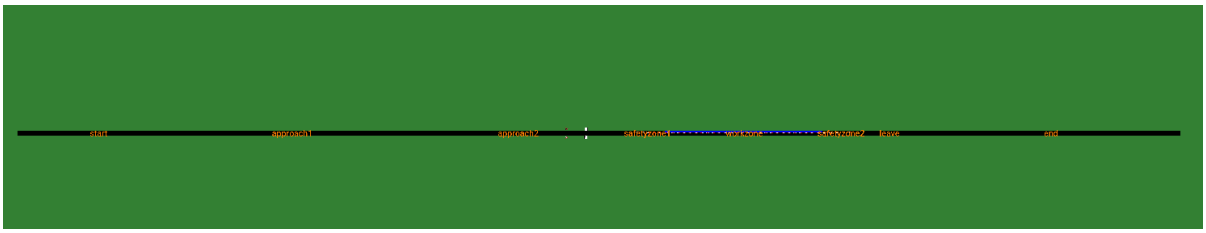

Road segments

n0→n1: Insertion and backlog area (300 m)
n1→n3: Approaching area (700 m)
n3→n4: Safety area (50 m)
n4→n5: Work zone (250 m)
n5→n6: Safety area (50 m)
n6→n8: Leaving area (500 m)

[1] The placement of the traffic signs is based on the German Guidelines for road job security (RSA).

[2] Required minimum safety distance according to the German Technical Rules for Workplaces ASR A5.2: 10m with allowed maximum speed 30 km/h; 50 m with allowed maximum speed 50 km/h; 100 m with allowed maximum speed 100 km/h.

Table 37. Network configuration details for Scenario 4.2 (motorway).

UC4.2_motorway	Settings	Notes
Road section length	2.15 km	
Road priority	3	
Allowed road speed	• 36.11 m/s • 27.78 m/s (700 m in front of the safety zone before entering the work zone area) • 22.22 m/s around the work zone	• 130 km/h • 100 km/h • 80 km/h
Number of nodes	9	• n0 – n8
Number of edges	8	
Number of O-D relations	1	• from n0 to n8
Number of lanes	2	
Construction location	from n4 to n5	• 150 m
Closed edge[3,4] (defined in the file: closeLanes.add.xml)	workzone	• the leftmost lane (150 m)
	safetyzone1	• the leftmost lane (100 m)
	safetyzone2	• the leftmost lane (100 m)
Filenames	• network: UC4_2_urban.net.xml • lane closure: closeLanes.add.xml • traffic signs: shapes.add.xml	

Intended control of lane usage

There is no control on lane usage. This situation is the same as the situation in an urban area, but on motorways. Speeds are higher, and more space and time are needed to execute the measures of this service.

Network layout

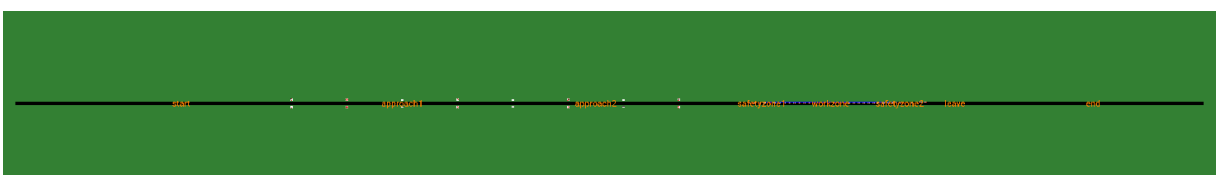

Road segments
n0→n1: Insertion and backlog area (600 m)
n1→n3: Approaching area (700 m)
n3→n4: Safety area (100 m)
n4→n5: Work zone (150 m)
n5→n6: Safety area (100 m)
n6→n8: Leaving area (500 m)

[3] The placement of the traffic signs is based on the German Guidelines for road job security (RSA).

[4] Required minimum safety distance according to the German Technical Rules for Workplaces ASR A5.2: 10m with allowed maximum speed 30 km/h; 50 m with allowed maximum speed 50 km/h; 100 m with allowed maximum speed 100 km/h.

4.1.4.2 Results

4.1.4.2.1 Urban Network

4.1.4.2.1.1 Impacts on Traffic Efficiency

Network-wide Impacts

Figure 43 depicts the average network speed for all Scenario 4.2 (urban network) baseline simulation experiments encompassing the different demand levels, traffic mixes, and parametrisation schemes. The two columns present the same data in a different format to facilitate the visual assessment with respect to the different traffic mixes (left column), and the different traffic demand levels (right column).

All plots indicate that average network speed does not decrease below 40 km/h despite the presence of the work zone (lane drop) and irrespective of the demand level, traffic mix, and parametrisation scheme. This implies that no major breakdown occurs due to the lane drop bottleneck.

Plots in the left column show that average network speed slightly decreases with increasing penetration rate of CAVs/CVs. As suggested in Section 4.1.2.1, this speed drop can be attributed to different factors, which affect the dynamics of automated vehicle models: (i) the required headway is estimated larger for automated vehicles, (ii) their acceleration rate is lower (i.e. the downstream end of jams dissolves slower), (iii) driver performance is decreased after a ToC, and (iv) MRMs may occur.

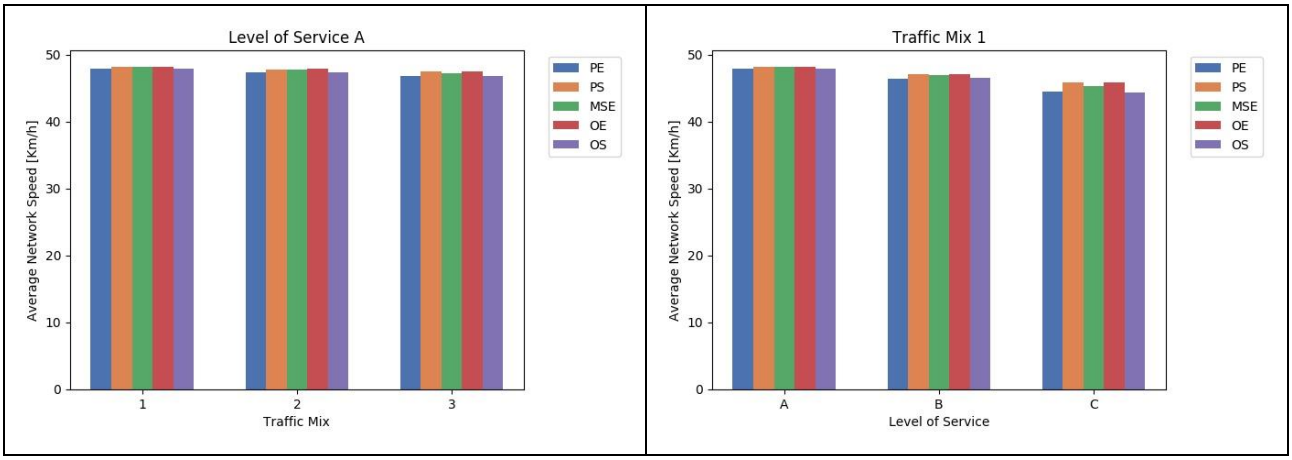

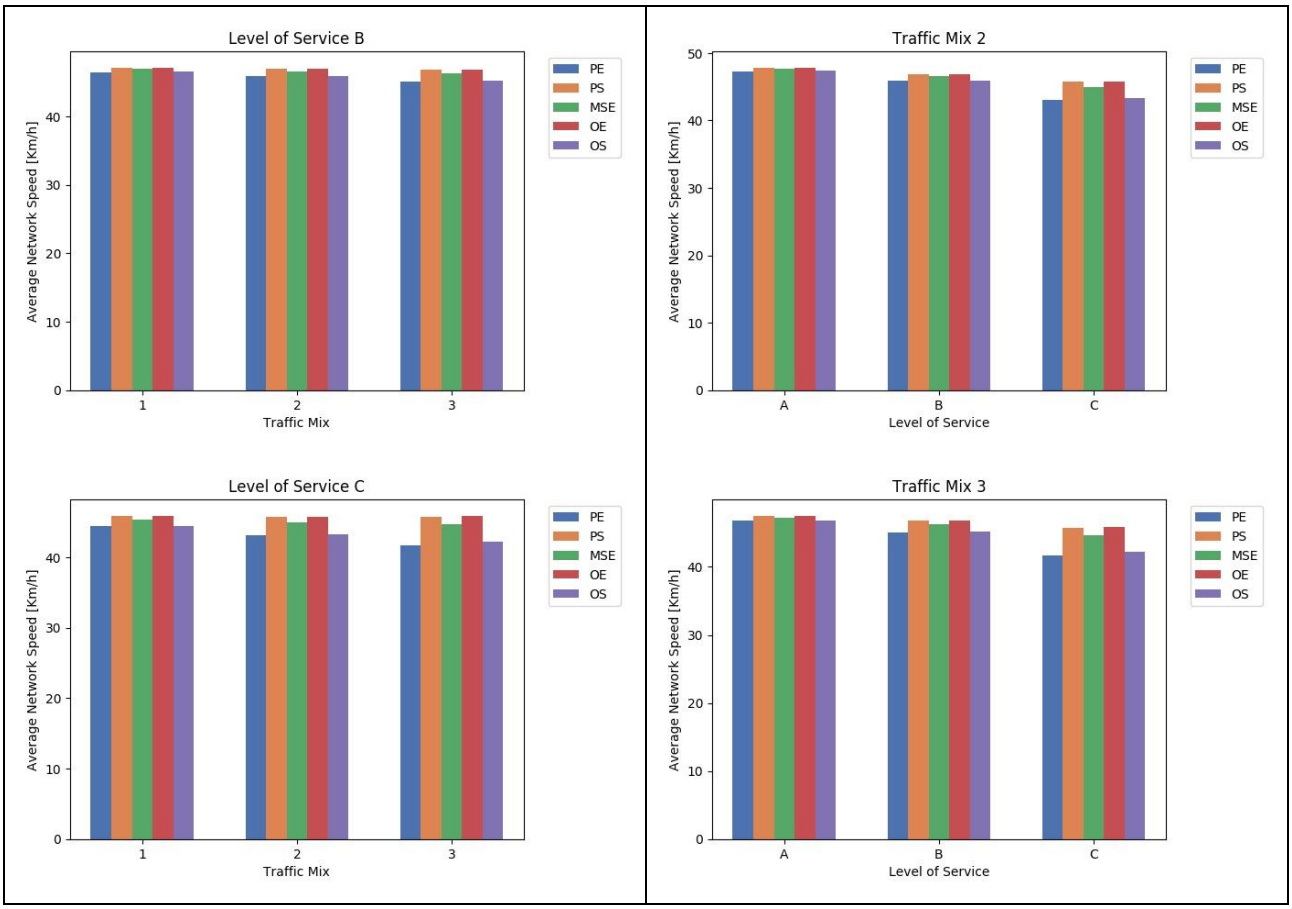

Figure 43. Average network speed for Scenario 4.2 (urban network) baseline simulation experiments (varying parameter scheme, LOS, and traffic mix). Different bar colours correspond to different parameter schemes.

We observe that the latter speed reduction is more significant for parametrisation schemes PE and OS, where driving behaviour was assumed more conservative. Finally, plots in the right column show that speed reduction is constant from LOS A to LOS B, and LOS B to LOS C for increasing penetration rate of CAVs/CVs.

Local Impacts

Figure 44 shows the average speed (taken over 5 minutes) on the edge 'approach_2', which is located just upstream of the subsequent lane drop at the beginning of the work zone (see network schematic in **Table 36**). The first row shows the results for different traffic demands (from LOS A to LOS C) and traffic mix 1. The average speed decreases for the parameter schemes OS and PE already at LOS B to some intermediate state, and drops slightly below 40 km/h at LOS C. Thus, we infer that merging operations remain smooth enough for traffic mix 1 irrespective of traffic demand. The latter picture deteriorates for higher traffic demands (lesser for LOS B, and more for LOS C) under traffic mixes 2 and 3. It is clear that traffic operations in the merging area upstream of the work zone become less efficient when both traffic demand (LOS C) and the penetration rate of CAVs/CVs are high. Observations regarding the local impacts coincide with the aforementioned network-wide ones.

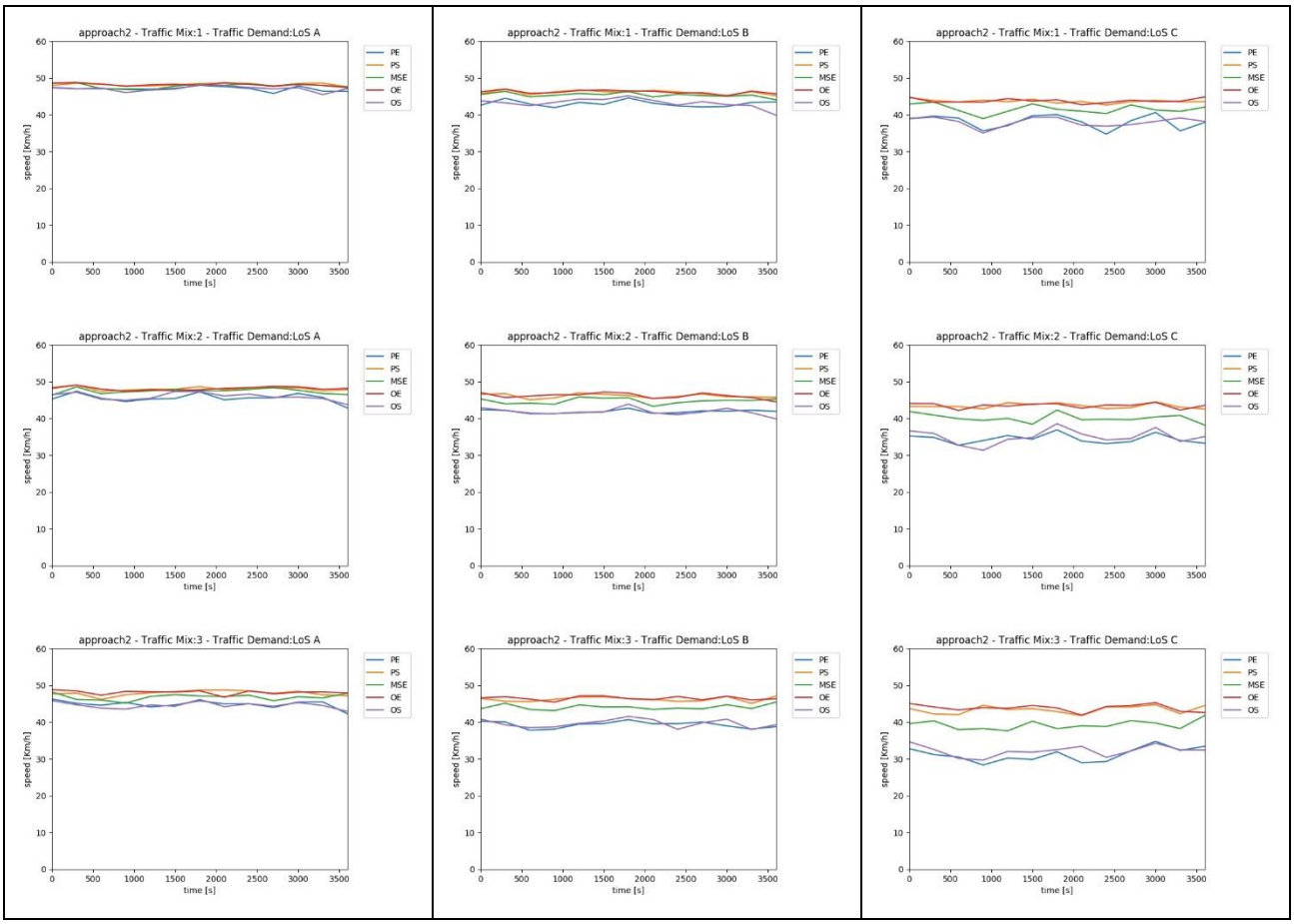

Figure 44. Average speed at the edge 'approach_2' for the different parameter sets. First row: varying LOS at traffic mix 1; second row: varying LOS at traffic mix 2; third row: varying LOS at traffic mix 3.

Moreover, no significant spillbacks are formed along edge 'appraoch_2' irrespective of the traffic mix, traffic demand level, and parametrisation scheme **(Figure 45)**. An average queue length of 20 m is observed in the worst case scenario (traffic mix 3, LOS c and parametrisation scheme PE), which is typical for lane drop locations due to construction site. Therefore, queue length statistics also demonstrate that merging operations at the lane drop are smooth for the examine scenarios.

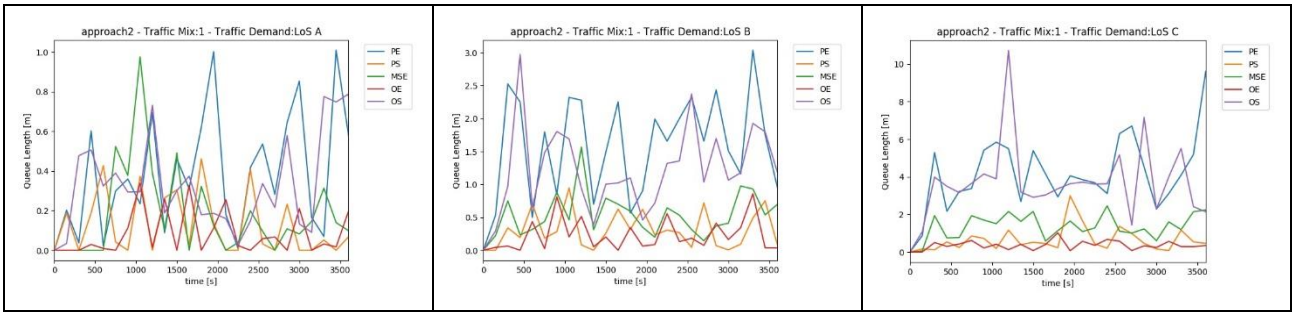

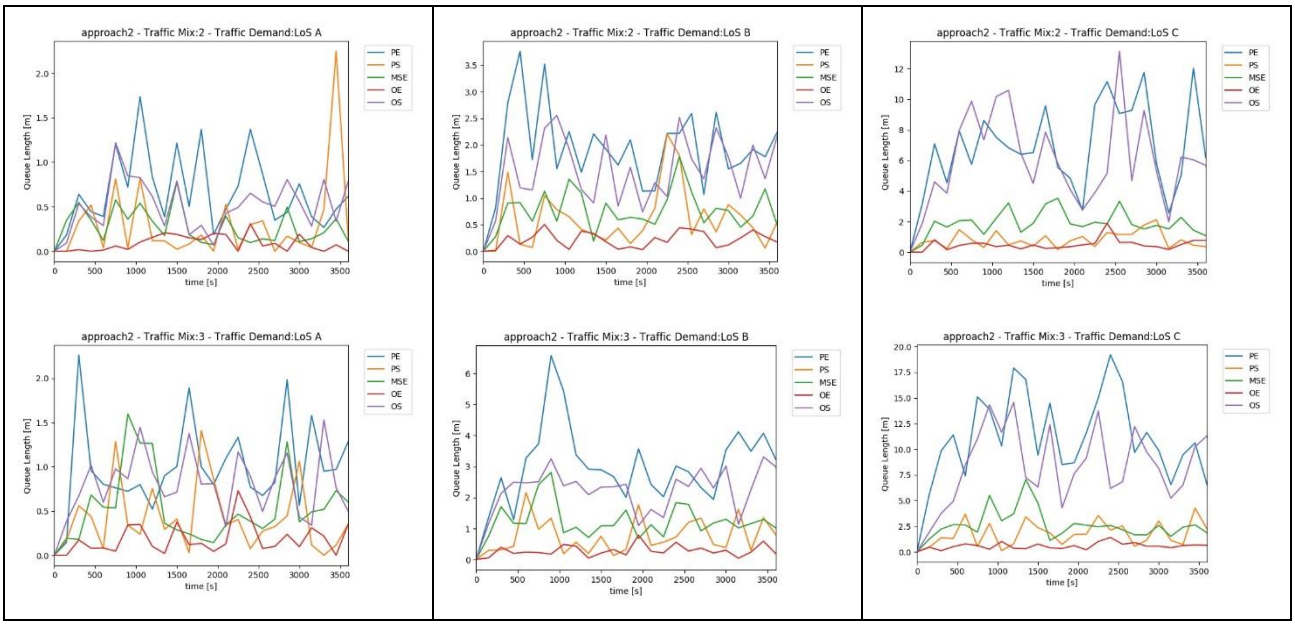

Figure 45. Average queue length at the edge 'approach_2' for the different parameter sets. First row: varying LOS at traffic mix 1; second row: varying LOS at traffic mix 2; third row: varying LOS at traffic mix 3.

4.1.4.2.1.2 Impacts on Traffic Dynamics

Figure 46 shows the total number of lane changes per simulated scenario. For traffic mix 1 the number of lane changes is proportional to the number of injected vehicles in the simulation network with a constant factor of approximately one lane change per vehicle (irrespective of LOS). As the share of CAVs/CVs increases, it can be observed that the number of lane changes per vehicle decreases (especially for traffic mix 3 and LOS B and C). This phenomenon is expected since the $lcAssertive$ parameter (i.e. the willingness to accept lower front and rear gaps on the target lane) is in general higher for LVs compared to CAVs/CVs. Moreover, for high share of CAVs/CVs (traffic mix 3) and traffic demand (LOS) it appears that parametrisation schemes corresponding to more congested conditions (MSE, PE and OS) result in more lane changes per vehicle compared to less congested ones (OE and PS). This observation complies similar findings in Section 4.1.2.2.

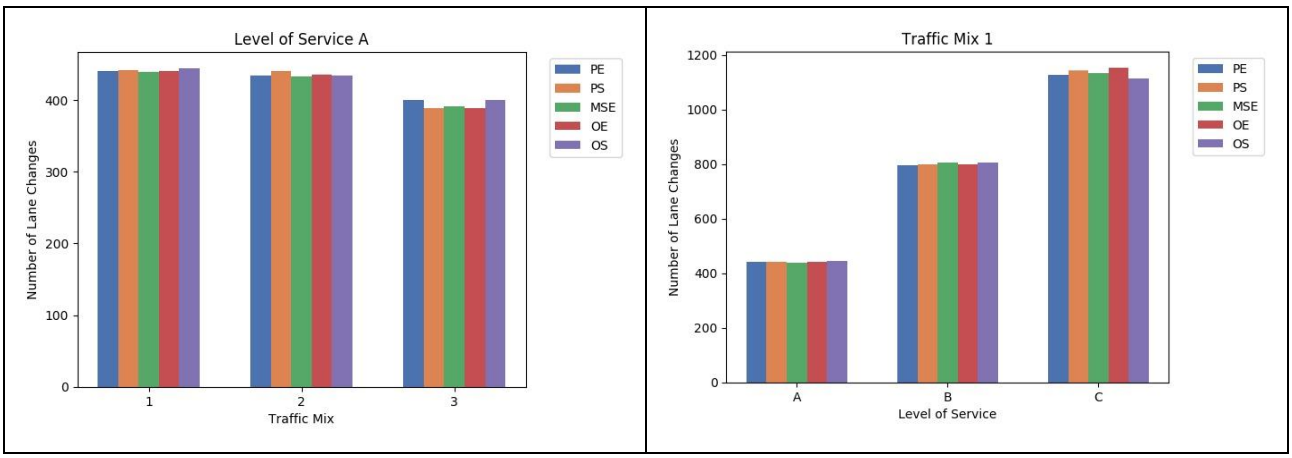

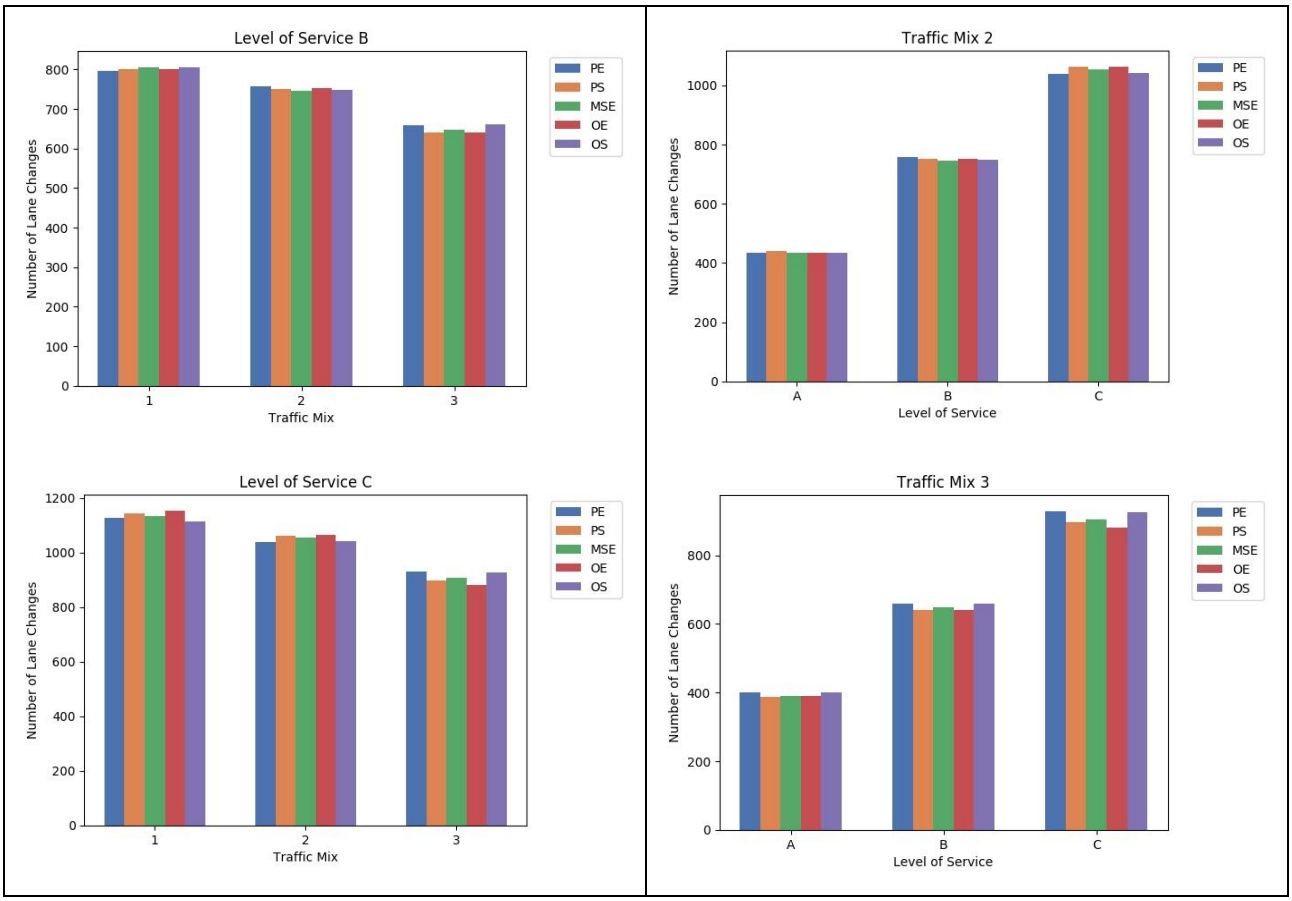

Figure 46. Number of lane changes for Scenario 4.2 (urban network) baseline simulation experiments (varying parameter scheme, LOS, and traffic mix). Different bar colours correspond to different parameter schemes. The left column groups results by LOS, the right column by traffic mix.

4.1.4.2.1.3 Impacts on Traffic Safety

Figure 47 presents the average number of events with $TTC < 3.0$ s (termed 'critical' below). Plots in the left column indicate that the number of critical events increases with increasing traffic demand. However, it has to be noted that this increase becomes more distinct for scenarios corresponding to lower average network speed (PE and OS schemes). An increase in the number of critical events is also observed for increasing penetration rate of CAVs/CVs.

As discussed in Section 4.4.2.1.2, CAVs/CVs accept larger gaps for lane-changing compared to LVs in baseline simulation experiments. Thus, the likelihood of finding a gap to merge early on the right-most lane (open lane) is lower and finally they have to come to a full stop (emergency braking) in front of the closed lane more frequently. This phenomenon causes several rear-end conflicts which are safety critical. This tendency is more pronounced for schemes PE and OS where CAVs/CVs become more unwilling to accept short gaps for lane-changing due to the corresponding driver model parameter values. However, it has to be stressed that based on this finding (which is counter-intuitive), schemes that were expected to favour efficiency explicitly, also generate safety benefits which would be expected when driving behaviour is more conservative in general.

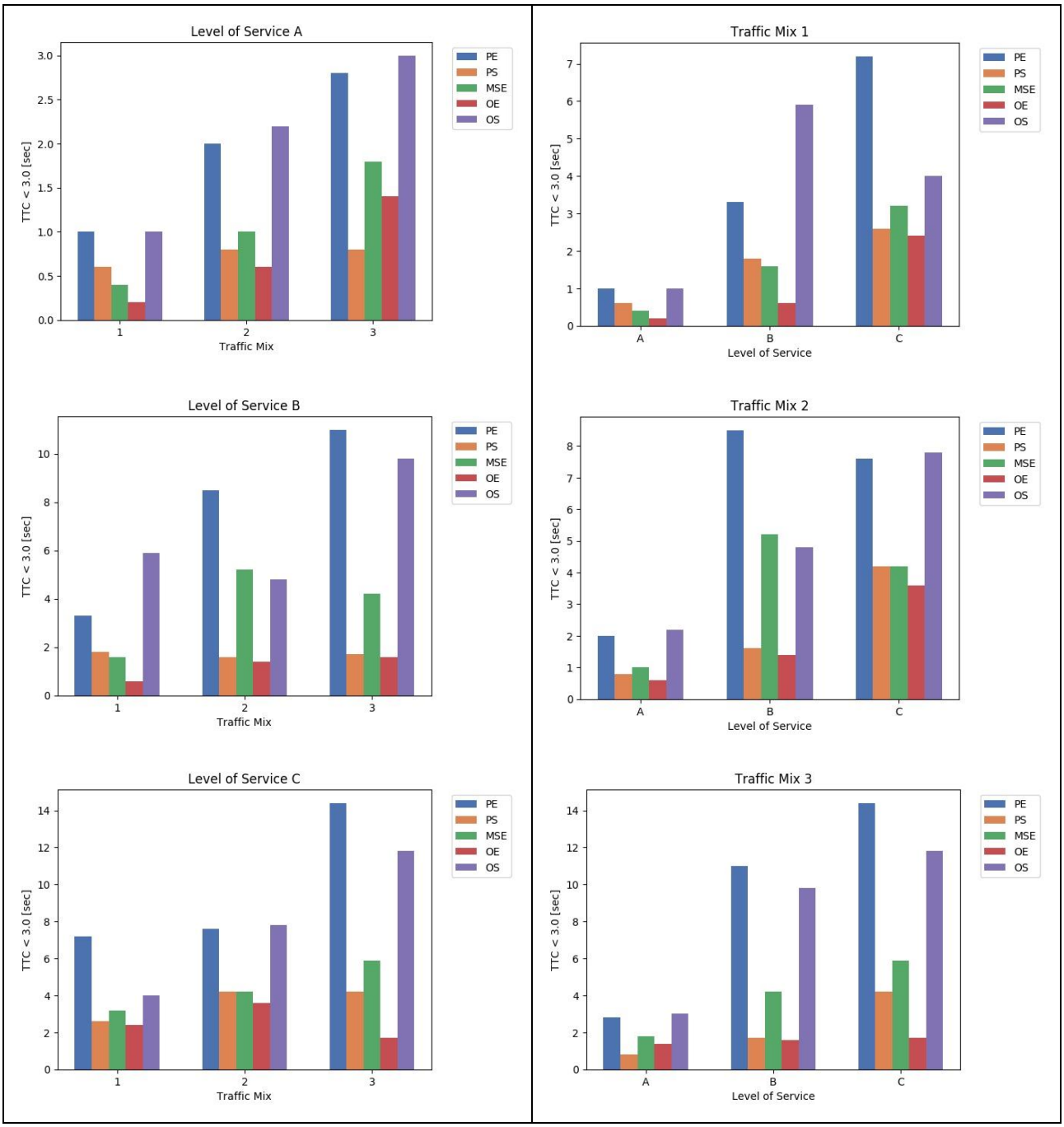

Figure 47. Average number of events with TTCs below 3.0 seconds for Scenario 4.2 (urban network) baseline simulation experiments (varying parameter scheme, LOS, and traffic mix). Different bar colours correspond to different parameter schemes. The left column groups results by LOS, the right column by traffic mix.

4.1.4.2.1.4 Environmental Impacts

Figure 48 depicts average CO_2 emissions per kilometre travelled. It can be seen that CO_2/km increases as traffic efficiency decreases **(Figure 43)**. Even for the same LOS and traffic mix, parametrisation schemes that favour efficiency exhibit reduced emissions levels compared to those favouring safety. This trend is uniform irrespective of the traffic demand level and traffic mix.

Moreover, it is shown that as the share of CAVs/CVs increases in the traffic mix, CO_2/km increases irrespective of the traffic demand level. The increased emission rates in the case CAVs/CVs are more in the traffic mix can be ascribed to the fact that 75% of them execute ToCs (a few leading to MRMs) at TAs, thus disturbing traffic operations at TAs as mentioned in Section 4.1.1.2.4. This phenomenon is more prominent for parametrisation scheme PE where driver awareness at the onset of ToC is reduced. Another reason is the fact that traffic composition is more homogeneous for traffic mix 1.

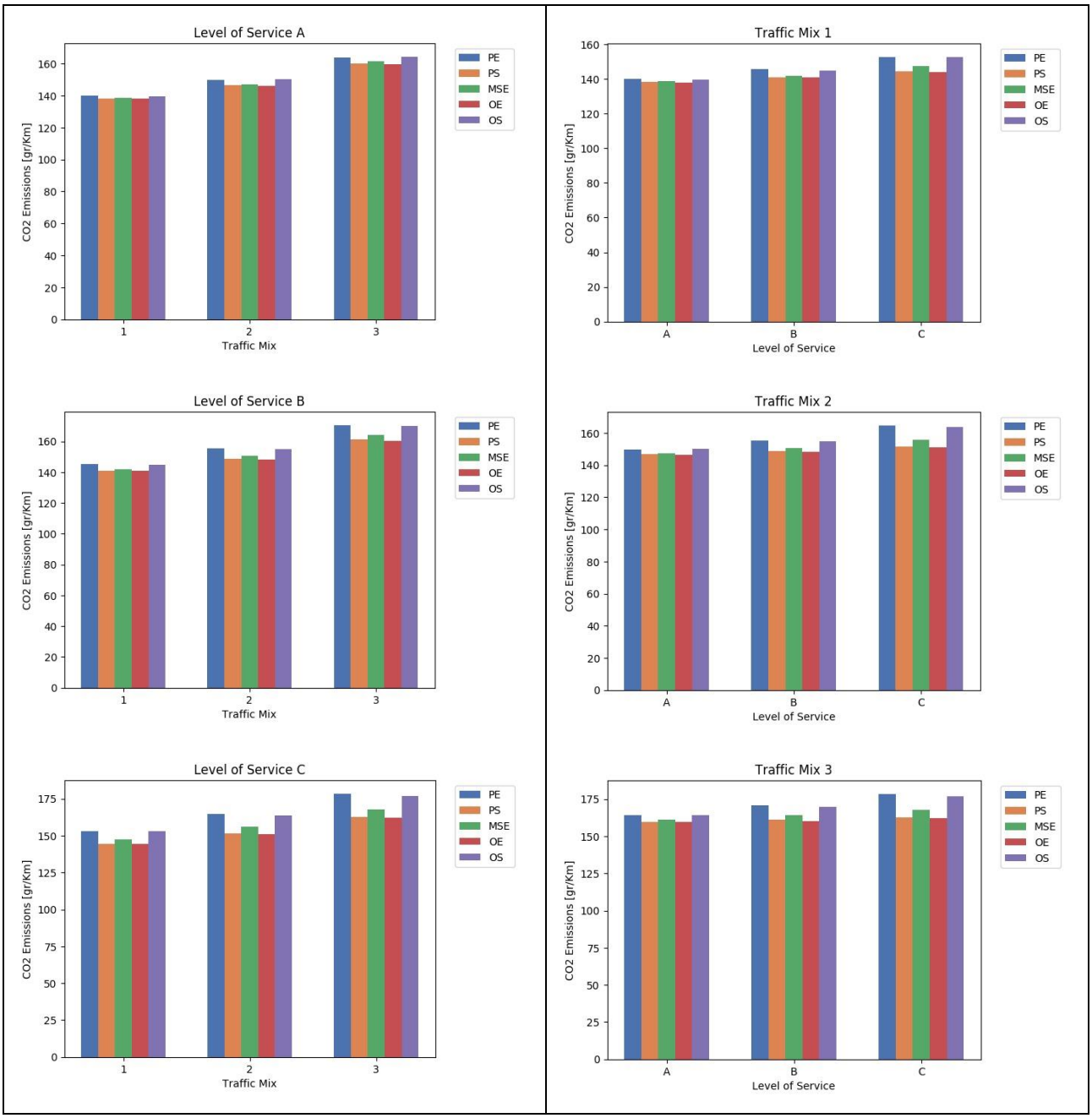

Figure 48. Average CO_2 emissions per km travelled for Scenario 4.2 (urban network) baseline simulation experiments (varying parameter scheme, LOS, and traffic mix). Different bar colours correspond to different parameter schemes. The left column groups results by LOS, the right column by traffic mix.

4.1.4.2.2 Motorway Network

4.1.4.2.2.1 Impacts on Traffic Efficiency

Network-wide Impacts

Figure 49 depicts the average network speed for all Scenario 4.2 (motorway network) baseline simulation experiments encompassing the different demand levels, traffic mixes, and parametrisation schemes. The two columns present the same data in a different format to facilitate the visual assessment with respect to the different traffic mixes (left column), and the different traffic demand levels (right column).

Plots in the left column indicate that average network speed decreases with increasing CAVs/CVs penetration rate. This effect becomes more significant as traffic demand increases. Moreover, it is shown that the influence of the different parametrisation schemes on average network speed exhibits the same trend irrespective of the traffic mix. Schemes PS and OE impact traffic efficiency positively (even in LOS C traffic conditions), while schemes PE and OS result in reduced levels of traffic efficiency.

Plots in the right column show that traffic efficiency is significantly decreased for LOS C. Parametrisation schemes MSE, PE and OS yield congested conditions (stop-and-go traffic) in this case, while schemes OE and PS result in less dense traffic. Free-flow traffic does not prevail even for LOS A, since merging at the lane drop area cannot be smooth due to the high injection rate of vehicles in the motorway network. The injection rate is higher compared to the urban case as shown in Section 3.4, because the capacity of a motorway lane is higher compared to an urban one. Thus, the differences in the operation of the urban and the motorway network can be explained.

As mentioned in previous sections, an important factor affecting merging operations upstream of the work zone is the desired longitudinal gaps by vehicles to change lane. For vehicle types that demand larger gaps, merging on the right-most open lane is less likely to occur upstream of the lane drop, thus resulting in full vehicle stops just upstream of the work zone. Therefore, stop-and-go traffic for LOS C and parametrisation schemes PE and OS is reasonable.

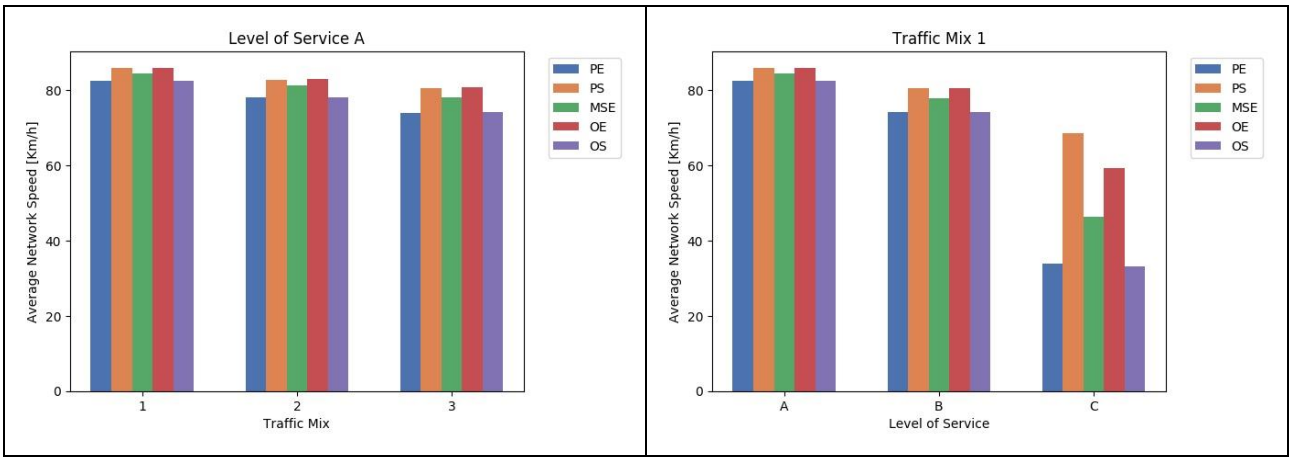

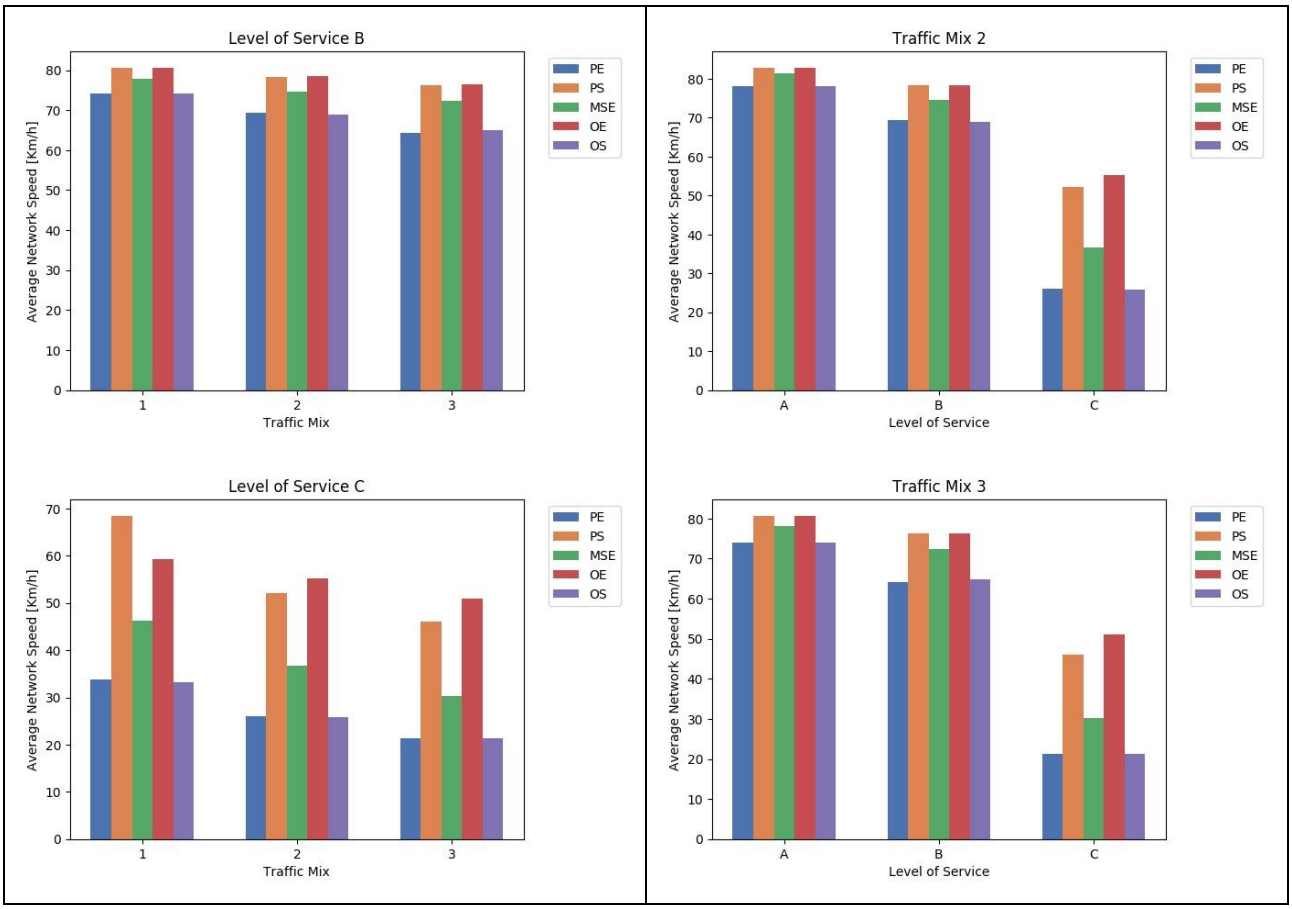

Figure 49. Average network speed for Scenario 4.2 (motorway network) baseline simulation experiments (varying parameter scheme, LOS, and traffic mix). Different bar colours correspond to different parameter schemes.

Local Impacts

Figure 50 shows the average speed (taken over 5 minutes) on the edge 'approach_2', which is located just upstream of the subsequent lane drop at the beginning of the work zone (see network schematic in **Table 37**). The first row shows the results for different traffic demands (from LOS A to LOS C) and traffic mix 1. As traffic increases, the efficiency of merging operations deteriorates until breakdown occurs for LOS C. The effect of the different parametrisation schemes becomes more distinct with the increase of traffic demand as well. Schemes PE and OS generate stop-and-go traffic due to conservative lane-changing. The latter distinction is more pronounced for higher penetration rate of CAVs/CVs, since these vehicles were modelled to accept larger gaps for lane-changing compared to LVs. Observations regarding the local impacts coincide with the aforementioned regarding the network-wide ones.

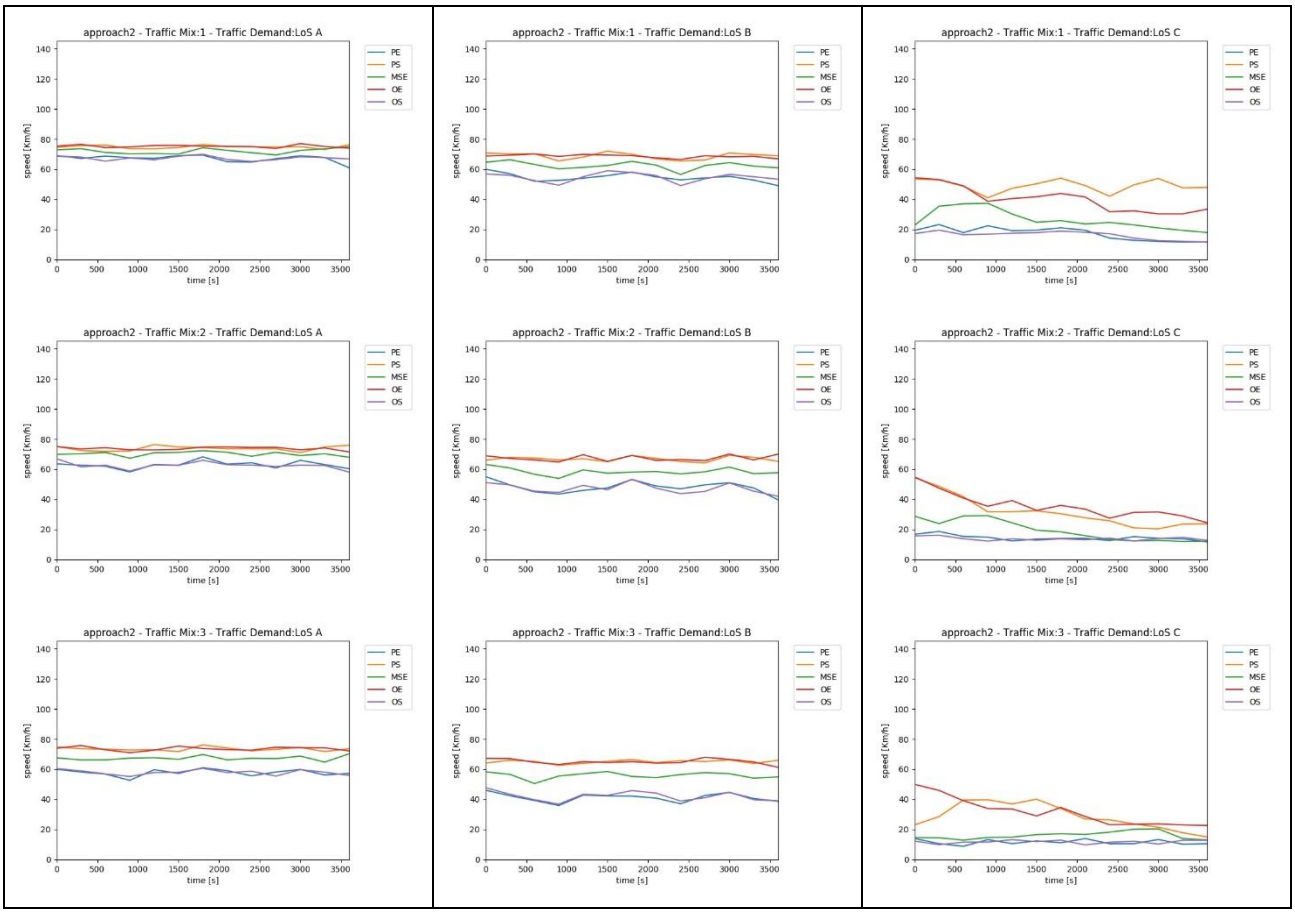

Figure 50. Average speed at the edge 'approach_2' for the different parameter sets. First row: varying LOS at traffic mix 1; second row: varying LOS at traffic mix 2; third row: varying LOS at traffic mix 3.

The breakdown occurring for LOS C is also reflected in terms of spillback formed along edge 'approach_2' **(Figure 51)**. Maximum queue length of approximately 320 m is observed for traffic mix 3, LOS C and parametrisation schemes PE and OS. However, long queues are created for the other parametrisation schemes as well for the aforementioned traffic mix and LOS. In general, observations regarding the local impacts coincide with the aforementioned regarding the network-wide ones.

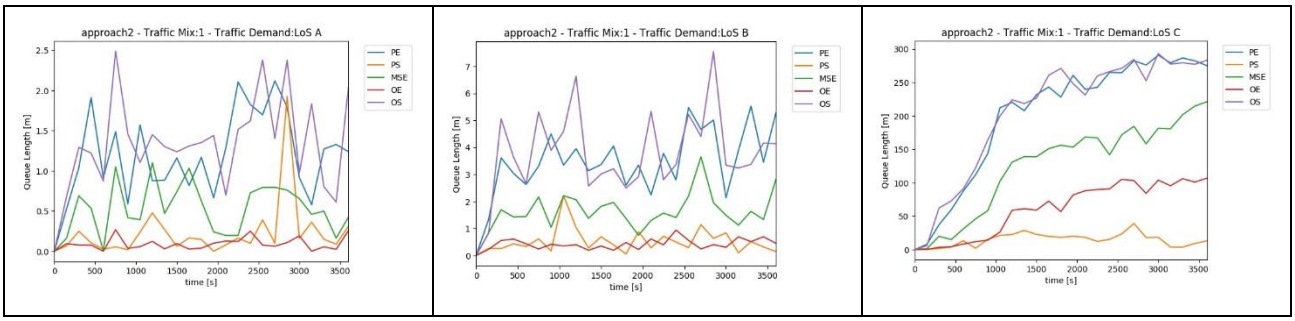

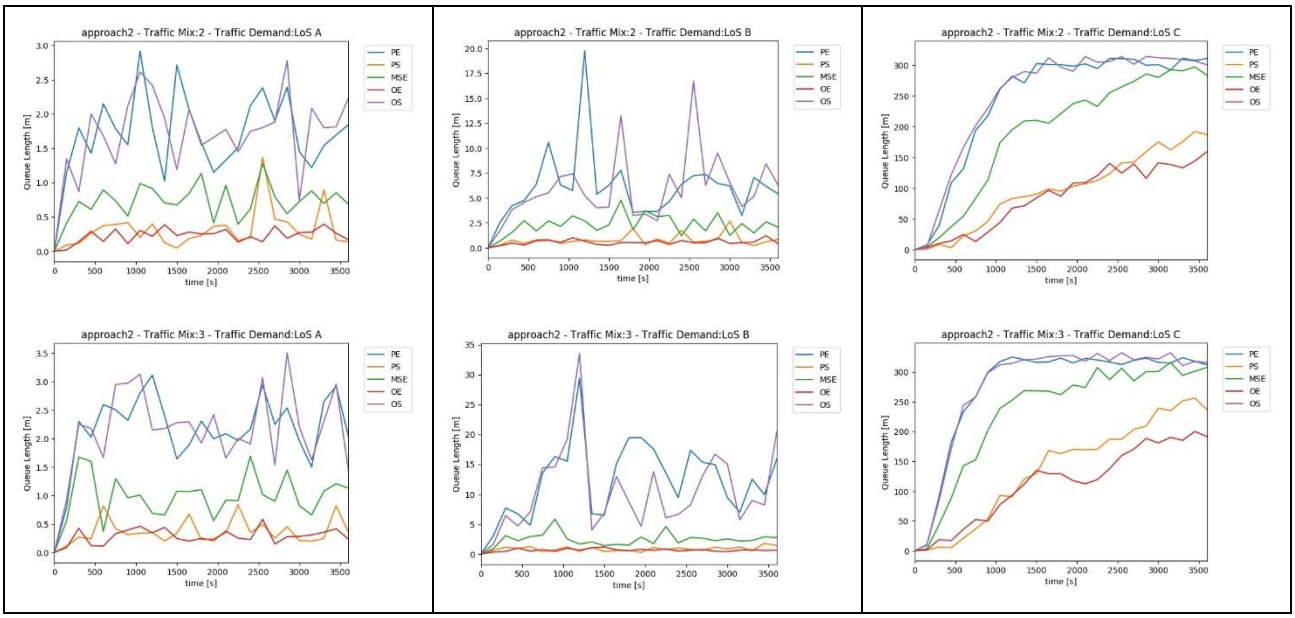

Figure 51. Average queue length at the edge 'approach_2' for the different parameter sets. First row: varying LOS at traffic mix 1; second row: varying LOS at traffic mix 2; third row: varying LOS at traffic mix 3.

4.1.4.2.2.2 Impacts on Traffic Dynamics

Figure 52 shows the total number of lane changes per simulated scenario. For traffic mix 1 and LOS A the number of lane changes is proportional to the number of injected vehicles in the simulation network with a constant factor of approximately one lane change per vehicle. However, for higher demand levels corresponding to lower average network speeds (LOS B and C), the lane change rate per vehicle is higher than one. It is clear that the smoother merging operations are at the lane drop, lesser lane changes are executed during the simulation. For congested conditions, conservative vehicle behaviour results in more lane changes compared to moderate or aggressive (parametrisation schemes PE and OS for traffic mixes 1 and 2, and LOS C). However, when the network is fully jammed (traffic mix 3, LOS C, and parametrisation schemes PE and OS) there is no room for tactical lane changes and the latter phenomenon vanishes. The overall picture with respect to lane changes is rather complex for this scenario and no generic conclusions can be drawn since congestion builds up upstream of the lane drop for most of the traffic mixes, traffic demand levels and parametrisation schemes.

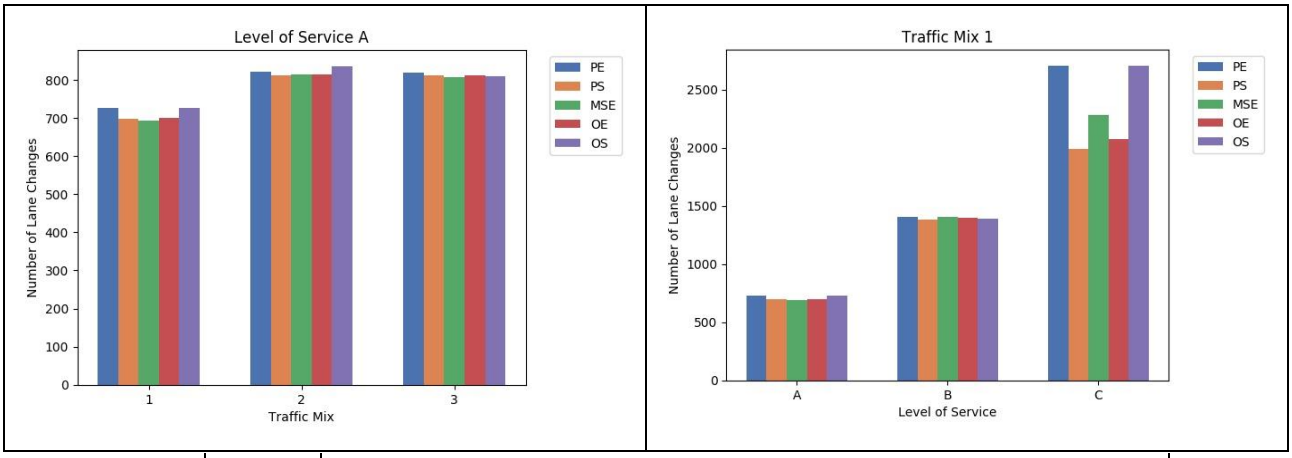

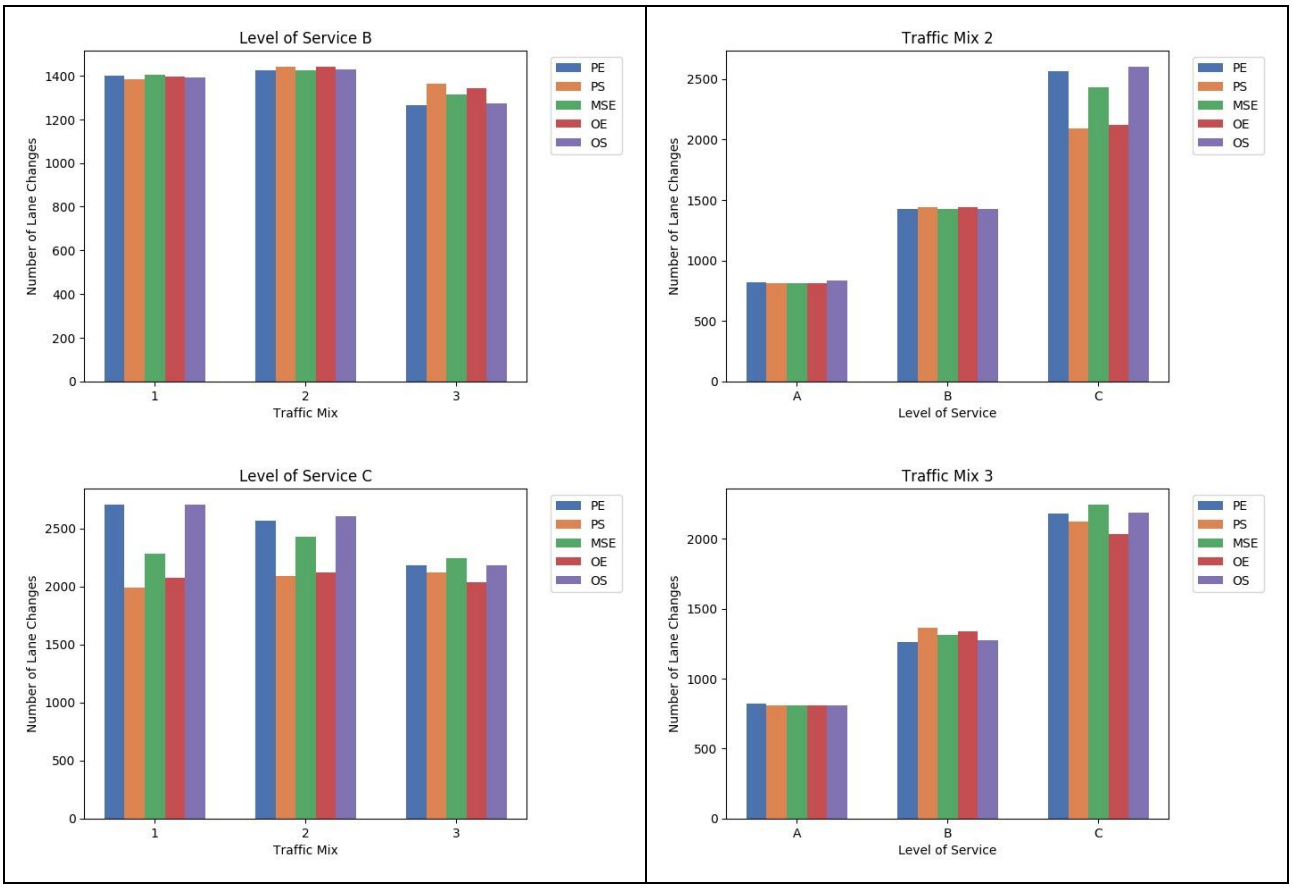

Figure 52. Number of lane changes for Scenario 4.2 (motorway network) baseline simulation experiments (varying parameter scheme, LOS, and traffic mix). Different bar colours correspond to different parameter schemes. The left column groups results by LOS, the right column by traffic mix.

4.1.4.2.2.3 Impacts on Traffic Safety

Figure 53 presents the average number of events with $TTC < 3.0$ s (termed 'critical' below). Plots in the left column indicate that the number of critical events increases with increasing traffic demand. However, it has to be noted that this increase becomes more distinct for scenarios corresponding to lower average network speed (PE and OS schemes). When the network becomes fully jammed (traffic mix 3, LOS C, and parametrisation schemes PE and OS) the latter difference in safety critical events between different parametrisation schemes diminishes since there is limited free space for lane-changing on the motorway network.

As discussed in Section 4.4.2.1.2, CAVs/CVs accept larger gaps for lane-changing compared to LVs in baseline simulation experiments. Thus, the likelihood of finding a gap to merge early on the right-most lane (open lane) is lower and finally they have to come to a full stop (emergency braking) in front of the closed lane more frequently. This phenomenon causes several rear-end conflicts which are safety critical. This tendency is more pronounced for schemes PE and OS where CAVs/CVs become more unwilling to accept short gaps for lane-changing due to the corresponding driver model parameter values. However, it has to be stressed that based on this finding (which is counter-intuitive), schemes that were expected to favour efficiency explicitly, als generate safety benefits which would be expected when driving behaviour is more conservative in general.

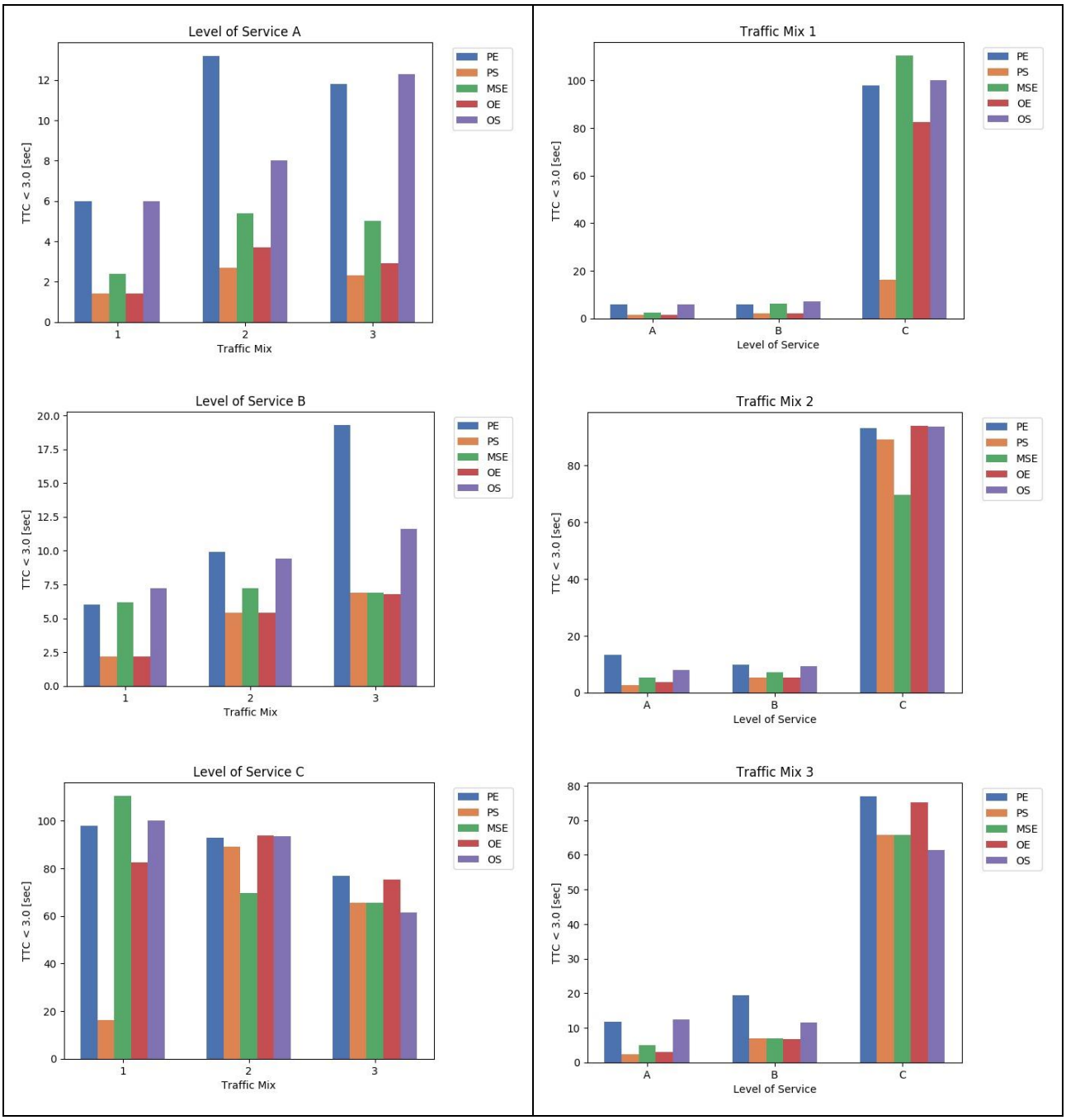

Figure 53. Average number of events with TTCs below 3.0 seconds for Scenario 4.2 (motorway network) baseline simulation experiments (varying parameter scheme, LOS, and traffic mix). Different bar colours correspond to different parameter schemes. The left column groups results by LOS, the right column by traffic mix.

4.1.4.2.2.4 Environmental Impacts

Figure 54 depicts average CO_2 emissions per kilometre travelled. It can be seen that CO_2/km increases as traffic efficiency decreases **(Figure 49)**. For congested conditions (LOS C and parametrisation schemes PE and OS), emission levels increase dramatically due to stop-and-go traffic. Even for the same LOS and traffic mix, parametrisation schemes that favour efficiency

exhibit reduced emissions levels compared to those favouring safety. This trend is uniform irrespective of the traffic demand level and traffic mix.

Moreover, it is shown that as the share of CAVs/CVs increases in the traffic mix, CO_2/km increases irrespective of the traffic demand level. The increased emission rates in the case CAVs/CVs are more in the traffic mix can be ascribed to the fact that 75% of them execute ToCs (a few leading to MRMs) at TAs, thus disturbing traffic operations at TAs as mentioned in Section 4.1.1.2.4. This phenomenon is more prominent for parametrisation scheme PE where driver awareness at the onset of ToC is reduced. Another reason is the fact that traffic composition is more homogeneous for traffic mix 1.

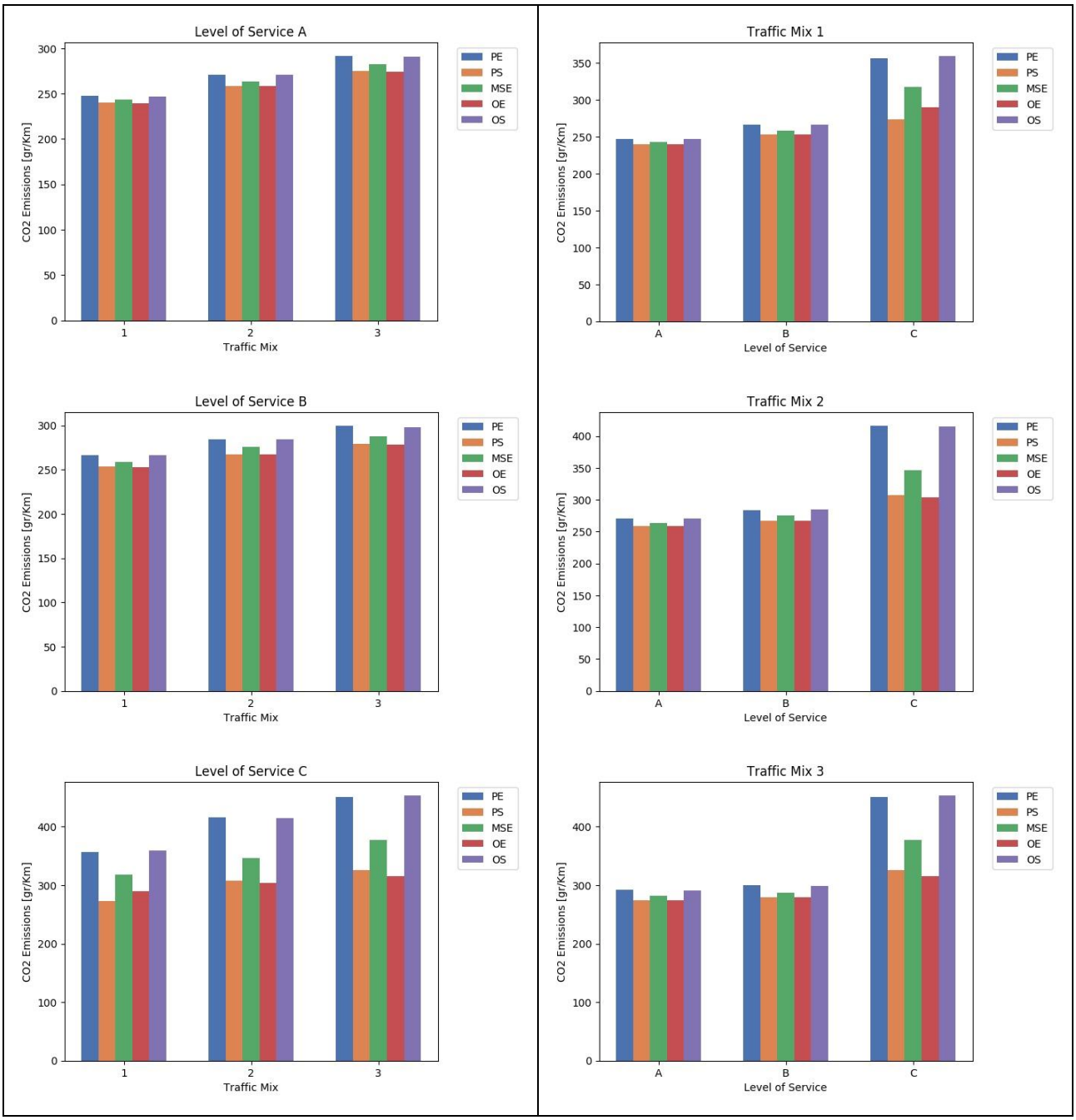

Figure 54. Average CO_2 emissions per km travelled for Scenario 4.2 (motorway network) baseline simulation experiments (varying parameter scheme, LOS, and traffic mix). Different bar colours correspond to different parameter schemes. The left column groups results by LOS, the right column by traffic mix.

4.1.5 Scenario 5.1: Schedule ToCs before no AD zone

4.1.5.1 Scenario Description

A (C)AV/CV is expected to behave more erratically after ToC. The dissimilarity between the driving behaviour during transitions and the driving behaviour shortly thereafter, might result in a significant disruption of traffic flow and safety. This effect is amplified when many ToCs occur in the same area. Hence, to avoid the latter amplification in mixed traffic scenarios, downward ToCs are distributed in time and space upstream of an area where no or limited automated driving is unavoidable (e.g., tunnels, geo-fenced areas, or complicated road works).

Figure 55 illustrates Scenario 5.1 where vehicles are approaching a no-AD zone consisting of two lanes. At some point upstream of the no-AD zone, the RSI defines through the collective perception process both the positions and speeds of vehicles and determines the optimal location and moment for CAVs/CVs to perform a downward ToC. Subsequently, ToC requests are provided to the corresponding CAVs/CVs; based on these ToC requests, CAVs/CVs perform ToCs at the desired location and time.

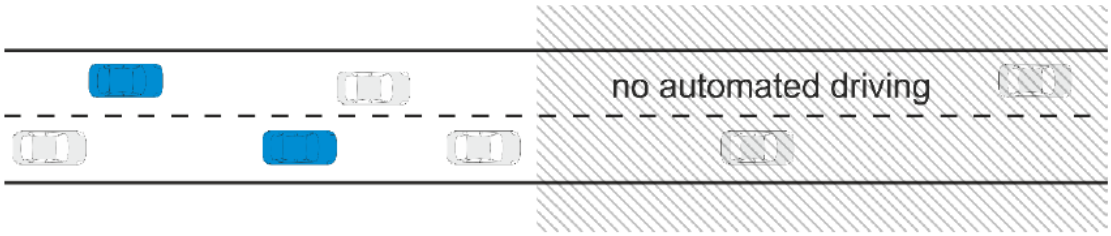

Figure 55. Schematic overview of Scenario 4.2.

Note: the figure is schematic. The blue CAVs have performed ToCs further upstream than the picture might suggest.

More details about the simulation network of Scenario 5.1 can be found in **Table 38.**

Table 38. Network configuration details for Scenario 5.1.

Scenario 5.1	Settings	Notes
Road section length	5.0 km	
Road priority	3	
Allowed road speed	27.78 m/s	• 100 km/h
Number of nodes	2	• n0 – n1
Number of edges	1	
Number of O-D relations	1	• n0 to n1
Number of lanes	2	• 2 normal lanes
Work zone location	-	
Closed edges	-	

Disallowed vehicle classes	• normal lanes: pedestrians, tram, rail_urban, rail, rail_electric, ship	• from n0 to n1
Filenames	• network: TransAID_UC5-1.net.xml	
Intended control of lane usage CAVs and other traffic are approaching a no-AD zone with 2 lanes. Starting about 3.0 km upstream from the no-AD zone, the RSI determines through collective perception the positions and speeds of vehicles and determines the optimal location and moment for CAVs to perform a downward ToC. Subsequently, ToC requests are provided to the corresponding CAVs. Based on the ToC requests, the CAVs perform ToCs at the desired location and moment in time and transition to manual mode. CVs are warned about the ToCs and possible MRMs. In the no-AD zone, the CAVs are in manual mode.		
Network layout 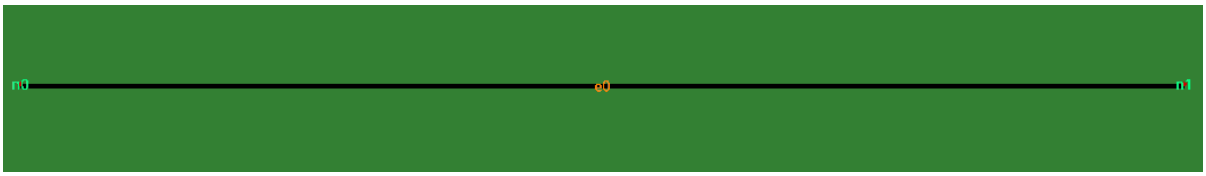		
Road segments n0→n1: (5.000 m)		

4.1.5.2 Results

4.1.5.2.1 Impacts on Traffic Efficiency

Network-wide Impacts

The results obtained for use case five using a demand of maximally LoS C for the two lane highway scenario did not show significant disruptions of the smooth traffic flow in the scenario, see **Figure 56** for some samples illustrating the average network speed, which remains approximately constant at the speed limit of 120 km/h for all scenarios and parameter schemes.

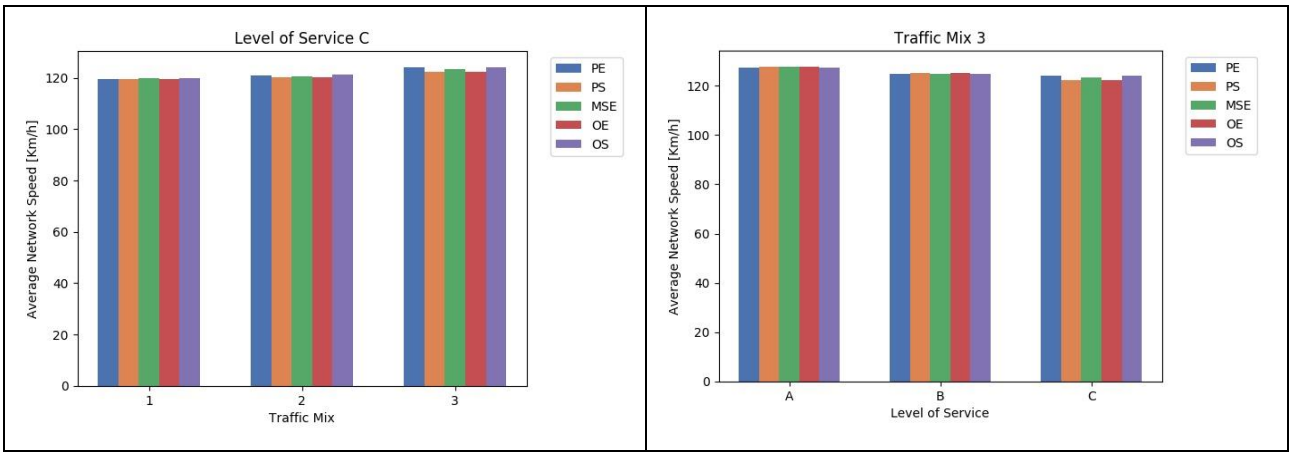

Figure 56. Average network speed for Scenario 5.1 baseline simulation experiments (varying parameter scheme, LOS, and traffic mix). Different bar colours correspond to different parameter schemes.

Local Impacts

Figure 57 reveals once more that there are no significant differences between the different scenarios. Apart from a small decrease of the free flow average speed on edge 'e0' for increasing demand no difference between the tested parametrisation schemes and traffic composition can be identified. This decreased average speed is due to the DVU's varying desired speeds and the slightly increased likelihood that a DVU with a smaller desired speed impedes another one from attaining its higher desired speed if there are more vehicles are on the road.

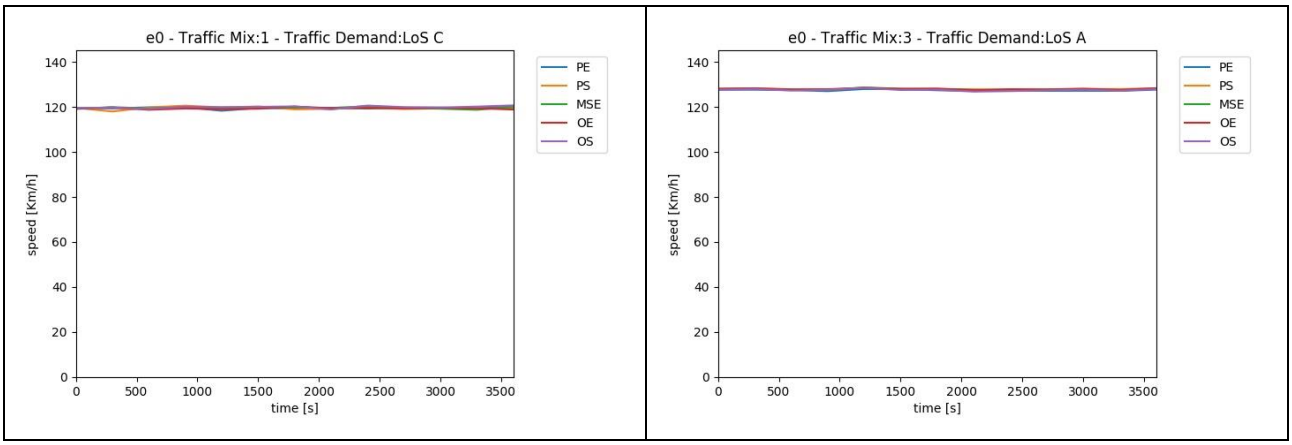

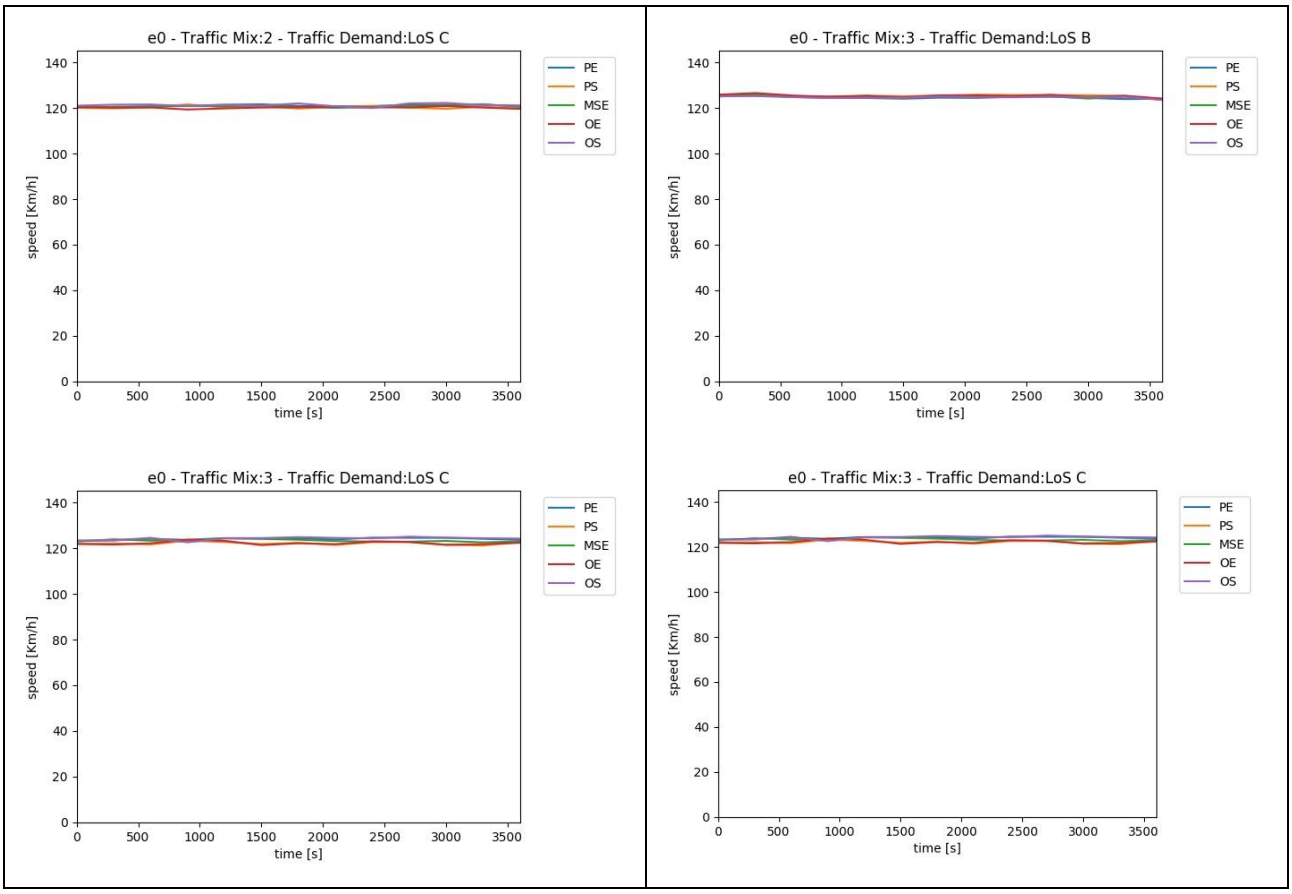

Figure 57. Average speed at the edge 'approach_2' for the different parameter sets. Left column: varying traffic mix at LOS C; right column: varying demand level at traffic mix 3.

4.1.5.2.2 Impacts on Traffic Dynamics

Figure 58 shows the total number of lane changes for each simulated scenario (accumulated over the ten executed runs). Interestingly, the number of changes decreases with an increasing share of AVs when the total demand is held constant, see left column. This may be explained by a more conservative lane change behavior of the AVs. Moreover, it does not increase linearly with the number of vehicles as might be expected. The increased number of lane changes for the parameter schemes PS and OE can be explained by the elevated willingness of DVUs to accept smaller gaps under that parameterisation.

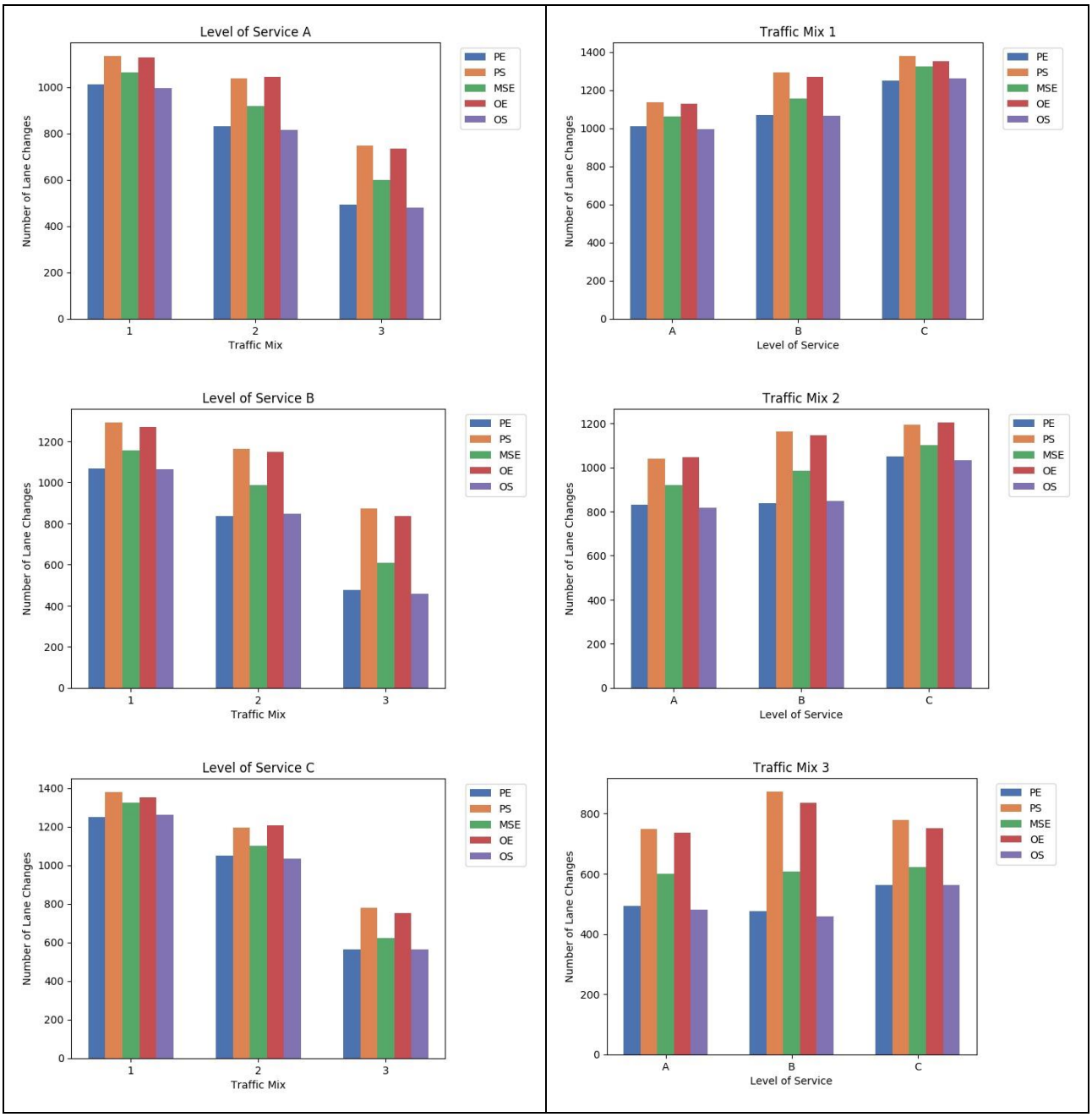

Figure 58 Number of lane changes for Scenario 5.1 baseline simulation experiments (varying parameter scheme, LOS, and traffic mix). Different bar colours correspond to different parameter schemes. The left column groups results by LOS, the right column by traffic mix.

4.1.5.2.3 Impacts on Traffic Safety

Due to the smoothness of the traffic flow in all scenarios, critical events (TTC below 3.0 seconds) are extremely rare for the simulated levels of demand. During all 450 runs only two instances have been observed (both for LoS C / Mix 3), see **Figure 57**.

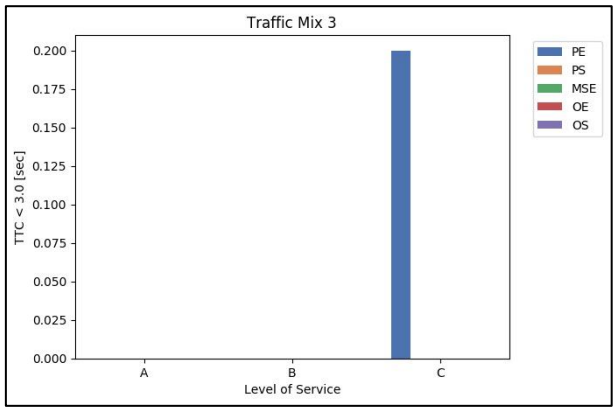

Figure 59. Average number of events with TTCs below 3.0 seconds for the different LoS with fixed traffic composition (Mix 3).

4.1.5.2.4 Environmental Impacts

As all scenarios exhibit highly similar dynamics, the differences between the corresponding emission levels are not large either, see **Figure 60**, which shows the average CO_2 emissions per travelled kilometre for different scenarios.

Two observations are perhaps notable. Firstly, the emissions increase with the share of CAVs/CVs in the scenario (correlating inversely with the number of lane changes, see Section 4.1.5.2.2). Probably, this is induced by the additional braking and accelerating occurring during ToCs and, more importantly, during MRMs. Perhaps, the slight disturbances due to not performing a lane change, which might be beneficial to the flow, also play a role. However, both factors are not reflected in the average network speed, see Section 4.1.5.2.1. Secondly, the emission level decreases with increasing demand, which may surprise at first glance. Keeping in mind that the situation is not congested, this is probably best explained by the slightly decreased average vehicle speeds, which correspond to a more efficient operation in terms of emissions per kilometre.

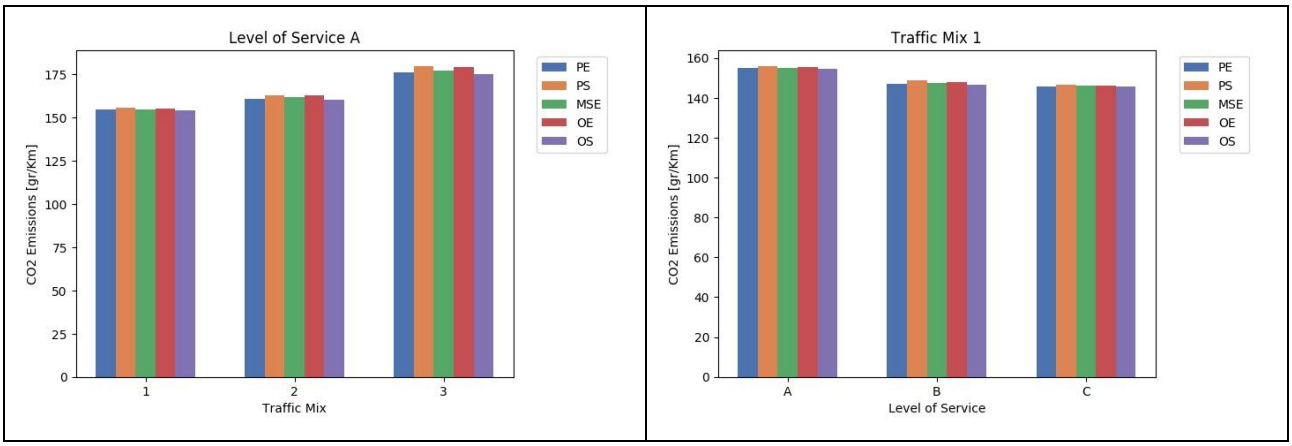

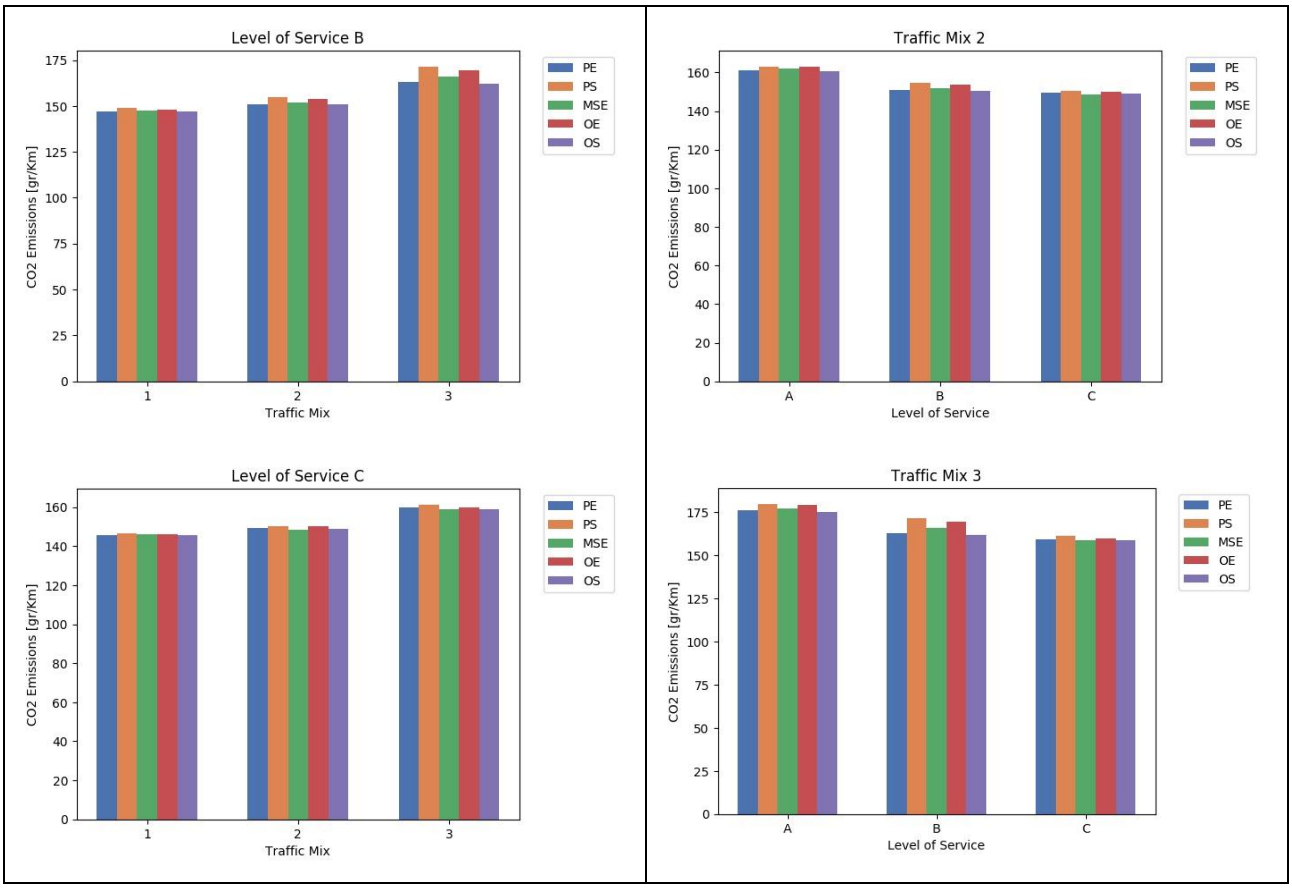

Figure 60. Average CO_2 emissions per km travelled for Scenario 5.1 baseline simulation experiments (varying parameter scheme, LOS, and traffic mix). Different bar colours correspond to different parameter schemes. The left column groups results by LOS, the right column by traffic mix.

4.2 Second Iteration

4.2.1 Scenario 1.3: Queue spillback at exit ramp

4.2.1.1 Scenario Description

CAVs, AVs, CVs, and LVs approach an exit on a motorway. There is a queue on the exit lane that spills back onto the motorway. We consider a queue to spill back on the motorway as soon as there is not enough space on the exit lane to decelerate comfortably (drivers will start decelerating upstream of the exit lane). Vehicles are not allowed to queue on the emergency lane, but queuing on right-most lane of the motorway will cause (a) a safety risk due to the large speed differences between the queuing vehicles and the regular motorway traffic, and (b) a capacity drop for all traffic (including vehicles that do not wish to use the exit). In the baseline of this scenario vehicles queue on the main road and the speed limit remains unchanged (drivers/AVs have to decide on their own to slow down when they notice the queue). When traffic management is introduced, the RSI will allow (and facilitate) vehicles to queue on a section of the emergency lane and gradually reduce the speed limit for traffic approaching the queue. This should reduce the capacity drop and safety risk.

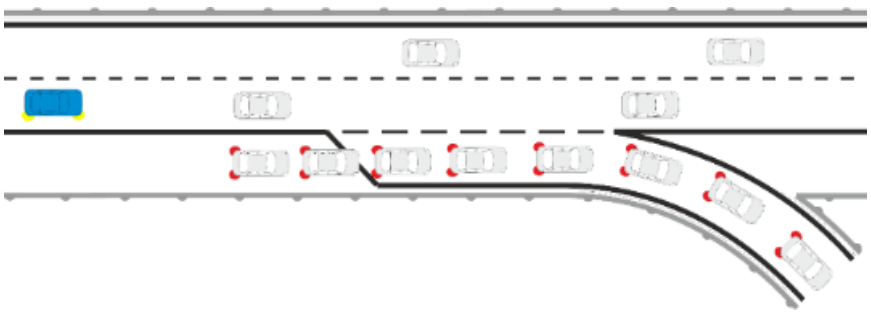

Figure 61. Schematic presentation of scenario 1.3. A queue at an exit ramp spills backs onto the motorway.

If an AV or CAV approaches the exit, it will try to merge into the exit lane. Usually the vehicle is capable of merging successfully and no driver interaction is required. However, if there is a queue on the exit lane, merging might be difficult. If the vehicle does not manage to merge into the exit lane, it can generate a TOR.

Since the AV will usually be able to merge into the exit lane autonomously, a TOR will not be generated until the AV has tried to merge autonomously, but – for whatever reason – did not manage to do so. The vehicle will slow down to a very low speed or come to a complete stop on the main road (next to the exit ramp) while it waits for the driver to perform the TOC. This is a potentially dangerous situation. If the TOC fails, the AV will perform an MRM. The vehicle most likely cannot stay on the main road, but in order to drive to the emergency lane (where it can perform a safe stop), the vehicle has to drive past the exit ramp. From there, the driver will take control again, merge into the main lane and drive to his/her destination using another exit. Merging from the emergency lane into high-speed traffic on the main lane is a dangerous manoeuvre. It would be safer (and faster) if the AV would not perform the MRM and autonomously decide to reroute after the TOR failed. This would imply that the AV solves the problem without interaction of the driver: when merging fails, the AV simply decides to reroute. Hence this use case did not require a TOR in the first place, as the AV knows how to solve the problem without interaction of

the driver. This is the approach we use in this scenario: the AV tries to merge into the exit lane, but when it fails to do so, it does not generate a TOR but decides to reroute instead.

In the baseline simulations of this scenario, AVs will continue to drive (slowly) while trying to merge into the exit lane, until they reach the very end of the exit ramp. They keep on trying to merge after they have stopped on the main road near the end of the exit ramp. If they fail to merge within 10 seconds after they have stopped on the main road near the end of the exit ramp, they are rerouted. Only AVs are rerouted this way, legacy vehicles are not rerouted and follow standard SUMO behaviour (they continue trying to merge for a longer time, and after one minute they are automatically removed by SUMO from the network). Once vehicles have passed the off-ramp traffic operations continue normally.

More details about the simulation network of Scenario 1.3 can be found in **Table 39**.

Table 39: Network configuration details for Scenario 1.3

UC1.3	Settings	Notes
Road section length	1.5 km	• both directions
Road priority	3	
Allowed road speed	• 33.33 m/s • 19.44 m/s (edges on the exit, after diverging from the motorway)	• 120 km/h • 70 km/h
Number of nodes	26	N/A
Number of edges	24	• both directions (opposite direction has 1 edge)
Number of O-D relations	3	• from ‘start’ to ‘end’ (on motorway) • from ‘start’ to ‘exit_north’ or ‘exit_south’
Number of lanes	2 + emergency lane (not used in baseline) 3 1	• both directions on motorway • motorway at exit lane • exit ramp after diverging from motorway
Detectors	Equidistant, on all lanes	Every 50 m
Exit lane	100m	
Traffic light	At the end of exit ramp, used to cause a queue on the exit ramp that eventually spills back to the motorway	• cycle time: 30 sec • green time for the exit ramp: 8 sec (LOS B), 9 sec (LOS C), 10 sec (LOS D)
Filenames	• network: UC13.net.xml • VMS: shapes.add.xml	• N/A • not used in baseline

Network layout

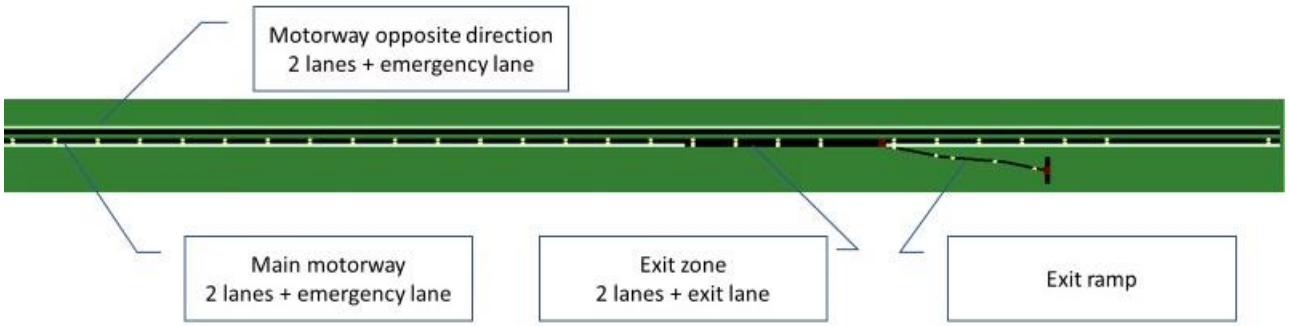

Road segments
Main motorway before exit zone: 800 m
Exit zone: 200 m
Exit ramp: 250 m

4.2.1.2 Results

The proposed scenario is simulated at three different traffic demand levels (LOS B, C, and D) with the consideration of three vehicle compositions as mentioned in Section 3.2.3. Furthermore, 10 simulation runs with different random seeds for each combination of LOS and vehicle composition are executed. In the following, the results are analysed and clarified for the aspects of traffic efficiency, traffic dynamics, traffic safety, and environment.

SUMO's lane change behaviour is not entirely realistic. Vehicles that want to use the exit lane tend to merge less aggressively than expected. In every simulation, both LVs and AVs fail to merge in the queue on the exit lane more often than we would expect in real-life situations. Eventually, the vehicles in the simulation drive all the way to the last point where they can merge, and sometimes come to a complete stop on the main road. This even occurs on the left lane, whereas in real-life situations drivers will usually merge to the right lane much earlier instead of using the left lane when they intend to take the exit (see **Figure 66** in the section on traffic dynamics).

Changing the lane change behaviour in SUMO to accommodate this specific case is beyond the scope of this study. As such, the results for this use case have been obtained using the default lane change behaviour in SUMO. This will be taken into account in the evaluation of the scenario with traffic management, especially in the comparison with the baseline scenario discussed below. The differences between the baseline scenario and the traffic management scenario will be critically analysed to assess which conclusions remain valid despite artefacts in SUMO's lane change behaviour.

4.2.1.2.1 Impacts on Traffic Efficiency

Network-wide Impacts

Figure 62 shows the average throughput (in veh/h) per LOS and traffic mix. The queue on the exit ramp causes a bottleneck with a capacity of about 2000 veh/h. The throughput is therefore expectedly increasing when going from LOS B to D, and almost constant within each LOS with only slight, random variations.

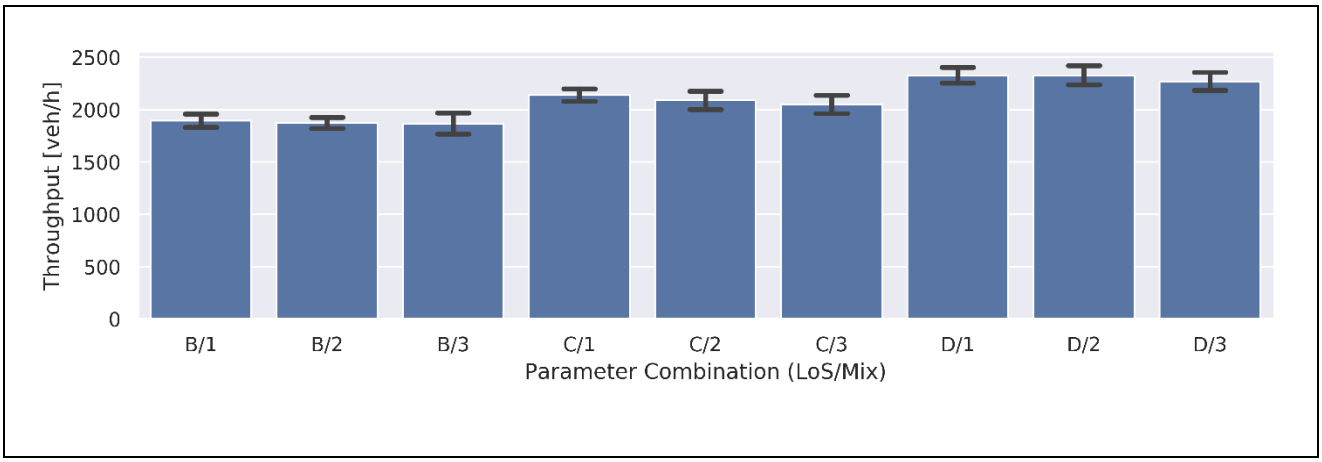

Figure 62. Average throughput (in veh/h) for use case 1.3 simulation experiments (varying LOS and traffic mix).

Free-flow travel time through the network is 0.50 min/km on the main route (only motorway) and 0.60 min/km on the exit route (motorway and exit ramp). There is a significant delay in every scenario, due to the queue on the exit ramp. The higher the traffic demand, the longer the queue upstream of the bottleneck, and the higher the travel time. The differences among the traffic mixes per LOS are not statistically significant. Between LOS however we can clearly see in **Figure 63** how the travel time significantly jumps up from LOS B to LOS C, with the differences between LOS C and LOS D less pronounced.

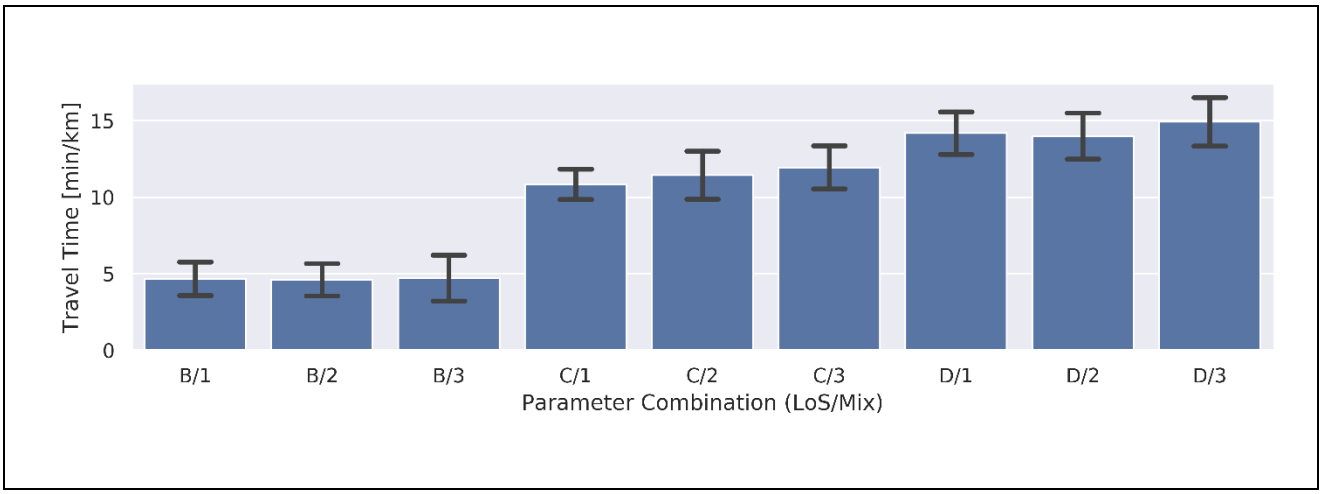

Figure 63. Average travel time (in min/km) for use case 1.3 simulation experiments (varying LOS and traffic mix).

Local Impacts

Figure 64 shows a tempo-spatial diagram (tx-diagram) for one of the simulations (LOS C, Traffic Mix 2, Driver Behaviour FSP, Seed 2). In this diagram, on every location in the network and at every minute of the simulation, the average speed is indicated by a corresponding colour. Each lane has its separate graph. The first two rows correspond to the left and the right lane on the main road. The third row shows (from bottom to top) the emergency lane, the exit lane on the main road (starting at 800 m), and finally the exit ramp. The speed on the exit ramp is always low, due to a lower speed limit in the first seconds of the simulation, and hence onwards due to the queue on the exit. The diagram clearly shows the location of the bottleneck (holding steady at about 1000 m, this is where the most downstream point of the exit lane is located). Queues grow upstream of the bottleneck. Traffic that continues on the main road after the bottleneck accelerates back to the free-flow speed.

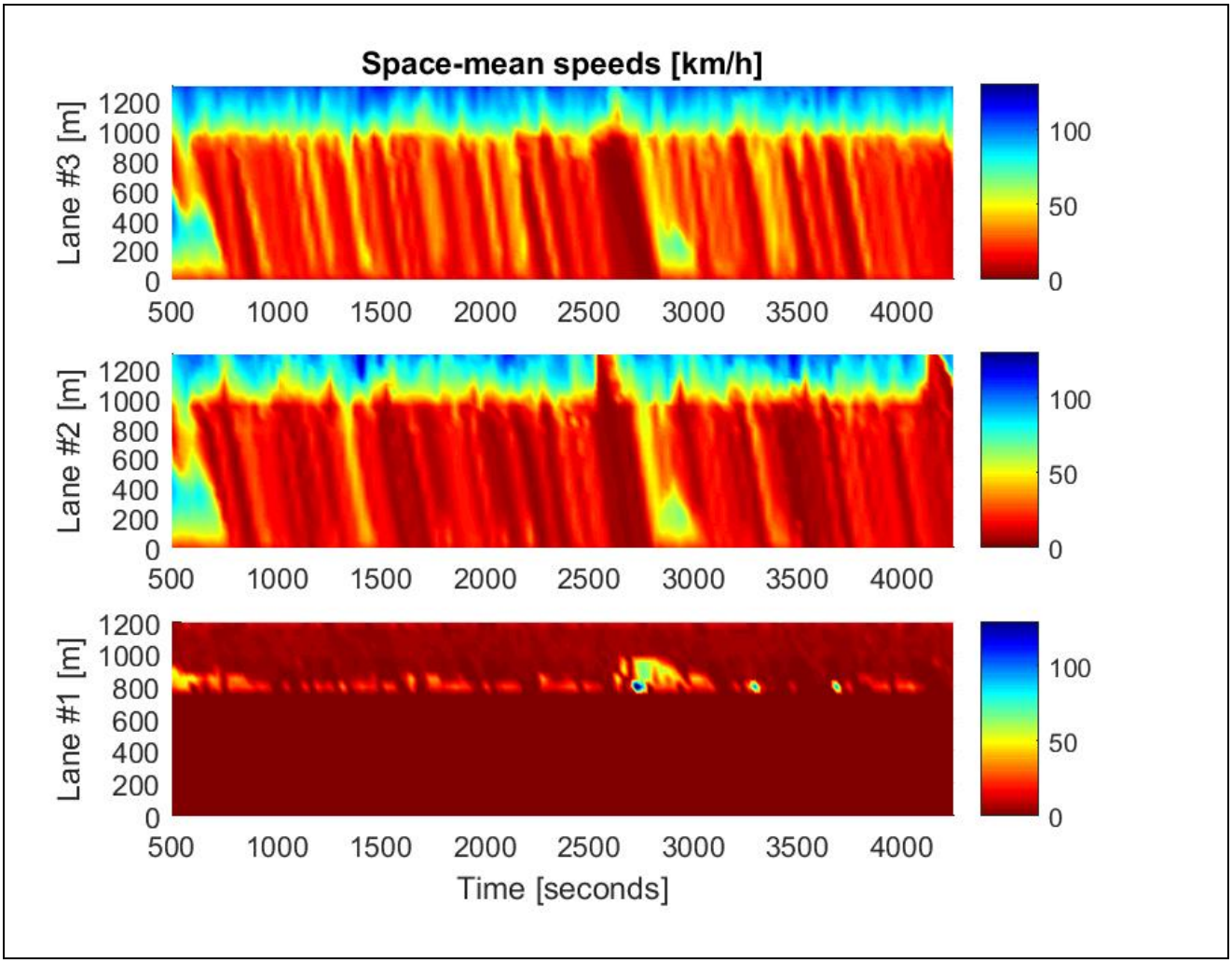

Figure 64. Example of a tempo-spatial diagram showing the speed per lane of the network at every location/time during the simulation (for LOS C, Traffic Mix 2, Driver Behaviour FSP, Seed 2).

In simulations pertaining to higher traffic demand (LOS D), there are usually longer queues, but the traffic mix does not affect the queue length. To illustrate this, a tempo-spatial diagram for another simulation is shown in **Figure 65**.

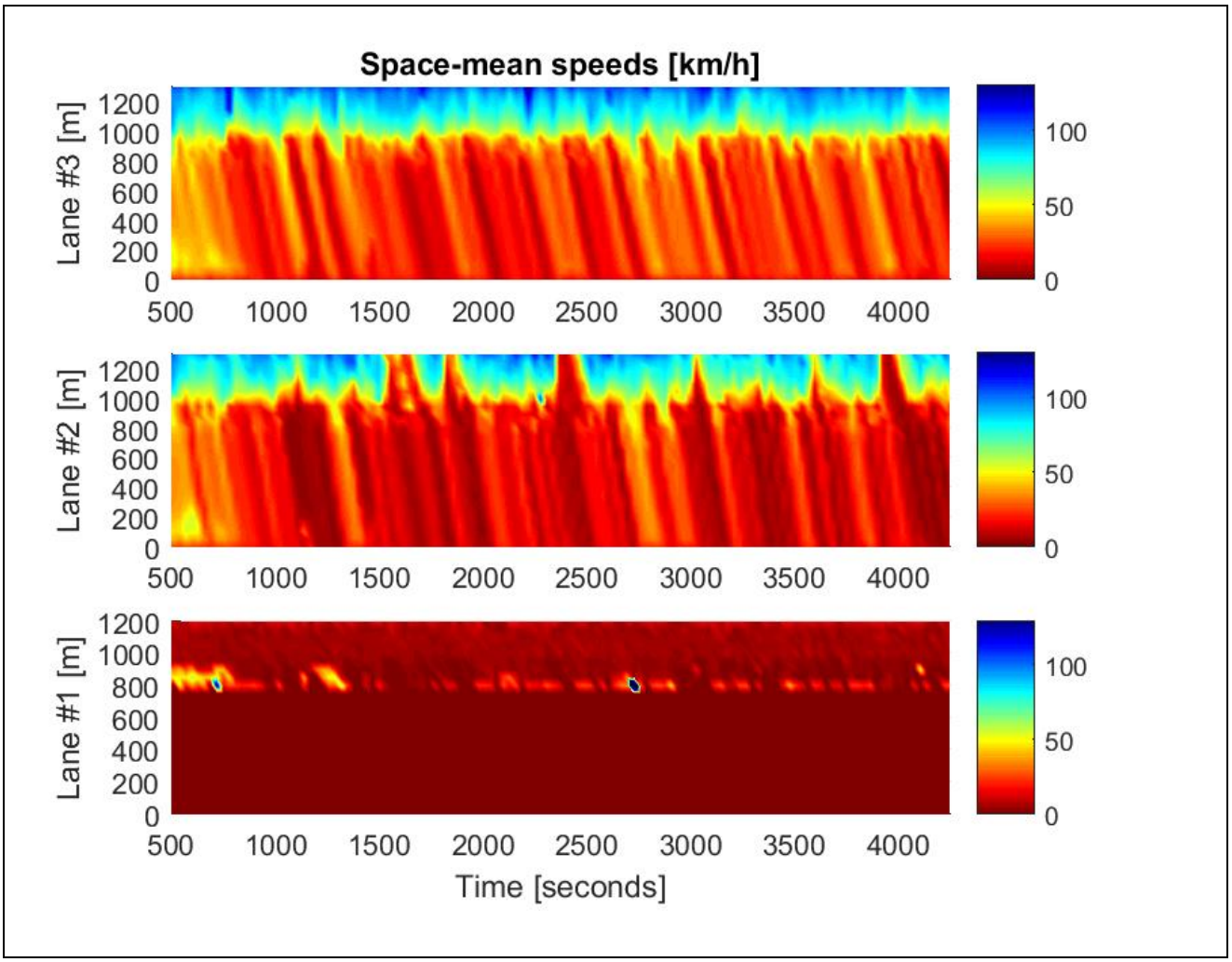

Figure 15. Example of a tempo-spatial diagram showing the speed per lane of the network at every location/time during the simulation (for LOS D, Traffic Mix 1, Driver Behaviour FSP, Seed 5).

The dynamics of the queues before the bottleneck are caused by vehicles that want to take the exit ramp but fail to merge. At some points during the simulation this even occurs on both lanes of the main road, blocking all traffic for a short while. One such occasion is shown in **Figure 66**.

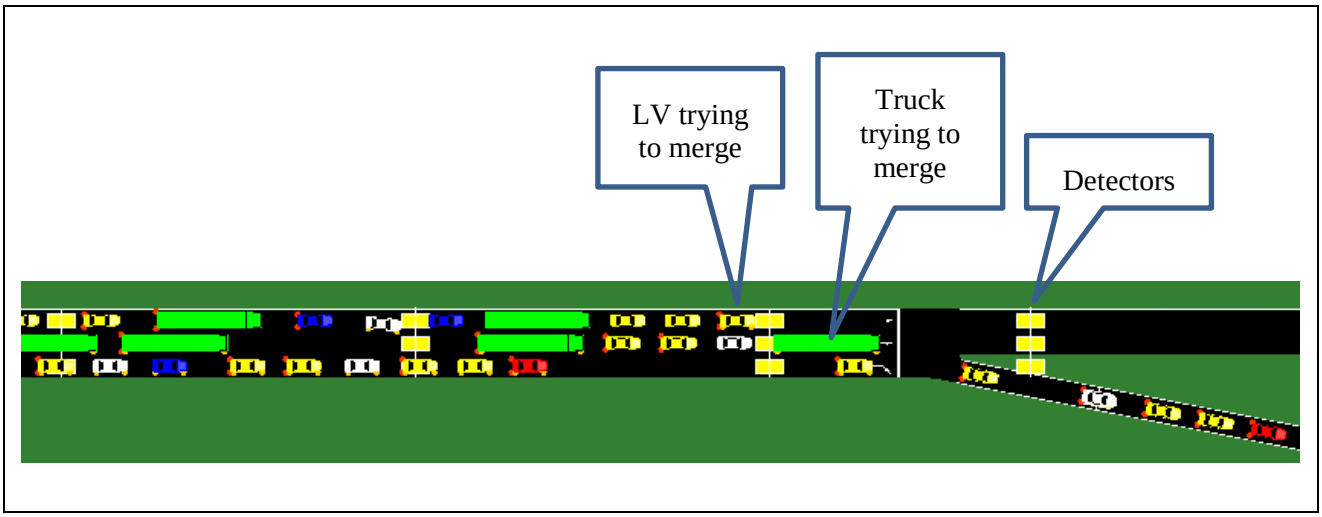

Figure 66. Screenshot of a SUMO simulation for use case 1.3, when vehicles trying to merge shortly block all traffic on the main road.

4.2.1.2.2 Impacts on Traffic Dynamics

The number of lane changes has no statistically significant differences among the traffic mixes per LOS individually. However, as the LOS increases, the number of lane changes drops. This decrease is more pronounced between LOS B and LOS C than between LOS C and LOS **(Figure 67)**. The latter is explained because the motorway already gets quite congested in LOS C. A additional possible reason for this may be that SUMO's lane change behaviour leads to vehicles get stuck in the queue, and therefore may be rerouted, hence skipping the lane change altogether as explained at the beginning of this section. The number of lane changes hovers about 0.45 lane changes per kilometre, so each vehicle will change lane a little over each 2 kilometres on average. Given that the length of the network (1.5 km) is shorter, this implies lane changes for about 70% of the vehicles, which fits with the vehicles' origin-destination patterns.

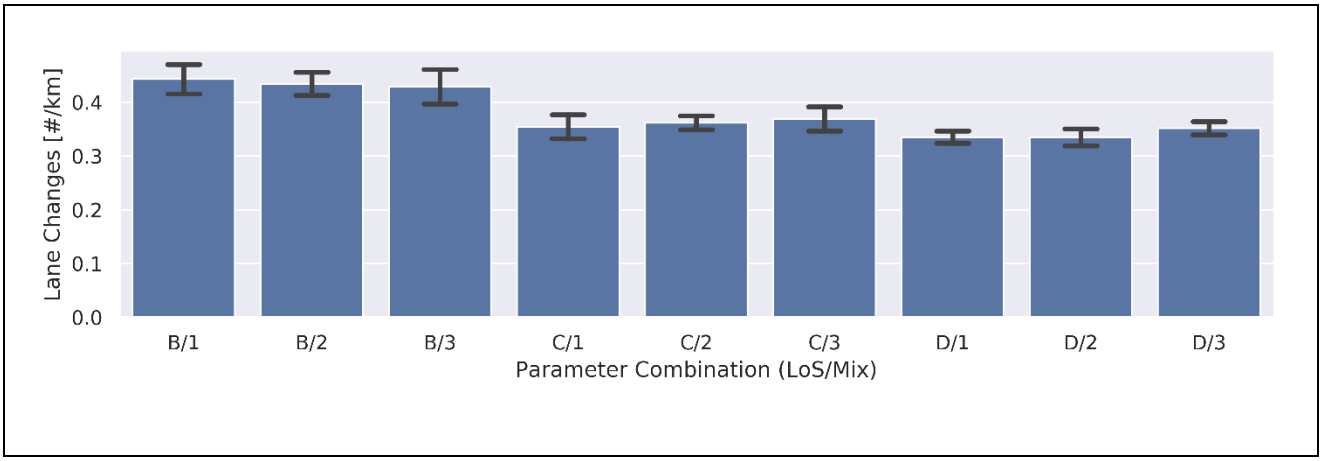

Figure 67. Lane changes (in #/km) for use case 1.3 simulation experiments (varying LOS and traffic mix).

4.2.1.2.3 Impacts on Traffic Safety

Figure 68 shows the number of critical events in the simulations. Every occurrence of a TTC smaller than 3 seconds is considered to be a critical event. There are no statistically significant differences between vehicle mixes within each LOS. Between LOS however the number of occurrences of critical events increases drastically. Especially when going from LOS B to LOS C, with the differences between LOS C and LOS D not statistically significant. These observations are in line with for example the travel time measurements as discussed before.

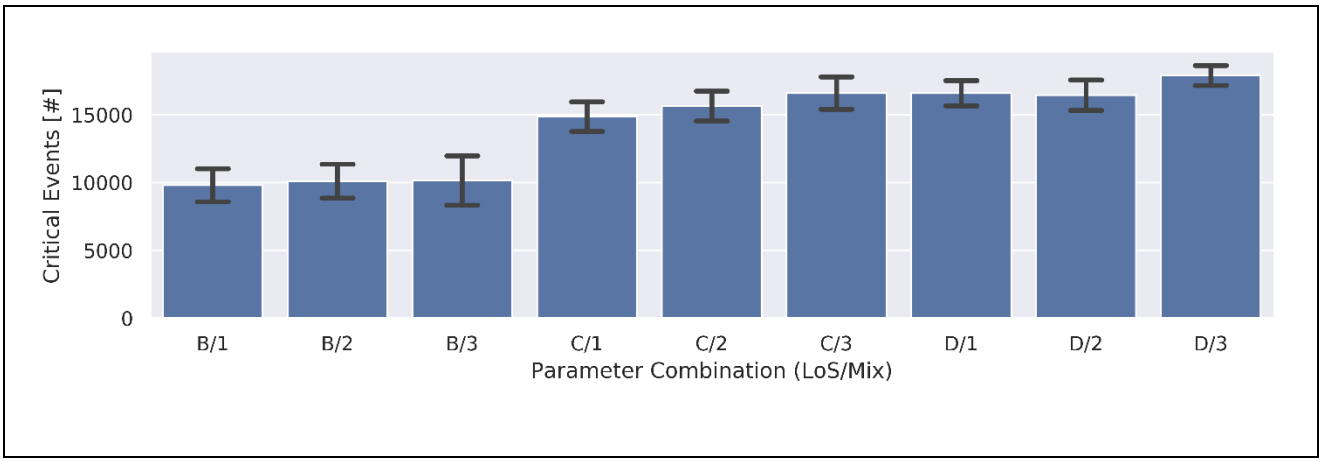

Figure 68. Critical events (# occurences where TTC < 3 s) for use case 1.3 simulation experiments (varying LOS and traffic mix).

The critical events occur mainly at the end of the queue and in the zone where a lot of lane changes occur. In LOS D congestion reaches the end of the network, reducing the number of critical events at the tail of the queue. This can be seen in the spatial distribution of the TTCs in **Figure 69**.

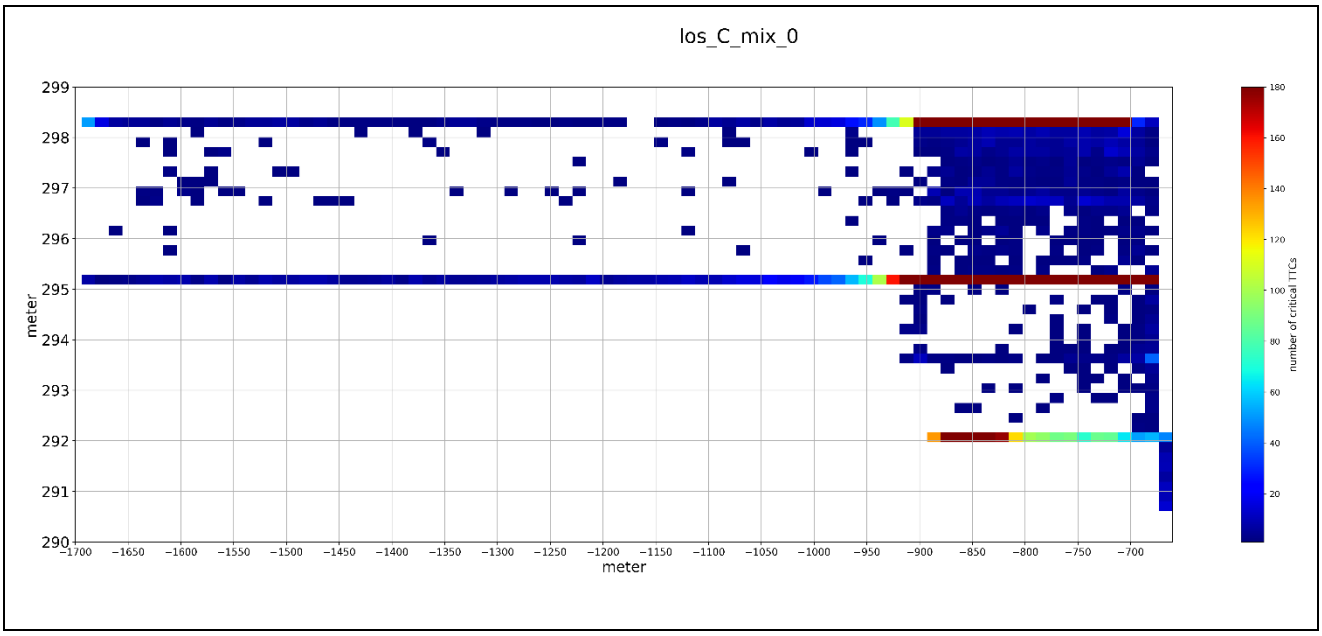

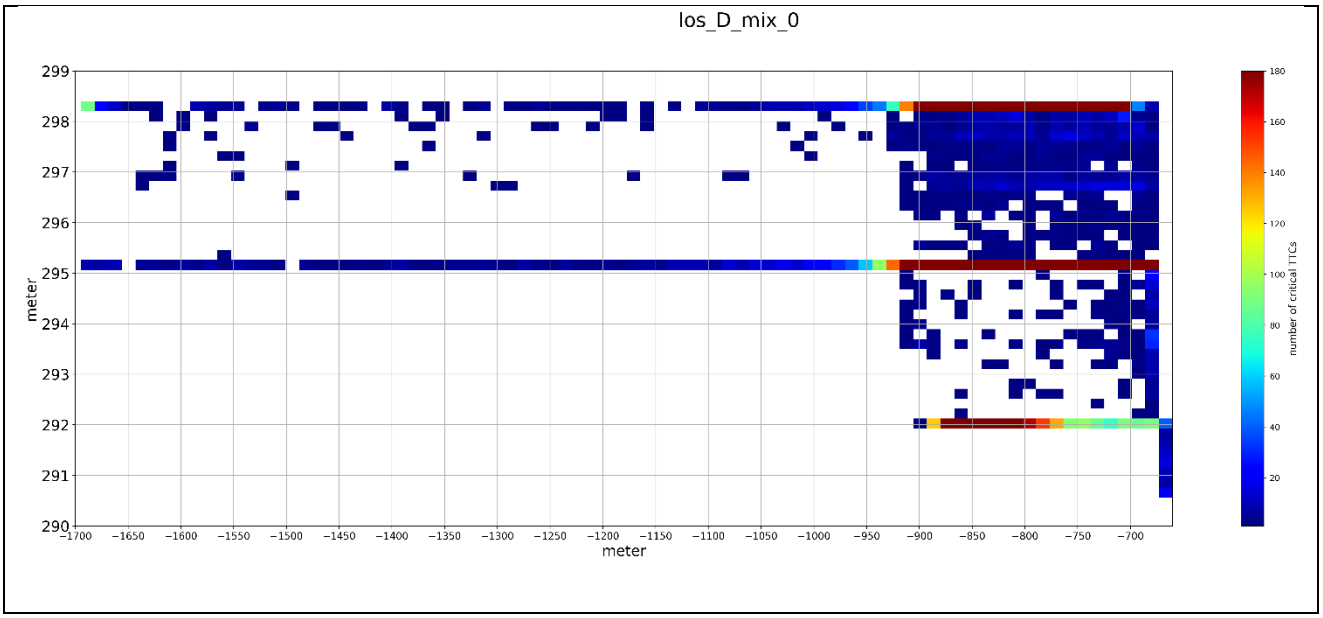

Figure 69: Spatial distribution of critical TTCs (< 3sec) for use case 1.3 for LOS C – Traffic Mix 0 and LOS D – Traffic Mix 0. Colours indicate the number of critical TTCs shown with discrete plotted bins (bin size ≈ 20 m x 0.3 m).

4.2.1.2.4 Environmental Impacts

Environmental impacts are assessed through the amount of CO_2 emissions per kilometre travelled. The results for each combination of LOS and traffic mix are shown in **Figure 70**. There, we can see that there are no real significant differences both among LOSs on the one hand, and within LOS between different traffic mixes on the other hand.

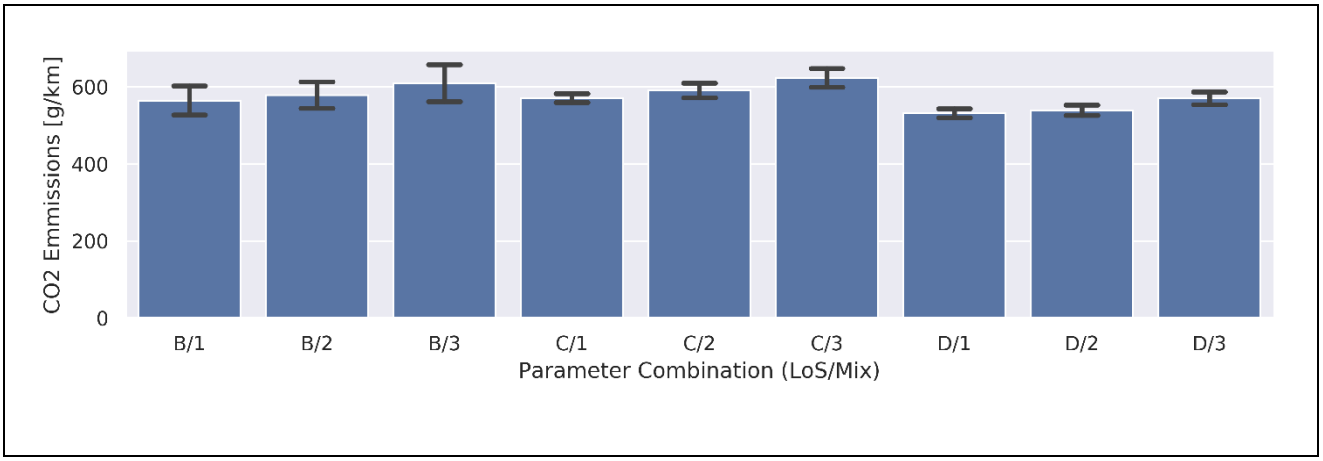

Figure 70: CO_2 emissions (in g/km) for use case 1.3 simulation experiments (varying LOS and traffic mix).

4.2.1.2.5 AV Rerouting

Figure 71 shows the number of vehicles that reroute (see also the explanation at the beginning of this section) during the entire simulation (for varying LOS and traffic mixes). Only automated vehicles that fail to merge into the exit lane (see scenario description for more details) are rerouted

and continue on the motorway instead of taking the exit lane as intended. The number of vehicles that reroute only varies among the traffic mixes (the differences between the LOSs are not statistically significant). This is as expected: it rises with increasing share of AVs in the vehicle mix).

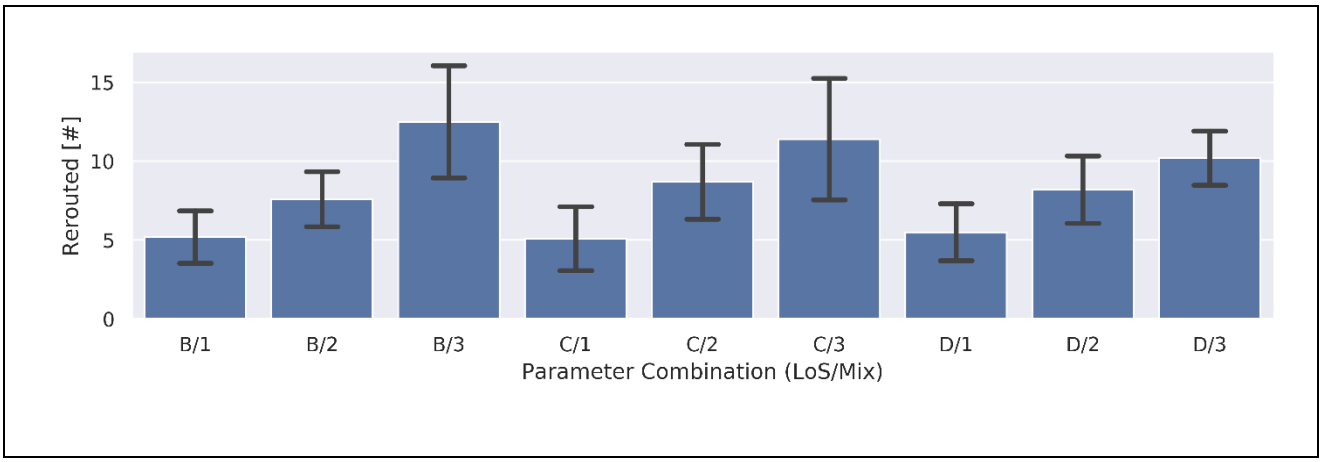

Figure 71. Number of vehicles that reroute during the simulation for use case 1.3 simulation experiments (varying LOS and traffic mix).

4.2.2 Scenario 2.1: Prevent ToC/MRM by providing speed, headway and /or lane advice

4.2.2.1 Scenario Description

The network in scenario 2.1 in the 2nd iteration is a continuation of the first iteration, representing a typical one-lane on-ramp joining a one-direction two-lane motorway segment **(Figure 72)**.

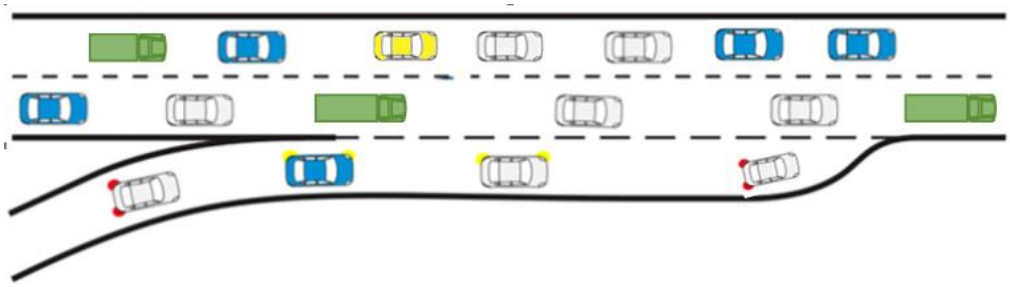

Figure 72. Schematic overview of Scenario 2.1.

Nevertheless, the following deviations need to be addressed for the baseline experiments in this iteration:

Regarding the network in the second iteration, the one-lane on-ramp was extended from 500 m to 1.0 km in order to accommodate the implementation of Day 1 C-ITS application and future traffic management measures (i.e. ramp metering). Considering the vehicle routes, the same two paths as in the 1st iteration are simulated: (C)AVs, CVs, and LVs travel along the mainline motorway (merging zone) and CAVs merge into the two-lane mainline motorway via the on-ramp/acceleration lane (see **Table 40)**.

Regarding the fleet composition, HGVs and LGVs are added to the LVs share on the mainline motorway, determined in **Table 23**. For the traffic composition, the same artificial mixes for (C)AVs/CVs are used as in the 1st project iteration **(Table 7)**. Based on observations from the 1st iteration, which already indicated the complexity of vehicle interactions in the presence of the vehicle classes that led to safety-critical events at the end of acceleration lane (lane drop) point, HGVs and LGVs are therefore not included on the on-ramp. Moreover, traffic management measures in WP4 such as speed advice and lane advice are currently targeting CAVs only and its predictability would be compromised with more vehicle classes on the on-ramp. Therefore, on-ramp vehicles in the 2nd iteration are CAVs only.

Regarding the ToC triggering, the (C)AVs/CVs on the mainline and the on-ramp should be handled separately:

1. On the mainline motorway route, merging zone in specific, all vehicles (despite their classes) are assumed not to trigger/initiate ToC but merely to keep safe distances with acceleration and deceleration according to their car-following models. This assumption is to emulate more realistically vehicles travelling on the mainline motorway in a mixed traffic situation in the near future.
2. While 75% of (C)AVs/CVs were assumed not be able to autonomously handle traffic situations at the TAs and thus trigger ToC (presented in D2.2), it is more likely that (C)AVs/CVs cannot assess/predict other vehicles' driving capabilities/behaviours or

communicate their reactions to all vehicle classes (especially LVs) due to the complexity and changing dynamics of traffic in the upcoming TAs. Furthermore, based on the 1st iteration baseline simulation experiments, safety-critical events were induced when vehicles on the mainline motorway were requested to take-over, which is caused by increasing the complexity with constantly varying traffic mixes. In addition, the assumption of mainline (C)AVs/CVs performing ToC renders any traffic management measures inefficient due to the unpredictability of these vehicles. Hence, the (C)AVs/CVs on the mainline motorway are presumed not to proceed with downward ToC in the 2nd iteration, which also corresponds to the egoistic behaviour of each individual road user.

3. On the on-ramp route, one-lane on-ramp acceleration lane in specific, we assume that Day 1 C-ITS applications are existent upon entry of on-ramp. Similar to the first iteration, 25% of the CAVs are supposed to be able to merge into the mainline along TAs in automated mode thanks to the aforementioned infrastructure-assisted measures, and 75% of the CAVs are not. The latter will request ToCs, perform ToCs (section 2.3.2.) or execute consequently MRMs on the on-ramp (mostly on-ramp-only according to the ToC model in section 2.3.2.3) and the acceleration lane. According to the definition of actors in section 3.2.2, they are categorized into 25% of CAV_G2 and 75% of CAV_G1.
4. A CAV_G1 will issue TOR upon message reception at 250 metres upstream to the first merge point (connection of on-ramp and acceleration lane), while a CAV_G2 will cope with merging in automated mode unless no imminent available gaps are found within the first 50 metres on the acceleration lane, where the CAV_G2 encounters a challenging merging situation due to dense mainline motorway traffic. In the latter case, a dynamic trigging of TOR with a reserving threshold distance of 450 metres is performed according to Section 2.3.2.2.

Based upon the aforementioned scenario description, **Table 40** shows the traffic composition on the mainline motorway route and on-ramp/acceleration lane route in a nutshell. The traffic flow inputs are calibrated according to this **Table 40** and **Table 25** in section 3.2.4.

Table 40. Traffic composition overview for Scenario 2.1.

	Fleet Composition			**Vehicle Mixes**				**CAV Category**		
	PC	**LGV**	**HGV**	**Class 1**	**Class 2**	**Class 3**	**Mix #**	**CAV (G1)**	**CAV (G2)**	**CAV (noToC)**
Mainline Motorway	77%	10%	13%	70%	15%	15%	1			100%
				50%	25%	25%	2			
				20%	40%	40%	3			
On-ramp → Acceleration lane	100%					100%		75%	25%	

The network configuration details are described in **Table 41**.

Table 41. Network configuration details for Scenario 2.1.

Scenario 2.1	Settings	Notes
Road section length	• Motorway: 2.5 km • On-ramp: 1.0 km	• Motorway two directions
Road priority	3	
Allowed road speed	• Motorway: 27.78 m/s • On-ramp: 27.78 m/s	• Motorway: 100 km/h • On-ramp: 100 km/h
Number of nodes	8	• n0 - n7 priority nodes
Number of edges	8	
Number of O-D relations	3	• from n1 to n7 • from n0 to n7 • from n7 to n1
Number of lanes	1-2-3	• 1 lane on-ramp • 2 normal lanes on motorway • 3 lanes at merging zone/ acceleration lane
Disallowed vehicle classes	• normal lanes: pedestrians, tram, rail_urban, rail, rail_electric, ship	• from n0 to n7
Filenames	• network: UC2_1.net.xml	
Network layout 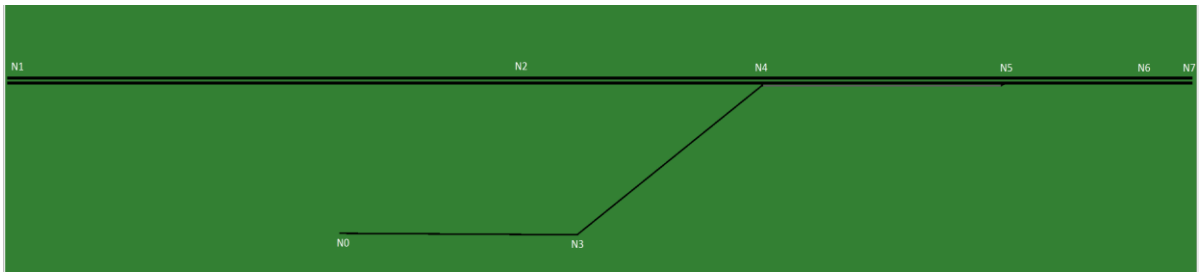		
Road segments n1→ n2: insertion and backlog area (1100 m, 2 lanes) n2→ n4: mainstream motorway (500 m, 2 lanes) n4→ n5: mainstream motorway with acceleration lane (150 m, 3 lanes) n5→ n6: mainstream motorway (300 m, 2 lanes) n6→ n7: exit (100 m, 2 lanes) n0→ n3: insertion and backlog area (500 m, 1 lane) n3→ n4: on-ramp (500 m, 1 lane) n7→ n1: mainstream motorway in opposite direction (2500 m, 2 lanes)		

To have a clear view of the merging zone, which is part of the TAs (transition area), a more detailed network schematic for the 2nd iteration (**Figure 73**) is added under the SUMO network layout.

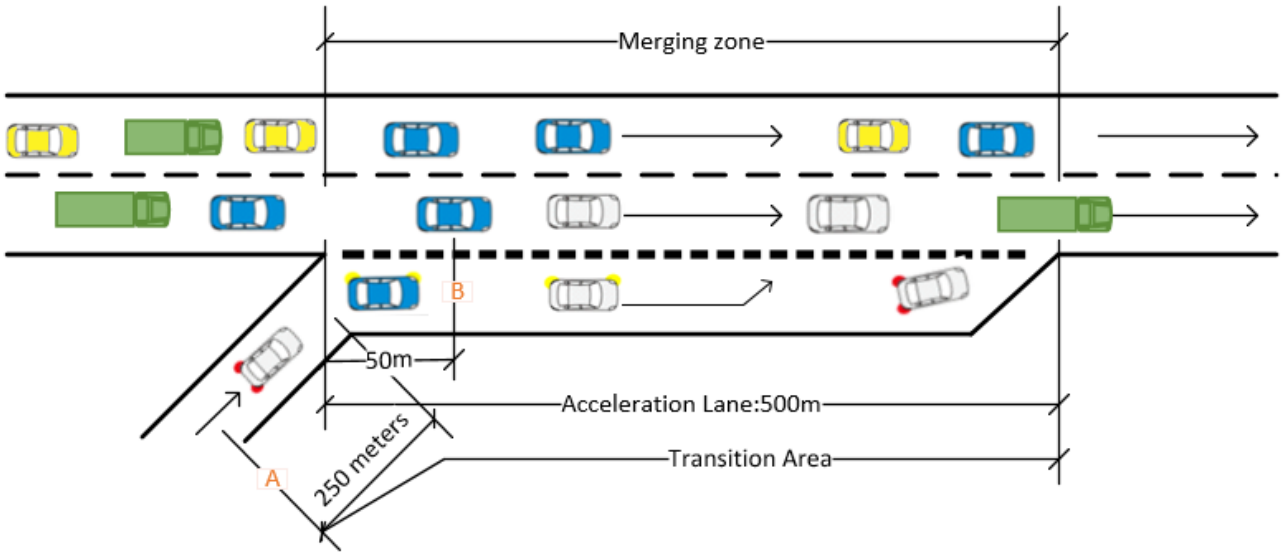

Figure 73. Merging zone schematic of UC2.1 network.

The merging zone is 500 m in length and is composed of one acceleration lane (right-most lane) and two mainline motorway lanes. At the end of the merging zone, a merging bottleneck is formed due to the lane drop. In the merging zone, mandatory lane changes (from the acceleration lane to main motorway lanes) frequently take place, which lead to downward ToCs of CAVs in the TA. In the 2nd iteration, the CAV_G1 vehicles issue a take-over request at 250 m (Point A) upstream of the merging zone on the on-ramp; The CAV_G2 vehicles will try to merge to mainline in automation mode, or proceed with ToC dynamically if they fail to merge successfully before Point B on the acceleration lane.

4.2.2.2 Results

4.2.2.2.1 Impacts on Traffic Efficiency

Network-wide Impacts

The average network speed is presented in the form of bar charts for three LOSs and three traffic mixes under full spectrum (FSP) parametrisation scheme (see **Figure 74**). This figure depicts the average network speed for traffic mix 1, 2 and 3, under LOS B, C or D. An overall comparison of different LOS/Mix combination is provided.

The average network speeds of 9 LOS/mix combinations are around 85-95 km/h. A slight decrease on the average network speed can be observed with increasing demand level and increasing CAVs/CVs, seemingly in a linear decrease pattern. This phenomenon corresponds with the fact that no significant congestion was observed on the network during the simulations of all 9 LOS/mix combinations. Regarding the slight decrease of this KPI when the share of CAVs/CVs is higher, the intuitive explanation is that the average network speeds decrease due to more mainline CAVs/CVs vehicles forming platoons, yielding less available gaps for on-ramp CAVs/CVs.

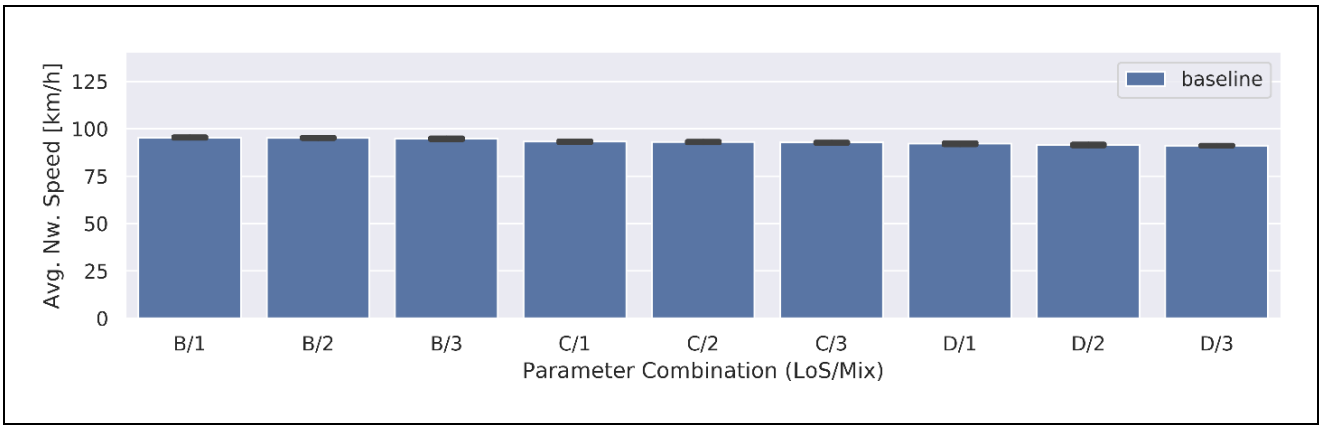

Figure 74. Average network speed for Scenario 2.1 2nd iteration baseline simulation experiments (varying LOS/traffic mix).

The travel time in **Figure 75** shows the same reflections as **Figure 74**. Small variations of value ranges for each group are observed from **Figures 74 and 75**, which is contributed by the refined ToC/MRM models and more accurate full spectrum parametrisation of vehicle/driver models in the second iteration.

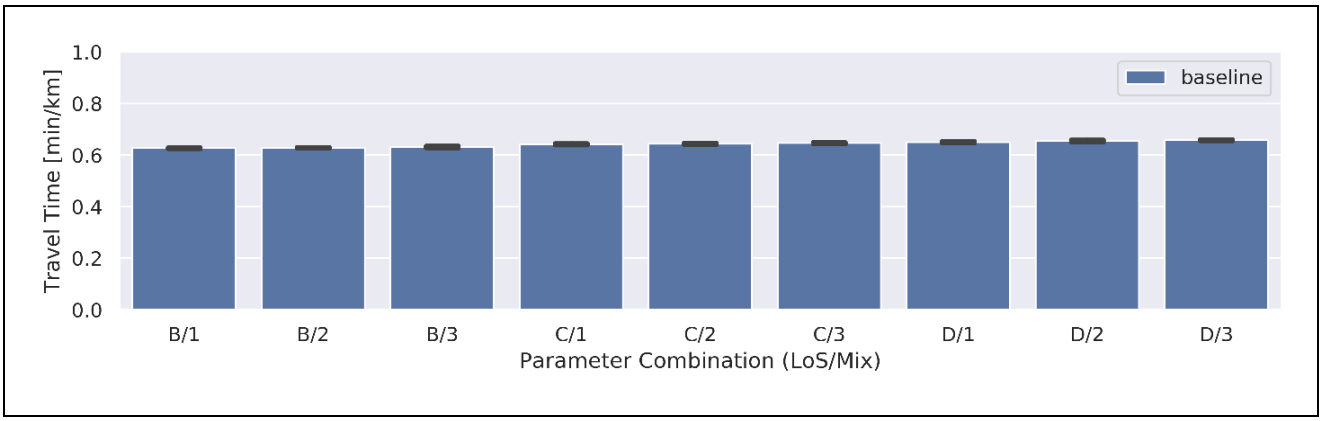

Figure 75. Travel time for Scenario 2.1 2nd iteration baseline simulation experiments (varying LOS/traffic mix).

Local Impacts

Under LOS D, vehicle mix 1-3, and random seed 5, **Figure 76** shows flow (upper row) and speed (bottom row) of the mainline motorway road stretch (around 2.5km), evolving through time (1 hour) and position. The merging zone on the mainline is from 1.6 km to 2.1 km. The upper three plots illustrate that, under LOS D, the mainline flow ranges between 600 veh/h/ln to 1000 veh/h/ln. On the one hand, these three plots show a slight intensification on the traffic flow when traffic mix increases. On the other hand, this phenomenon cannot be supported by the bottom three plots due to near free-flow traffic conditions.

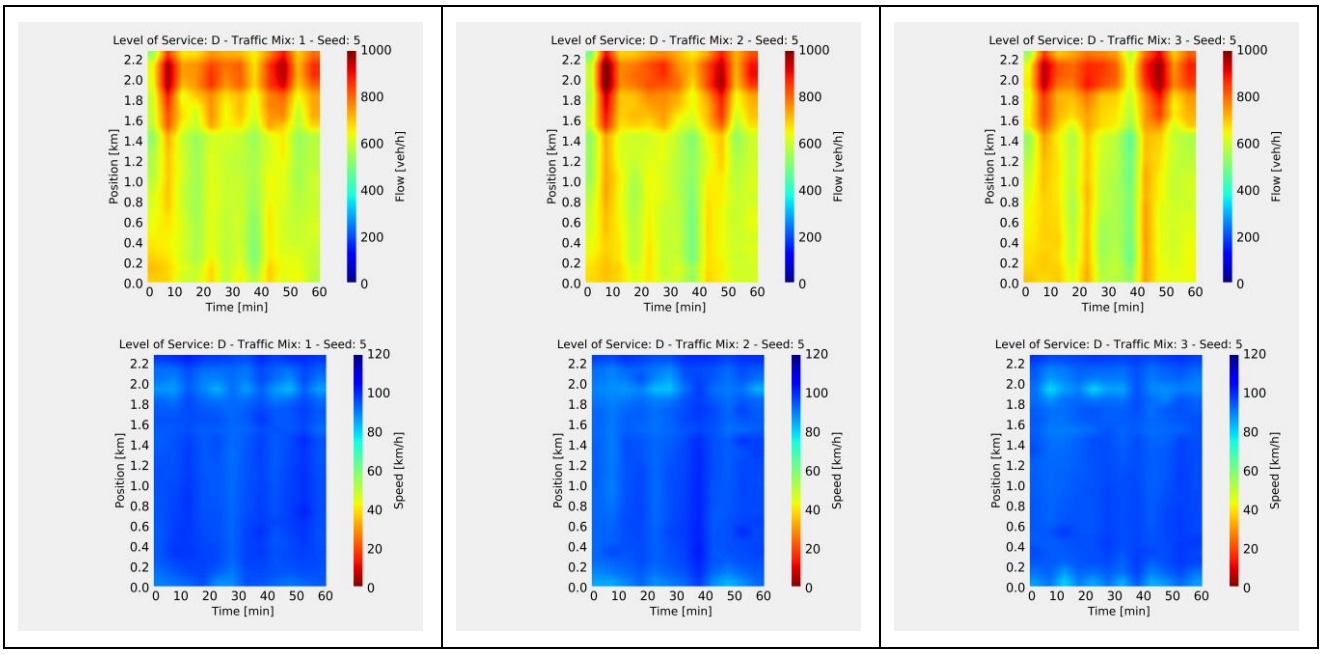

Figure 76. Examplary time-space-diagrams (mainline) of measured speeds (upper row) and flows (bottom row) for use case 2.1 baseline under LOS D, vehicle mix 1-3 (left, middle and right column), seed 5.

Under traffic mix 3, LOS B to D, and random seed 5, **Figure 77** shows flow (upper row) and speed (bottom row) of the same road stretch as **Figure 76**. The upper three plots illustrate that under one traffic mix, the mainline motorway flow increases as the traffic demand increases from LOS B to LOS D. The corresponding effect can be observed from the lower three plots, where speed heat graph shows more propagation across time and position. But all three LOSs under mix 3 didn't encounter severe traffic congestion.

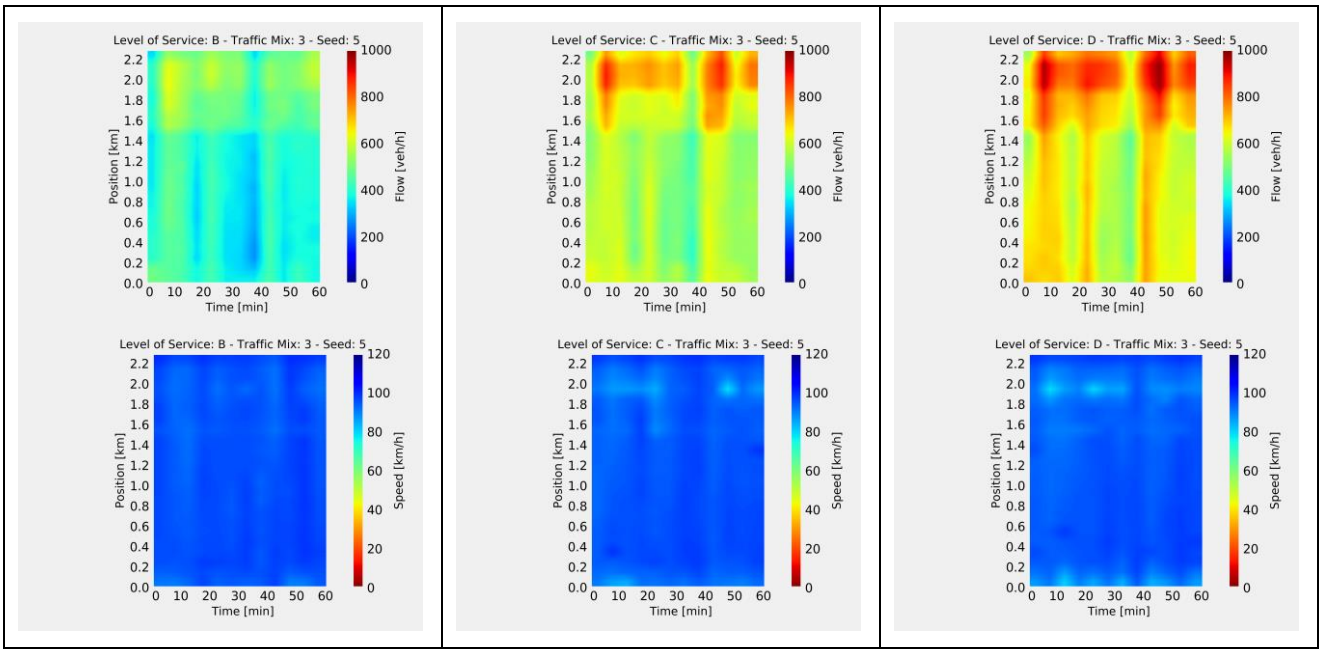

Figure 77. Examplary time-space-diagrams (mainline) of measured speeds (upper row) and flows (bottom row) for use case 2.1 baseline under vehicle mix 3, LOS B-D (left, middle and right column), seed 5.

Under LOS D, vehicle mix 1-3, and random seed 5, **Figure 78** shows flow (upper row) and speed (bottom row) of a 1.5 km road stretch: on-ramp (0~1.0 km) plus acceleration lane (1.0~1.5 km), evolving through time (1 hour) and position. The First Merge Point is at 1.0 km and the acceleration lane starts from 1.0 km until the Lane Drop Point 1.5 km.

The upper three plots illustrate that the on-ramp flow is around 600 veh/h/ln and the acceleration lane flow is around 200 veh/h/ln since on-ramp vehicles merge into the mainline motorway, thus leaving the acceleration lane between the First Merge Point and the Lane Drop Point (1.5 km). Regarding the traffic flow, no change can be easily observed because there are only CAVs on the on-ramp.

The lower three plots illustrate that free-flow traffic prevails on the on-ramp except for the last 200 metres, where the CAV_G1 vehicles perform ToC. As the traffic mix increases on the mainline motorway, the last 200 metres of acceleration lane shows more significant speed drop (yellow/red on the right-bottom plot). The reasoning here is twofold: 1) This could be caused by the increased share of CAVs/CVs on the mainline merging zone that are unwilling to break up their platoon and create gaps for the on-ramp merging vehicles. 2) This could be caused by the CAV_G2 vehicles that perform dynamic ToC at relatively random position on the acceleration lane, inducing shock wave on the acceleration lane.

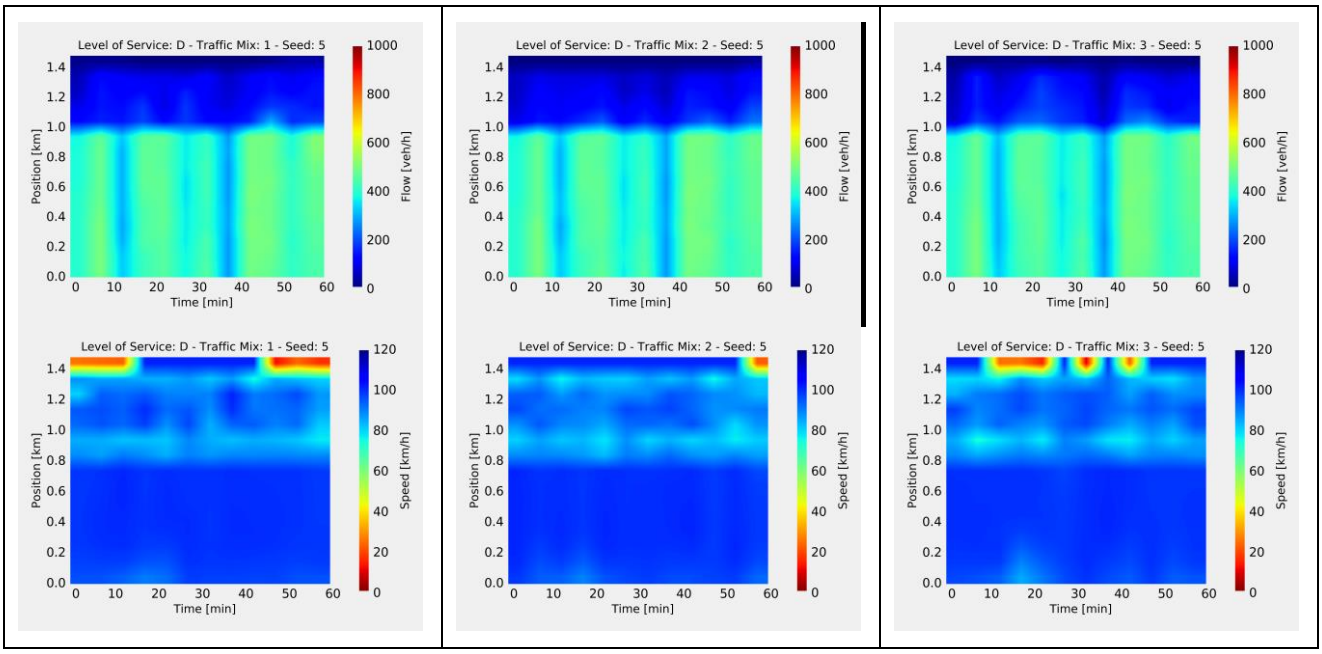

Figure 78. Examplary time-space-diagrams (on-ramp) of measured speeds (upper row) and flows (bottom row) for use case 2.1 baseline under LOS D, vehicle mix 1-3 (left, middle and right column), seed 5.

Under traffic mix 3, LOS B-D, and random seed 5, **Figure 79** shows flow (upper row) and speed (bottom row) of the same road stretch as **Figure 78**. The upper three plots illustrate that under one traffic mix, the on-ramp flow increases as the traffic demand increases from LOS B to LOS D. The corresponding effect can be observed from the lower three plots, where the speed heat graphs show more disturbances close to Lane Drop Point.

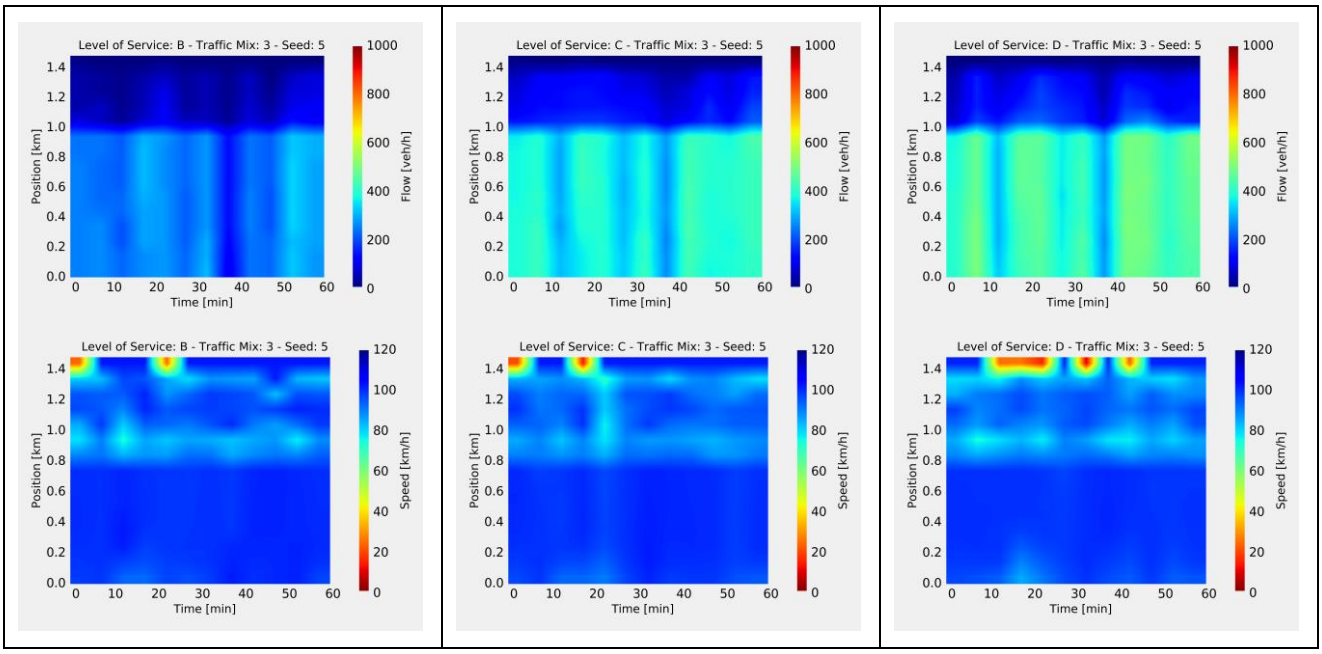

Figure 79. Examplary time-space-diagrams (on-ramp) of measured speeds (upper row) and flows (bottom row) for use case 2.1 baseline under vehicle mix 3, LOS B-D (left, middle and right column), seed 5.

4.2.2.2.2 Impacts on Traffic Dynamics

As a continuation of the first iteration, the total number of lane changes is used to show the disruption caused in the traffic flow by lane change manoeuvres per demand level and per traffic mix. Results are depicted in **Figure 80** below.

Within a fixed demand level, the total number of lane changes decreases slightly when the CAV share on the mainline increases. The possible logic here is that, the parameter *lcAssertive* of CAVs/CVs is smaller compared to LVs. This could lead to less willingness to perform lane change manoeuvres in the TAs, which in turn contributes to slight reduction of the total number of lane changes.

The total number of lane changes for LOS B, C and D under each traffic mix generally has no change or subtle reduction as traffic demand increases. Lane change behaviour can be generally categorized into mandatory lane change, such as on-ramp vehicles merging into mainline motorway, and discretionary lane change, such as lane change to gain speed in the TAs. In this case, the total number of mandatory lane changes could increase as traffic demand level increases from LOS B to LOS D. In contrast, the total number of discretionary lane changes could decrease because the traffic intensifies on the mainline motorway. The offset between these two phenomena could result in diversification in traffic dynamics regarding lane change behaviour.

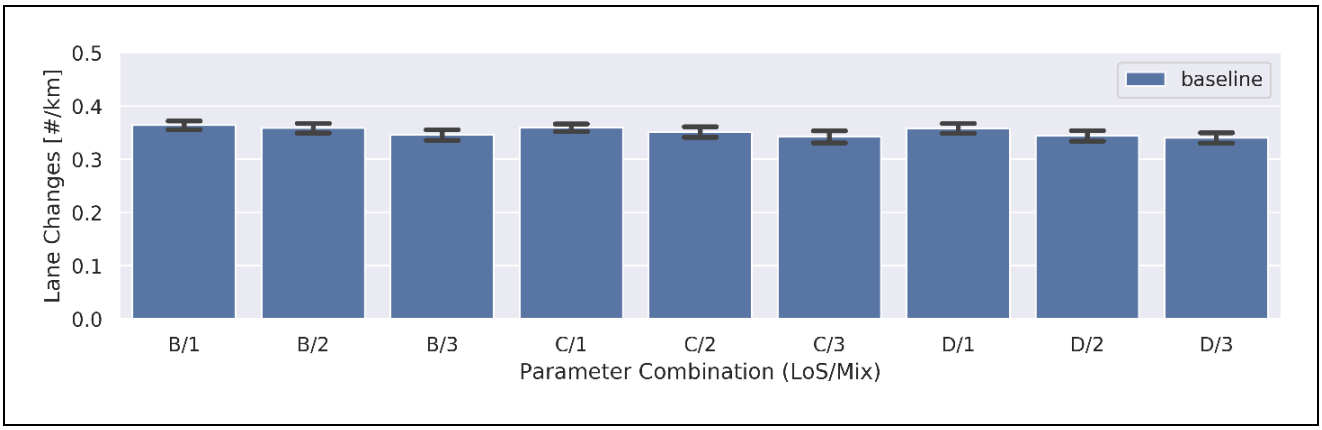

Figure 80. Lane changes for Scenario 2.1 2nd iteration baseline simulation experiments (varying LOS/traffic mix).

The results of the network throughput (veh/h) are presented with bar charts in **Figure 81**. From **Figure 81**, the network throughput increases for higher LOS and decreases slightly for higher traffic mixes under a fixed LOS, which correlates to the total number of lane changes in **Figure 80** and the average network speed in **Figure 74,** since no significant congestion and spillbacks were formed during the simulations.

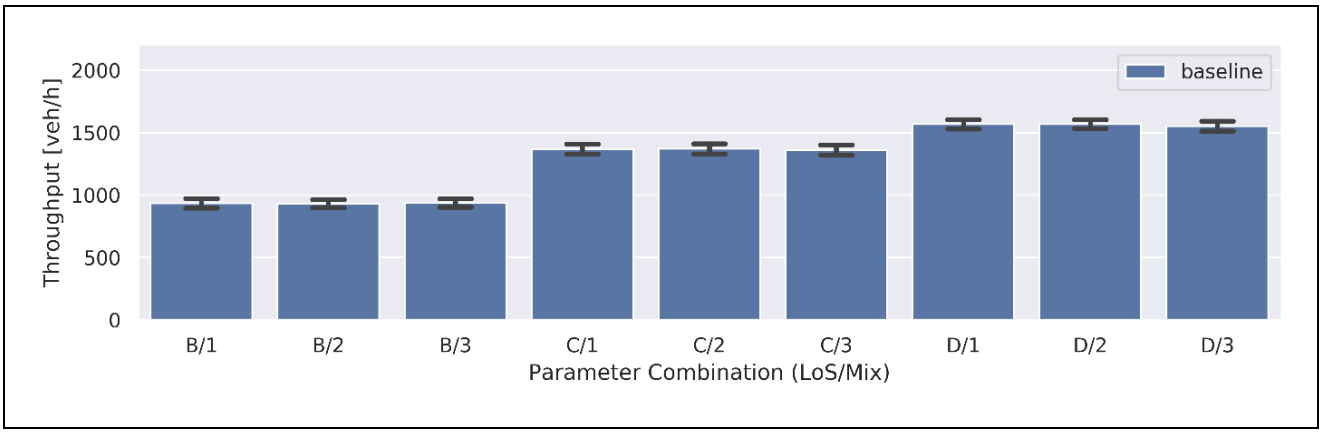

Figure 81. Throughput for Scenario 2.1 2nd iteration baseline simulation experiments (varying LOS/traffic mix).

4.2.2.2.3 Impacts on Traffic Safety

In the 2nd iteration baseline simulation experiments, the number of critical events continue to be an indicator of traffic safety by depicting the number of conflicts corresponding to TTC < 3.0 s. TTC measures a longitudinal margin to lead vehicles or objects and is a proxy for traffic safety.

Figure 82 shows the number and value range of safety critical events for three different LOSs and three different traffic mixes. When traffic mix increases under each traffic demand, the number of critical events stays unchanged or increases slightly. Unlike the generally increasing number of critical events when traffic mix increases, this could be that the parameter set of CAVs are refined in the second project iteration, where the driver's desired (minimum) time headway are generally larger than the LVs only when switching from CACC to ACC model. Another observation is that the number of critical events and its data range increases as traffic demand increases. This is self-

explanatory since higher demand (before capacity drop) induces more critical events when vehicles interact in the merging zone. Additionally, more CAVs/CVs are requesting TOR, performing ToC and eventual MRM on the on-ramp, thus creating more critical events in general.

The value range of critical events under each LOS and each traffic mix basically shows random pattern, with a tendency of a wider range when the number of critical events is higher, which could be explained by the increasing complexity of mixed traffic. For traffic mix 2, the number of critical events is slightly lower comparing to traffic mix 1 and 3. This could be caused by this relatively balanced traffic mix in term of vehicle behaviour heterogeneity. The other way around, the relative high number of critical events for traffic mix 1 could be explained by the greater vehicle behaviour heterogeneity. For traffic mix 3, the relative high number of critical events can be explained by the aforementioned fact that high share of CAVs/CVs forming platoons, creating more critical events for on-ramp merging vehicles.

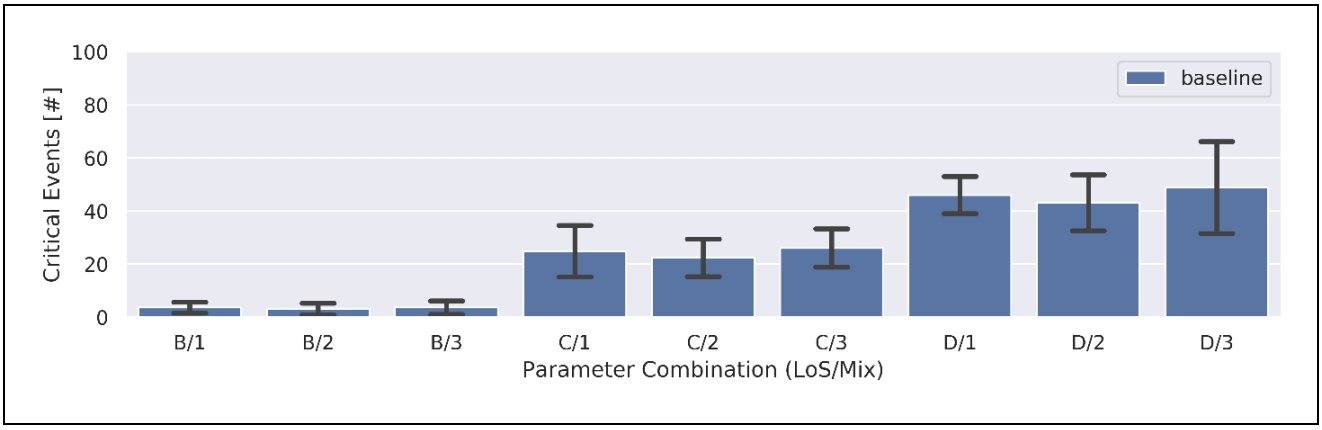

Figure 82. Critical events for Scenario 2.1 2nd iteration baseline simulation experiments (varying LOS/traffic mix).

In this iteration, a TTC location plot script is developed to show the locations of critical events on each use case network. For example, **Figure 83** maps the locations of critical events of 10 seeds under LOS D, traffic mix 1-3. The following patterns can be observed:

- The critical events mostly occur at two locations, namely lane drop location on the motorway and the last 250 meter of on-ramp. The lane drop location has a greater speed variation due to the lane changes (at the end of acceleration lane) that could not be performed earlier. The last 250 meters of the on-ramp is the location where the CAV_G1 vehicles request TOR, perform ToC and eventual MRM, which causes speed variations as each CAV driver behaviour becomes unpredictable.
- At a higher traffic mix, the situation at lane drop location seems slightly worse with a chain reaction spillback of critical events. Nevertheless, it is difficult to draw preliminary conclusions here since the patterns are scattered and case sensitive based on simulation observations.

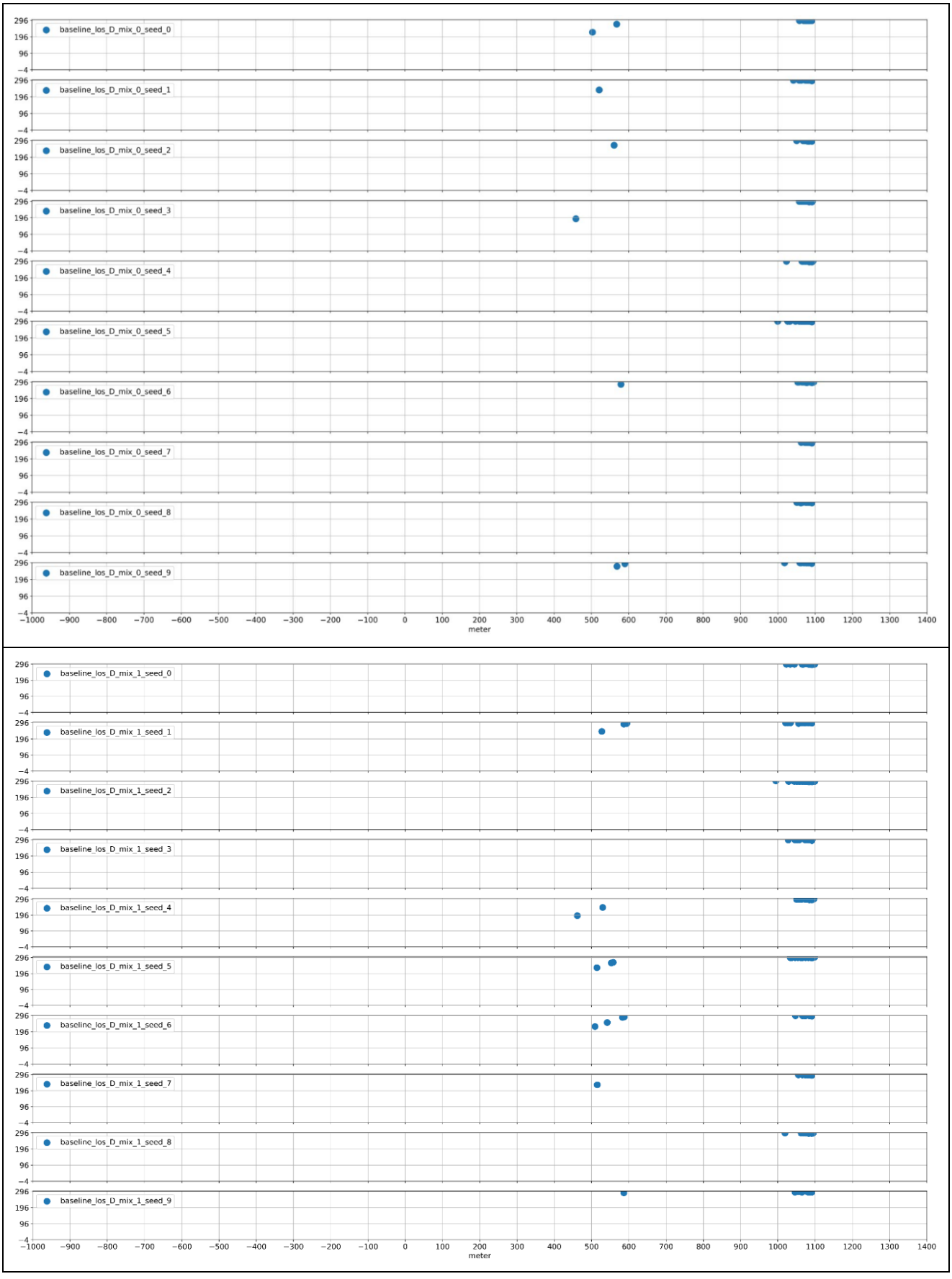
baseline_los_D_mix_0_seed_0
baseline_los_D_mix_0_seed_1
baseline_los_D_mix_0_seed_2
baseline_los_D_mix_0_seed_3
baseline_los_D_mix_0_seed_4
baseline_los_D_mix_0_seed_5
baseline_los_D_mix_0_seed_6
baseline_los_D_mix_0_seed_7
baseline_los_D_mix_0_seed_8
baseline_los_D_mix_0_seed_9
296
196
96
−4
−1000 −900 −800 −700 −600 −500 −400 −300 −200 −100 0 100 200 300 400 500 600 700 800 900 1000 1100 1200 1300 1400
meter
baseline_los_D_mix_1_seed_0
baseline_los_D_mix_1_seed_1
baseline_los_D_mix_1_seed_2
baseline_los_D_mix_1_seed_3
baseline_los_D_mix_1_seed_4
baseline_los_D_mix_1_seed_5
baseline_los_D_mix_1_seed_6
baseline_los_D_mix_1_seed_7
baseline_los_D_mix_1_seed_8
baseline_los_D_mix_1_seed_9
meter

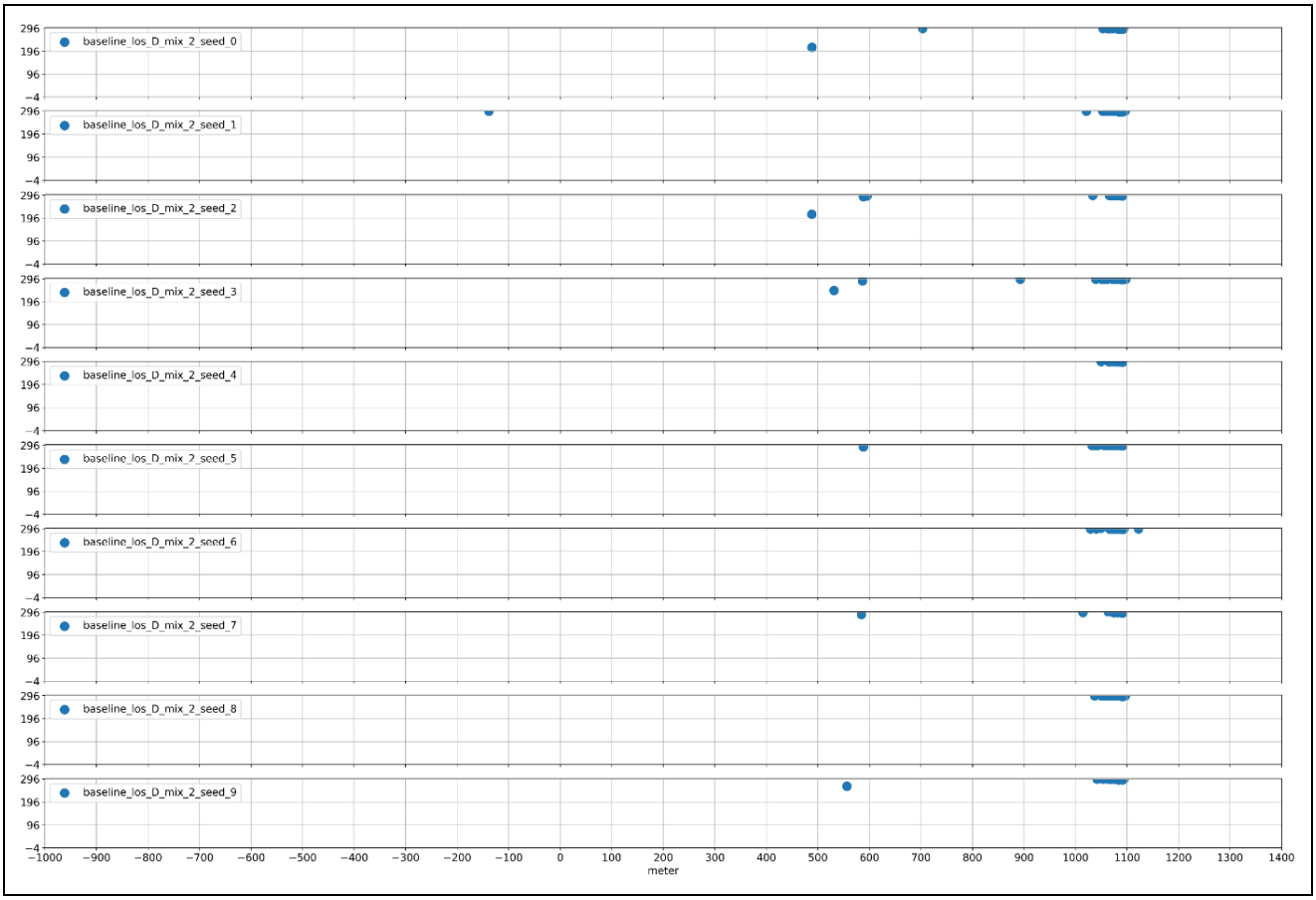

Figure 83. Spatial distribution of critical events (TTC< 3sec) for seed 0-9, LOS D, traffic mix 1-3 and Scenario 2.1 2nd iteration baseline simulation experiments.

Figure 84 shows the numbers (colour of bins) and locations (location of bins) of critical events under LOS B, traffic mix 1-3 on a 2D histogram (colour bar indicating the critical event intensity). It can be seen that the critical events are happening on the two aforementioned locations. But the numbers of critical events are not visually clear due to the small amount**.**

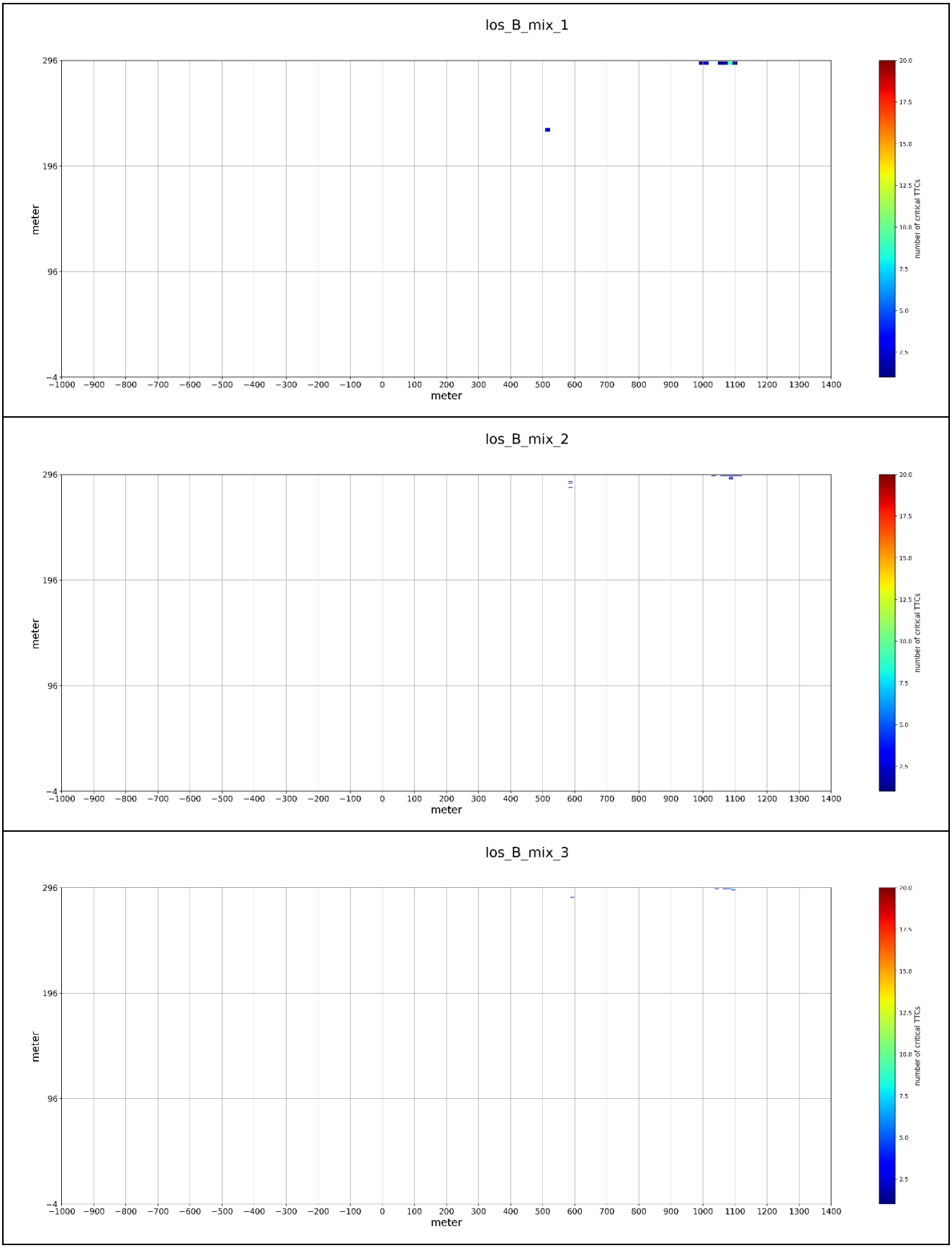
los_B_mix_1
los_B_mix_2
los_B_mix_3
meter
number of critical TTCs

Figure 84. Spatial distribution of critical events (TTC< 3sec) for Scenario 2.1 2nd iteration baseline simulation experiments (LOS B/varying traffic mix).

Figure 85 shows the numbers (colour of bins) and locations (location of bins) of critical events under LOS C, traffic mix 1-3. The critical events locations correspond with previous findings in this section. The numbers of critical events seem higher under LOS C/mix 1 and LOS C/mix 3 than LOS C/mix 2. This corresponds with the findings related to **Figure 82**. The correlation between traffic mix and critical event is case sensitive. Therefore, the possible hypotheses are provided preliminarily case by case in the findings.

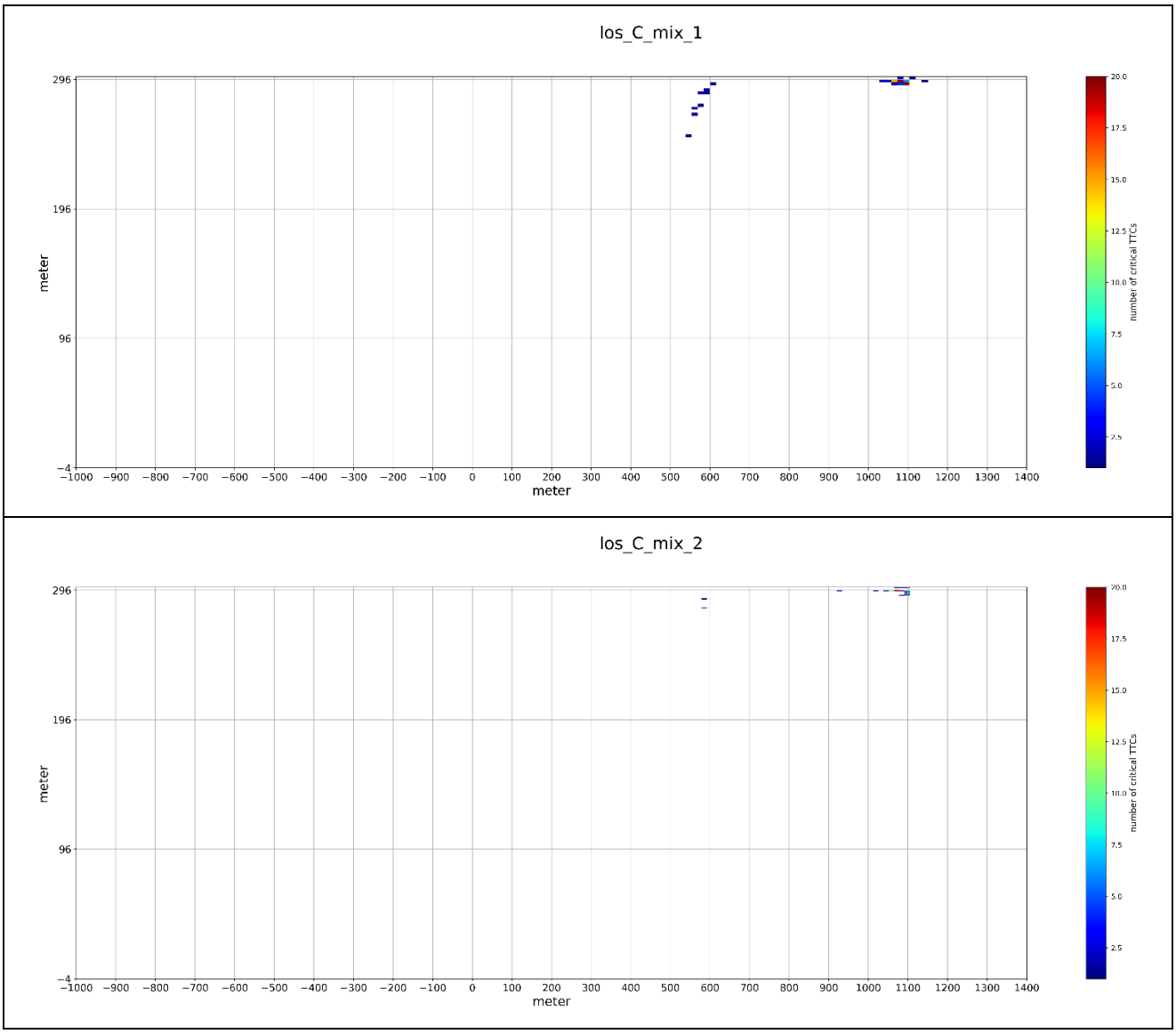

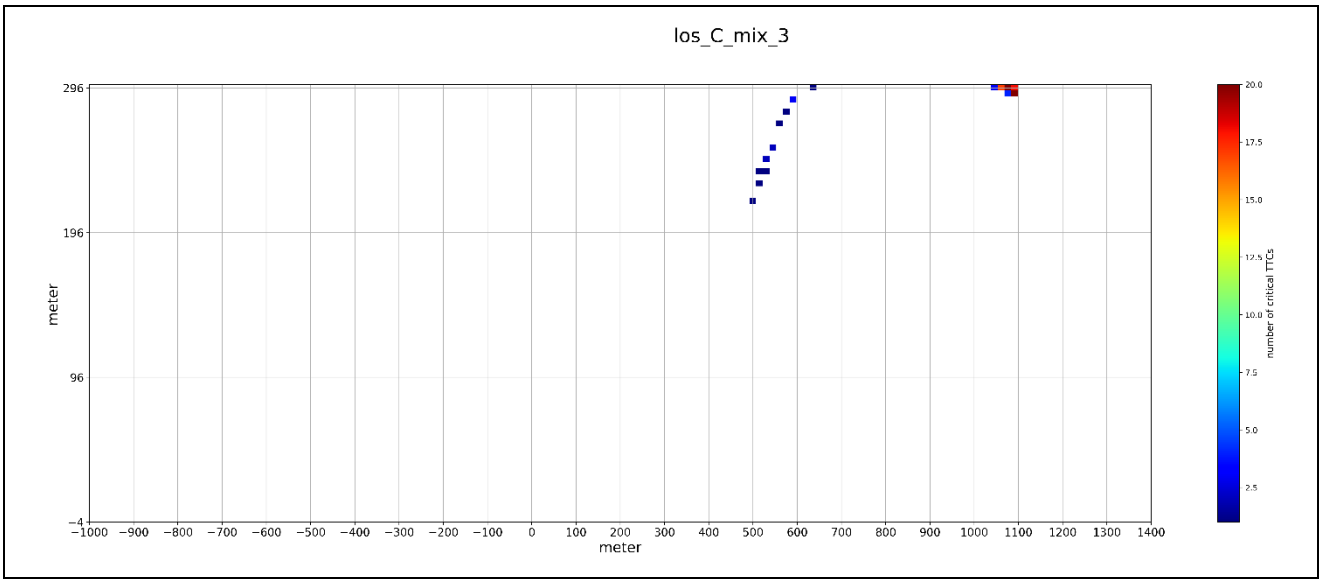

Figure 85. Spatial distribution of critical events (TTC< 3sec) for Scenario 2.1 2nd iteration baseline simulation experiments (LOS C/varying traffic mix).

Figure 86 shows the numbers (colour of bins) and locations (location of bins) of critical events under LOS D, traffic mix 1-3. The critical events locations still correspond with previous findings in this section. The numbers of critical events seem to be highest under LOS D/mix 3, followed by LOS D/mix 1 and then LOS D/mix 2.

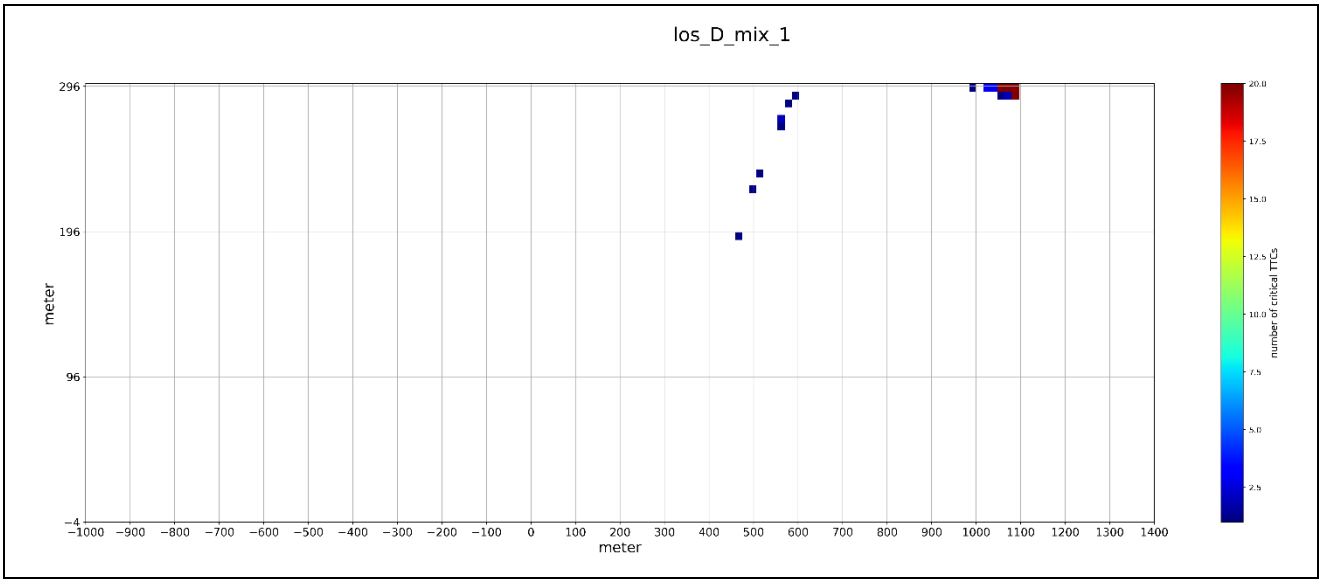

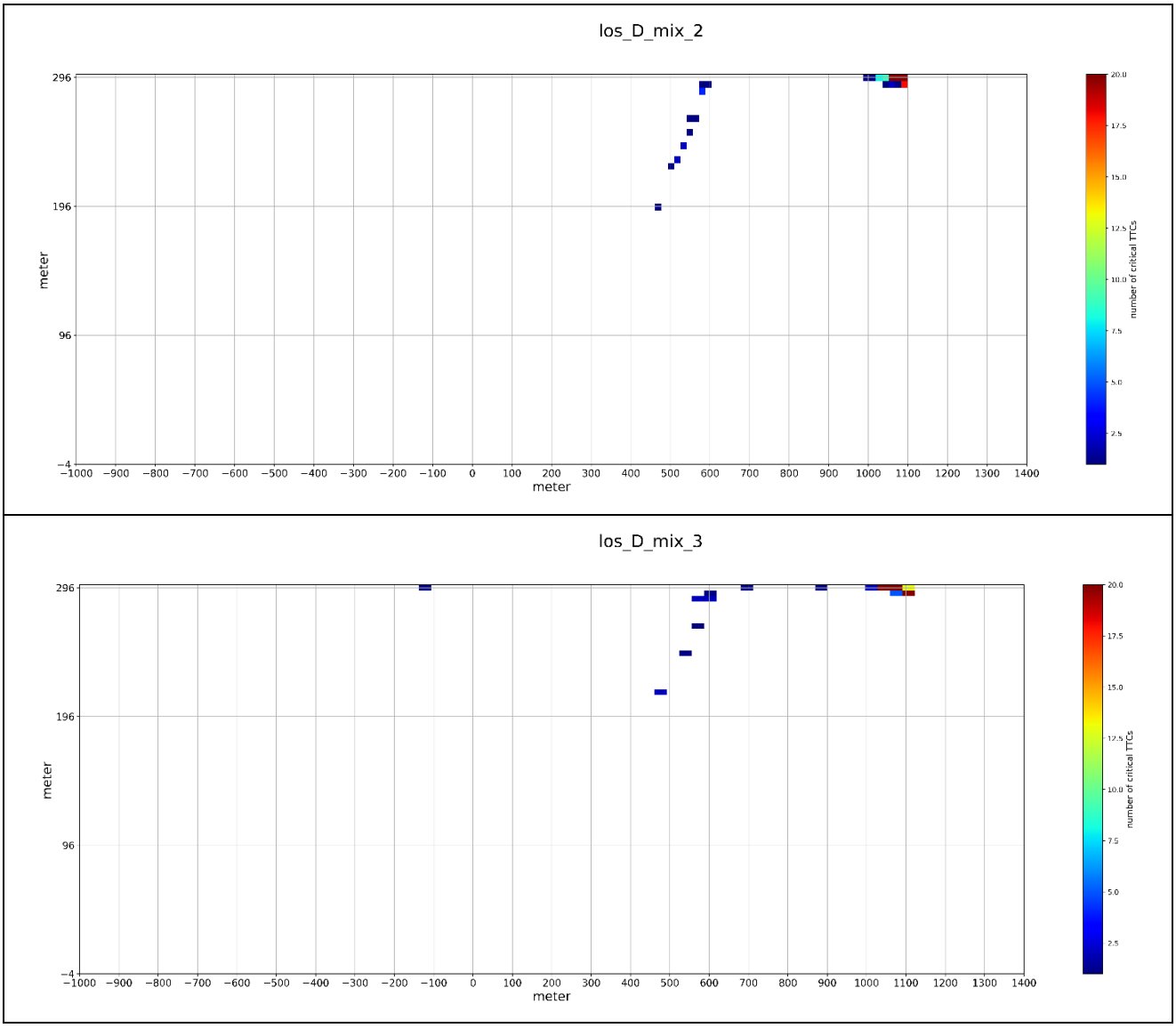

Figure 86. Spatial distribution of critical events (TTC< 3sec) for Scenario 2.1 2nd iteration baseline simulation experiments (LOS D/varying traffic mix).

4.2.2.2.4 Environmental Impacts

Figure 87 shows the total CO_2 emissions for all 9 LOS/Mix combinations. The total CO_2 slightly increases when the traffic mix increases under the same traffic demand, and when the traffic demand increases from LOS B to LOS D. This result complies with average network speed values in section 4.2.2.2.1, where lower average network speed showed less optimal in terms of traffic efficiency. It is probable that the CO_2 emissions increase slightly due to the variation of individual vehicle speed, but the increase is much less comparing to the 1st project iteration. It is mainly contributed by the modification in parametrisation in the second project iteration and the fact that the mainline vehicles don't perform ToC where the individual speed variation is likely to be higher.

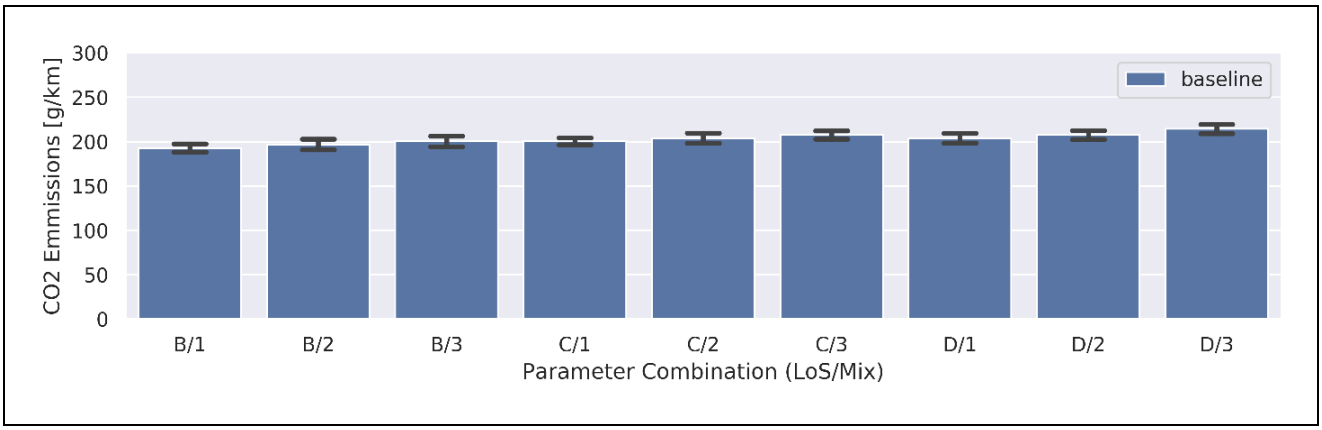

Figure 87. CO_2 emissions for Scenario 2.1 2nd iteration baseline simulation experiments (varying LOS/traffic mix).

4.2.3 Scenario 2.3: Intersection handling due to incident

4.2.3.1 Scenario Description

In scenario 2.3, an incident takes place at the intersection. The location of the incident is on lane 5 at approximately 35 metres before the stop line (see **Figure 88**).

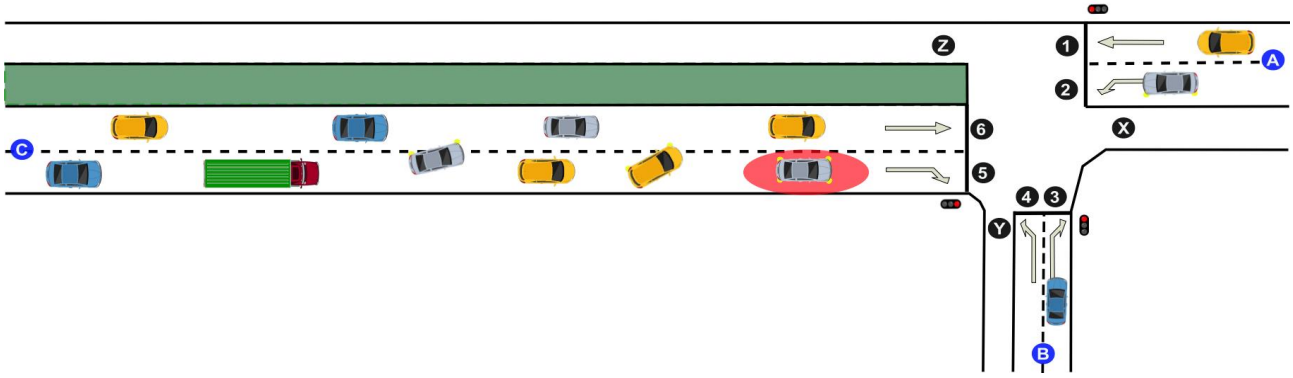

Figure 88. Schematic presentation of use case 2.3.

Based on findings from scenario 4.2 (1st iteration), we consider that Day 1 C-ITS applications are existent in the baseline simulations, and that CAVs are also able to dynamically trigger TORs according to the complexity of the traffic conditions in the proximity of the intersection.

As soon as the RSU is informed about the incident on lane 5 it shares its relevant information with the approaching CAVs/CVs. The information is shared via DENM and SPATEM messages that are broadcasted by the RSU located at the intersection. Upon DENM reception, warning messages are issued to the CV/CAV drivers to inform about the downstream incident. Since CVs are equipped with lower automation systems that cannot cope with the broadcasted information, and their drivers are expected to continuously monitor the primary driving tasks, we assume that they are manually and instantly taking over vehicle control at approximately 350 - 300 m upstream of the intersection (see **Figure 89**).

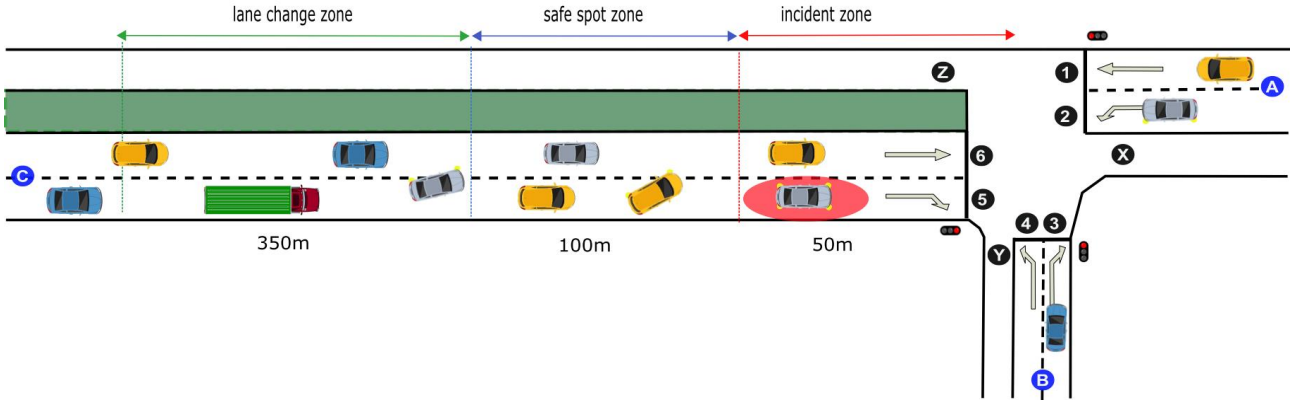

Figure 89. Traffic zones of use case 2.3

On the other hand, based on findings from the 1st project iteration we know that CAVs will be able to cope with upcoming events/incidents like work zones depending on the capabilities of their automation systems. Thus, we assume, as described in paragraph 3.2.2, that 75% of CAVs (CV and CAV_G1) will have to issue a TOR request upon DENM reception (350 m upstream of the intersection, 320 m upstream of the incident), while the remaining 25% of CAVs (CAV_G2) can pass the incident zone in automated mode. The ToC location for the first group of CAVs (CAV_G1) will depend on the driver's response time. If the driver does not respond to the TOR within the available lead time (10 s in this case), an MRM will take place on the CAV's current lane. CAVs from the second group (CAV_G2 – the one that can cope with the incident) which are driving in lane 5 and are within visual range of the incident will attempt to merge into lane 6. If the first attempt to merge is blocked, a TOR is issued by the automation (see **Figure 90)**. In this case, the driver will either take-over control successfully within the situation-specific available lead time (cf. Section 2.3.2.2), or an MRM will be initiated if the driver fails to respond to the TOR. Considering that the dynamic TOR location is a function of vehicle speed (see Section 2.3.2.2) and that different vehicles (CAVs_G2) might have different capabilities in terms of field of view, we define a specific distribution for the *dynamicToCThreshold* parameter **(Table 41)** for the urban traffic situation that is simulated in UC2.3. It must be noted that the situation awareness of the CAV drivers is expected to be increased in the case of the dynamical TOC triggering, due to the prior information received via the ETSI messages about the incident.

Table 41. ToC Model parameter value for dynamical TOR triggering in Scenario 2.3.

Dynamic TOR Parameter	Urban Network
dynamicToCThreshold (s)	normal(9.0, 0.5); [8.0, 10.0]

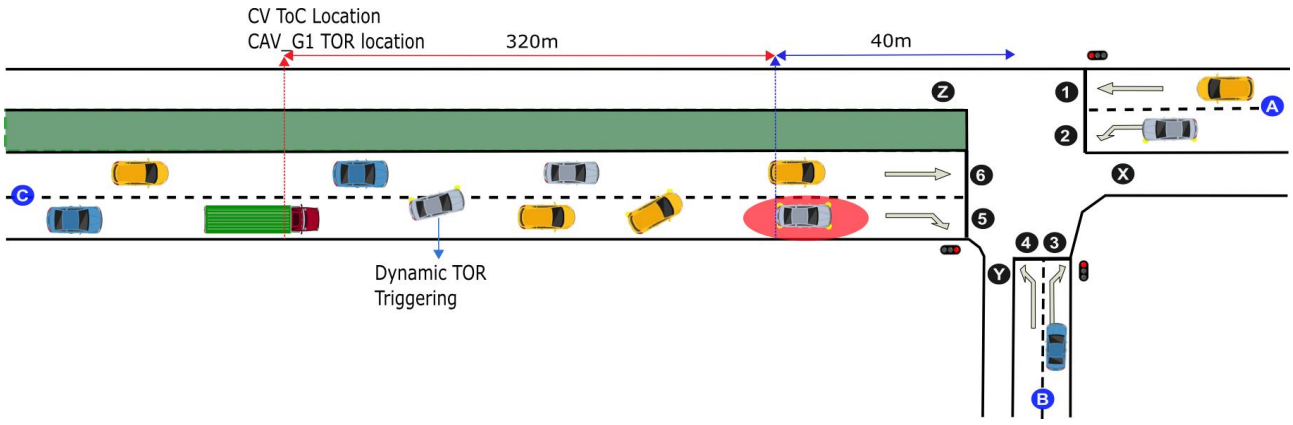

Figure 90. ToC triggering conditions for CVs and CAVs in use case 2.3

More details about the simulation network of Scenario 2.3 can be found in **Table 42**.

Table 42. Network configuration details for use case 2.3

Scenario 2.3	Settings	Notes
Road section length	1.6 km	• both directions
Road priority	3	
Allowed road speed	13.89 m/s	• 50 km/h
Number of nodes		• n0 – n8
Number of edges		• both directions
Number of O-D relations	2	• from n0 to n8 • from n8 to n0
Number of lanes	4	• both directions
Incident location		• 250 m
Closed edge[1, 2] (defined in the file: UC2_3Incident.add.xml)	Incident zone	• lane 6 (50 m)
	Safe spot zone	• lane 6 (100m)
	Lane change zone	• lane 6 (350 m)
Filenames	• network: UC23.net.xml	

Intended control of lane usage

Around the incident location CAVs are rerouted due to a vehicle that is coming to a stop in the right turn lane. CAVs are informed about the incident and are rerouted via the left thru lane and are being able to turn right at the junction due to a temporary adaptation of the RSU in the vicinity.

Network layout

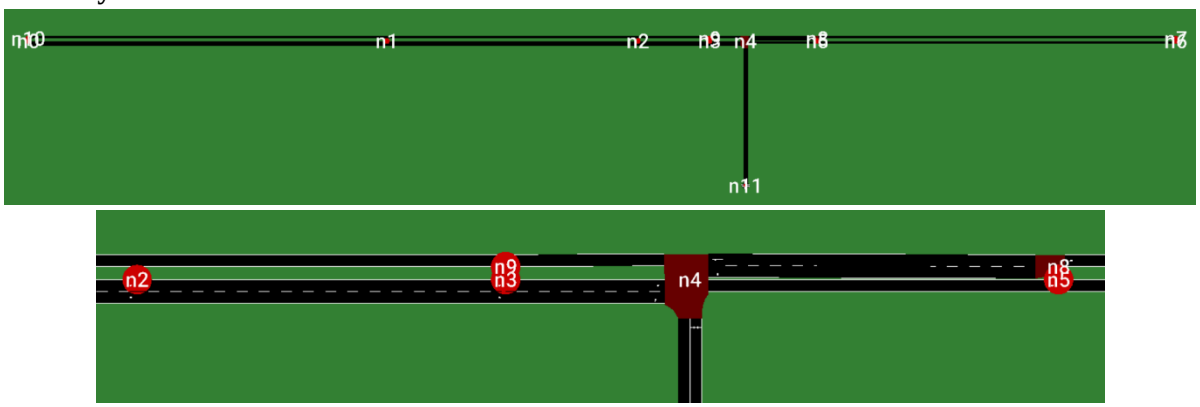

Road segments

n0	n1	500	start
n1	n2	350	lane change zone
n2	n3	100	safe spot zone
n3	n4	50	incident zone
n4	n5	100	leave
n5	n6	500	end
n6	n7	500	reverse1
n7	n8	100	reverse2
n8	n9	50	reverse3
n9	n10	950	reverse4
n4	n11	200	minor road end
n11	n4	200	minor road start

4.2.3.2 Results

The proposed scenarios are simulated at three traffic demand levels (LOS B, C and D) with the consideration of three vehicle compositions as mentioned in Section 3.2. Furthermore, 10 simulation runs with different random seeds for each combination of LOS demand and vehicle composition are executed. In the following, the results are analysed and clarified in the aspects of traffic efficiency, traffic dynamics, traffic safety and environment.

Due to simulating an urban network including a traffic light-controlled junction, the intensities of the proposed LOS as stated in paragraph 3.2.4 are lowered appropriately to represent LOS levels B, C and D. The volumes were calculated with COCON. This is a Dutch software tool to calculate fixed time signal control plans. It is the most used software suite in the Netherlands (see https://www.wegenwiki.nl/COCON). The hourly volumes per lane corresponding to the proposed LOS and the respective intensity/capacity ratios are depicted in **Table 43**.

Table 43. Vehicles/hour/lane for LOS B, C and D for UC2.3 urban situation with TLC.

Facility Type	Capacity (veh/h/l)	Level of Service (LOS)		
		B	C	D
Urban with TLC (50km/h)	1200 veh/h/l	780	960	1108
Intensity / Capacity (IC) ratio		0,65	0,80	0.92

When implementing the LOS for two lanes, due to the blocked lane, even when simulating LOS B a queue one lane 6 builds up very quickly and spills back to the start of the network within 600 s of the simulation. For all levels of service there will be little difference between the scenarios to observe regarding the effects of vehicle behaviour, traffic merging, TORs, TOCs and MRMs. Therefore, the simulations are run with the LOS for just one lane.

4.2.3.2.1 Impacts on Traffic Efficiency

Traffic efficiency is analysed both network-wide and locally.

Network-wide Impacts

Figure 91 shows that traffic is quite smooth for LOS B and LOS C mix 2 and 3 with an average travel time of approximately 1.6 min/km. There is also no significant difference in travel time with different vehicle mixes. LOS C shows only a slight increase in travel time (31%) with the highest proportion of CAV's, i.e. mix 3 (C/3). When traffic demand further increases to LOS D, an increase in travel time is already notable at mix 2 and grows even more at mix 3. To summarise, when the LOS increases to C and higher the impact of a higher penetration rate of CAVs influences the travel time negatively. As the graph shows for LOS D mix1, 2 and 3 the travel time increases by 25%, 125% and 290% respectively in comparison to LOS B.

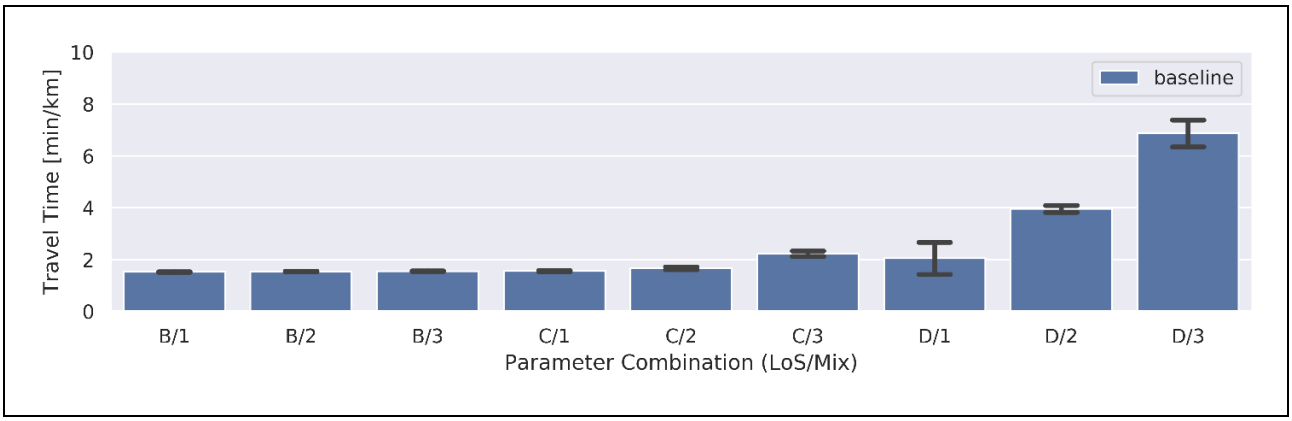

Figure 91. Travel time (min/km) for use case 2.3 simulation experiments (varying LOS and traffic mix).

Local Impacts

Following the aforementioned network-wide analysis the local impacts at LOS D are further investigated based on time-space plots for traffic speed and flow. **Figures 92** and **93** show the time-space diagrams for measured speeds and flows at LOS D with 26% (mix 1) and 70% (mix 3) share of CVs and CAVs respectively. As the figures show in LOS D mix 1 a queue builds up behind the incident, red area of **Figure 92** (a), which in time grows (between 0.3 and 0.4 km) but also reduces occasionally. **Figure 92** (b) shows that indeed the throughput varies from time to time as marked by darker and lighter blue areas running from position 0.3 km up until position 0.95 km. When the throughput is disrupted by the build-up of the queue some turbulence in speed and flow occurs at the tail of the queue around position 0.3 - 0.4 km. At this point the vehicle throughput at the tail of the queue is compacted.

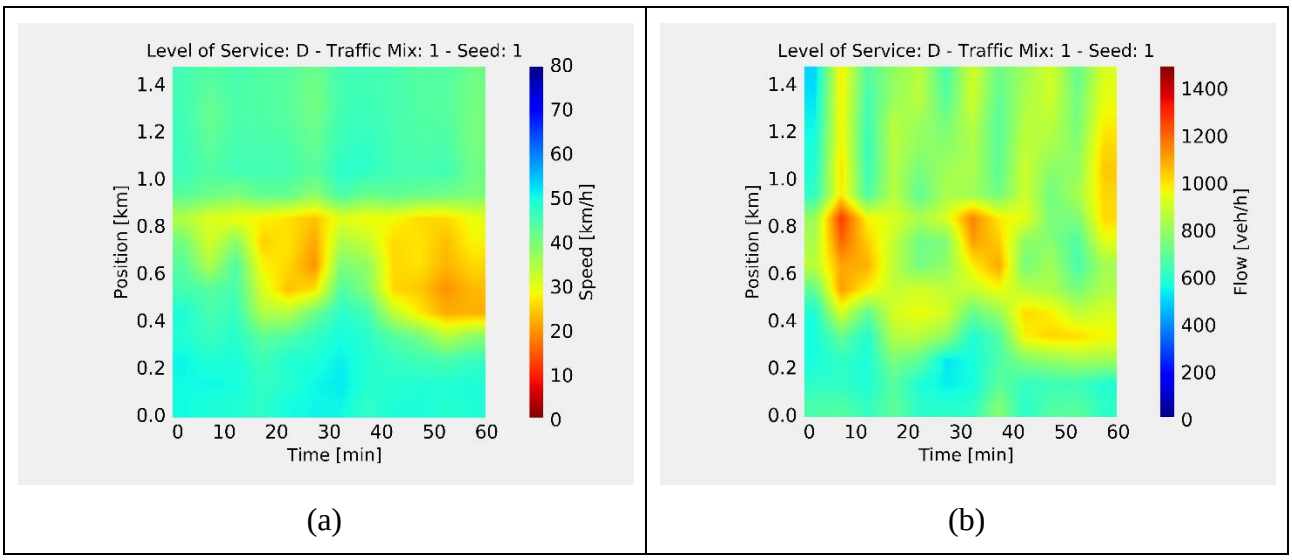

(a) (b)

Figure 92. Exemplary time-space-diagrams for LOS D – traffic mix 1 (seed 1) measured speed (left column a) and flow (right column b) for use case 2.3.

Figure 93 (a) and (c) shows that from the start of the simulation the queue builds up and spills back to the beginning of the network. The capacity drops in LOS D mix 3 is too significant to cope with the traffic demand. Also, here we observe a compacted throughput just behind the tail of the queue.

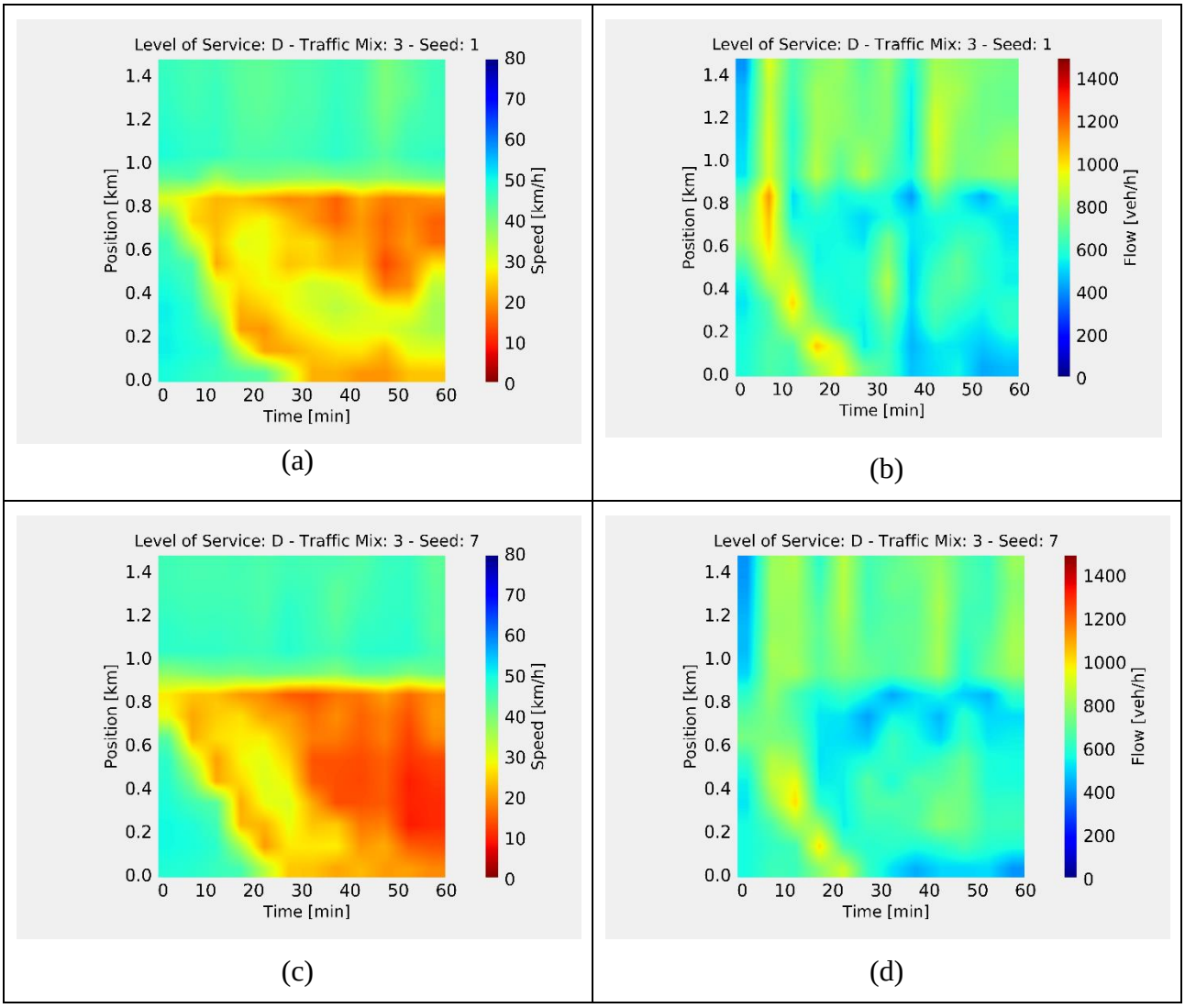

Figure 93. Exemplary time-space-diagrams for LOS D – traffic mix 3 (seed 1 and sees 7) measured speed (left column a and c) and flow (right column b and d) for use case 2.3.

The figures show that speed will reduce when the proportion of CAVs increase. The drop in the network capacity is the result of the increased number of ToCs due to the increased number of CAVs. During ToC, a vehicle will only interact in the safest possible way with the surrounding traffic and will not increase speed or preform a lane change which results in the observed capacity drop.

4.2.3.2.2 Impacts on Traffic Dynamics

To elaborate on traffic dynamics, the average throughput **(Figure 94)** and the number of lane changes **(Figure 95)** were used as KPIs. An increase of the proportion of CAVs has a positive effect on the vehicle throughput at LOS B (10% increase) and LOS C (11%). On the contrary the

throughput at LOS D decreases when the proportion of CAVs increases by 10%. When reaching the capacity of the road network the performance of ToCs influences the network throughput. The spread between the seeds is minimal as shown by the black lines per bar.

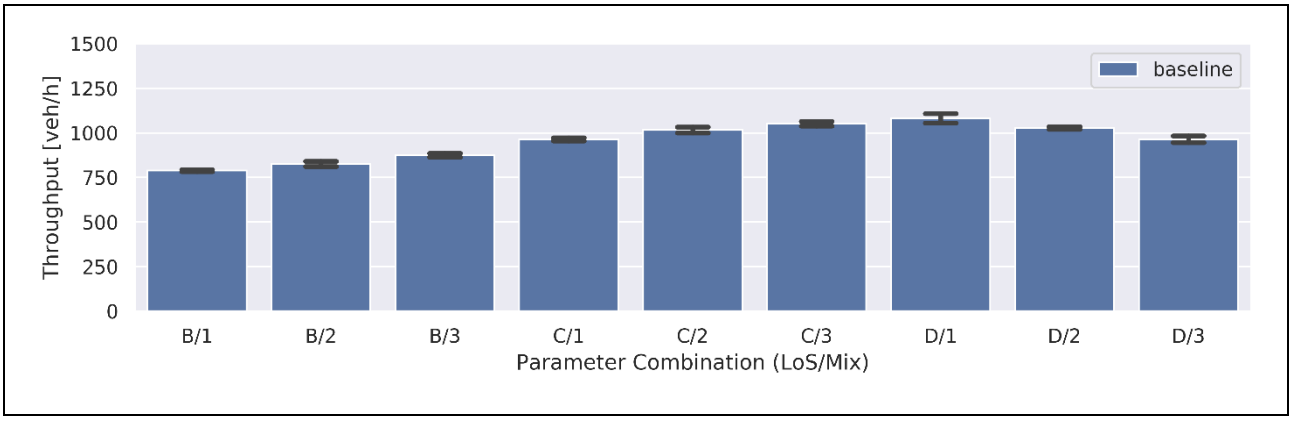

Figure 94. Throughput [veh/h] for use case 2.3 (varying LOS and traffic mix).

As **Figure 95** shows for LOS B the number of lane changes differ marginally. For LOS C mix 1 and mix 2 the number of lane changes even drop a little. LOS C Mix 3 shows a slight increase of lane changes. But then at LOS D an increasing number of lane changes occur when the proportion of CAVs increases.

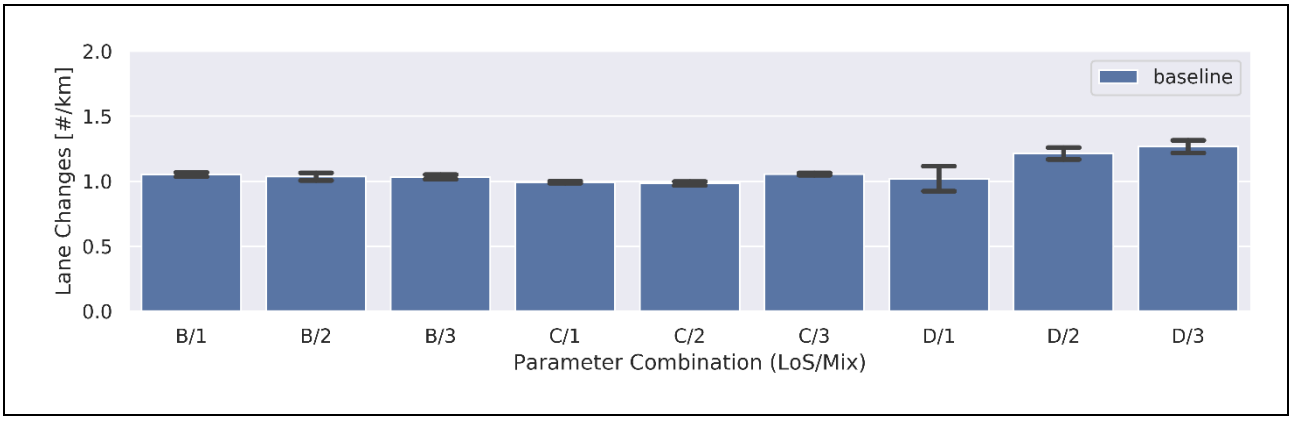

Figure 95. Number of lane changes per kilometre [#/km] for use case 2.3 (varying LOS and traffic mix).

When looking in more detail at the simulations, we observe that more lane changes occur when the queue spills all the way back on lane 6. When there is room on lane five more and more vehicles will change to lane 5 but also almost directly want to change back (left indicators are turned on). **Figure 96** shows this for the vehicle in the red circle. The vehicle changes to lane 5 at timestamp 953 (frame (a)), then drives for just 10 seconds on lane 5 (frame (b)) and as soon there is a gap on lane 6 changes back to lane 6 (frame (c)).

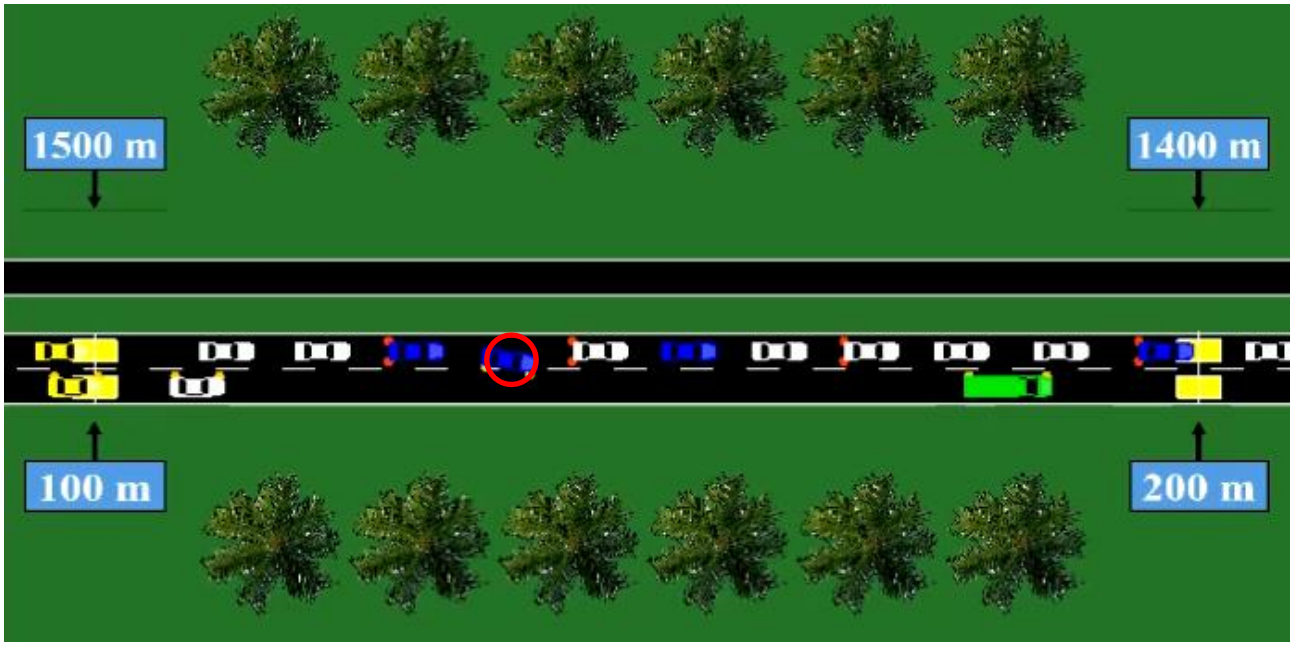

(a)

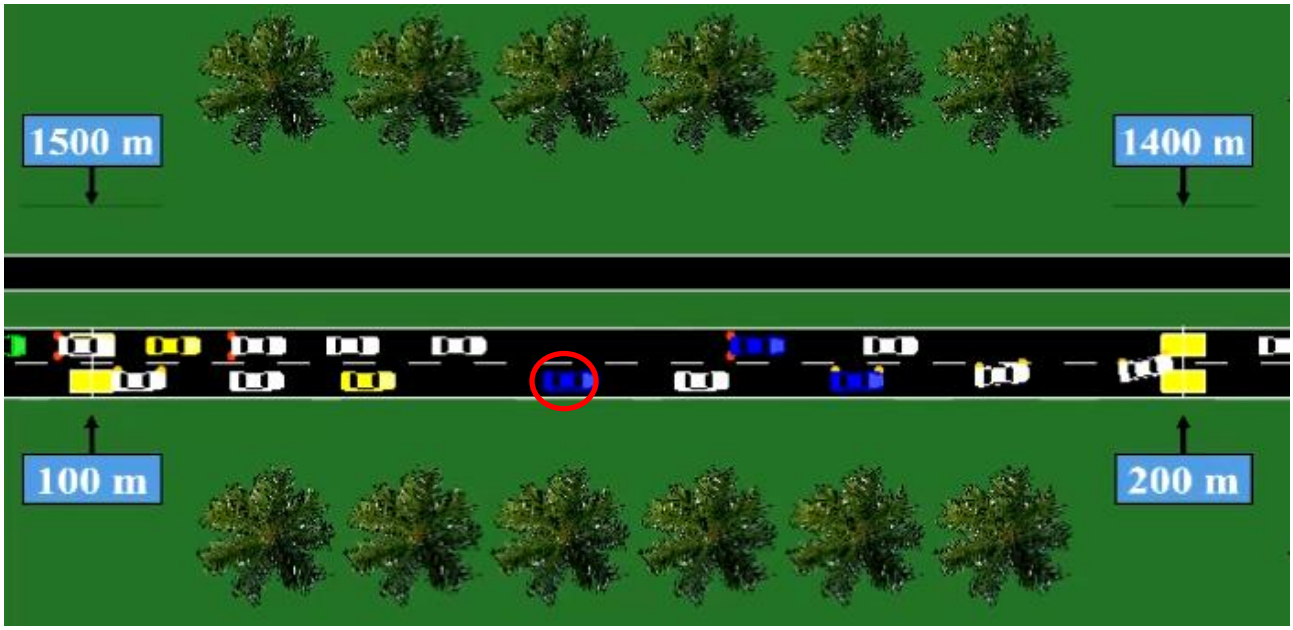

(b)

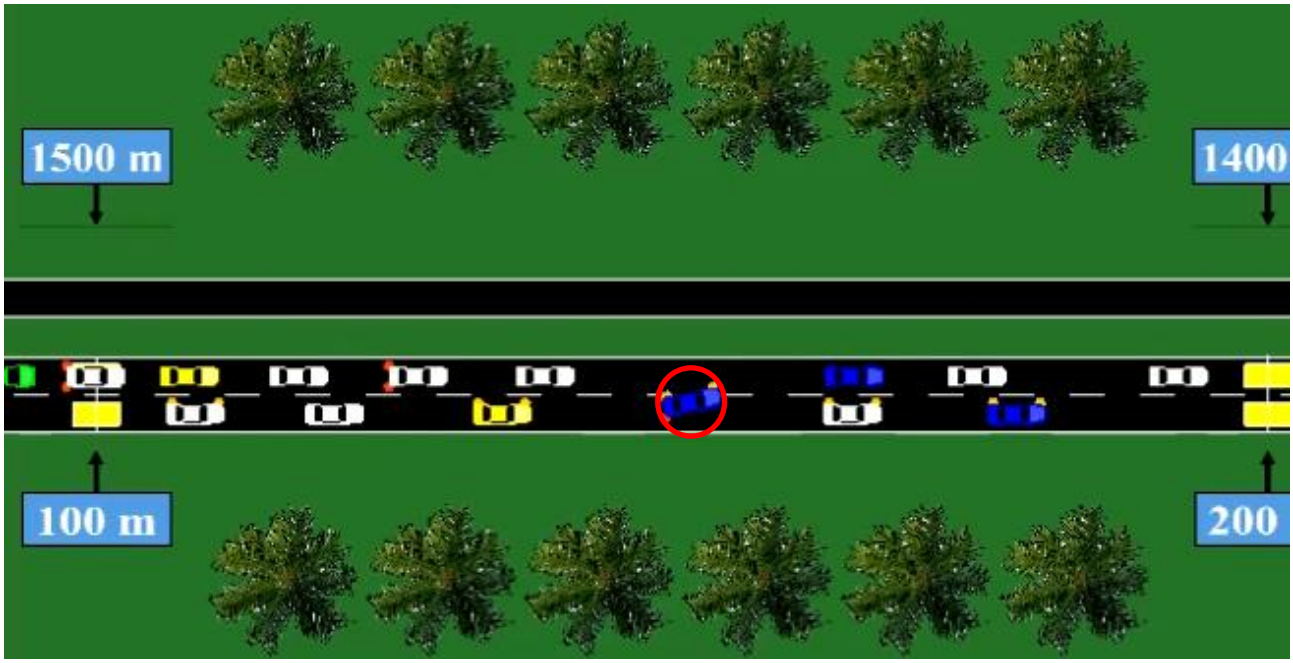

(c)

Figure 96. UC 2.3 Los D mix 3 seed1, Lane change back and forth.

4.2.3.2.3 Impacts on Traffic Safety

Traffic safety is analysed both network-wide and locally. On the network-wide level, the number of critical TTC events is used as a KPI. Locally we evaluate the aggregated TTC distributions within the incident zone by using two different examples.

Network-wide Impacts

Figure 97 shows the average number of critical events for all combinations of traffic states and vehicle compositions. An increase in critical events is shown for LOS C Mix 3, but moreover for LOS D, especially mix 2 and mix 3. This is analysed in the next paragraph.

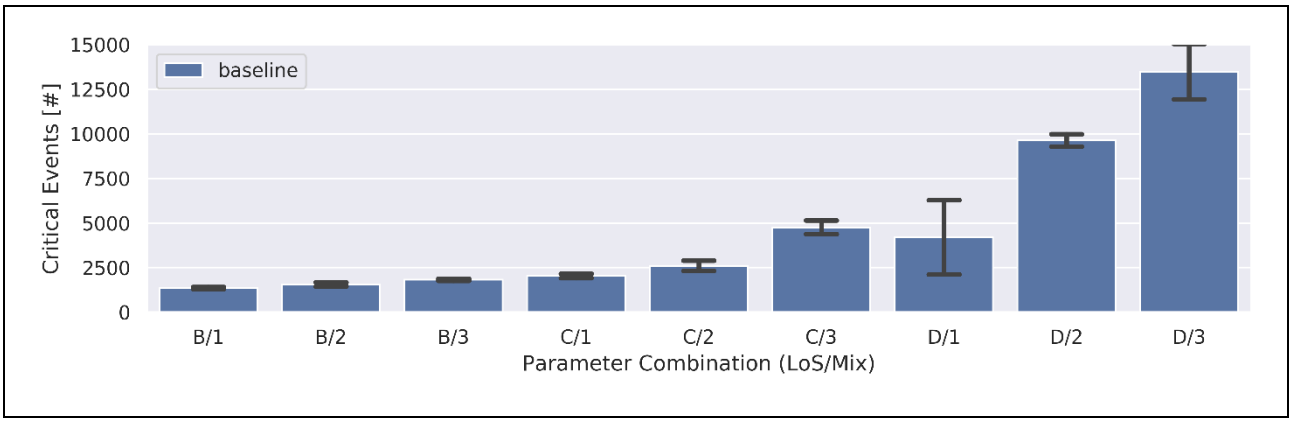

Figure 97. Average number of events with TTCs below 3.0 seconds for use case 2.3 (varying LOS and traffic mix).

Local Impacts

When looking at the spatial distribution of the critical events, local impacts can be further identified. Mix 1 and 3 are shown for LOS B, C and D in **Figures 98**, **99**, and **100** where each plot features the aggregated number of critical TTCs of 10 seeds (per LOS/mix) marked as bins within the approach area. Each plotted bin means that at least one TTC occurred at this position. The colour of a bin then indicates the amount of TTCs at this marked position. So, when e.g. several TTCs concentrate within a certain area, the colours translate as a spatial density for interpretation of the TTC distribution.

As indicated by the latter figures, when the percentage of CAVs increases, the density of safety critical events increases. As the traffic jam intensifies and progresses upstream the density of TTC events also increases. Moreover, lane change activity behind the incident location undermines traffic safety further. LOS B and LOS C – Mix 1 mostly show TTC's on lane 6 (upper most bar region above 58 meter) and not many TTCs during lane changing (the scattered locations). At LOS C mix 3 and LOS D the number of TTCs during lane change grows strongly, mainly on lane 5.

Moreover, safety critical events occur between the incident location and the headway of Traffic Light Controller. The number of critical events seem to grow at the same rate as the increase in traffic demand (LOS) and percentage of CAVs. The reason of these TTCs is due to the braking for the traffic light and lane changes in just a few meters to lane 6 by vehicles which want to turn right.

Looking at the aforementioned figures of mix 3 with LOS C and D, TTCs during lane change occur mostly between 50 and 500 meters. This occurs due to the build-up of the queue mainly on lane 6 and vehicles trying to merge from lane 5 into the traffic queue.

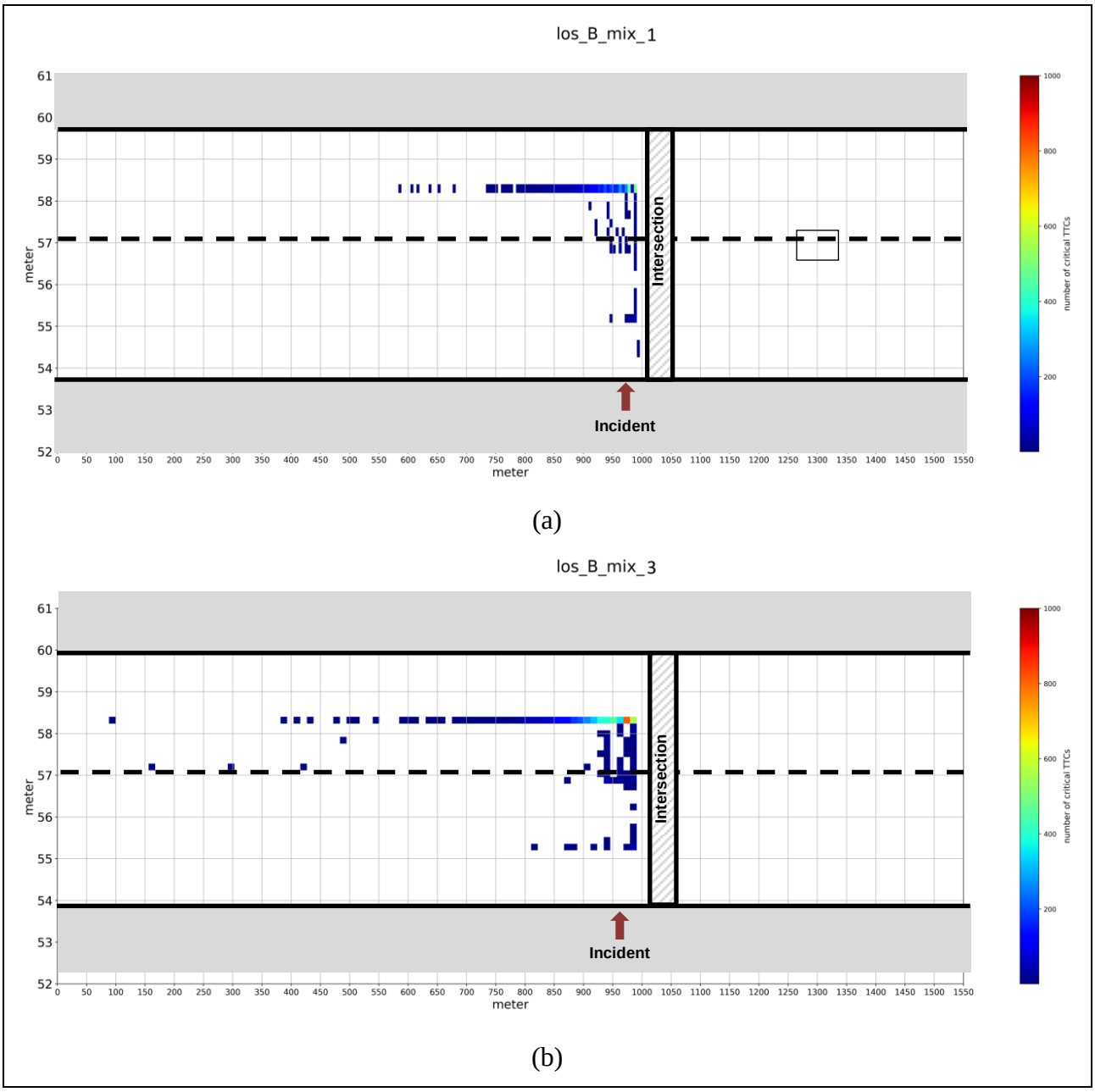

Figure 98. Spatial distribution of critical TTCs (< 3sec) for UC2.3, upper plot (a): LOS B – Traffic Mix 1 (code 0); bottom plot (b): LOS D – Traffic Mix 3 (code 2). Colours indicate the number of critical TTCs shown with discrete plotted bins (bin size ≈ 20m x 0,3m).

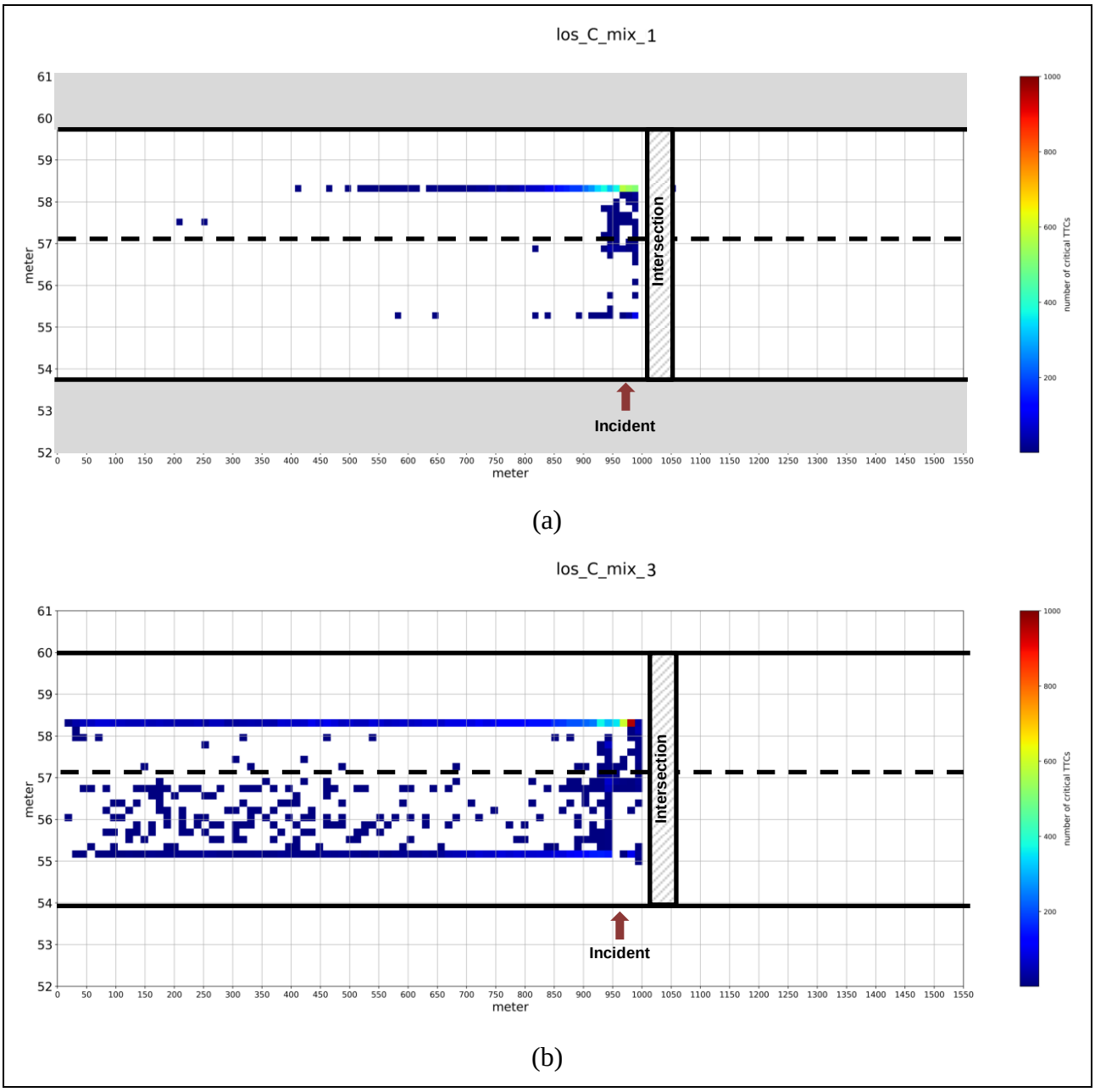

Figure 99. Spatial distribution of critical TTCs (< 3sec) for UC2.3, upper plot (a): LOS C – Traffic Mix 1 (code 0); bottom plot (b): LOS C – Traffic Mix 3 (code2).

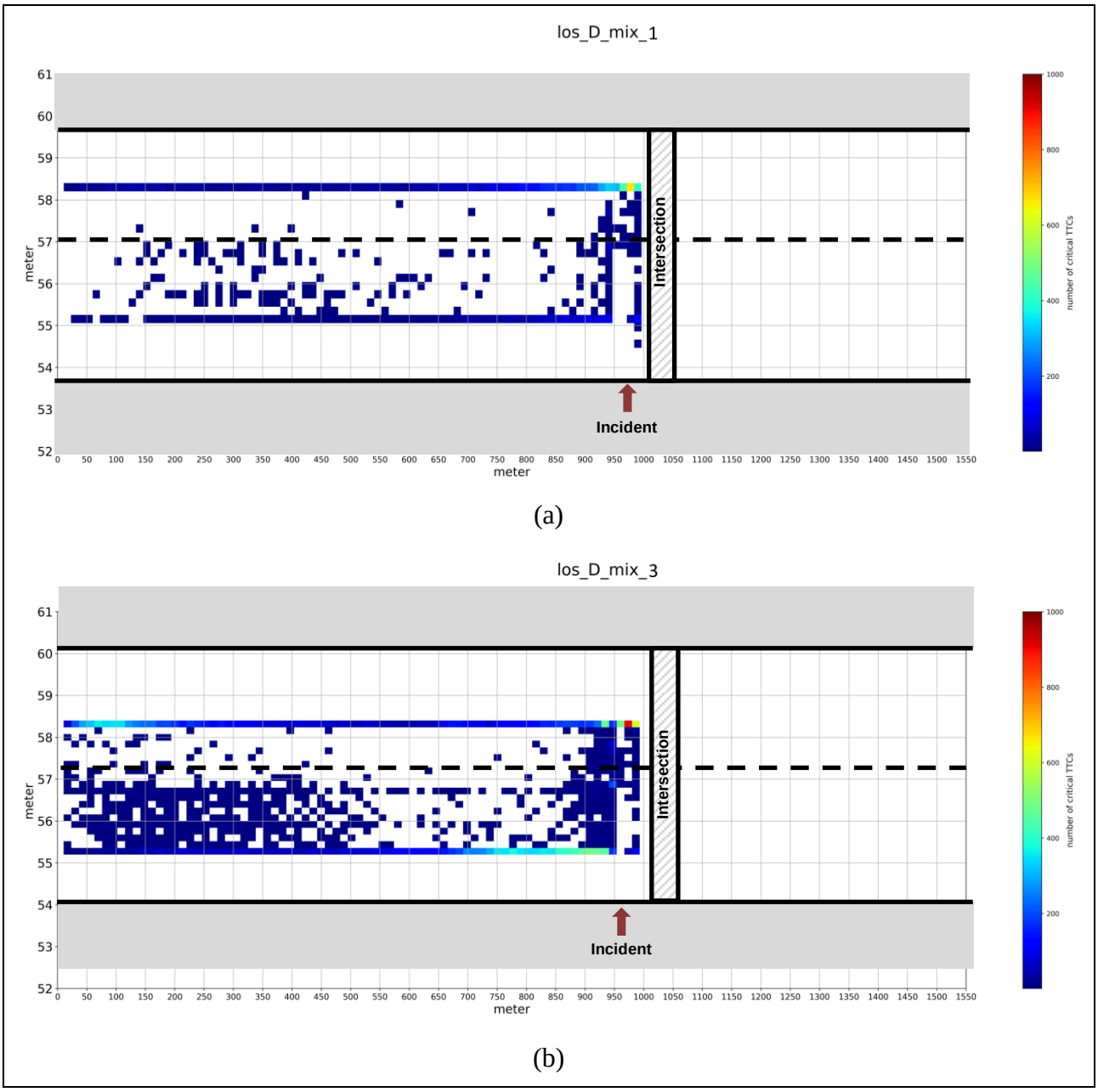

Figure 100. Spatial distribution of critical TTCs (< 3sec) for UC2.3, upper plot (a): LOS D – Traffic Mix 1 (code 0); bottom plot (b): LOS D – Traffic Mix 3 (code 2).

4.2.3.2.4 Environmental Impacts

CO_2 is selected as the indicator for investigating the environmental impacts of mixed traffic and control transitions in the context of scenario 2.3. **Figure 101** shows the average CO_2 emissions per travelled kilometre for the different traffic mixes.

The level of CO_2 remains roughly the same for all mixes at LOS B and LOS C (Mix 1 and Mix 2). For LOS C – Mix 3 and LOS D – Mix 1 the CO_2 levels are a bit higher, while for LOS D – Mix 2 the CO_2 levels are doubled and LOS D – Mix 3 the CO_2 emissions are increasing up to 140%.

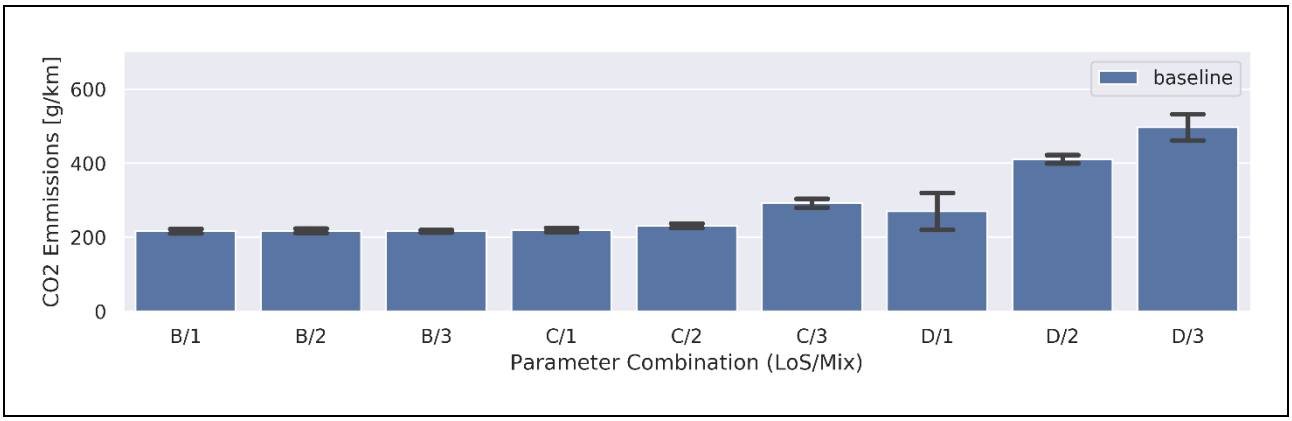

Figure 101. Average CO_2 emissions per kilometres travelled [g/km] for use case 2.3 (varying LOS and traffic mix).

When analysing the simulation results the CO_2 emissions are increasing in the line with the growth of the total travel time (see **Figure 91)**. At LOS D the speeds are much lower as well as the amount of stop and go traffic which results in higher CO_2 emissions. **Figure 102** illustrates this with exemplary speed patterns of LOS B, C and D.

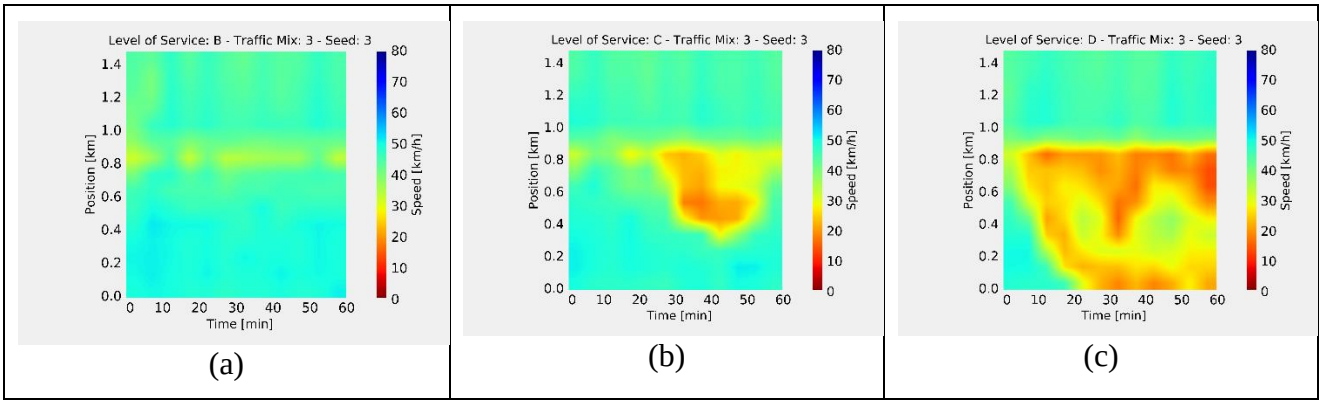

Figure 102. UC 2.3 Measured speed for Los B, C and D mix 3 seed 3

4.2.3.3 Discussion

Analysis of the baseline shows that increased percentage of CAVs increases throughput at LOS B and C but disrupts it at LOS D. Therefore, at lower intensities the traffic flow is better with higher percentages of CAVs but when the traffic density increases to LOS D the impact is reversed.

In this scenario, CVs and CAVs_G1 preform a TOC 350m upstream of the signalized junction based on the reception of DENM messages. CAVs_G2 try to pass the incident in automated mode. At LOS D, the decreasing performance due to a higher percentage of CAVs is due to the initiated TOCs of CAVs_G1 upstream of the incident and CAV_G2s issuing a TOR when a lane change is thwarted by surrounding traffic. CAVs_G1 have to prepare a ToC (preparation phase and driver recovery phase), especially if they are in CACC mode, and need to enlarge car-following headways prior to transition (which requires time and reduces capacity). When CAVs_G2 issue a TOR the driver is already informed about the incident by the DENM message, and thus his initial awareness is higher. Therefore, ToC will be performed more quickly but still affect traffic flow performance.

Traffic management measures should focus on providing a safe situation (reduced speed limit etc.) and provide information to the CAVs so they (for the largest part) can pass the incident zone without disengaging automated mode. In addition, cooperative manoeuvring of surrounding CAVs can support lane change by providing a minimum safe gap needed to perform a lane change.

4.2.4 Scenario 4.2: Safe Spot in Lane of Blockage & Lane Change Assistant

4.2.4.1 Scenario Description

A construction site occupies the left lane of a two-lane road in Scenario 4.2 **(Figure 102)**. In the 1st project iteration it was assumed that 25% of CVs/CAVs will be able to pass along the work zone in automated mode, while the rest 75% will need to issue a TOR upstream of the construction site. The TOR location was fixed both for the urban and the motorway networks (230 m and 250 m upstream of the work zone respectively). Among the CAVs that issued TOR upstream of the work zone, a few implemented MRM on their driving lane. However, given the parametrization of the ToC model in the 1st project iteration with respect to CAVs, the MRM duration was rather short and did not inflict serious disturbance to the traffic flow. Thus, the baseline simulations for Scenario 4.2 were adapted in the context of Deliverable D4.2 (Maerivoet et al., 2019), where a specific CAV (named "MRM_CAV_01") entered the network (both urban and motorway) at time 8.33 min and came to a full stop after MRM on the open lane upstream of the work zone (near the lane drop). The "MRM_CAV_01" remained stopped for 75 s after the MRM, thus blocking traffic upstream of the lane drop. The latter vehicle was guided to the safe spot in the traffic management scenario to prevent the blockage of the open right lane.

In the 2nd project iteration we revise our previous assumptions with respect to the occurrence of ToCs (frequency and location) in the baseline simulation experiments in order to increase the realism of our analysis. Thus, we consider that Day 1 C-ITS applications are existent in the baseline, and that CAVs are also able to dynamically trigger ToCs according to the complexity of the traffic conditions in the proximity of the work zone.

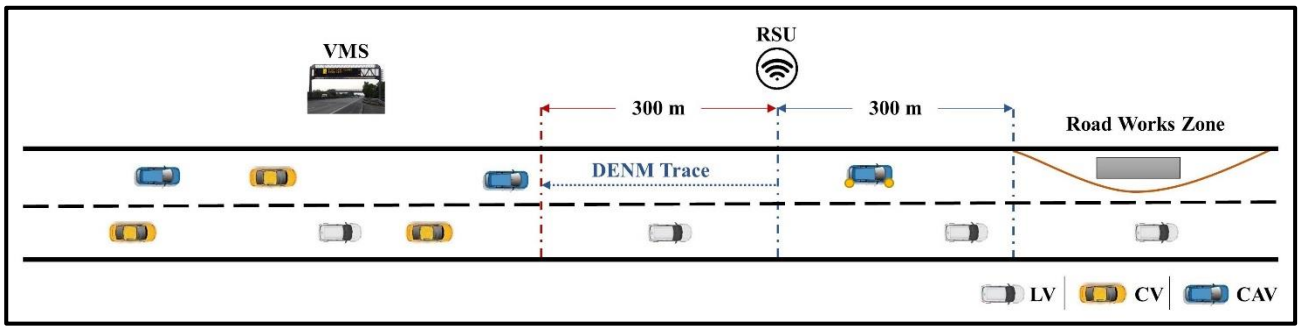

Figure 102. Schematic overview of Scenario 4.2.

The RSI is informed about the construction site and the surrounding environment, and shares the relevant information with the approaching CAVs/CVs. The information is shared via DENM messages that are broadcasted by a single RSU located 300 m upstream of the work zone. Upon DENM reception, warning messages are issued to the CV/CAV drivers to inform about the downstream work zone. Since CVs are equipped with lower automation systems that cannot cope with road works and their drivers are expected to continuously monitor the primary driving tasks we assume that they are manually and instantly taking over vehicle control 600 m upstream of the work zone **(Figure 103,** 600m before the work zone is assumed to be the start of the zone, conveyed in the DENMs traces, where oncoming vehicles identify that the roadworks warning is relevant to their driving direction**)**.

On the other hand, based on findings from the 1st project iteration we know that CAVs will be able to cope with work zones depending on the capabilities of their automation systems. Thus, we assume that 75% of CAVs will have to issue a TOR upon DENM reception (600 m upstream of the construction site), while the remaining 25% of CAVs can pass the work zone in automated mode. The ToC location for the first group of CAVs (CAV_G1) will depend on the driver's response time. If the driver does not respond to the TOR within the available lead time (10 s in this case), a MRM will take place on the CAV's current lane. Thus, TORs regarding CVs and CAVs_G1 are issued further upstream from the work zone compared to the 1st project iteration. Moreover, we assume that the "MRM_CAV_01" belongs to the CAV_G1 group in the 2nd project iteration. Hence, it will issue TOR upon DENM reception and come to a full stop after MRM at the open lane. It is simulated to enter the network at the same time as in the 1st project iteration and stay stopped after MRM the same amount of time.

If any CAV from the second group (CAV_G2 – the one that can cope with road works) is driving on the left closed lane and is unable to merge to the right lane in automated mode due to dense surrounding traffic, then a downward control transition is issued dynamically by the automation **(Figure 103)**. In this case, the driver will either take-over control successfully within the situation-specific available lead time (cf. Section 2.3.2.2), or MRM will be initiated if the driver fails to respond to the TOR. We assume that the lane change intention of CAVs_G2 to shift to the open lane is provoked when the work zone enters their field of view. Hence, the $dynamicToCThreshold$ parameter is adjusted to induce TORs when the first lane change attempt of CAVs_G2 towards the open lane is blocked. Considering that the dynamic TOR location is a function of vehicle speed (see Section 2.3.2.2) and that different vehicles (CAVs_G2) might have different capabilities in terms of field of view, we define separate distributions for urban and motorway conditions with respect to the $dynamicToCThreshold$ parameter **(Table 44)**. Moreover, it has to be noted that the situation awareness of the CAVs_G2 drivers is expected to be increased in the case of dynamical TOC triggering, due to the prior information received via the DENM messages about the work zone (this is reflected in the ToC model parametrization for CAVs_G2 presented in **Table 29**).

Table 44. ToC Model parameter values for dynamical TOR triggering in Scenario 4.2.

Dynamic TOR Parameter	Urban Network	Motorway Network
$dynamicToCThreshold\ (s)$	normal(11, 0.5); [9.0, 13.0]	normal(7.0, 0.5); [6.0, 8.0]

Additionally, CAVs driving in CACC mode upstream of the work zone should deactivate CACC and enlarge their desired headways with their leading vehicles upon DENM reception. CACC deactivation is translated as initiation of the ToC preparation phase for CAVs_G1, and switching to ACC mode for CAVs_G2. Finally, we assume that the presence of Day 1 C-ITS applications does not enhance the lane change capability of CAVs (more conservative compared to manual driving).

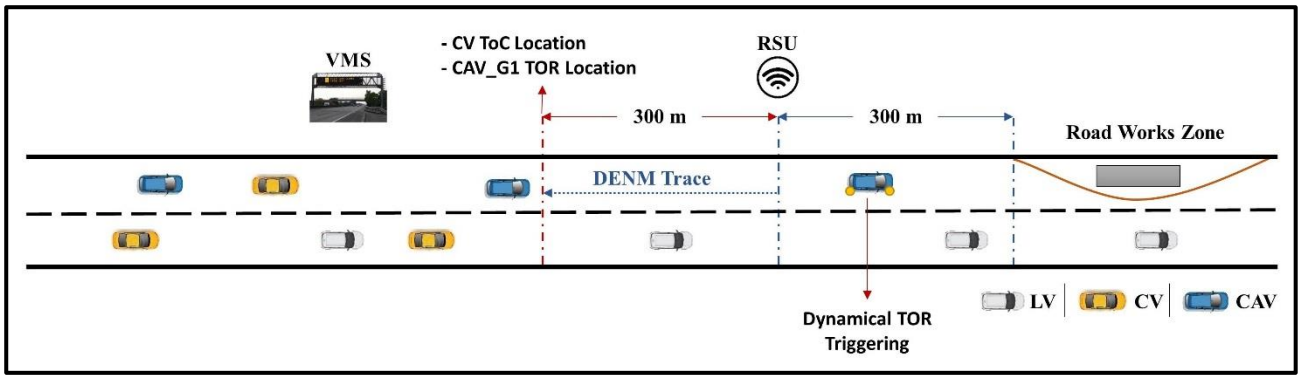

Figure 103. ToC triggering conditions for CVs and CAVs in Scenario 4.2.

More details about the simulation networks of Scenario 4.2 (urban and motorway network) can be found in **Table 45** & **46.**

Table 45. Network configuration details for Scenario 4.2 (urban).

Scenario 4.2_urban	**Settings**	**Notes**
Road section length	3.7 km	• both directions
Road priority	3	
Allowed road speed	13.89 m/s	• 50 km/h
Number of nodes	9	• n0 – n8
Number of edges	16	• both directions
Number of O-D relations	2	• from n0 to n8 • from n8 to n0
Number of lanes	4	• both directions
Work zone location	from n4 to n5	• 250 m
Closed edge[1, 2] (defined in the file: closeLanes.add.xml)	workzone	• the leftmost lane (250 m)
	safetyzone1	• the leftmost lane (50 m)
	Safetyzone2	• the leftmost lane (50 m)
Filenames	• network: UC4_2_urban.net.xml • lane closure: closeLanes.add.xml • traffic signs: shapes.add.xml	
Intended control of lane usage This situation is the same as the situation in motorways, but speeds on urban roads are lower, and thus less space and time are needed to execute the measures of this service.		
Network layout 		
Road segments n0→n1: Insertion and backlog area (300 m) n1→n3: Approaching area (700 m) n3→n4: Safety area (50 m)		

n4→n5: Work zone (250 m) n5→n6: Safety area (50 m) n6→n8: Leaving area (500 m) n8→n0: Opposite direction (1850 m)

Table 46. Network configuration details for Scenario 4.2 (motorway).

UC4.2_motorway	Settings	Notes
Road section length	4.3 km	• both directions
Road priority	3	
Allowed road speed	• 36.11 m/s • 27.78 m/s (700 m in front of the safety zone before entering the work zone area) • 22.22 m/s around the work zone	• 130 km/h • 100 km/h • 80 km/h
Number of nodes	9	• n0 – n8
Number of edges	16	• both directions
Number of O-D relations	2	• from n0 to n8 • from n8 to n0
Number of lanes	4	• both directions
Construction location	from n4 to n5	• 150 m
Closed edge[3,4] (defined in the file: closeLanes.add.xml)	workzone	• the leftmost lane (150 m)
	safetyzone1	• the leftmost lane (100 m)
	safetyzone2	• the leftmost lane (100 m)
Filenames	• network: UC4_2_urban.net.xml • lane closure: closeLanes.add.xml • traffic signs: shapes.add.xml	
Intended control of lane usage A Lane Change Assistant service is providing lane change advice to CAVs upstream of the work zone to facilitate merging in the free right lane. Some CAVs cannot merge on free lane early and are not able to pass the construction site due to the capabilities of their driving automation system. Thus, they perform a ToC. Some of the ToCs are unsuccessful, so the respective CAV must perform an MRM. It uses the safe spot information just in front of the construction site to come to a safe stop.		

Network layout

Road segments
n0→n1: Insertion and backlog area (600 m)
n1→n3: Approaching area (700 m)
n3→n4: Safety area (100 m)
n4→n5: Work zone (150 m)
n5→n6: Safety area (100 m)
n6→n8: Leaving area (500 m)
n8→n0: Opposite direction (2150 m)

4.2.4.2 Results

The proposed scenario is simulated at three different traffic demand levels (LOS B, C and D) with the consideration of three vehicle compositions as mentioned in Section 3.2.3. Furthermore, 10 simulation runs with different random seeds for each combination of LOS and vehicle composition are executed. In the following, the results are analysed and clarified in the aspects of traffic efficiency, traffic dynamics, traffic safety, and environment. Simulation results are presented explicitly for the urban and the motorway networks.

4.2.4.2.1 Urban Network

4.2.4.2.1.1 Impacts on Traffic Efficiency

Network-wide Impacts

The length of the urban network in Scenario 4.2 is 1.85 km (westbound direction) and the speed limit is 50 km/h. Thus, a vehicle travelling with speed limit needs 1.2 min to traverse 1 km. **Figure 104** depicts the average travel time required by a vehicle to travel 1 km for each parameter combination (traffic demand level – traffic mix) examined in the context of Scenario 4.2. Hence, it is visible that for LOS B traffic is free flowing irrespective of the CV/CAV share since travel time per kilometre travelled is marginally higher than 1.2 min. Free-flow traffic conditions are also maintained for LOS C since travel time per kilometre travelled slightly increases to 1.3 min for the three examined traffic mixes. A further increase to 1.5 min is observed for LOS D and traffic mixes 1 and 2. However, when the share of CVs/CAVs rises to 70% in the total vehicle fleet (traffic mix 3) travel time per kilometre travelled increases to 1.7 min. This is a 30% increase in contrast to free flow traffic conditions which indicates that traffic operations become less smooth. Moreover, we observe that the standard deviation for parameter combination LOS D – Traffic Mix 3 is significantly higher compared to the other parameter combinations. Hence, depending on stochastic factors of the simulations traffic congestion can set in for the latter parameter combination.

Considering, that the majority of CVs/CAVs arrive at the work zone in manual mode due to the deployment of Day 1 C-ITS applications, it is evident that dynamical TOR triggering and the presence of CAVs_G2 (in automated mode) around the work zone (which are more conservative in terms of car-following and lane changing compared to manually driven vehicles), adversely impact traffic operations only for the highest demand level and share of CAVs. Finally, it is noted that according to the network-wide traffic efficiency results, the negative impacts of the

"MRM_CAV_01" (being stopped after MRM) materialize only for the highest traffic demand level. When the arrival rate of vehicles is lower (LOS B and C), the queue formed behind the "MRM_CAV_01" dissolves faster thus not generating a traffic breakdown.

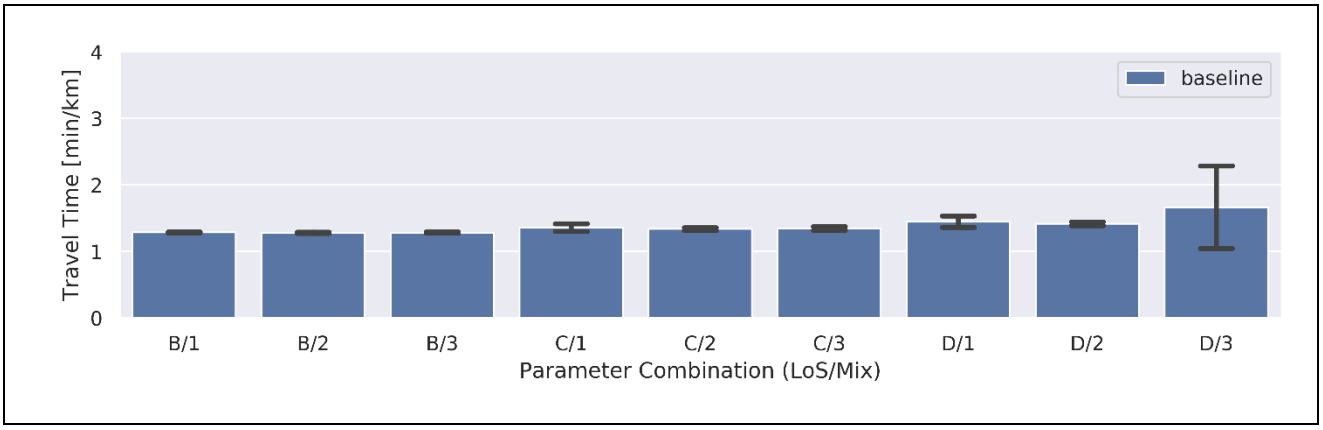

Figure 104. Travel time (min/km) for use case 4.2 (urban) simulation experiments (varying LOS and traffic mix).

Local Impacts

Following the aforementioned network-wide statistics regarding traffic efficiency we also present the corresponding local impacts for traffic mix 3 and traffic demand levels LOS B – D in terms of speed and flow tempo-spatial plots. The latter traffic mix has been selected since it encompasses the highest share of CVs/CAVs (and inherently CAVs_G2). Thus, we can examine the most detrimental impacts of: a) ToCs upon DENM reception at location 0.4 km, and b) dynamical TOR triggering upstream of the work zone at location 1.0 km (work zone ends at location 1.4 km).

Figure 105 shows the tempo-spatial plots for measured speeds and flows at LOS B with 70% share of CVs and CAVs. Indeed free flow traffic conditions prevail on the network as indicated by the network-wide results. An insignificant traffic disruption occurs at the lane drop location (entry to the work zone) due to merging operations which does not propagate upstream though. Due to lower demand and decreased density in the proximity of the work zone entry point, dynamical TOR triggering is less frequent and does not degrade traffic flow performance.

Figure 106 shows the tempo-spatial plots for measured speeds and flows at LOS C with 70% share of CVs and CAVs. In this case, traffic operations are more disrupted in the proximity of the work zone, but speed does not drop below 40 km/h. Thus, traffic conditions can be still considered as free flowing. However, due to increased demand and increased frequency of dynamical TOR triggering, merging at the lane drop becomes more turbulent. Given that CAVs_G2 are more conservative in terms of lane changing compared to manually driven vehicles, the increased rate of dynamical TORs is normal while demand increases (lesser opportunities for unobstructed merging on the open right lane).

Figure 107 shows the tempo-spatial plots for measured speeds and flows at LOS D with 70% share of CVs and CAVs. Seed 9 represents the worst case with respect to reduced traffic flow performance and is presented for two reasons. Firstly, to indicate that traffic breakdown can occur at the lane drop for the highest demand level and share of CVs/CAVs (inherently CAVs_G2 also). The breakdown is an outcome of both increased demand and rate of dynamical TORs. Secondly, to

demonstrate that the ToC preparation phase can also generate independent traffic disruption (see location 0.4 km) when ToCs are initiated at the same location and traffic is dense.

Finally, we can observe in **Figure 107** that the "MRM_CAV_01" also plays a significant role in the creation of the traffic breakdown in LOS D, since abrupt speed drop occurs after 10 min (time when "MRM_CAV_01" stops after MRM) which propagates upstream and is maintained until the end of the simulation due to increased traffic demand. Similar disturbances in time and space can be also observed for LOS B **(Figure 105)** and LOS C **(Figure 106)**, but dissolve smoothly due to the decreased vehicle arrival rate in the latter traffic demand levels as mentioned previously in the analysis of the network-wide results.

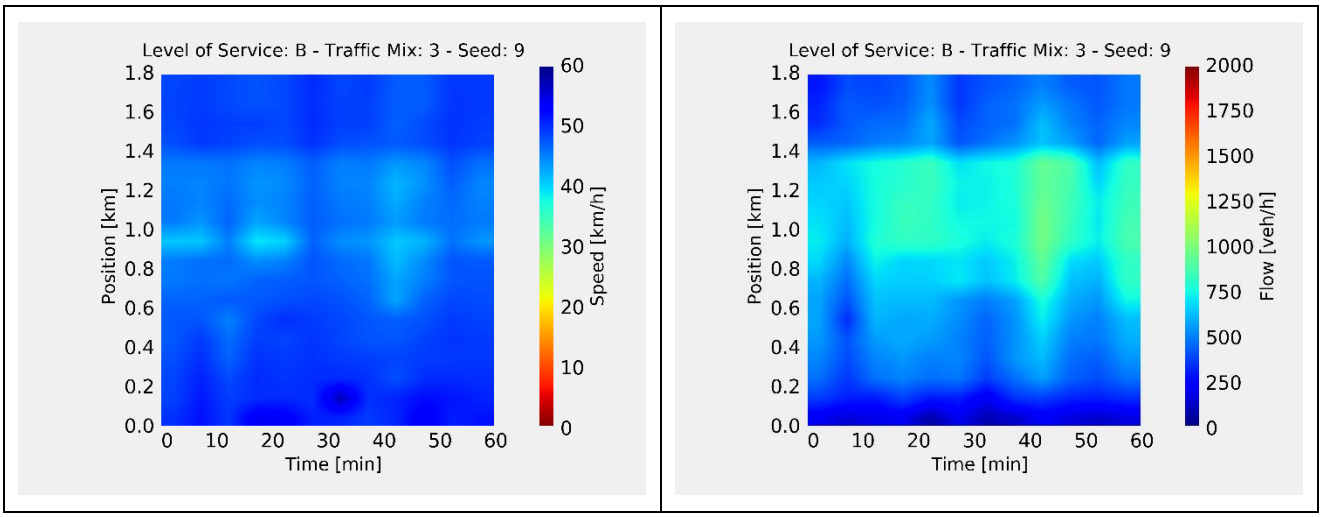

Figure 105. Exemplary time-space-diagrams for measured speed (left column) and flow (right column) for use case 4.2 (urban) simulation experiments (LOS B – Traffic Mix 3 – Seed 9).

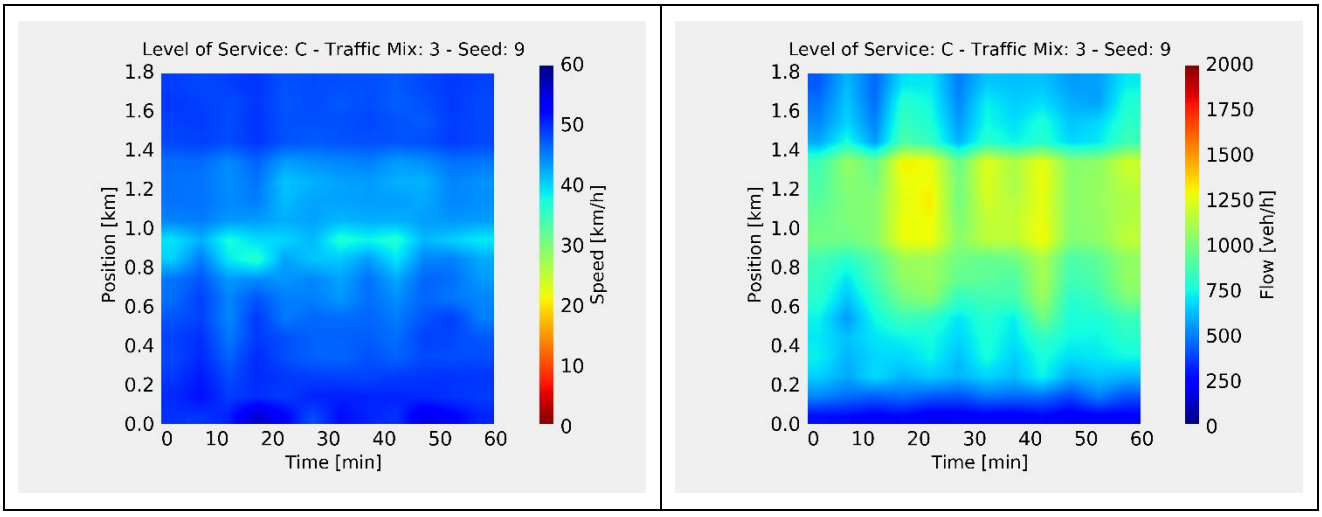

Figure 106. Exemplary time-space-diagrams for measured speed (left column) and flow (right column) for use case 4.2(urban) simulation experiments (LOS C – Traffic Mix 3 – Seed 9).

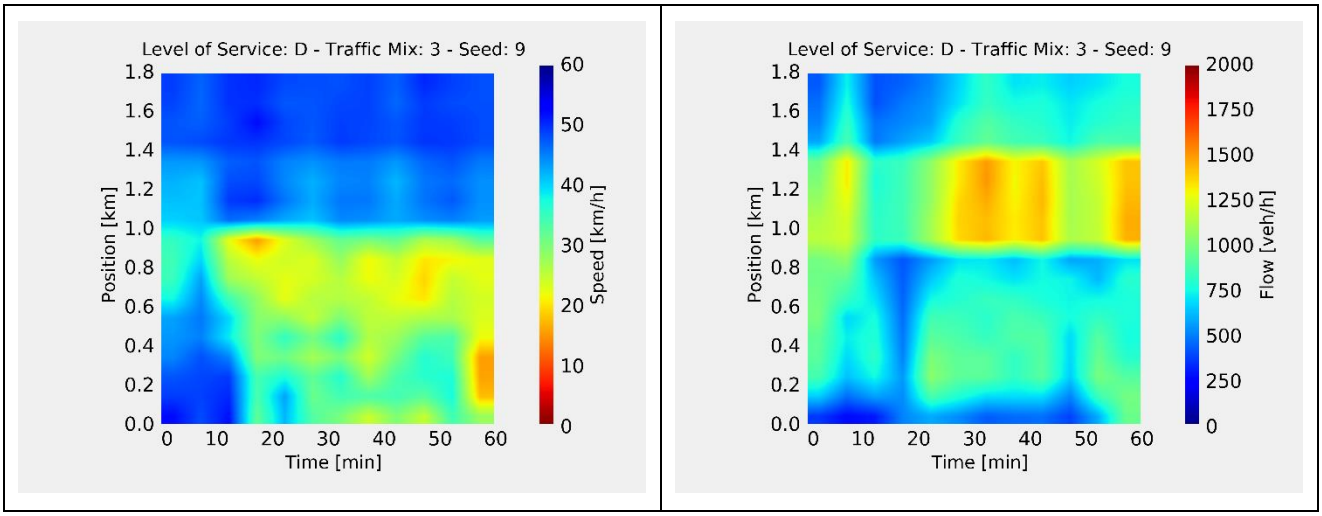

Figure 107. Exemplary time-space-diagrams for measured speed (left column) and flow (right column) for use case 4.2 (urban) simulation experiments (LOS D – Traffic Mix 3 – Seed 9).

4.2.4.2.1.2 Impacts on Traffic Dynamics

The average throughput is used as KPI to elaborate on traffic dynamics hereafter. **Figure 108** shows the number of vehicles that were serviced (exited the network) within an hour of simulation per parameter combination. Considering that traffic demand input was 825 veh/h for LOS B, 1155 veh/h for LOS C, and 1386 veh/h for LOS D, it is clear that input traffic can be serviced on average for every parameter combination. However, we can also observe a marginal decrease of throughput when CV/CAV share increases that persists for each examined traffic demand level. The latter decrease can be ascribed to the conservativeness of CAV lane changing and the ToC operations (i.e. ToC preparation phase, dynamical TOR triggering near the work zone) which generate traffic flow disturbances as explained in the analysis of the traffic efficiency above.

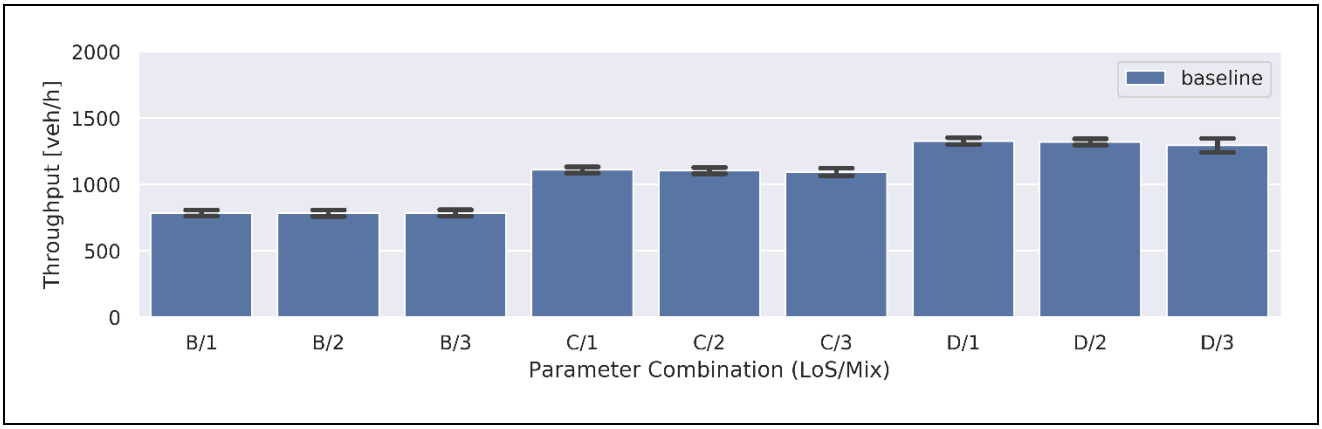

Figure 108. Throughput (veh/h) for use case 4.2 (urban) simulation experiments (varying LOS and traffic mix).

Lane changing is also investigated as a factor significantly affecting traffic dynamics. The number of lane changes per kilometre travelled is used as KPI in this case. According to **Figure 109**, approximately one lane change is performed per 2 kilometres. Considering that the urban network stretches to 1.8 km and that one lane change is required for a vehicle inserted on the blocked lane to reach its destination (by passing the work zone) the reported numbers are reasonable. Moreover,

Figure 109 indicates that lane changing is slightly reduced for higher shares of CVs/CAVs. The latter result is expected since conservative CAV lane changing creates more turbulence around the lane drop area and thus there is less space for tactical lane changing. Likewise, higher traffic demand (LOS D) yields denser traffic conditions in the proximity of the work zone which results in less space for tactical lane changing and thus reduced lane change intensity.

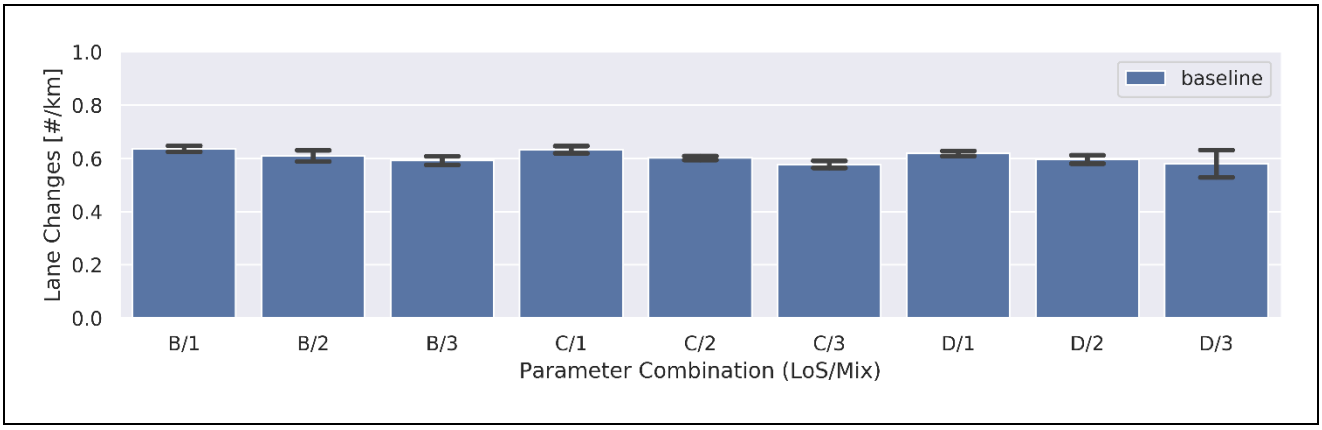

Figure 109. Number of lane changes per kilometre (#/km) for use case 4.2 (urban) simulation experiments (varying LOS and traffic mix).

4.2.4.2.1.3 Impacts on Traffic Safety

In the 2nd iteration we analyse traffic safety both network-wide and locally. On the network-wide scale we use the same KPI as in the 1st iteration (i.e. the number of critical TTC events less than 3 sec). Locally we evaluate aggregated TTC distributions upstream of the work zone.

Network-wide Impacts

Figure 110 illustrates the average number and standard deviation of safety critical events for every examined parameter combination of traffic state and vehicle composition. We can observe that the average number of safety critical events approximately ranges between 30 and 350. Moreover, it is shown that for every traffic demand level the average number of safety critical events increases with increased share of CVs and CAVs. The latter finding coincides with observations made based on simulation results of the 1st project iteration. Conservativeness of CV/CAV lane change behaviour (compared to manual driving) and ToC/MRM operations induce higher numbers of safety critical events.

Figure 110 also indicates that increasing traffic demand leads to increased occurrence of safety critical events. As explained in the analysis of the traffic efficiency results, traffic is free flowing for parameter combinations LOS B/Mix 1 – LOS D/Mix 2. However, as demand increases (from LOS B to LOS D) traffic becomes denser and the vehicle interactions in the mixed traffic stream are rendered more complex. Thus, denser traffic generates higher collision risk when traffic flow remains in the uncongested regime and there is space available for vehicle interactions. On the contrary, this is not the case for parameter combination LOS D/Mix 3 when traffic conditions can get congested for specific simulation seeds. Hence, we observe the high standard deviation of safety critical events which indicates that in the case of congestion there is limited space for vehicle interactions and consequently safety critical events can be significantly lower.

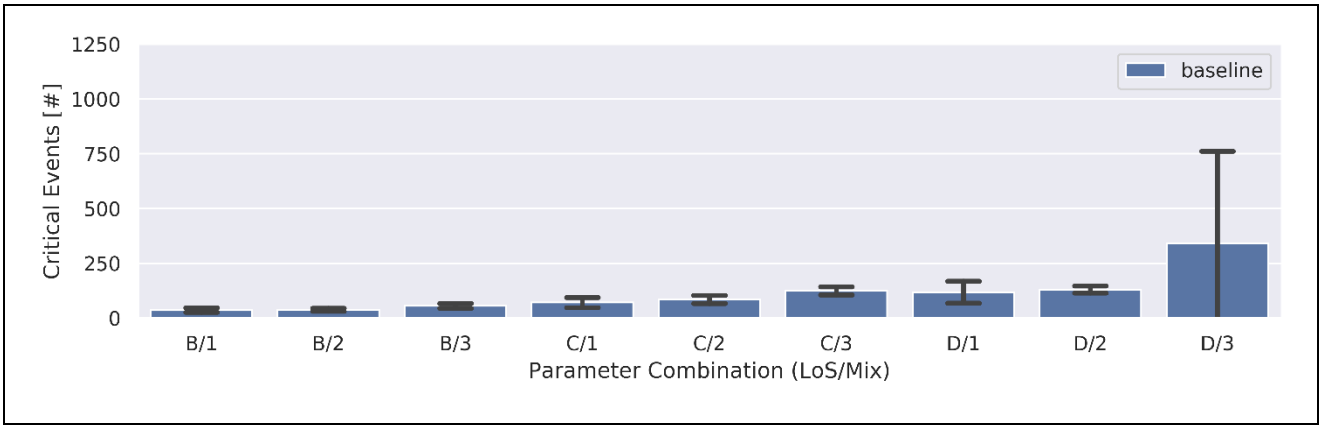

Figure 110. Average number of events with TTCs below 3.0 seconds for use case 4.2 (urban) simulation experiments (varying LOS and traffic mix).

Local Impacts

When looking at the spatial distribution of safety critical events, local impacts can be further identified. Three examples are shown in **Figure 111** where each plot features the aggregated number of critical TTCs of 10 seeds (per LOS/mix) marked as bins along the urban network. Each plotted bin means that at least one TTC occurred at this position. The colour of a bin then indicates the amount of TTCs at this marked position. So, when e.g. several TTCs concentrate within a certain area, the colours translate as a spatial density for interpretation of the TTC distribution.

The focus of the analysis on the local scale is placed explicitly on traffic state LOS D where most of the safety critical events were observed in the bar plots of the network-wide analysis. **Figure 111** indicates that there are two main areas where safety critical events are generated: a) in front of the work zone (location = 1.0 km), and b) downstream of the DENM reception point (location = 0.4 – 0.55 km). Safety critical events on the right lane upstream of the work zone (lane centre at y = 55.3) occur due to braking episodes which take place to facilitate merging of stopped vehicles (located on the left lane in front of the work zone) onto the open lane. On the other hand, safety critical events on the left lane (lane center at y = 58.3) occur due to hard braking events from vehicles which cannot freely merge onto the right open lane.

Safety critical events taking place downstream of the DENM reception point are induced due to the following two reasons. Firstly because of ToCs/MRMs occurring in the latter area, and secondly due to the "MRM_CAV_01" which also stops for a few seconds within this area. Moreover, we can observe that several safety critical events occur due to lane change activity. This phenomenon can be ascribed to lane change activity of CVs/CAVs trying to move to the open lane upon DENM reception, as well as lane change activity to overpass the stopped "MRM_CAV_01" (location = 0.4 – 0.55 km). Finally, it is shown that increased CV/CAV share (higher ToC/MRM rate – conservative lane changing) generates higher frequency of safety critical events (colour spectrum shifts from blue to red) around the aforementioned areas of interest where safety issues are identified.

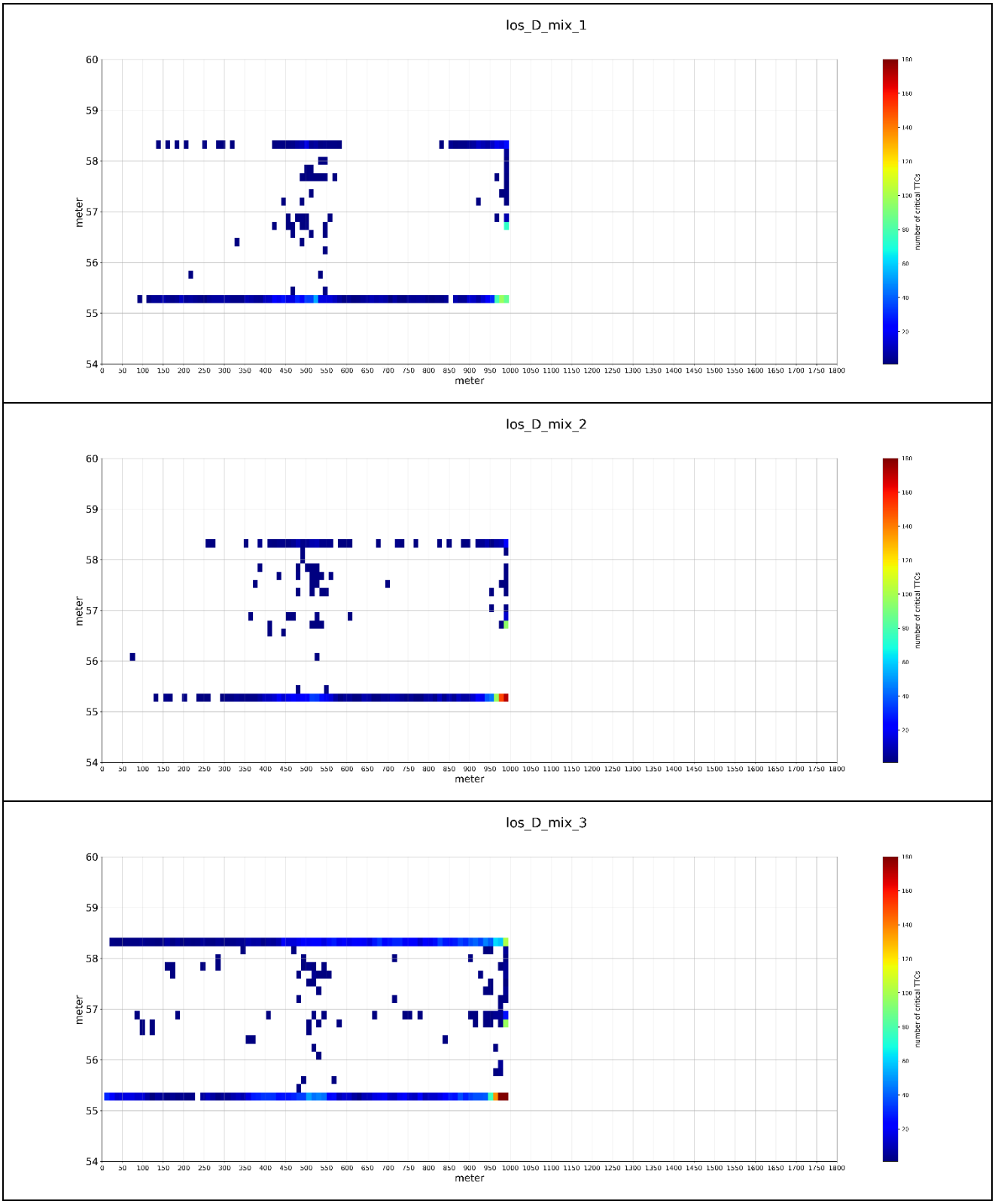

Figure 111. Spatial distribution of critical TTCs (< 3sec) for use case 4.2 (urban) for three different runs (upper plot (a): LOS D – Traffic Mix 1; middle plot (b): LOS D – Traffic Mix 2; bottom plot (c): LOS D – Traffic Mix 3). Colours indicate the number of critical TTCs shown with discrete plotted bins (bin size ≈ 20m x 0,3m).

4.2.4.2.1.4 Environmental Impacts

The environmental impacts of system-initiated control transitions in the context of Scenario 4.2 are assessed in terms of CO_2 emissions per kilometre travelled. **Figure 112** depicts the average CO_2 emissions per travelled kilometre for the examined parameter combinations. In general, the trends observed for emissions match those for travel times. CO_2 emissions gradually increase from 150 g/km (LOS B – Traffic Mix 1) to 180 g/km (LOS D – Traffic Mix 2) following the increase in traffic disruption (longer travel times) due to higher demand and CAV share. Maximum CO_2 emission rate is observed for parameter combination LOS D – Traffic Mix 3, when ToC operations and especially the behaviour of the "MRM_CAV_01" induce excessive traffic congestion for specific simulation seeds. Thus, the standard deviation for CO_2 emissions is also significantly higher for this parameter combination.

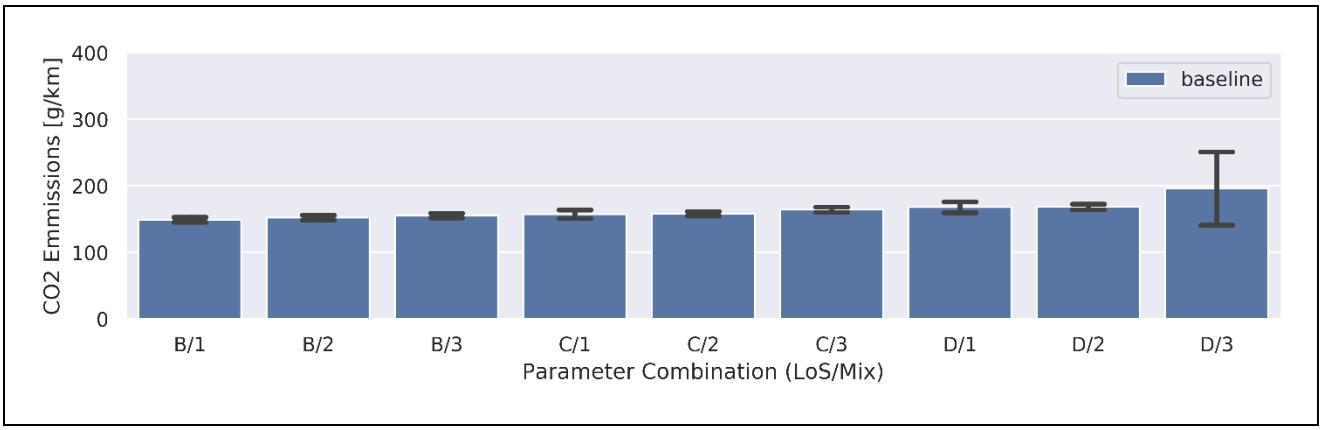

Figure 112. Average CO_2 emissions per kilometres travelled [g/km] for use case 4.2 (urban) simulation experiments (varying LOS and traffic mix).

4.2.4.2.2 Motorway Network

4.2.4.2.2.1 Impacts on Traffic Efficiency

Network-wide Impacts

The length of the motorway network in Scenario 4.2 is 2.15 km (westbound direction) and the average speed limit is 103.25 km/h (the speed limit gradually drops from the insertion edge towards the work zone for safety reasons). Thus, a vehicle travelling with speed limit needs approximately 0.58 min to traverse 1 km. **Figure 113** depicts the average travel time required by a vehicle to travel 1 km for each parameter combination (traffic demand level – traffic mix) examined in the context of Scenario 4.2. Hence, it is visible that for LOS B traffic is free flowing irrespective of the CV/CAV share since travel time per kilometre travelled is marginally higher than 0.58 min. However, free-flow traffic conditions are not maintained for LOS C. On the contrary, in the latter traffic state travel time per kilometre travelled ranges between 2.3 – 3 min for the three examined parameter combinations. A further increase is observed for the three traffic mixes in traffic state LOS D. Thus, we can infer that traffic conditions for LOS C and D are congested.

The prevalence of congestion in LOS C and D follows from increased demand (compared to the urban case) and more complex vehicle interactions due to higher driving speeds on the motorway network. Particularly, ToC/MRM operations can induce sharper braking events for following vehicles with higher travelling speeds. Moreover higher speeds mean longer safe gaps for lane

changing. Hence, merging operations in the proximity of the lane drop location (work zone) are adversely affected considering the increased conservativeness of CAVs in lane changing. Notably, travel time per kilometre travelled is more increased when the share of CAVs in the vehicle mix is higher. Finally, another contributing factor in the onset of congestion for LOS C and D is the behaviour of the "MRM_CAV_01" which stops after implementing MRM upstream of the work zone.

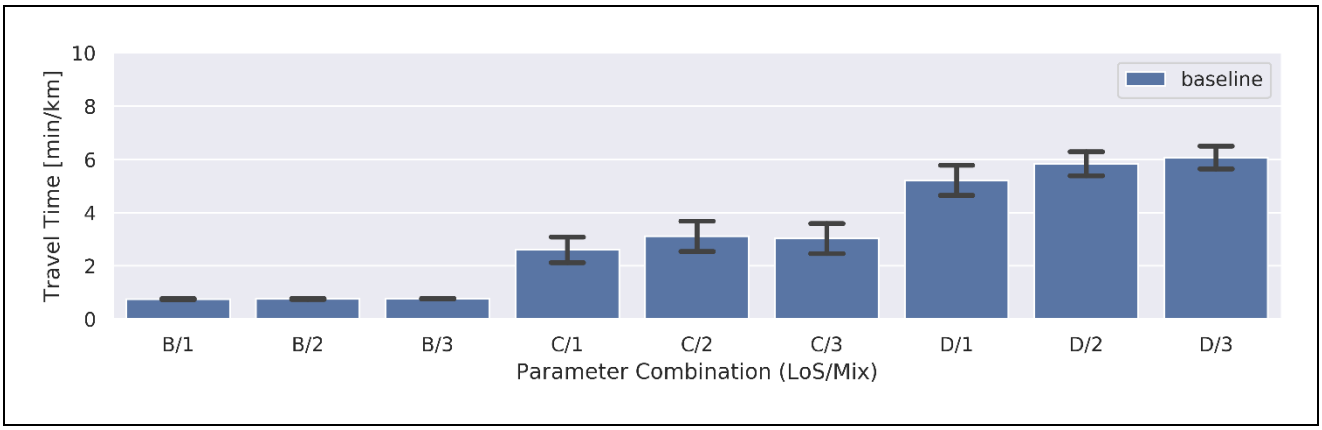

Figure 113. Travel time (min/km) for use case 4.2 (motorway) simulation experiments (varying LOS and traffic mix).

Local Impacts

Following the aforementioned network-wide statistics regarding traffic efficiency we also present the corresponding local impacts for traffic mix 1 and traffic demand levels LOS B – D in terms of speed and flow tempo-spatial plots. The latter traffic mix has been selected to demonstrate the detrimental impacts of: a) ToCs upon DENM reception at location 0.4 km, b) dynamical TOR triggering upstream of the work zone at location 1.0 km (work zone ends at location 1.4 km), and c) conservative CAV lane change behaviour, for a low share of CVs/CAVs (and inherently CAVs_G2) in the fleet mix.

Figure 114 shows the tempo-spatial plots for measured speeds and flows at LOS B with 23% share of CVs and CAVs. Indeed free flow traffic conditions prevail on the network as indicated by the network-wide results. Traffic disruption occurs at the lane drop location (entry to the work zone) due to inefficient merging operations, which can be ascribed to conservative CAV lane changing and dynamical TOR triggering, but does not propagate upstream though. However, we can observe that several traffic disruptions of approximately the same magnitude occur at different time points throughout the simulation timeline.

Figure 115 shows the tempo-spatial plots for measured speeds and flows at LOS C with 23% share of CVs and CAVs. In this case, traffic breaks down at the lane drop location (entry to the work zone) and congestion steeply propagates to the motorway network entry within 20 min. Due to increased demand (compared to the urban case), merging at the lane drop becomes more problematic (since the rate of dynamical TORs is higher and CAV are more conservative compared to manually driven vehicles in terms of lane changing), and the formed queue cannot dissipate. However, it can be also noted that a second significant speed drop can be observed within location 0.4 – 0.5 km, which also propagates upstream until the network entry. This phenomenon occurs as a result of ToC/MRMs which are performed by CAVs_G1 as the aftermath of the DENM message

reception. Moreover, the behaviour of the "MRM_CAV_01" which stops after MRM at location 0.7 km and around time 8 min expedites the queue propagation to the motorway entry area.

Figure 116 shows the tempo-spatial plots for measured speeds and flows at LOS D with 70% share of CVs and CAVs. Similar phenomena and traffic operations with LOS C can be observed for this traffic state, but intensified due to increased demand. In general, traffic breakdown mainly occurs at the work zone entry due to increased demand (compared to the urban case), dynamical TOR triggering and conservative CAV lane changing. Additionally, speed tempo-spatial contour plots indicate that ToC/MRM operations upon DENM reception and the behaviour of the "MRM_CAV_01" can further deteriorate traffic flow performance during congestion.

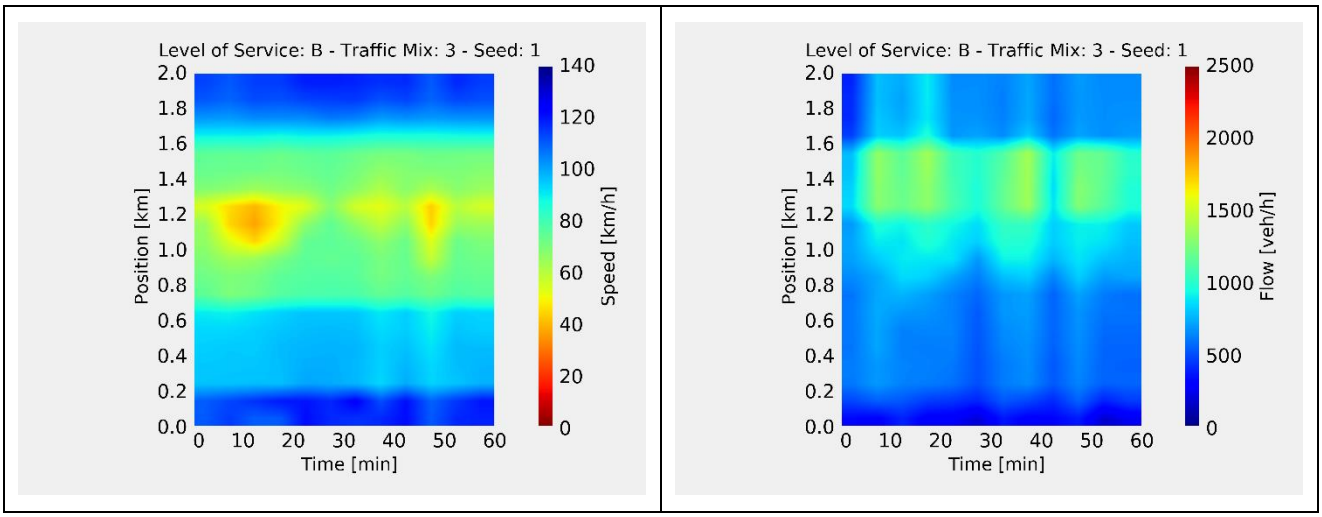

Figure 114. Exemplary time-space-diagrams for measured speed (left column) and flow (right column) for use case 4.2 (urban) simulation experiments (LOS B – Traffic Mix 3 – Seed 9).

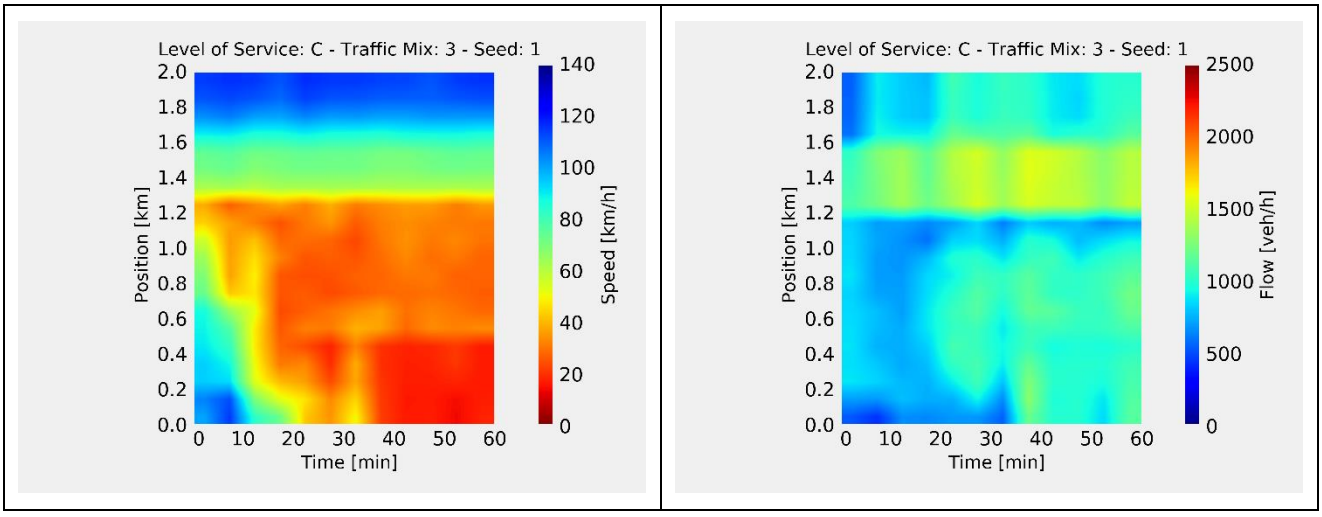

Figure 115. Exemplary time-space-diagrams for measured speed (left column) and flow (right column) for use case 4.2(urban) simulation experiments (LOS C – Traffic Mix 3 – Seed 9).

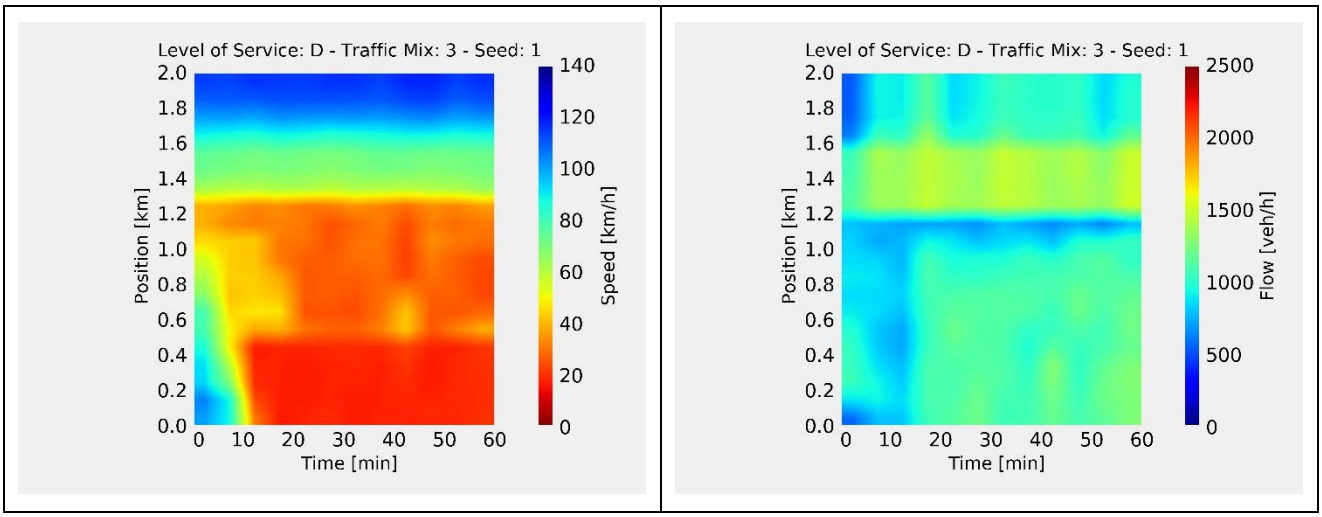

Figure 116. Exemplary time-space-diagrams for measured speed (left column) and flow (right column) for use case 4.2 (urban) simulation experiments (LOS D – Traffic Mix 3 – Seed 9).

4.2.4.2.2.2 Impacts on Traffic Dynamics

The average throughput is used as KPI to elaborate on traffic dynamics hereafter. **Figure 117** shows the number of vehicles that were serviced (exited the network) within an hour of simulation per parameter combination. Considering that traffic demand input was 1155 veh/h for LOS B, 1617 veh/h for LOS C, and 1940 veh/h for LOS D, it is clear that input traffic can only be serviced on average for traffic state LOS B. Due to congestion, lesser vehicles can exit the motorway network within a simulated hour compared to input flow rates for traffic states LOS C and D. Interestingly, average throughput is similar between LOS C and D for the same traffic mixes. Thus, it can be deduced that the network has already reached capacity in traffic state C.

Moreover, we can also observe a marginal decrease of throughput when CV/CAV share increases that persists for each examined traffic demand level. The latter decrease can be ascribed to the conservativeness of CAV lane changing and the ToC operations (i.e. ToC preparation phase, dynamical TOR triggering near the work zone) which generate traffic flow disturbances as explained in the analysis of the traffic efficiency results above.

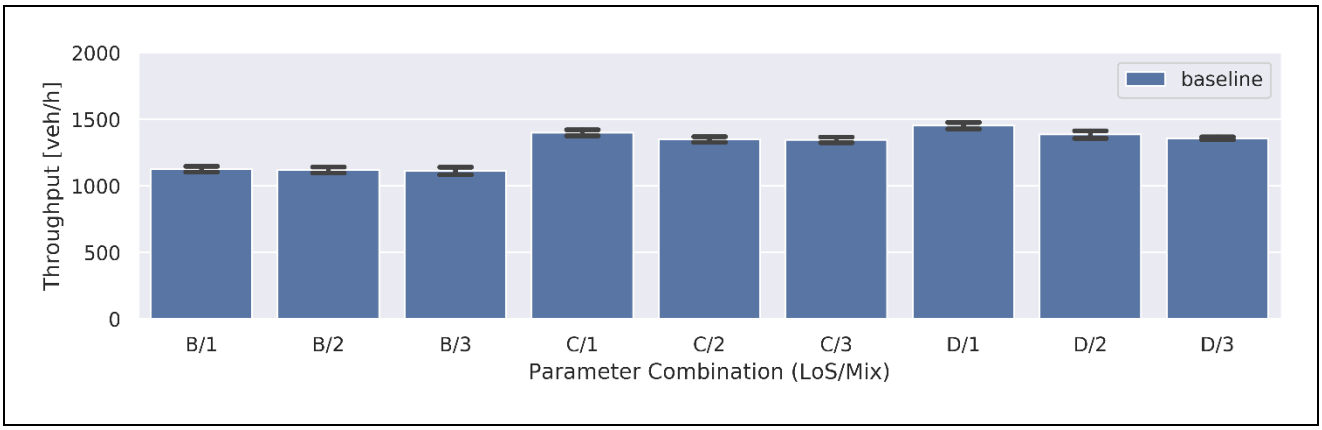

Figure 117. Throughput (veh/h) for use case 4.2 (motorway) simulation experiments (varying LOS and traffic mix).

Lane changing is also investigated as a factor significantly affecting traffic dynamics. The number of lane changes per kilometre travelled is used as KPI in this case. According to **Figure 118**, approximately one lane change is performed per 2.5 kilometres for traffic state LOS B. Considering that the motorway network stretches to 2.15 km and that one lane change is required for a vehicle inserted on the blocked lane to reach its destination (by passing the work zone) the reported numbers are reasonable for uncongested conditions.

In contrast, lane change intensity is significantly increased during congested traffic conditions (LOS C and D). However, when congestion is higher (LOS D) and the available space for lane change manoeuvers further decreases we can also observe a decrease in lane change intensity. Finally, an interesting finding is that lane changes per kilometre travelled increase for higher shares of CVs/CAVs and congested traffic conditions. The latter trend is opposite to the one regarding uncongested conditions (LOS B) where conservative CAV lane change behaviour results in reduced tactical lane changing. Nonetheless, a more comprehensive analysis that encompasses spatial distribution of lane changes, distribution of lane changes per lane change intention and per lane change direction (left or right lane changes) is required to explain the observed trends during congested conditions. This type of analysis will be conducted in the context of traffic management simulation experiments.

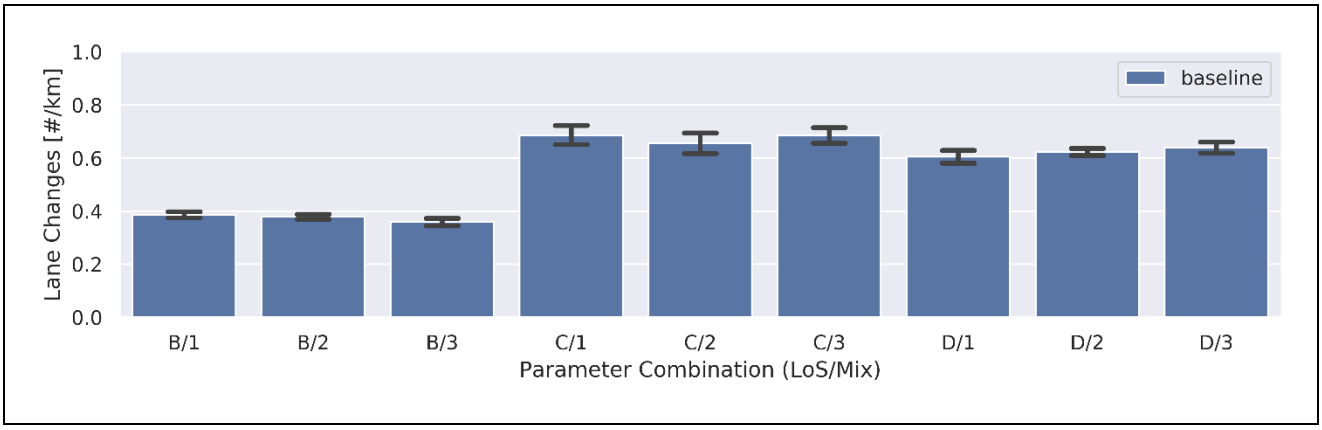

Figure 118. Number of lane changes per kilometre (#/km) for use case 4.2 (motorway) simulation experiments (varying LOS and traffic mix).

4.2.4.2.2.3 Impacts on Traffic Safety

Network-wide Impacts

Figure 119 illustrates the average number and standard deviation of safety critical events for every examined parameter combination of traffic state and vehicle composition. We can observe that the average number of safety critical events approximately ranges between 50 and 150 for uncongested conditions (LOS B). This finding complies with similar observations made with respect to the urban case where mostly free flowing conditions prevail for the examined traffic demand levels. However, it is also shown that safety critical events increase excessively (more than one critical event per simulated vehicle) during uncongested conditions (traffic states LOS C and D). The latter result is rather contradictory considering that there is limited space for high-speed and complex vehicle interactions during congestion. Thus, unless the spatial and temporal distribution of safety critical events is analysed it is difficult to conclude on the assessment of traffic safety in the context of Scenario 4.2 (motorway network).

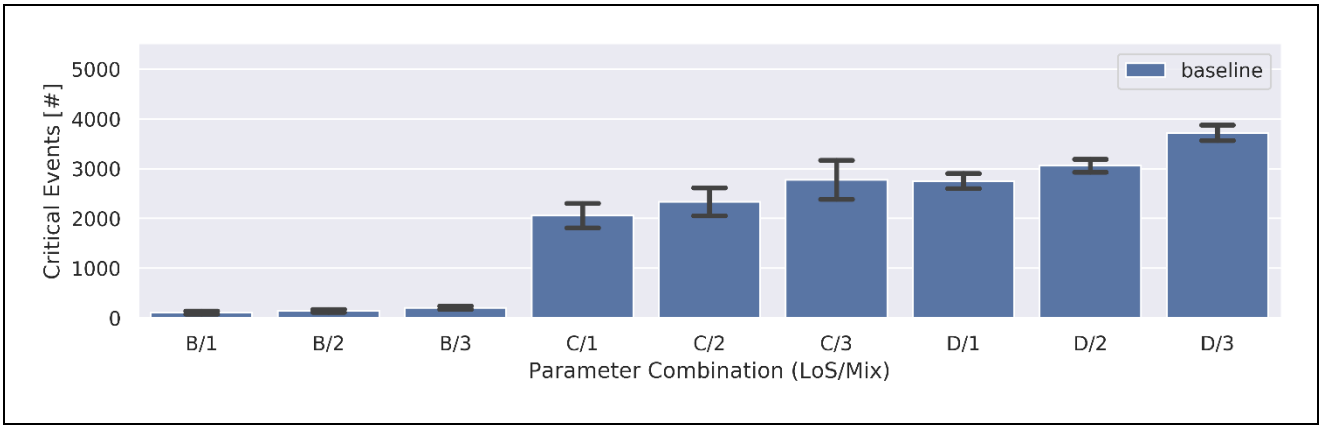

Figure 119. Average number of events with TTCs below 3.0 seconds for use case 4.2 (motorway) simulation experiments (varying LOS and traffic mix).

Local Impacts

When looking at the spatial distribution of safety critical events, local impacts can be further identified. Three examples are shown in **Figure 120** where each plot features the aggregated number of critical TTCs of 10 seeds (per LOS/mix) marked as bins along the urban network. Each plotted bin means that at least one TTC occurred at this position. The colour of a bin then indicates the amount of TTCs at this marked position. So, when e.g. several TTCs concentrate within a certain area, the colours translate as a spatial density for interpretation of the TTC distribution.

Figure 120 indicates that there are two main areas where safety critical events are generated: a) in front of the work zone (location = 1.2 km) b) downstream of the DENM reception point (location = 0.5 – 0.7 km). Safety critical events on the right lane upstream of the work zone (lane center at y = 55.3) occur due to braking episodes which take place to facilitate merging of stopped vehicles onto the open lane. On the other hand, safety critical events on the left lane (lane center at y = 58.3) occur due to hard braking events from vehicles which cannot freely merge onto the right open lane. However, since demand is increased in traffic states LOS C and D we can observe that in congested traffic conditions the number of safety critical events due to car-following reasons is significantly higher on the left lane compared to the right one.

Safety critical events taking place downstream of the DENM reception point are induced due to the following two reasons. Firstly because of ToCs/MRMs occurring in the latter area, and secondly due to the "MRM_CAV_01" which also stops (after implementing MRM) for a few seconds within this area. Moreover, we can observe that several safety critical events occur due to lane change activity. This phenomenon can be ascribed to lane change activity of CVs/CAVs trying to move to the open lane upon DENM reception, as well as lane change activity to overpass the stopped "MRM_CAV_01". **Figure 120** also shows that increased CV/CAV share (higher ToC/MRM rate – conservative lane changing) generates higher frequency of safety critical events (colour spectrum shifts from blue to red) around the aforementioned areas of interest where safety issues are identified.

Nonetheless, to justify the excessive number of safety critical events it is important to understand if the latter are induced prior to the onset of congestion or afterwards when congestion has reached the motorway network entry point (temporal distribution of safety critical events). Finally, the distribution of critical events per reason (car-following or lane change activity) needs to be defined, as well as the vehicle types that are involved in potential conflicts (share of critical events between

similar of different vehicle types). The aforementioned analysis will be conducted in the context of the traffic management simulations (WP4).

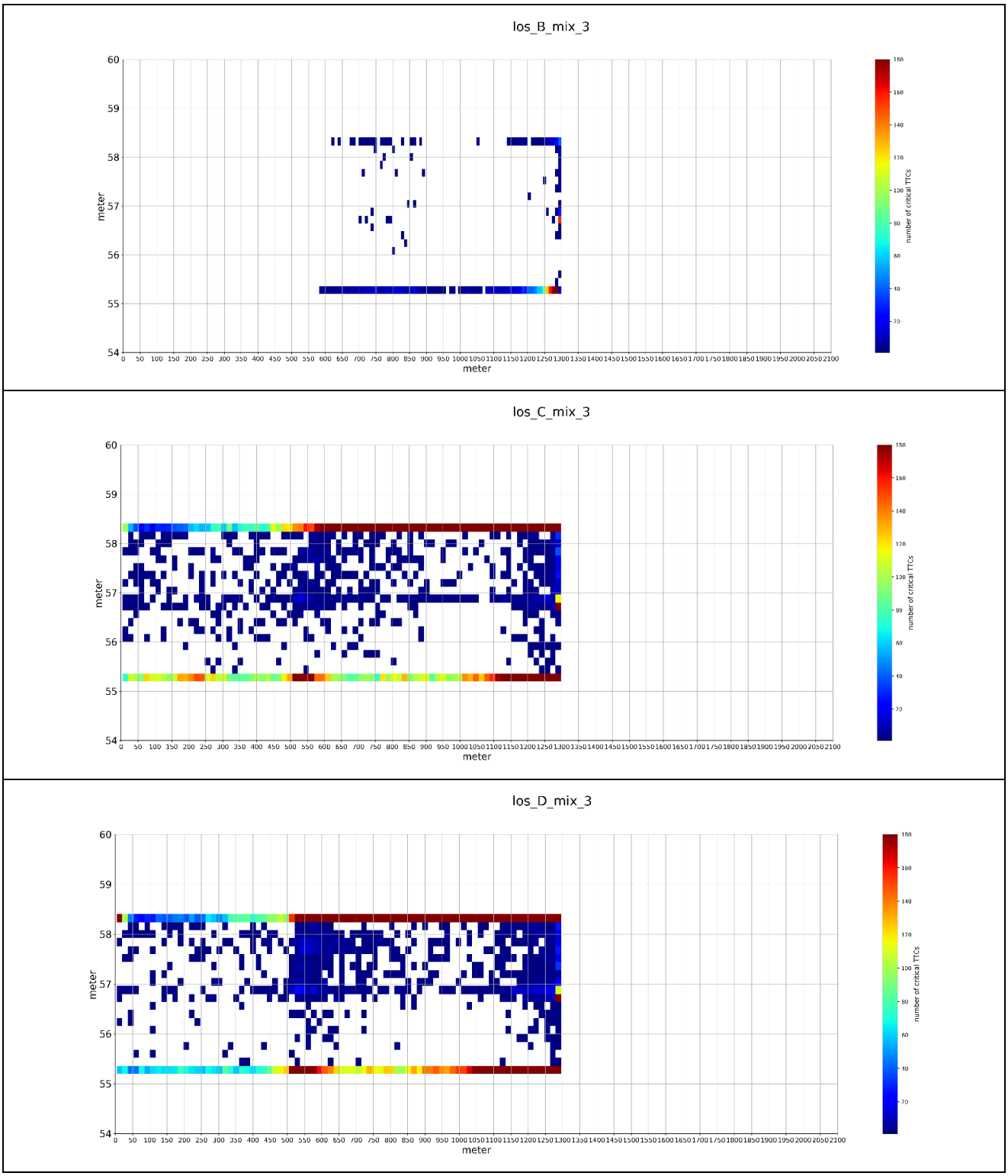

Figure 120. Spatial distribution of critical TTCs (< 3sec) for use case 4.2 (urban) for three different runs (upper plot (a): LOS B – Traffic Mix 3; middle plot (b): LOS C – Traffic Mix 3; bottom plot (c): LOS D – Traffic Mix 3). Colours indicate the number of critical TTCs shown with discrete plotted bins (bin size ≈ 20m x 0,3m).

4.2.4.2.2.4 Environmental Impacts

The environmental impacts of system-initiated control transitions in the context of Scenario 4.2 are assessed in terms of CO_2 emissions per kilometre travelled. **Figure 121** depicts the average CO_2 emissions per travelled kilometre for the examined parameter combinations. In general, the trends observed for emissions match those for travel times. CO_2 emissions gradually increase from 240 g/km (LOS B – traffic mix 1) to 590 g/km (LOS D – traffic mix 2) following the increase in traffic disruption (longer travel times) and the onset of congestion in traffic state LOS C and D due to higher demand and CAV share. Maximum CO_2 emission rate is observed for parameter combination LOS D – Traffic Mix 3, when ToC operations and the behaviour of the "MRM_CAV_01" intensify traffic congestion. The excessive CO_2 emissions rates for LOS C and D are observed due to stop and go traffic which extends from the work zone entry point until the motorway network entry. Finally, CO_2 emissions are higher compared to the urban conditions for uncongested conditions due to the higher travelling speeds on the motorway network.

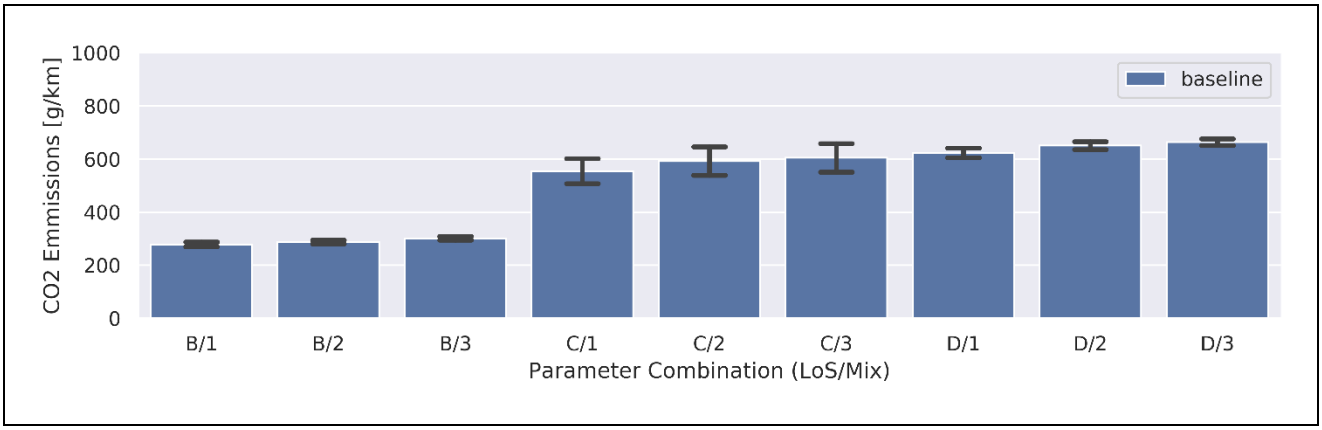

Figure 121. Average CO_2 emissions per kilometres travelled (g/km) for use case 4.2 (motorway) simulation experiments (varying LOS and traffic mix).

4.2.4.3 Discussion

According to the aforementioned analysis, ToC/MRM operations do not inflict serious traffic disruption during low traffic demand levels even in the proximity of the work zone (lane drop bottleneck location). Although the "MRM_CAV_01" stops upstream of the work zone on the right open lane for approximately 1 min, no traffic breakdown is observed when traffic demand is low (< 1200 veh/h). However, it should be noted that the impacts of the "MRM_CAV_01" actions are strongly related to the driver response time after MRM and the entry time of the latter vehicle in the simulation. On the other side, ToCs upon DENM reception, dynamic ToCs on the left lane close to the work zone, conservative CAV lane change behaviour, and the actions of the "MRM_CAV_01" expedite the onset of congestion, prolong its duration, and intensify its severity for higher traffic demand levels (motorway case). However, it remains to be identified what the impacts of MRM that compulsory lead to full vehicle stop due to system design would be in the case of multiple MRMs which has not been examined in the context of this analysis.

As far as traffic dynamics are concerned, the simulation results indicate that input traffic demand can be serviced (exit the simulation network) within the simulation timeline for the urban scenarios. On the contrary, input demand cannot be serviced for traffic states LOS C and D when motorway driving conditions are examined. When the latter traffic states are considered, maximum throughput cannot surpass 1500 veh/h. Moreover, it can be observed that higher CV/CAV share in the vehicle

mix reduces throughput for both uncongested and congested traffic conditions. This phenomenon can be ascribed to the fact that CAV lane change behaviour is more conservative compared to manual driving. In contrast with the similar effect of higher CV/CAV share on the throughput KPI during both congested and uncongested conditions, conflicting trends are identified with respect to the lane change intensity KPI (number of lane changes per kilometre travelled) for different traffic conditions. In the uncongested regime of traffic higher share of CV/CAVs results in reduced lane change intensity, while the opposite takes places in the congested regime or traffic. Even though this result is reasonable for free-flow traffic due to decreased tactical lane changes from CAV, it would be expected that in congested traffic conditions when there is limited space for lane change manoeuvers lane change intensity would be reduced too. In order to discover the reasoning behind the latter behaviour the tempo-spatial distribution of lane changes, distribution of lane changes per lane change intention, and per lane change direction (left or right lane changes) need to be investigated.

The baseline simulation results of Scenario 4.2 suggest that ToC/MRM operations and conservative CAV lane change behaviour generate safety critical issues. According to the spatial distribution of safety critical events, it becomes clear that they are mostly concentrated upstream of the lane drop location (work zone entry point) and downstream of the DENM reception point where CVs and CAVs_G1 implement ToCs/MRM. Moreover, we can observe that the prominent reason inducing safety critical events is car-following, but several of the latter event can be ascribed to lane change operations (especially downstream of the DENM reception point). It is also shown that increasing share of CV/CAVs results in decreased traffic safety and that the number of safety critical events is excessively high during congested traffic conditions.

Considering that conservative CAV lane change behaviour and dynamic TOCs can cause safety critical events due to hard braking events in the proximity of the work zone, and that increased rate of ToC/MRMs due to higher share of CVs/CAVs can render traffic interactions more complex in the area downstream of the DENM message reception, traffic safety results pertaining to uncongested conditions appear to be reasonable. However, the excessive number of safety critical events pertaining to congested conditions, when limited available space and lower traffic speed would be expected to yield lesser safety issues, cannot be justified by this analysis. To explain the excessive number of safety critical events during congestion it is important to understand if the latter are induced prior to the onset of congestion or afterwards when congestion has reached the motorway network entry point (temporal distribution of safety critical events). Additionally, the distribution of critical events per reason (car-following or lane change activity) needs to be defined, and especially the vehicle types that are involved in potential conflicts (share of critical events between similar of different vehicle types). The aforementioned analysis is planned to be conducted in the context of the traffic management simulations (WP4).

Finally, the observed CO_2 emission rates observed per parameter combination are in compliance with the corresponding traffic efficiency results. Excessive emissions rates reported during congested traffic conditions result from stop and go traffic prevailing on a large proportion of the motorway simulation network, while CO_2 emissions are lower in the case of the urban network when uncongested conditions are concerned due to lower vehicle travelling speeds (which are closer to fuel-efficient driving speed for free-flowing traffic in an urban network).

4.2.5 Scenario 4.1 + Service 5 (4.1-5): Distributed safe spots along an urban corridor

4.2.5.1 Scenario Description

In scenario 4.1 we consider an urban corridor with a generic No-AD zone, i.e., a road section where automated driving is not permitted **(Figure 122)**.

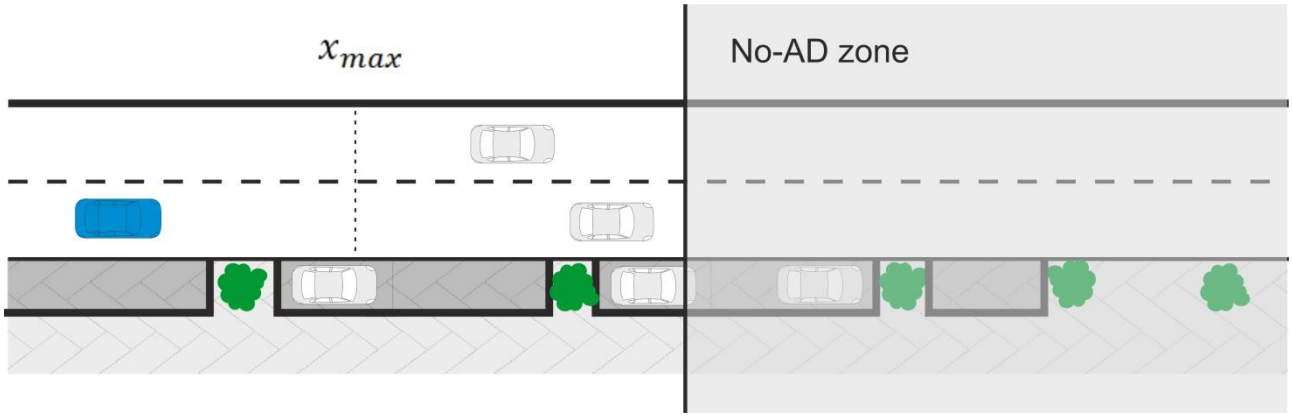

Figure 122. Schematic presentation of the scenario. The cross-section x_{max} is the latest point, where a TOR has to be issued to ensure that the automated (blue) vehicle does not enter the No-AD zone. Present roadside parking places may be assigned as safe spots when traffic management is considered.

As proposed in the previous work concerning No-AD zones on motorways, this situation may be suitable for distribution of TORs (Maerivoet et al., 2019). As in such an urban scenario it is often the case that parking lots are available at the road side, it seems worth studying their use as safe spots, i.e., their use as proximate navigation targets in case of failing takeovers of vehicles approaching the No-AD zone. One logistically interesting aspect of this endeavour is that the parking spaces will be occasionally occupied by regularly parking vehicles. Hence their availability as safe spots has to be monitored constantly.

Although the availability of safe spots will only be relevant for later work in WP4, the basic environment for their application will be modelled in the baseline simulation already. Here we assume that a fraction p of vehicles in the simulation carries the desire to stop at a parking place for an average duration of $T = 10\ min$. Such that for the whole time of the simulation approximately half of the available spaces are occupied. This is achieved by setting the parking desire rate to $p = \frac{0.5N}{T \cdot r_{veh}}$ for the number N of parking spaces and the total vehicle insertion rate r_{veh}.

At approximately minute 30 of the simulation, one vehicle is inserted whose driver fails to comply with the TOR issued and performs an MRM at the rightmost lane (we refer to this CAV as vehicle "MRM_CAV_01" in this section). The management of these vehicles and their proper assignment to available safe spots will be the task of the traffic management algorithm to be devised later in WP4. Here we only provide the KPIs observed for the situation in absence of the traffic management measures. We assume an identical failure characteristic for all simulation runs, i.e. the driver is assigned a prolonged response time of 200 seconds. We assume that the automation logic has implemented a simple strategy for the case of a MRM, which consists in stopping on the

rightmost lane if the traffic situation allows this (i.e. lane changing succeeds for a vehicle traveling on the left lane as the MRM is initiated).

For the unmanaged case that MRMs are performed on the lane just where the vehicle happens to be located when the available lead time for the transition expires, it is clear that severe disruptions of the traffic flow do result. **Figure 123** (a) shows the situation, where the transition of "MRM_CAV_01" failed and the CAV came to a full stop after performing the MRM (red vehicle). Other vehicles are required to slow down and manoeuvre around the stopped vehicles carefully, which leads to a large queue even at low traffic volumes as can be observed in **Figure 123** (a). **Figure 123** shows the situation a few seconds later after the CAV had successfully performed its ToC and the human driver continued driving. The queue quickly dissolved after this.

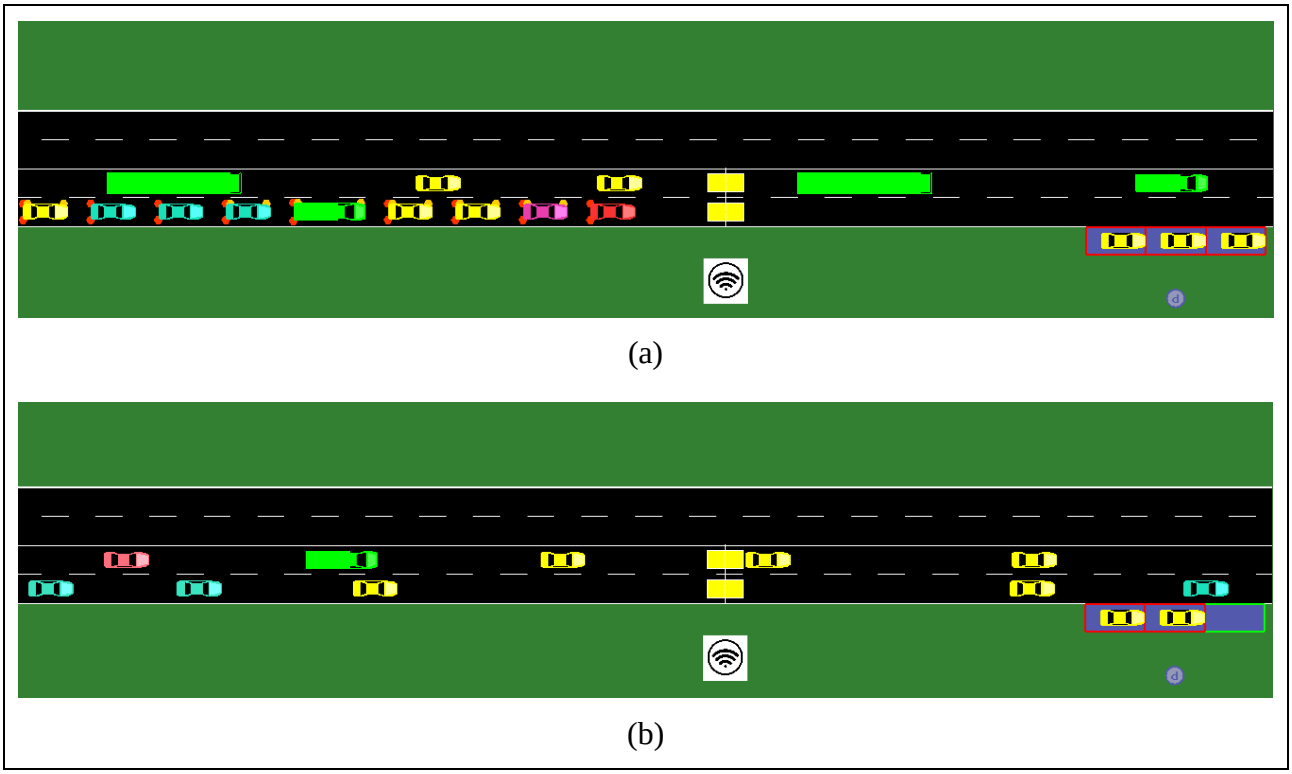

(a)

(b)

Figure 123. Snapshots of the simulation showing the key event of the scenario: one CAV performing an MRM (red vehicle).

The detailed network information for use case 4.1-5 is listed in **Table 47**.

Table 47. Network configuration details for Scenario UC 4.1-5.

UC4.1_5	Settings	Notes
Road section length	1.82 km	
Road priority	-	
Allowed road speed	13.89 m/s	• 50 km/h
Number of nodes	6	• n0 – n5
Number of edges	5	•
Number of O-D relations	1	• from n0 to n5

Number of lanes	2	• per direction
No-AD zone location	from n2 to n3	• length: 250 m, disallowed vClasses: custom1/2
Parking facilities	Located along edge "approach"	• five parking areas, equidistantly distributed at 150m. distance
Filenames	• network: UC45.net.xml • visualization: view.xml • parking facilities: UC45.add.xml	

Intended control of lane usage
The section named "No-AD" is not allowed to be entered by automated vehicles. Therefore TMC provides this information to approaching CAVs. Vehicles are free to choose lanes. The CAV inserted at minute 30 uses the rightmost lane.

Network layout

Detail: No-AD zone entry, parking spaces

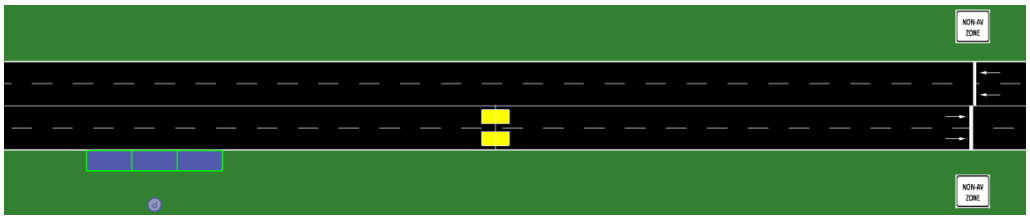

Road segments
"entry" (n0→n1): Insertion area (100 m)
"approach" (n1→n2): Approaching area with parking places (870 m)
"NoAD" (n2→n3): No-AD zone (250 m)
"upward" (n3→n4): Area for upward transitions (500 m)
"exit" (n4→n5): Leaving area (100 m)

4.2.5.2 Results

The proposed scenarios are simulated at three traffic loading levels (LOS B, C and D) with the consideration of three vehicle compositions as mentioned in Section 3.2. Furthermore, 10 simulation runs with different random seeds for each combination of LOS and vehicle composition are executed. In the following, the results are analysed and clarified in the aspects of traffic efficiency, traffic dynamics, traffic safety, and environment.

4.2.5.2.1 Impacts on Traffic Efficiency

As in the first iteration, traffic efficiency will be analysed both network-wide and locally.

Network-wide Impacts

Figure 124 shows that traffic is quite smooth with the travel time of approximately 1.6 min and there is no significant difference in travel time with different vehicle compositions when the travel load is low, i.e. at LOS B. The MRM performance of vehicle "MRM_CAV_01" shows no influence on these aggregated travel times for lower traffic demands. When the share of the CVs/CAVs increases from 44% (Mix 2) to 70%, (Mix 3) the travel time average gets 2.5 times higher than at LOS B (from 1.6 min to approximately 4 min) with the medium traffic demand LOS C. In a high

traffic state (LOS D), the average travel time increases to about 7.6 min. It is almost 5 times longer than that for LOS B. This is mainly because CVs/CAVs have higher requirements for traffic safety than conventional cars, which are controlled by human drivers and react more flexibly for dealing with unexpected traffic interactions and situations. CVs/CAVs' higher requirements for traffic safety result in a reduction of road capacity because of their increased headways. When an MRM is performed in this situation additionally, the road capacity is further reduced and it causes much higher travel times.

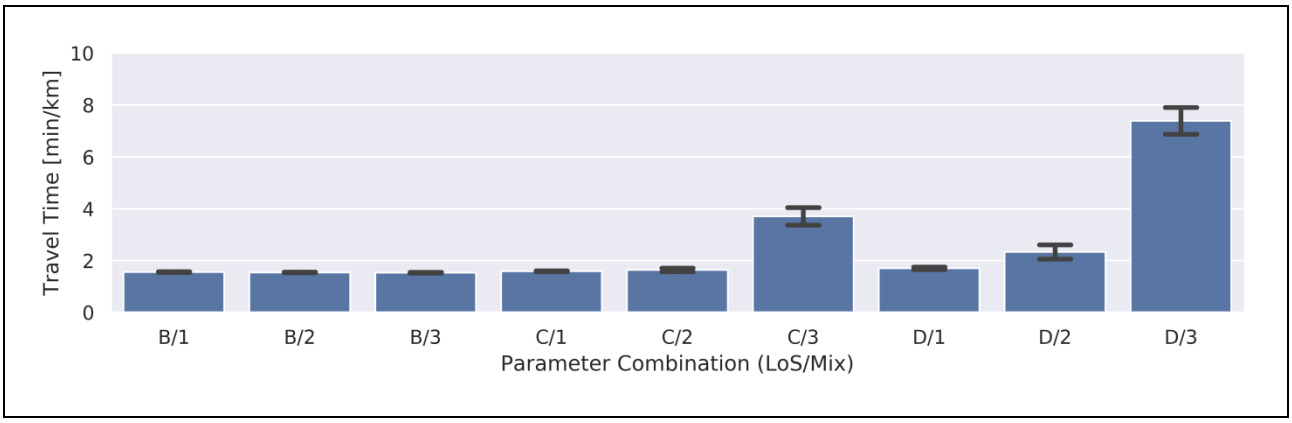

Figure 124. Travel time (min/km) for use case 4.1-5 simulation experiments (varying LOS and traffic mix).

Local Impacts

Following the aforementioned network-wide analysis the local impacts at LOS C and D are further investigated based on time-space plots for traffic speed and flow. **Figure 125** shows the time-space diagrams for measured speeds and flows at LOS C with 70% share of CVs and CAVs.

With a high CV/CAV share and the MRM performance of vehicle "MRM_CAV_01" the road capacity dramatically drops due to increased headways, and therefore disruptions in traffic flow occur which lead to a decreasing network speed (see **Figure 125**, Panel (a) – blue area). The spillback occurs around the 10th minute. It continues to grow to the start position of the network and lasts until the end of the observed simulation period, i.e. (the blue area in **Figure 125** (a)). Due to this spillback, the number of vehicles per hour (flow) drops to approximately less than 1000 veh/h (see **Figure 125** (b)), where colours vary mostly from blue to light green after about the 40th minute). This is the same phenomenon we observed in use case 5 in iteration 1 for the unmanaged scenarios, although ToCs are distributed for CAVs ahead of the No-AD zone in this use case (Notably, these were simulated with different LOS and traffic mix parametrizations) (Maerivoet et al., 2019).

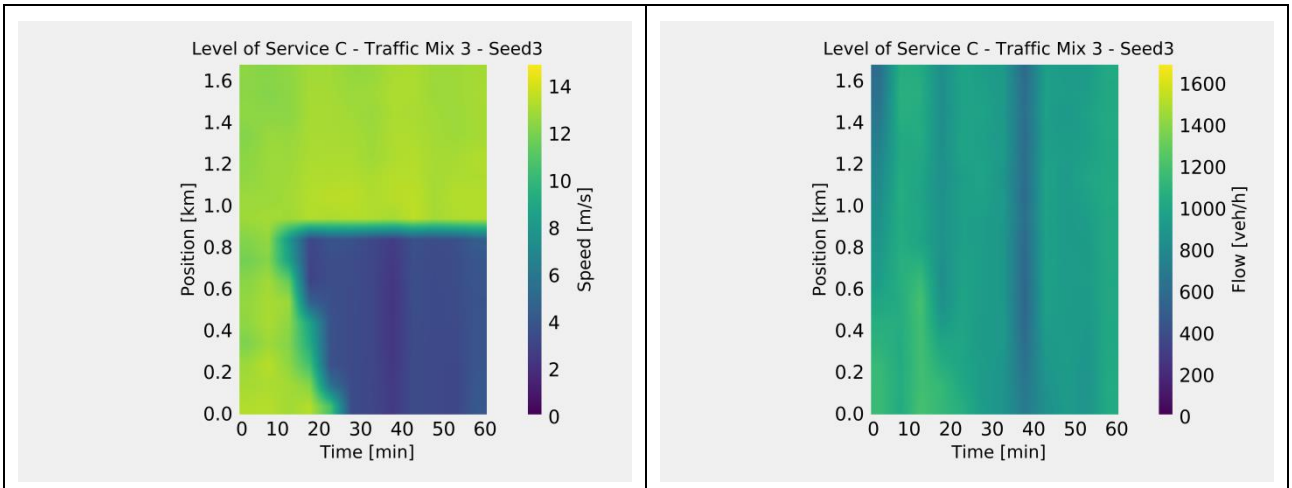

(a) (b)

Figure 125. Exemplary time-space-diagrams for measured speed (left column) and flow (right column) for use case 4.1-5 (LOS C – traffic mix 3 – seed 3).

Figure 126 specifically illustrates the impact of vehicle "MRM_CAV_01" which was induced to the traffic flow with the departure time at the 30th minute (see explanation in section 4.2.5.1 and **Figure 123**). The time-space diagrams represent the speed and the flow distributions at LOS D with 26% share of CVs and CAVs (Traffic Mix 1) respectively. At the 30th minute, i.e. the time to insert the vehicle "MRM_CAV_01" into the network there is a drop in speed and traffic flow, which dissipates shortly after several minutes, and remains at a relatively constant and high level for the remaining simulation time (see **Figure 126** Panel (a) and (b)). The dark blue spots, appearing at about the 30th minute, indicate the presence of "MRM_CAV_01" and light green and yellow indicates relatively smooth traffic flow).

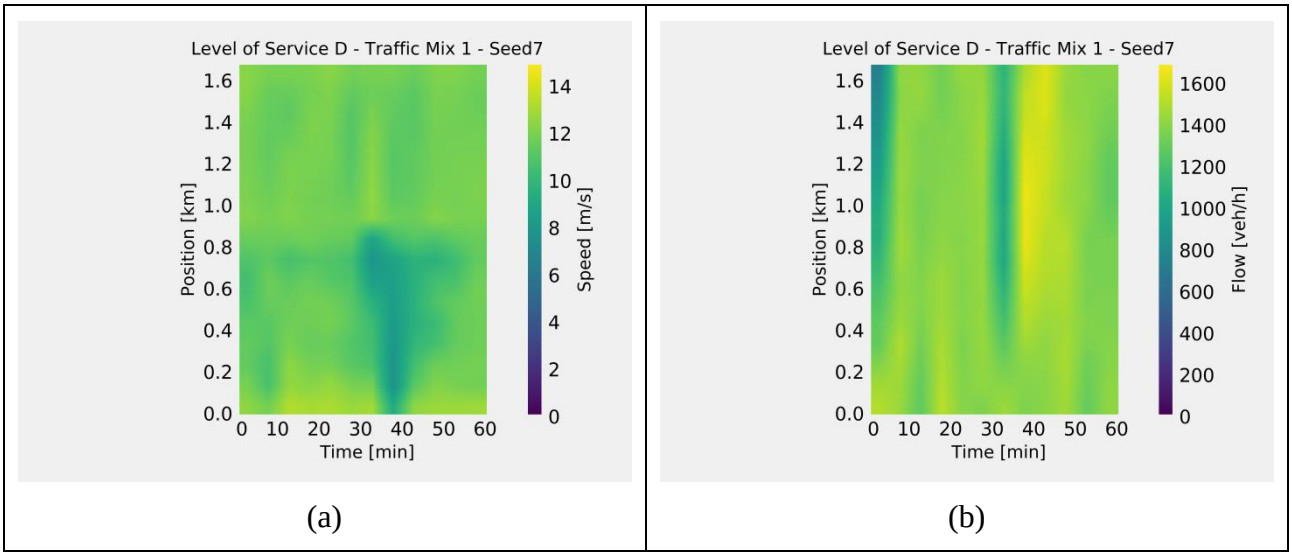

(a) (b)

Figure 126. Exemplary time-space-diagrams for measured speed (left column) and flow (right column) for use case 4.1-5 (LOS D – traffic mix 1 –seed 7).

4.2.5.2.2 Impacts on Traffic Dynamics

The average throughput and the number of lane changes are used as KPIs to elaborate on traffic dynamics hereafter. **Figure 127** indicates that the vehicle compositions and the MRM performance of vehicle "MRM_CAV_01" do not have much impact on the amount of traffic throughput when the traffic state is low (LOS B). We observe that as the traffic demand (LOS C and LOS D) and the share of CVs and CAVs (Mix 2 and Mix 3) increase, the traffic throughput becomes less. The reason for this is again the impact of CAV shares as described in section 4.2.5.2.1.

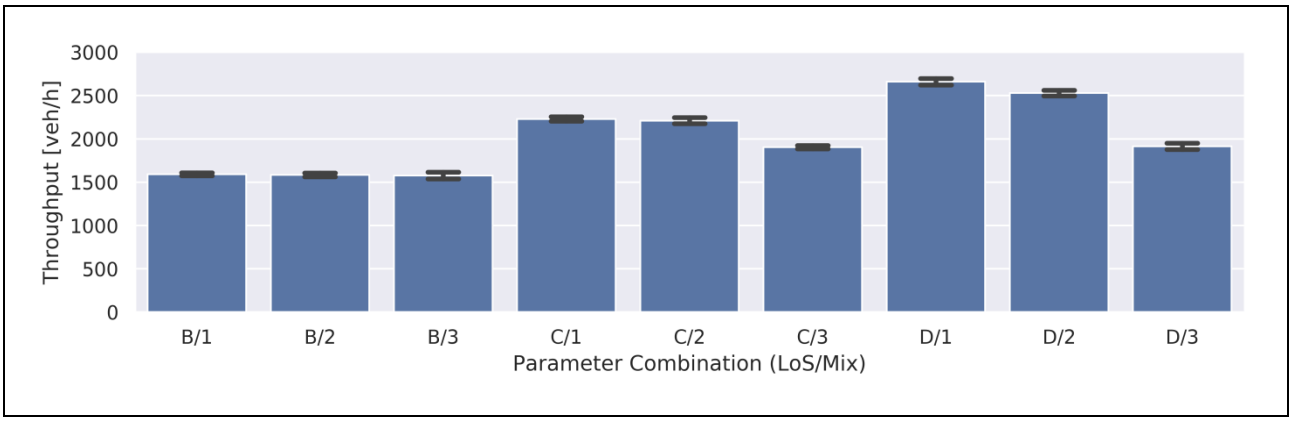

Figure 127. Throughput (veh/h) for use case 4.1-5 (varying LOS and traffic mix).

In addition, lane changing behaviour is also investigated. The number of lane changes per kilometre is used as indicator here. **Figure 128** shows an overall decline of the number of lane changes throughout the increasing traffic demands and CV/CAV shares (LOS/Mix). This should relate to the wider driving speed spectrum and driving behaviours when traffic condition is not saturated. Available road space is one of the prerequisites for lane changing. When traffic state is saturated, road space for lane changing is limited. Therefore, the number of lane changes per kilometre continues to decrease from LOS B to LOS D.

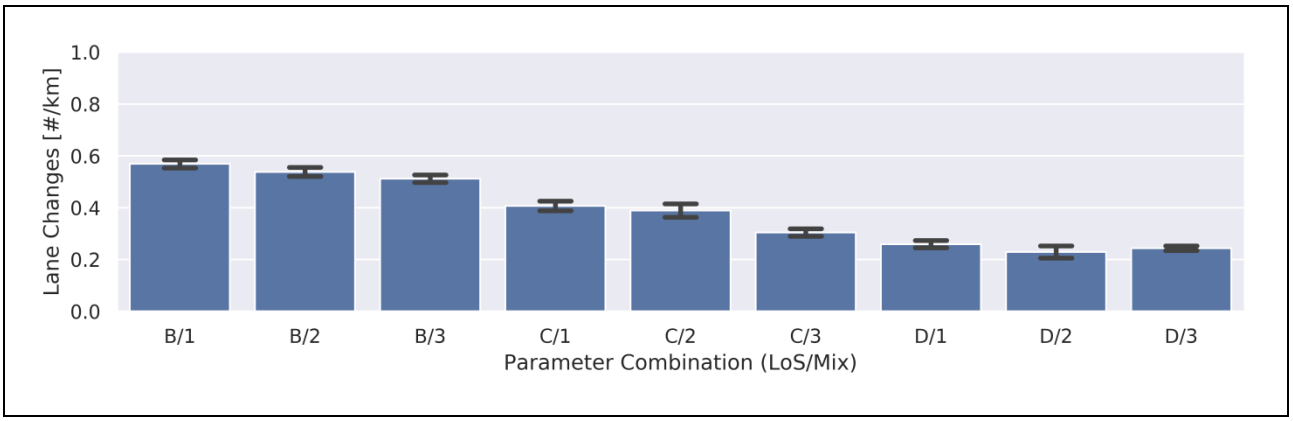

Figure 128. Number of lane changes per kilometre (#/km) for use case 4.1-5 (varying LOS and traffic mix).

4.2.5.2.3 Impacts on Traffic Safety

In the second iteration we analyse traffic safety network-wide and also locally. Network-wide we use the same KPI as in the first iteration with the number of critical TTCs less than 3 sec. Locally we evaluate aggregated TTC distributions within the interesting No-AD approach zone by using two different examples.

Network-wide Impacts

Regarding the impacts on traffic safety time to collision (TTC) is used as indictor. When a vehicle's TTC is less than 3 sec, we consider this as a critical event. **Figure 129** shows the average number of critical events for all combinations of traffic states and vehicle compositions. We observe that the number of critical events is between 124 and 273 in all scenarios. At LOS B, a higher share of CVs and CAVs results in a higher number of critical events, increasing from 158 to 204. This should also mainly relate to a wider vehicles' speed spectrum due to free road capacity and human driving behavior.

For LOS C we observe a similar trend. However, the number of critical events decreases when the share of CVs and CAVs reaches 70% (mix 3). When the traffic state is at LOS D, the traffic condition is saturated with limited speed variation. The interaction between vehicles is not as dynamic as at LOS B. Therefore, the number of critical events recedes (dropping from 210 (D/1) to 124 (D/3)).

With the consideration of the different traffic demands at LOS B, C and D we additionally calculated the number of critical events per vehicle. This ratio varies between 0.09 and 0.26, and becomes less than 0.15 only at saturated traffic conditions (LOS D). This means that approximately one out of every four vehicles has a TTC less than 3 sec in most of the parameter combinations, i.e. from B/1 to C/3. This phenomenon should be further investigated in WP4 and taken into consideration in the TM strategy development if necessary.

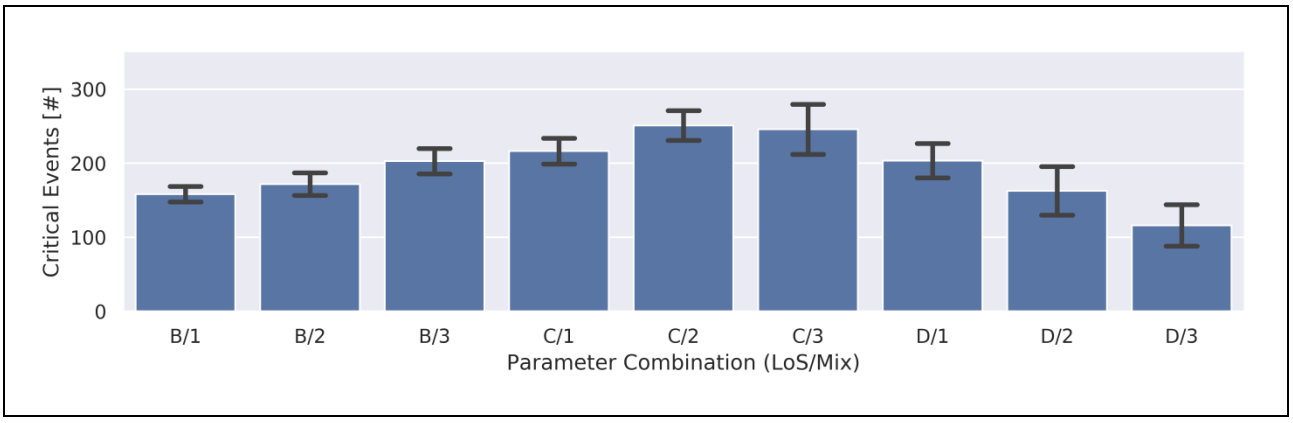

Figure 129. Average number of events with TTCs below 3.0 seconds for use case 4.1-5 (varying LOS and traffic mix).

Local Impacts

When looking at the spatial distribution of the critical events, local impacts can be further identified. Two examples are shown in **Figure 130** where each plot features the aggregated number of critical TTCs of 10 seeds (per LOS/mix) marked as bins within the approach area. Each plotted bin means that at least one TTC occurred at this position. The colour of a bin then indicates the

amount of TTCs at this marked position. So, when e.g. several TTCs concentrate within a certain area, the colours translate as a spatial density for interpretation of the TTC distribution.

Panel (a) shows that most of the critical events occur in the front of the No-AD zone and on the rightmost lane in the areas next to the parking spaces at LOS B with 70% share of CVs and CAVs. The lighter colour spectrum from cyan to light green on the rightmost lane indicates that the critical events concentrate next to the parking areas which relates either to the merging of parking vehicles into the traffic flow or the braking of vehicles before entering a free parking slot. Both situations cause disruptions in traffic flow and induce heavy braking manoeuvres made by following vehicles and result in critical TTC events. Notably, few critical events also happen within the parking spaces. This is due to the fact that each parking space has three separate slots. So when vehicles merge into or out of a slot, it may result in a TTC below 3 seconds.

Panel (b) shows that the most critical events occur on the rightmost lane in the area next to the parking spaces at LOS D with 61% LV share, but distribute more evenly than the aforementioned condition. Here, the lighter colour spectrum from cyan to yellow indicates that the critical events occur more frequently next to parking areas as in Panel (a). Again, some critical events occur in three parking spaces, but the respective amount is quite limited.

Also **Figure 130** shows that some critical TTC events occur between the left and right lane centres which are obviously caused by lane changes (see the dark blue markers aside from the lane centres at y= 45.2 or y=48.4). These events are widely distributed within the whole approach road section ahead of the No-AD zone. The dark blue colours of these markers indicate that there is no heavy concentration of critical TTC events related to these lane changes.

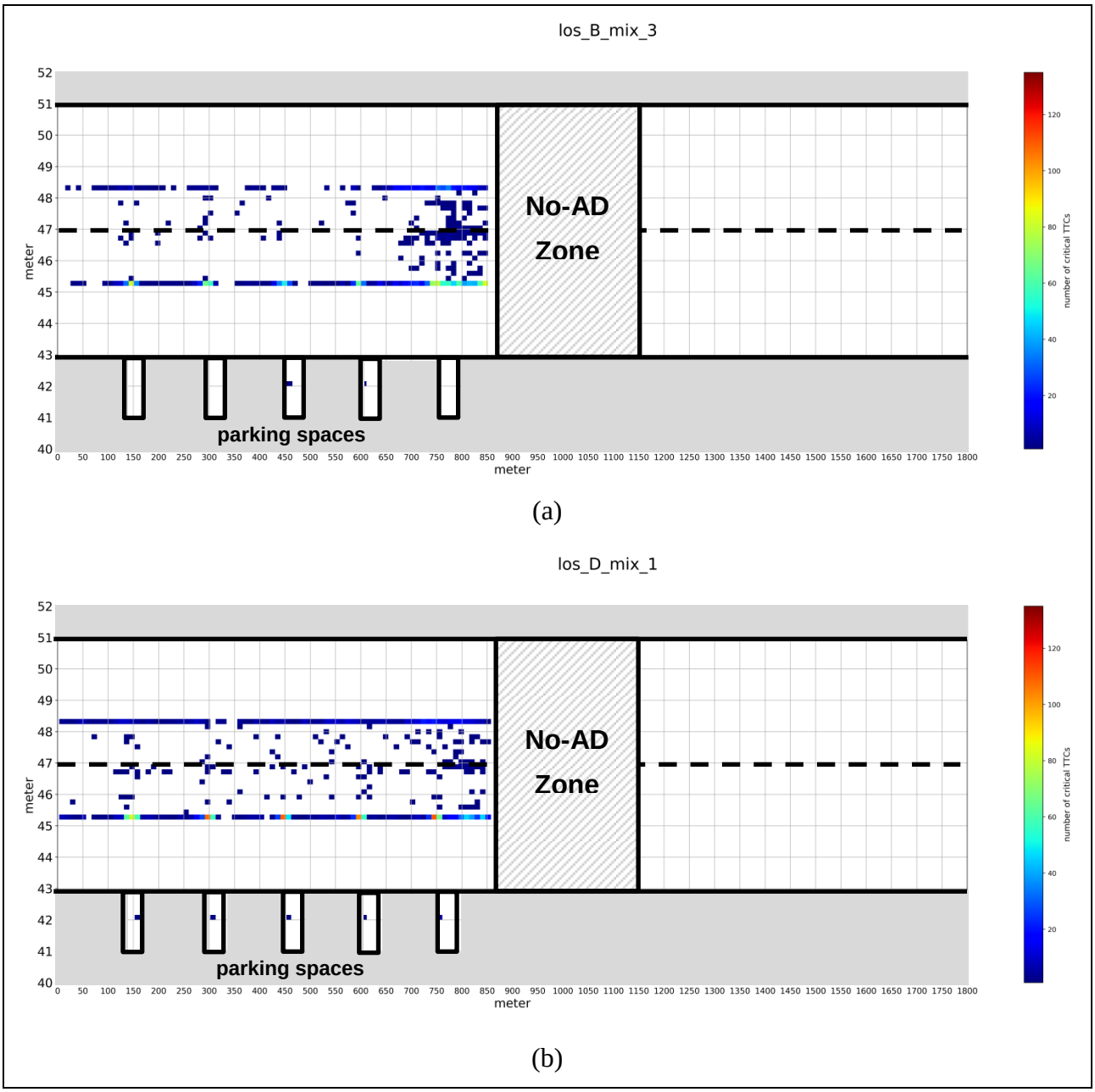

Figure 130. Spatial distribution of critical TTCs (< 3sec) for use case 4.1-5 for two different runs (upper plot (a): LOS B – traffic mix 3; bottom plot (b): LOS D – traffic mix 1). Colours indicate the number of critical TTCs shown with discrete plotted bins (bin size ≈ 20m x 0,3m).

4.2.5.2.4 Environmental Impacts

CO_2 is selected as the indicator for investigating use case 4.1-5's impacts on environment. **Figure 131** shows the average CO_2 emissions per travelled kilometre for the different traffic mixes. Emissions remain relatively constant through most of the simulations (between 150 and 160 g/km to 200 g/km) except for the situations with higher demand and high CVs/CAVs share (C/3 and D/3). These parameter variations present significantly higher emissions. In these cases traffic flow is less smooth due to disruptions (as described in section 4.2.5.2.1), which ultimately results in higher emissions and also longer travel times. The trend depicted here for emissions looks similar to the trend for travel time.

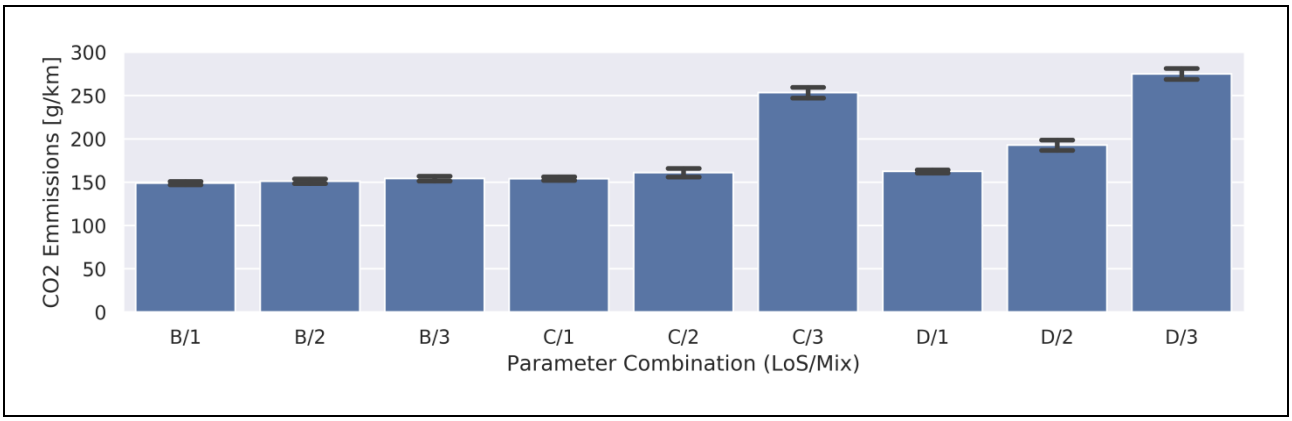

Figure 131. Average CO_2 emissions per kilometres travelled (g/km) for use case 4.1-5 (varying LOS and traffic mix).

4.2.5.3 Discussion

Aim of this baseline simulation 4.1-5 was to investigate the impact of severe MRM manoeuvres with a prolonged driver response time which results in full stops of automated vehicles on the rightmost lane. Here we only inserted one vehicle with such behaviour called "MRM_CAV_01" within a very heterogenic traffic composition. The designed roadside parking activities reflect the complex traffic operation in real life without traffic management assistance and help to highlight the possible issues/drawbacks of the above mentioned MRM performances of automated vehicles in such urban scenarios. These issues will be taken into consideration in the TM development of WP4. Moreover, the impact of only one vehicle with such behaviour of "MRM_CAV_01" dissipates within an hour of simulation time. Therefore we also investigated the overall scenario performance by means on the basis of pre-selected KPIs. Especially, cases with high traffic demand and higher CV/CAV shares up to 70% were of interest in the presence of ToC distribution traffic management from use case 5.

Overall, the results of use case 4.1-5 show significant negative effects for traffic efficiency, CO_2 production and throughput when LOS and traffic mix are highest due to the saturation effects in the scenario. Because of the presence of a No-AD zone in this use case every CV/CAV received a TOR from the TM application of UC 5. This leads consequently to ToCs/MRMs and therefore its negative effects on the overall traffic performance occurred for high traffic demands. These impacts become even worse in presence of the dynamic parking activities and also of the severe MRM performance of "MRM_CAV_01". The negative impact of vehicle "MRM_CAV_01" becomes obvious when analysing its local impact in traffic efficiency with the help of time-space-diagrams. These showed major disruptions after the MRM performance and only dissolved under easier traffic conditions. The results also reveal that the threat of such a MRM performance to traffic safety may not be as critical when looking at the TTCs. Because the deceleration rate during a MRM performance is quite moderate (3 m/s^2), TTCs do not increase as much locally close to "MRM_CAV_01" as we expected. However, the results also point out that approximately one out of every four vehicles has a TTC less than 3 sec in most of the parameter combinations. This phenomenon should be further investigated in WP4 and the KPI of critical TTCs as well as its distribution will be of interest then.

The abovementioned aim of the investigation has been principally achieved with the executed simulation study, covering the major LOS spectrum and vehicle compositions in urban areas. Different issues are already identified solely with one vehicle performing a severe MRM

manoeuvre in addition to the designed daily parking activities in the baseline simulation. Together with these revealed issues the influence of the frequency of such severe MRM manoeuvres on traffic will be taken into account in WP4.

5 Conclusions

5.1 First Iteration

In this Deliverable D3.1 we developed driver models to emulate vehicle automations for CAVs/CVs. These models dictate CAV/CV longitudinal motion, lateral motion, and driving behaviour during ToC/MRM. We adopted an ACC model from a previous study and modified it to ensure collision-free car-following and to simulate CAV/CV longitudinal motions in SUMO. We also parametrised SUMO's default lane change model (LC2013) to reflect the actual (OEM-specific) CAV/CV lane change behaviour by means of a sensitivity analysis. Finally, we developed a ToC/MRM model based on literature findings to mimic ToC/MRM at TAs.

Our baseline simulations experiments encompassed three distinct dimensions (the traffic demand level, the traffic mix, and the driver model parametrisation scheme) to capture the effects of ToCs/MRM for varying traffic conditions, traffic composition, and vehicle properties. We addressed six scenarios, previously defined in Deliverable D2.2, with respect to the investigation of ToC/MRM impacts at work zones (Scenarios 1.1 and 4.2), motorway merge segments (Scenarios 2.1 and 3.1), and no-AD zones (Scenario 5.1). We presented simulation results and analysed them in terms of traffic efficiency, traffic dynamics, traffic safety, and environmental impacts at TAs.

The analysis of the simulation results indicated that congestion at lane drops is highly correlated with safety-critical events. Moreover, it is found that traffic safety is further undermined as the share of CAVs/CVs in the traffic mix increases. The rationale behind this behaviour is that CAVs/CVs were simulated more conservative in terms of their lane change behaviour in comparison to LVs. Therefore, they cannot merge early enough to the desired lane, which in return leads to sudden braking in front of the dead-end lane and consequently to rear-end conflicts due to car-following. It is also noteworthy that conflicts are higher for parametrisation schemes that were expected to benefit traffic safety (PE and OS). However, since the parameter values of these schemes result in reduced merging efficiency, the aforementioned phenomenon is more pronounced.

A noteworthy finding is that parametrisation schemes OE and PS exhibit similar performance for most of the simulated scenarios and output statistics. The same applies to parametrisation schemes PE and OS. These pairs represent similar behaviour in terms of car-following and lane-changing, but different in terms of driver response to ToC/MRM **(Table 18)**. Thus, it can be deduced that ToCs and MRMs do not heavily impact traffic operations given their current implementation in baseline simulation experiments. This is rather exemplified by simulation results of Scenario 5.1, where ToCs/MRMs have no effects on traffic operations given the examined demand levels, traffic mixes, and parametrisation schemes. The reason behind this behaviour can be two-fold. Firstly, the unexpectedness of MRMs for non-cooperative vehicles is only captured rudimentarily in the given model structure, and secondly, MRMs do not necessarily result in a full vehicle stop. By adapting the ToC/MRM model to incorporate more realism concerning following vehicle reaction to MRMs, and assuming MRM logic that mandates a full vehicle stop, the most deteriorating effects of ToCs/MRMs might be captured.

Simulation results also show that there is no clear relationship between lane-changing and traffic efficiency. However, it is stressed that no investigation was conducted with respect to the allocation of lane changes per reason, location, and vehicle type. This work will be done in future deliverables to identify the impacts of lane changes in the proximity and along TAs. Finally, it is demonstrated

that emissions levels decrease for improved traffic efficiency, and increase significantly for stop-and-go traffic (Scenario 4.2, Motorway Network).

According to simulation results, it is clear that traffic operations are significantly degraded at lane drop locations leading to adverse impacts on traffic efficiency, safety, and environment. Thus, facilitating merging operations at lane drops by providing lane advice seems to be a promising measure for improving traffic conditions at TAs. The latter traffic management measure was proposed by TransAID in D2.1 and will be evaluated in D3.2.

Finally, we emphasise that within the context of this Deliverable D3.1 some important assumptions were made with respect to vehicle model parameter values and respective driving behaviour for CAVs, CVs, and LVs. Thus, the investigation of ToCs/MRMs at TAs was done to a theoretical level which provided an initial understanding of traffic operations at TAs in the absence of traffic management. Simulation results indicate that a rigorous calibration of the LVs lane change behaviour is also necessary to replicate overall merging operations more accurately. Parameters pertaining to ToC/MRM model need to be also tuned in more detail based on actual CAV/CV behaviour. Moreover, an actual road network needs to be simulated (with calibrated demand) in the next project iteration to examine the effects of ToCs/MRMs in real traffic conditions.

5.2 Second Iteration

In the 2nd version of Deliverable D3.1 we introduce new driver models for (C)AVs and adapt existing ones (presented in the 1st version of Deliverable D3.1) to increase their realism in reflecting AV behaviour during lane changing and downward control transitions. A Cooperative Adaptive Cruise Control (CACC) model is used to replicate (C)AV car-following behaviour in the presence of V2X communications, while the previous parametrization of the default SUMO lane change model is refined to better capture AV lane change behaviour, and the ToC model is extended so that it can emulate dynamical TOR triggering based on the prevailing traffic conditions.

Our baseline simulations experiments in the 2nd project iteration also encompassed three distinct dimensions (the traffic demand level, the traffic mix, and the driver model parametrisation scheme) to capture the effects of ToCs/MRM for varying traffic conditions, traffic composition, and vehicle properties. However, a single parametrization scheme that encapsulates the full spectrum of vehicle behaviour was adopted in the 2nd iteration in order to focus more on actual traffic conditions, rather than theoretically investigate the impacts of different parametrizations of the driver models. Moreover, we addressed six scenarios in the 2nd iteration as well, previously defined in Deliverable D2.2, with respect to the investigation of ToC/MRM impacts at work zones (Scenarios 4.2), motorway merge and diverge segments (Scenarios 2.1 and 1.3), incident locations (Scenario 2.3), and no-AD zones (Scenario 4.1 – 5.1). A new feature of the baseline simulation experiments in the 2nd project iteration was the consideration of Day 1 C-ITS applications in the context of Scenarios 2.1, 2.3 and 4.2, which substantially enhances the realism of our simulation experiments. We presented simulation results and analysed them in terms of traffic efficiency, traffic dynamics, traffic safety, and environmental impacts at TAs.

The baseline simulation results of the 2nd project iteration indicate that unmanaged MRMs can cause significant traffic disruption. The magnitude of the disruption is a function of the driver response time and the prevailing traffic intensity. It is also noted that in our baseline simulation experiments we assumed that the majority of drivers manage to take-over vehicle control during ToC or shortly after MRM. In the case that multiple MRMs with long duration (> 100s) occur in the simulation network the probability of traffic breakdown can significantly increase. The latter

phenomenon can be further intensified if these MRMs take place on the same temporal window and spatial domain.

On the other hand, successful ToC operations can only induce disruption when the CV/CAV share is high, traffic intensity is high, and TORs are concurrently initiated within a short distance interval. The disruption becomes more significant if (C)AVs are driving in CACC mode and have to enlarge car-following headways prior to ToC initiation (ToC preparation phase). Otherwise, the impacts of successful ToCs on traffic efficiency are insignificant. However, we did not model erratic driver behaviour during control transitions that eventually lead to successful takeover of vehicle control, nor did we comprehensively capture the unexpectedness of ToCs/MRMs for non-cooperative vehicles in the given model structure. Thus, in real-life conditions ToCs might generate traffic disruption even for lower shares of CVs/CAVs in the fleet composition.

Simulation findings also indicate that throughput increases with increasing traffic intensity until traffic breaks down and congestion propagates on the network. Then throughput stabilizes since network capacity is reached. Moreover, we observe that throughput slightly decreases with increasing CV/CAV share. This is expected considering that CAVs are more conservative in lane change behavior and that the number of ToCs/MRMs increases during the simulation timeline. However, inconsistent results are reported when lane change intensity is examined. During uncongested conditions lane change activity is reduced for higher share of CVs/CAVs since the latter vehicles accept larger safe gaps for lane changing (compared to manually driven vehicles). However, for Scenarios 2.3 and 4.2 the same behavior is identified during congested conditions when limited available space and lower speeds would normally result in lesser lane changes. Thus, a more comprehensive analysis that encompasses spatial distribution of lane changes, distribution of lane changes per lane change intention and per lane change direction (left or right lane changes) is required to explain the observed trends during congested conditions. Additionally, the lane change behaviour of vehicles upstream of static blockages (incident – work zone) under congested conditions as reported in section 4.2.3.2.2 should be also investigated.

According to the traffic safety KPIs, the number of safety critical events increases in the presence of more CVs/CAVs in the fleet mix. At first glance this can be ascribed to ToC/MRM events that increase with higher CV/CAV share and to conservative CAV lane change behaviour which can generate complex merging operations at lane drops locations. However, the ACC/CACC model uses speed differences in a linear way although speed actually impacts braking gaps and thus safety requirements in a quadratic way. Hence, the TTCs that are reported due to car-following reasons (which are the majority among safety critical events) can also occur due to systematic issues concerning the ACC/CACC model. Moreover, we have replicated the CAV lane change behaviour based on a single prototype vehicle as described in section 2.2. Nonetheless, considering rapid advancements in the automated driving domain, market available AVs might be capable of more human-like lane change behaviour in the near future. Additionally, safety critical events are rather high during congested conditions when limited available space and lower speeds would normally result in reduced safety issues. Therefore, to conclude on the traffic safety impacts of automated driving and control transitions it is important to analyse the distribution of critical events per reason (car-following or lane change activity), the vehicle types that are involved in potential conflicts (share of critical events between similar of different vehicle types), and understand if safety critical events are induced prior to the onset of congestion or afterwards when congestion has reached the motorway network entry point (temporal distribution of safety critical events). Attention also needs to be placed on the accuracy of available AV driver models in replicating actual AV driving behaviour.

Finally, it is demonstrated that CO_2 emission levels decrease for improved traffic efficiency, and increase significantly for stop-and-go traffic.

References

Behrisch, M., Bieker, L., Erdmann, J., & Krajzewicz, D. (2011). SUMO – Simulation of Urban MObility: An Overview. *Proceedings of SIMUL 2011, The Third International Conference on Advances in System Simulation*. Presented at the SIMUL 2011, Barcelona. Retrieved from http://www.thinkmind.org/index.php?view=instance&instance=SIMUL+2011

Blommer, M., Curry, R., Swaminathan, R., Tijerina, L., Talamonti, W., & Kochhar, D. (2017). Driver brake vs. Steer response to sudden forward collision scenario in manual and automated driving modes. *Transportation Research Part F: Traffic Psychology and Behaviour*, *45*, 93–101. https://doi.org/10.1016/j.trf.2016.11.006

Blythe, P., & Curtis, A. (2004). *Advanced driver assistance systems: Gimmick or reality?* Presented at the 11th World Congress on ITS, Nagoya. Retrieved from https://www.researchgate.net/profile/Philip_Blythe/publication/233932657_Advanced_Driver_Assistance_Systems_gimmick_or_reality/links/56b8843f08aebbde1a7f7907.pdf

Clark, H., & Feng, J. (2017). Age differences in the takeover of vehicle control and engagement in non-driving-related activities in simulated driving with conditional automation. *Accident Analysis & Prevention*, *106*, 468–479. https://doi.org/10.1016/j.aap.2016.08.027

Cukier, R. I., Fortuin, C. M., Shuler, K. E., Petschek, A. G., & Schaibly, J. H. (1973). Study of the sensitivity of coupled reaction systems to uncertainties in rate coefficients. I Theory. *The Journal of Chemical Physics*, *59*(8), 3873–3878. https://doi.org/10.1063/1.1680571

Davis, L. C. (2004). Effect of adaptive cruise control systems on traffic flow. *Physical Review E*, *69*(6). https://doi.org/10.1103/PhysRevE.69.066110

de Winter, J. C. F., Happee, R., Martens, M. H., & Stanton, N. A. (2014). Effects of adaptive cruise control and highly automated driving on workload and situation awareness: A review of the empirical evidence. *Transportation Research Part F: Traffic Psychology and Behaviour*, *27*, 196–217. https://doi.org/10.1016/j.trf.2014.06.016

Erdmann, J. (2014). Lane-Changing Model in SUMO. *Proceedings of the SUMO2014 Modeling Mobility with Open Data*, *24*, 77–88. Retrieved from http://elib.dlr.de/89233/

Eriksson, A., & Stanton, N. A. (2017). Takeover Time in Highly Automated Vehicles: Noncritical Transitions to and From Manual Control. *Human Factors: The Journal of the Human Factors and Ergonomics Society*, *59*(4), 689–705. https://doi.org/10.1177/0018720816685832

Fuller, R. (2005). Towards a general theory of driver behaviour. *Accident Analysis & Prevention*, *37*(3), 461–472. https://doi.org/10.1016/j.aap.2004.11.003

Gold, C., Damböck, D., Lorenz, L., & Bengler, K. (2013). "Take over!" How long does it take to get the driver back into the loop? *Proceedings of the Human Factors and Ergonomics Society Annual Meeting*, *57*(1), 1938–1942. https://doi.org/10.1177/1541931213571433

Hasebe, K., Nakayama, A., & Sugiyama, Y. (2003). Dynamical model of a cooperative driving system for freeway traffic. *Physical Review E*, *68*(2). https://doi.org/10.1103/PhysRevE.68.026102

Hausberger, S., Rexeis, M., & Luz, R. (2011). *PHEM - the model of the TU Graz for the calculation of vehicle emissions and its database at Euro 5 and Euro 6*. Presented at the Symposium: Emissions and potential for reduction in road traffic, Stuttgtart, Germany.

Horst, R. V. D., & Hogema, J. (1993). *Time-to-Collision and Collision Avoidance Systems*. Presented at the 6th ICTCT Workshop, Salzburg.

Kesting, A., & Treiber, M. (2008). Calibrating Car-Following Models by Using Trajectory Data: Methodological Study. *Transportation Research Record: Journal of the Transportation Research Board*, *2088*, 148–156. https://doi.org/10.3141/2088-16

Kesting, A., Treiber, M., Schönhof, M., & Helbing, D. (2008). Adaptive cruise control design for active congestion avoidance. *Transportation Research Part C: Emerging Technologies*, *16*(6), 668–683. https://doi.org/10.1016/j.trc.2007.12.004

Krauß, S. (1998). *Microscopic Modeling of Traffic Flow: Investigation of Collision Free Vehicle Dynamics* (Ph.D. Thesis). University of Cologne.

Liang, C.-Y., & Peng, H. (1999). Optimal Adaptive Cruise Control with Guaranteed String Stability. *Vehicle System Dynamics*, *32*(4–5), 313–330. https://doi.org/10.1076/vesd.32.4.313.2083

Liu, H., Kan, X., Wei, D., Chou, F.-C., Shladover, S. E., & Lu, X.-Y. (2018). *Using Cooperative Adaptive Cruise Control (CACC) to Form High-Performance Vehicle Streams—Microscopic Traffic Modeling* (FHWA Exploratory Advanced Research Program No. Cooperative Agreement No. DTFH61-13-H-00013). University of California, Berkeley: California PATH Program.

Louw, T., Kountouriotis, G., Carsten, O., & Merat, N. (2015). Driver Inattention During Vehicle Automation: How Does Driver Engagement Affect Resumption Of Control? *4th International Conference on Driver Distraction and Inattention (DDI2015)*. Presented at the Sydney. Retrieved from http://eprints.whiterose.ac.uk/91858/

Lu, Z., Coster, X., & de Winter, J. (2017). How much time do drivers need to obtain situation awareness? A laboratory-based study of automated driving. *Applied Ergonomics*, *60*, 293–304. https://doi.org/10.1016/j.apergo.2016.12.003

Lu, Z., Happee, R., Cabrall, C. D. D., Kyriakidis, M., & de Winter, J. C. F. (2016). Human factors of transitions in automated driving: A general framework and literature survey. *Transportation Research Part F: Traffic Psychology and Behaviour*, *43*, 183–198. https://doi.org/10.1016/j.trf.2016.10.007

Maerivoet, S., Akkermans, L., Carlier, K., Flötteröd, Y.-P., Lücken, L., Alms, R., … Blokpoel, R. (2019). *Preliminary simulation and assessment of enhanced traffic management measures* [TransAID Deliverable D4.2].

Marsden, G., McDonald, M., & Brackstone, M. (2001). Towards an understanding of adaptive cruise control. *Transportation Research Part C: Emerging Technologies*, *9*(1), 33–51. https://doi.org/10.1016/S0968-090X(00)00022-X

Merat, N., Jamson, A. H., Lai, F. C. H., & Carsten, O. (2012). Highly Automated Driving, Secondary Task Performance, and Driver State. *Human Factors: The Journal of the Human Factors and Ergonomics Society*, *54*(5), 762–771. https://doi.org/10.1177/0018720812442087

Merat, N., Jamson, A. H., Lai, F. C. H., Daly, M., & Carsten, O. M. J. (2014). Transition to manual: Driver behaviour when resuming control from a highly automated vehicle. *Transportation Research Part F: Traffic Psychology and Behaviour*, *27*, 274–282. https://doi.org/10.1016/j.trf.2014.09.005

Milanés, V., & Shladover, S. E. (2014). Modeling cooperative and autonomous adaptive cruise control dynamic responses using experimental data. *Transportation Research Part C: Emerging Technologies*, *48*, 285–300. https://doi.org/10.1016/j.trc.2014.09.001

Milanés, V., & Shladover, S. E. (2016). Handling Cut-In Vehicles in Strings of Cooperative Adaptive Cruise Control Vehicles. *Journal of Intelligent Transportation Systems*, *20*(2), 178–191. https://doi.org/10.1080/15472450.2015.1016023

Milanes, V., Shladover, S. E., Spring, J., Nowakowski, C., Kawazoe, H., & Nakamura, M. (2014). Cooperative Adaptive Cruise Control in Real Traffic Situations. *IEEE Transactions on Intelligent Transportation Systems*, *15*(1), 296–305. https://doi.org/10.1109/TITS.2013.2278494

Mok, B., Johns, M., Miller, D., & Ju, W. (2017). Tunneled In: Drivers with Active Secondary Tasks Need More Time to Transition from Automation. *Proceedings of the 2017 CHI Conference on Human Factors in Computing Systems*, 2840–2844. https://doi.org/10.1145/3025453.3025713

National Research Council (U.S.) (Ed.). (2010). *Highway Capacity Manual*. Washington, D.C.: Transportation Research Board, National Research Council.

Naus, G. J. L., Vugts, R. P. A., Ploeg, J., van de Molengraft, M. J. G., & Steinbuch, M. (2010). String-Stable CACC Design and Experimental Validation: A Frequency-Domain Approach. *IEEE Transactions on Vehicular Technology*, *59*(9), 4268–4279. https://doi.org/10.1109/TVT.2010.2076320

Ott, L., & Longnecker, M. (2004). *A first course in statistical methods*. Belmont, CA: Thomson-Brooks/Cole.

Punzo, V., & Ciuffo, B. F. (2011). *Sensitivity Analysis of Car-following Models: Methodology and Application*. Presented at the Transportation Research Board 90th Annual MeetingTransportation Research Board. Retrieved from https://trid.trb.org/view/1092680

Punzo, V., Montanino, M., & Ciuffo, B. (2015). Do We Really Need to Calibrate All the Parameters? Variance-Based Sensitivity Analysis to Simplify Microscopic Traffic Flow Models. *IEEE Transactions on Intelligent Transportation Systems*, *16*(1), 184–193. https://doi.org/10.1109/TITS.2014.2331453

Saltelli, A. (Ed.). (2008). *Global sensitivity analysis: The primer*. Chichester, England ; Hoboken, NJ: John Wiley.

Saltelli, Andrea, Annoni, P., Azzini, I., Campolongo, F., Ratto, M., & Tarantola, S. (2010). Variance based sensitivity analysis of model output. Design and estimator for the total sensitivity

index. *Computer Physics Communications*, *181*(2), 259–270. https://doi.org/10.1016/j.cpc.2009.09.018

Saltelli, Andrea, Tarantola, S., Campolongo, F., & Ratto, M. (2002). *Sensitivity Analysis in Practice*. https://doi.org/10.1002/0470870958

Samuel, S., Borowsky, A., Zilberstein, S., & Fisher, D. L. (2016). Minimum Time to Situation Awareness in Scenarios Involving Transfer of Control from an Automated Driving Suite. *Transportation Research Record: Journal of the Transportation Research Board*, *2602*, 115–120. https://doi.org/10.3141/2602-14

Shladover, S. E. (2009). *Effects of Cooperative Adaptive Cruise Control on Traffic Flow: Testing Drivers ' Choices of Following Distances*. University of California.

Shladover, S., Su, D., & Lu, X.-Y. (2012). Impacts of Cooperative Adaptive Cruise Control on Freeway Traffic Flow. *Transportation Research Record: Journal of the Transportation Research Board*, *2324*, 63–70. https://doi.org/10.3141/2324-08

Sobol, I. M. (1993). Sensitivity estimates for nonlinear mathematical models. *Mathematical Modelling and Computational Experiments*, *1*(4), 407–414.

Sobol, I. M., Tarantola, S., Gatelli, D., Kucherenko, S. S., & Mauntz, W. (2007). Estimating the approximation error when fixing unessential factors in global sensitivity analysis. *Reliability Engineering & System Safety*, *92*(7), 957–960. https://doi.org/10.1016/j.ress.2006.07.001

Todosiev, E. P. (1963). *The action point model of the driver-vehicle system* (Ph.D. Thesis). The Ohio State University.

Treiber, M., & Helbing, D. (2001). Microsimulations of Freeway Traffic Including Control Measures. *At - Automatisierungstechnik*, *49*(11/2001). https://doi.org/10.1524/auto.2001.49.11.478

Treiber, M., Hennecke, A., & Helbing, D. (2000). Congested traffic states in empirical observations and microscopic simulations. *Physical Review E*, *62*(2), 1805–1824. https://doi.org/10.1103/PhysRevE.62.1805

Treiber, M., & Kesting, A. (2013). *Traffic Flow Dynamics: Data, Models and Simulation*. Retrieved from //www.springer.com/us/book/9783642324598

van Arem, B., van Driel, C. J. G., & Visser, R. (2006). The Impact of Cooperative Adaptive Cruise Control on Traffic-Flow Characteristics. *IEEE Transactions on Intelligent Transportation Systems*, *7*(4), 429–436. https://doi.org/10.1109/TITS.2006.884615

VanderWerf, J., Shladover, S., Kourjanskaia, N., Miller, M., & Krishnan, H. (2001). Modeling Effects of Driver Control Assistance Systems on Traffic. *Transportation Research Record: Journal of the Transportation Research Board*, *1748*, 167–174. https://doi.org/10.3141/1748-21

VanderWerf, J., Shladover, S., & Miller, M. A. (2004). Conceptual Development and Performance Assessment for the Deployment Staging of Advanced Vehicle Control and Safety Systems. *PATH Research Report*. Retrieved from https://trid.trb.org/view/1157086

VanderWerf, J., Shladover, S., Miller, M., & Kourjanskaia, N. (2002). Effects of Adaptive Cruise Control Systems on Highway Traffic Flow Capacity. *Transportation Research Record: Journal of the Transportation Research Board*, *1800*, 78–84. https://doi.org/10.3141/1800-10

Wagner, P. (2012). Analyzing fluctuations in car-following. *Transportation Research Part B: Methodological*, *46*(10), 1384–1392. https://doi.org/10.1016/j.trb.2012.06.007

Wijbenga, A., Mintsis, E., Vreeswijk, J., Correa, A., Luecken, L., Schindler, J., … Markowski, R. (2019). *Scenario definitions and modelling requirements* [TransAID Deliverable D2.2 Final Report].

Xiao, L., & Gao, F. (2011). Practical String Stability of Platoon of Adaptive Cruise Control Vehicles. *IEEE Transactions on Intelligent Transportation Systems*, *12*(4), 1184–1194. https://doi.org/10.1109/TITS.2011.2143407

Xiao, Lin, Wang, M., & van Arem, B. (2017). Realistic Car-Following Models for Microscopic Simulation of Adaptive and Cooperative Adaptive Cruise Control Vehicles. *Transportation Research Record: Journal of the Transportation Research Board*, *2623*, 1–9. https://doi.org/10.3141/2623-01

Xin, W., Hourdos, J., Michalopoulos, P., & Davis, G. (2008). The Less-Than-Perfect Driver: A Model of Collision-Inclusive Car-Following Behavior. *Transportation Research Record: Journal of the Transportation Research Board*, *2088*, 126–137. https://doi.org/10.3141/2088-14

Young, M. S., & Stanton, N. A. (2002). Malleable Attentional Resources Theory: A New Explanation for the Effects of Mental Underload on Performance. *Human Factors: The Journal of the Human Factors and Ergonomics Society*, *44*(3), 365–375. https://doi.org/10.1518/0018720024497709

Young, M. S., & Stanton, N. A. (2007). Back to the future: Brake reaction times for manual and automated vehicles. *Ergonomics*, *50*(1), 46–58. https://doi.org/10.1080/00140130600980789

Zeeb, K., Buchner, A., & Schrauf, M. (2015). What determines the take-over time? An integrated model approach of driver take-over after automated driving. *Accident Analysis & Prevention*, *78*, 212–221. https://doi.org/10.1016/j.aap.2015.02.023

Ziegler, J., Bender, P., Schreiber, M., Lategahn, H., Strauss, T., Stiller, C., … Zeeb, E. (2014). Making Bertha Drive-An Autonomous Journey on a Historic Route. *IEEE Intelligent Transportation Systems Magazine*, *6*(2), 8–20. https://doi.org/10.1109/MITS.2014.2306552

Appendix A

SUMO network files were created within the context of D2.2. Information pertinent to the dimensions of the simulation experiments (three different vehicle mixes for CAVs, CVs, and LVs, three different traffic demand levels (LOS A, LOS B, LOS C), five different driver model parameter sets (PS, PE, MSE, OE, OS), all corresponding to six baseline scenarios) was input to the appropriate SUMO configuration files in D3.1.

Initially, parameter values for the driver models were specified (either in the form of constant values or normal distributions) for each parametrisation scheme, through a configuration file **(Figure A.1)**. Subsequently, using the Python script 'createVehTypeDistribution.py', along with the corresponding configurations (text) files, the desired heterogeneous flows are generated **(Figure A.2)**.

```
# Create automated vType distribution.

# Parametrization Scheme: Pessimistic Safety (PS)

##############################################
# Attribute distributions for the ACC model. #
# Aggressive ACC.                            #
##############################################
carFollowModel ; ACC
tau            ; normal(1.2, 0.1); [1.1, 1.3]
accel          ; normal(1.5, 1.0); [0.75, 2.0]
decel          ; normal(3.0, 1.0); [2.0, 4.0]
emergencyDecel ; 9.0

####################
# Generic Attributes.#
####################
color; white
actionStepLength ; 0.1

##############################################
# Attribute distributions for the SL2015 model.#
# Aggressive SL2015.                         #
##############################################
lcAssertive ; normal(0.9, 0.1); [0.8, 1.0]

##############################################
# Attribute distributions for the TOC/MRM model.#
# Conservative TOC/MRM.                      #
##############################################
param; has.toc.device              ; true
param; device.toc.manualType       ; vehLVPS
param; device.toc.automatedType    ; vehCAVToCPS
param; device.toc.responseTime     ; normal(7, 3); [2, 60]
param; device.toc.initialAwareness ; normal(0.3, 0.3); [0.1, 1.0]
param; device.toc.recoveryRate     ; normal(0.2, 0.1); [0.01, 0.5]
param; device.toc.mrmDecel         ; 3.0
param; device.toc.useColorScheme   ; true
```

normal(mu, sd): with mu and sd being floating numbers: Normal distribution with mean mu and standard deviation sd.

Figure A.1 Configure file – defines the car-following parameter distributions for the pessimistic safety parametrisation scheme.

```
<vTypeDistribution id="vehLVMSE">
        <vType accel="1.503" actionStepLength="0.100" carFollowModel="Krauss" color="yellow"decel="3.362"
               emergencyDecel="9.000" id="vehLVMSE0" lcAssertive="1.300" sigma="0.483" speedFactor="0.905" tau="0.723"/>
        <vType accel="1.675" actionStepLength="0.100" carFollowModel="Krauss" color="yellow" decel="3.035"
               emergencyDecel="9.000" id="vehLVMSE1" lcAssertive="1.300" sigma="0.383" speedFactor="1.174" tau="1.469"/>
        <vType accel="1.069" actionStepLength="0.100" carFollowModel="Krauss" color="yellow" decel="3.810"
               emergencyDecel="9.000" id="vehLVMSE2" lcAssertive="1.300" sigma="0.671" speedFactor="1.014" tau="0.925"/>
        <vType accel="3.314" actionStepLength="0.100" carFollowModel="Krauss" color="yellow" decel="2.965"
               emergencyDecel="9.000" id="vehLVMSE3" lcAssertive="1.300" sigma="0.910" speedFactor="1.129" tau="0.821"/>
        <vType accel="2.673" actionStepLength="0.100" carFollowModel="Krauss" color="yellow" decel="2.386"
               emergencyDecel="9.000" id="vehLVMSE4" lcAssertive="1.300" sigma="0.638" speedFactor="0.864" tau="1.034"/>
```

(a)

```
</vType>
<vType accel="1.868" actionStepLength="0.100" carFollowModel="ACC" color="white" decel="2.343"
       emergencyDecel="9.000" id="vehCAVToCMSE1" lcAssertive="0.737" tau="1.507">
    <param key="device.toc.automatedType" value="vehCAVToCMSE"/>
    <param key="device.toc.manualType" value="vehLVMSE"/>
    <param key="has.toc.device" value="true"/>
    <param key="device.toc.mrmDecel" value="3.000"/>
    <param key="device.toc.recoveryRate" value="0.348"/>
    <param key="device.toc.initialAwareness" value="0.218"/>
    <param key="device.toc.useColorScheme" value="true"/>
    <param key="device.toc.responseTime" value="4.630"/>
```

(b)

```
</vType>
<vType accel="1.868" actionStepLength="0.100" carFollowModel="ACC" color="blue" decel="2.343"
       emergencyDecel="9.000" id="vehCVToCMSE1" lcAssertive="0.605" tau="1.507">
    <param key="device.toc.automatedType" value="vehCVToCMSE"/>
    <param key="device.toc.manualType" value="vehLVMSE"/>
    <param key="has.toc.device" value="true"/>
    <param key="device.toc.mrmDecel" value="3.000"/>
    <param key="device.toc.recoveryRate" value="0.348"/>
    <param key="device.toc.initialAwareness" value="0.218"/>
    <param key="device.toc.useColorScheme" value="true"/>
    <param key="device.toc.responseTime" value="0.000"/>
```

(c)

Figure A.2 Portion of the output ‘vTypeDistributions’ file including information of the driver models of each vehicle type: (a) LVs, (b) CAVs and (c) CVs.

The process of running all baseline simulation scenarios is automated, through the use of the Python script ‘batchRunner.py’ **(Figure A.3)**, for all possible combinations of the different vehicle mixes, traffic demand levels, and driver model parameter sets. In addition, an important aspect of reproducing realistic results in a simulation scenario is the stochasticity introduced into the simulation experiments. SUMO uses two different RNG instances, one for random numbers used on creating vehicles and one for dynamic behaviour. In order to secure that simulation results were statistically significant, ten simulations were performed using different seeds that were randomly generated.

```
# Number of simulations per Demand/Parameter configuration
Nsim = 10
# Number of lanes (regarding the LOS) in the current scenario
Nlanes = 1

# Number of restarts if a run fails
MAXTRIES = 10

# List of genral additional files to be loaded for all runs
generalAddFiles = ["../../../shapes.add.xml, ../../../closeLanes.add.xml, ../../../view.add.xml "]

# Demand levels (levelID->veh/(h*l))
demand_urban = {"los_A":735, "los_B":1155, "los_C":1617}

# levels to be used for simulations
demand_levels = demand_urban
demand_ID_map = {"los_A":0, "los_B":1, "los_C":2}

# Vehicle mix (mix_ID->class->share [in %])
veh_mixes = {"mix_0":{"LV":0.7, "CVToC":0.15, "CAVToC":0.15},
             "mix_1":{"LV":0.5, "CVToC":0.25, "CAVToC":0.25},
             "mix_2":{"LV":0.2, "CVToC":0.4, "CAVToC":0.4}}

# Parameter assumptions regarding (E)fficiency/(S)afety and (O)ptimism/(P)essimism
param_schemes = ["PS", "OS", "PE", "OE", "MSE"]

# template file for the routes
routefile_template = "routes_template.rou.xml"

# config file
config_file = "sumo.cfg"

# runner script for single runs
runner_file = "runner.py"
```

Figure A.3 Part of the Python script used for the automated running of the baseline simulation scenarios.

The collection of the simulation output files was conducted in four different XML-format files, using commands lanechange-file, summary-file, emission-file and queue-file in the Python script 'batchRunner.py', as depicted in **Figure A.4**, while the output for the SSM device is specified at the corresponding route definition file **(Figure A.5).** Finally, as illustrated in **Figure A.4**, the Python script 'batchRunner.py' calls the 'runner.py' script which triggers the ToC device for the specified vehicle types.

```
# this is the main entry point of this script
if __name__ == "__main__":
    options = get_options()
    downwardEdgeID = None
    distance = None
    # this script has been called from the command line. It will start sumo as a
    # server, then connect and run
    if options.gui:
        sumoBinary = checkBinary('sumo-gui')
    else:
        sumoBinary = checkBinary('sumo')
    # sumoBinary = checkBinary('sumo-gui')

    traci.start([sumoBinary, "-c", options.sumocfg, "--seed", options.seed,
    "--summary", "outputSummary%s"%options.suffix, "-a", options.additionals, "-r", options.routes,
    "--lanechange-output", "outputLaneChanges%s"%options.suffix,
    "--queue-output", "outputQueue%s"%options.suffix])

    downwardEdgeID = "approach2"
    distance = 10.
    #~ upwardEdgeID = "e0"
    #~ upwardDist = 3500.0

    run(downwardEdgeID, distance) #, upwardEdgeID, upwardDist)

    traci.close()
    sys.stdout.flush()
```

Figure A.4 Part of the Python script ‘batchRunner.py’ including the desired commands/arguments for the generation of the output files.

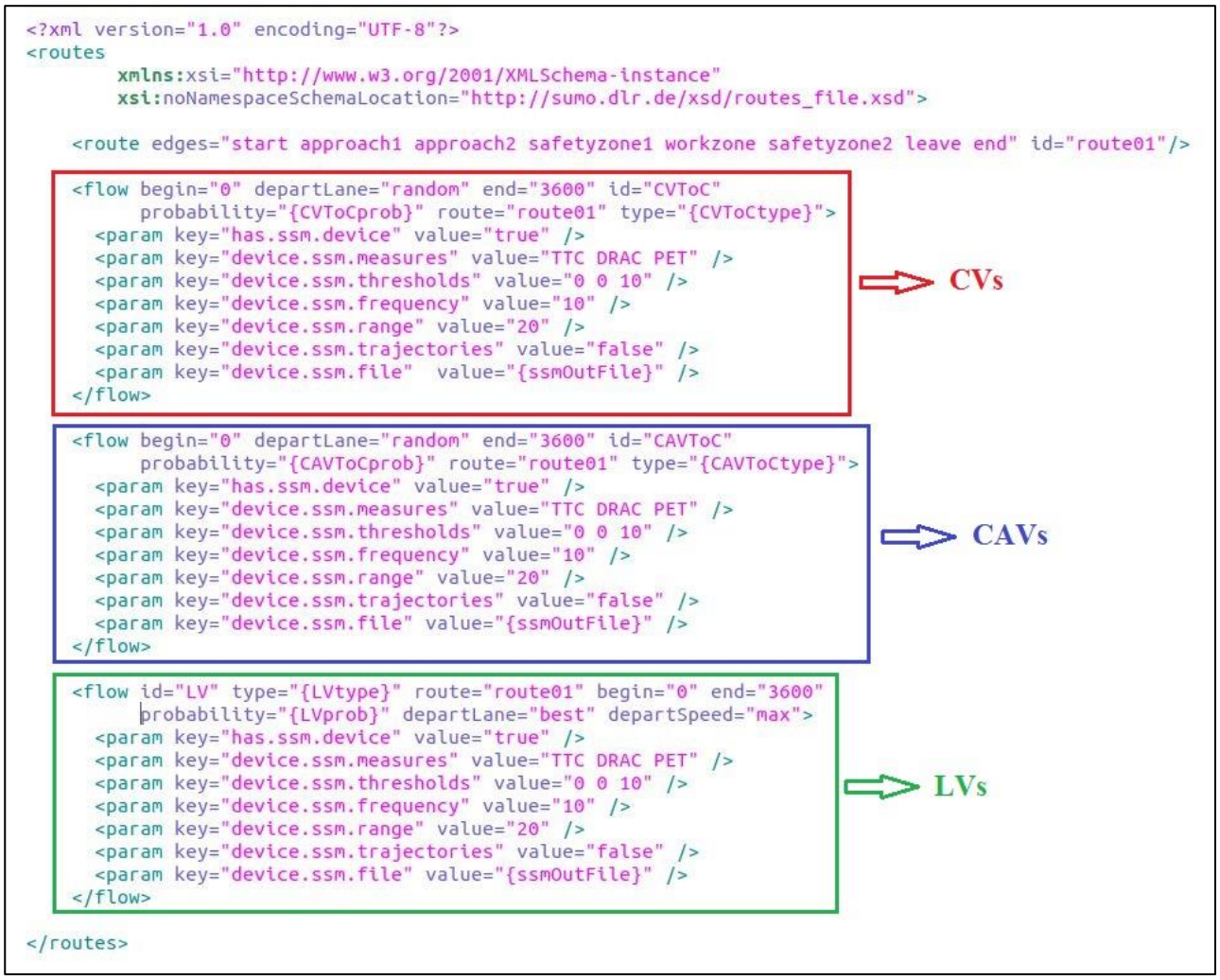

Figure A.5 The route definition file, '.rou.xml', to attach an SSM device to the vehicles.

Appendix B

The source code that generates situation specific driver response times in the cases of dynamical TOR triggering is thoroughly presented in **Table B.1**.

Table B.1 Source code generating response times for dynamical TOR triggering events.

```
#! /usr/bin/python3
#
# File: generateResponseTimeDistributions.py
# Author: Leonhard Luecken (leonhard.luecken@dlr.de)
# Date: 2019/05/22
#
# This script generates a lookup table for the parameters of the
# truncated Gaussian from which response times are sampled in case
# of dynamic ToCs, see MSDevice_ToC::responseTimeVars
# Also: TransAID Deliverable 3.1v2
#
# These tables provide mappings p_MRM, T_lead -> var, assuming
# that the mean of response times scales as
# min(2*sqrt(T_lead), 0.7*T_lead)

import numpy as np
from scipy import stats
from scipy.optimize import bisect

# define grid for looup table
pMRMSpan = np.linspace(0.0, 0.5, 11)
# ~ leadTimeSpan = list(np.linspace(0.1, 1.0, 4))
leadTimeSpan = list(np.linspace(0.1, 2.0, 20)) + list(np.linspace(2.25, 5.0, 12)) + list(np.linspace(5.5, 20.0, 30)) + list(np.linspace(21, 50.0, 30))

def responseMeanFromLeadTime(leadTime):
    # Assumed functional dependence for mean from given lead time
    return np.min([2*np.sqrt(leadTime), 0.7*leadTime])
```

```
def Ntrunc_GE(mu, sigma, x):
    # calculate the probability that a variable distributed according to a truncated Gaussian
    # is is greater or equal x
    if x < 0:
        print("ERROR: expected x>=0")
        sys.exit(1)
    # Truncated probability mass of normal
    pLE0 = stats.norm.cdf(0, loc=mu, scale=sigma)
    # Probability mass of rescaled gaussian above x
    pGEx = (1.0 - stats.norm.cdf(x, loc=mu, scale=sigma))/(1.0 - pLE0)
    return pGEx

def responseVariance(meanResponse, leadTime, pMRM):
    # fit v -> P(N_trunc(meanResponse, v)>leadTime) = pMRM
    f = lambda v: Ntrunc_GE(meanResponse, v, leadTime) - pMRM
    vMax = 100.0

    if (f(vMax) < 0):
        print("ERROR: leadTime or pMRM too large (or meanResponse too low).")
        sys.exit(1)

    v = bisect(f, 0.0001, vMax)
    return v

if __name__ == "__main__":
    # Generate parameters
    means = {}
    variances = {}
    for p in pMRMSpan:
        means[p] = {}
        variances[p] = {}
        for t in leadTimeSpan:
            print("# pMRM = %s, leadTime = %s"%(p, t))
```

```
            m = responseMeanFromLeadTime(t)
            # determine variance
            v = responseVariance(m, t, p)
            means[p][t] = m
            variances[p][t] = v
            print("  -> m = %s, v = %s"%(m,v))

    # Write lookup table in Cpp format (see MSDevice_ToC.cpp)
    lines = []

    # Write grid
    lines.append("// Grid of the response time distribution.\n")
    lines.append("// Generated by the script generateResponseTimeDistributions.py, see Appendix to TransAID Deliverable 3.1v2.\n")
    lines.append("// Probability for an MRM to occur (start with 0.0, end with 0.5)\n")
    lines.append("std::vector<double> MSDevice_ToC::lookupResponseTimeMRMProbs = ")
    l = "{" + str(pMRMSpan[0])
    for p in pMRMSpan[1:]:
        l += ", " + str(p)
    l += "};\n"
    lines.append(l)

    lines.append("// Lead time grid\n")
    lines.append("std::vector<double> MSDevice_ToC::lookupResponseTimeLeadTimes = ")
    l = "{" + str(leadTimeSpan[0])
    for t in leadTimeSpan[1:]:
        l += ", " + str(t)
    l += "};\n\n"
    lines.append(l)

    # ~ # Write means
    # ~ lines.append("// Means of the response time distribution.\n")
    # ~ lines.append("std::vector<std::vector<double> > MSDevice_ToC::lookupResponseTimeMeans = {\n")
```

```
    # ~ for p in pMRMSpan:
        # ~ l = "{" + str(means[p][leadTimeSpan[0]])
        # ~ for t in leadTimeSpan[1:]:
            # ~ l += ", " + str(means[p][t])
        # ~ l += "},\n"
        # ~ lines.append(l)
    # ~ lines.append("};\n\n")
    # ~ # Mean function
    # ~ lines.append("// Mean of the response time distribution.\n")
    # ~ lines.append("double MSDevice_ToC::lookupResponseTimeMean(double leadTime) {\n")
    # ~ lines.append("    return MIN2(2*sqrt(leadTime), 0.7*leadTime);\n")
    # ~ lines.append("};\n\n")

    # Write variances
    lines.append("// Variances of the response time distribution.\n")
    lines.append("std::vector<std::vector<double>>
MSDevice_ToC::lookupResponseTimeVariances = {\n")
    for p in pMRMSpan:
        l = "{" + str(variances[p][leadTimeSpan[0]])
        for t in leadTimeSpan[1:]:
            l += ", " + str(variances[p][t])
        l += "},\n"
        lines.append(l)
    lines.append("};\n\n")

    with open("responseTimeLookup.cpp", "w") as f:
        f.writelines(lines)

    print(lines)
```